Investigation of the role of the 5'-3' exoribonuclease *pacman* in *Drosophila* wound healing

Melanie Jane Sullivan

A thesis submitted in partial fulfilment of the requirements of the University of Brighton and the University of Sussex for the degree of Doctor of Philosophy

September 2008

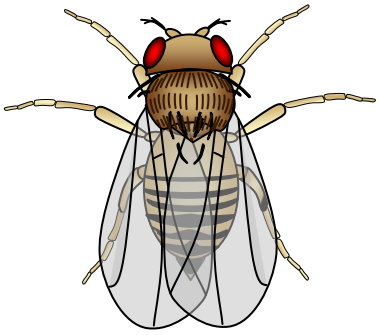

brighton and sussex medical school

i Abstract:

Investigation of the role of the 5'-3' exoribonuclease *pacman* in *Drosophila* wound healing.

The *Drosophila* gene *pacman* encodes a 5'-3' exoribonuclease, which is involved in RNA degradation. *pacman* mutants were created by P-element excision. These mutants have phenotypes including dull and blistered wings, kinked legs and thoracic closure defects. Also, *pacman* mutant embryos show a dorsal closure defect. The thorax and dorsal closure phenotypes in *pacman* mutants closely resemble those observed in flies mutant for genes of the highly conserved JNK signalling pathway, for example *hemipterous* (JNKK), *basket* (JNK) and *kayak* (Dfos). These similarities suggest *pacman* may be involved in regulating the JNK pathway. The JNK signalling pathway is known to regulate morphological processes such as dorsal closure during *Drosophila* development and wound healing. The phenotypes of our *pacman* mutants suggest *pacman* may have a role in these processes possibly through interactions with the JNK signalling pathway.

In this thesis the role of *pacman* in wound healing of *Drosophila melanogaster* is under investigation, firstly through survival experiments. These experiments show wounded *pacman* mutant flies do not survive as long as wounded wild type flies. These results suggest that *pacman* affects epithelial sheet sealing during wound healing. Secondly the role of *pacman* in regulating the JNK signalling pathway was investigated. Double mutant flies were created containing mutations for both *pacman* and *puckered*, a gene of the JNK signalling pathway. Results suggest there is a genetic interaction between *pacman* and *puckered.* This was researched further through Western Blotting experiments, QRT-PCR and staining experiments. Overall *pacman* has been shown to be involved in regulating wounding healing in *Drosophila melanogaster*, possibly through a genetic interaction with the JNK signalling pathway. However whether this interaction is direct or indirect is still unknown. Further studies should focus on other genes of the JNK pathway for example *hemipterous*, *basket* and *kayak* or upstream activators of this pathway.

ii Table of Contents:

Table of Contents:

Table of Contents:

Table of Contents:

Table of Contents:

Table of Contents:

Table of Contents:

Table of Contents:

iii Table of Figures:

Table of Figures:

Table of Figures:

iv Tables:

v Acknowledgements:

I would like to take this opportunity to thank the many people who have supported me throughout my thesis:

To Dr Dom Grima, Dr Steve Hebbes and Dr Maria Zabolotskaya: Thank you so much for allowing me to pester you with all my endless questions! Your wisdom, knowledge, support and advice were greatly appreciated.

I would like to thank Dawn Field and Helen Glenwright for their technical assistance and lending me their ears when I needed to chat.

To Nancy and Lauren my fellow PhD students: I'm glad we experienced the ups and downs of PhD life together. Thanks for always being there.

To Liz McQueeney: Thanks so much for the loan of the laptop the write up would have taken twice as long without it!!

To my supervisor Dr Sarah Newbury: A huge thanks to Sarah for being an amazing supervisor. From day one you were always there for me providing advice, support and encouragement.

Lastly I thank my mum and dad for being my rock. I couldn't have done it without you both. Thanks for pushing me on when I felt like I couldn't continue, for all the late night calls and for keeping me strong.

vi Candidate's Declaration:

Declaration

I declare that the research in this thesis, unless otherwise formally indicated within the text, is the original work of the author. The thesis has not been previously submitted to this or any other university for a degree, and does not incorporate any material already submitted for degree.

Signed:

Dated:

vii Abbreviations:

Abbreviation	Meaning
1˚ Ab	Primary Antibody
2˚ Ab	Secondary Antibody
ANOVA	Analysis of Variants
cDNA	Complementary DNA
Ct	Threshold Cycle
DC	Dorsal Closure
DNase	Deoxyribonuclease
dR	Relative Quantity
ECL	Electrochemiluminescence
ED	Effective Dose
ERK	Extracellular Signal Regulated Kinase
GFP	Green Fluorescent Protein
GTPase	Guanosine Triphosphatase
Hom	Homozygous
IRE	Iron Response Element
JNK	Jun N Terminal Kinase
JNKK	Jun N Terminal Kinase Kinase
JNKKK	Jun N Terminal Kinase Kinase Kinase
MAPK	Mitogen-Activated Protein Kinase
MAPKK	Mitogen-Activated Protein Kinase Kinase
MAPKKK	Mitogen-Activated Protein Kinase Kinase Kinase
mRNA	Messenger RNA
NRT	No Reverse Transcriptase
NTC	No Template Control
P-Body	Processing Body
PBS	Phosphate Buffered Saline
PCR	Polymerase Chain Reaction
Phospho	Phosphorylated
pJNK	Phosphorylated JNK
QPCR	Quantitative PCR
RNase	Ribonuclease
Rsq	Pearson Correlation Coefficient
RT	Reverse Transcription
SDS	Sodium Dodecyl Sulfate
TGF-β	Transforming Growth Factor-Beta
UAS	Upstream Activator Sequence
W.T	Wild type

Chapter 1 Introduction

1.1 Introduction to *Drosophila melanogaster*

Over the last century *Drosophila melanogaster* has become an invaluable research tool for scientists. There are several factors that make *Drosophila* an ideal model organism to study. Firstly they are cheap to breed and maintain. Secondly they have a quick generation time i.e. 10 days from mating until the emergence of new offspring. Importantly they possess unique mobile sequences called P elements similar to transposons which can move around the fly genome. These P elements can be used to genetically modify flies leading to new mutants. Another useful characteristic *Drosophila* possess are balancer chromosomes. Balancer chromosomes contain inversions which prevent crossing over (recombination) between homologous chromosomes during meiosis meaning heterozygous mutations can be maintained across generations. Balancer chromosomes also carry a dominant marker gene such as curly wings therefore heterozygotes can be distinguished by looking for the dominant marker. Lastly *Drosophila* genes are highly conserved across evolution. They have only 4 chromosomes therefore genetic crosses are simpler in *Drosophila* than higher organisms. Thus studying genes of interest in *Drosophila* will enhance our knowledge of human genetics. Geneticists have used *Drosophila* for many years to understand the role that genes play during development. Analysing mutants and genetic manipulation has allowed the identification of key developmental genes particularly those controlling embryonic development (Ashburner 1989).

1.1.1 *Drosophila* life cycle

Drosophila melanogaster development from egg to adult fly takes 9-10 days at 25˚C (Figure 1.1). After fertilization of the egg embryonic development takes 24 hours. This is followed by hatching of the larval stage. There are three larval stages separated by molts. The 3rd instar larvae undergo pupation at day 5. Inside the pupa metamorphosis occurs developing the larval imaginal discs into the adult structures. Adult flies reach sexual maturity at 8 hours and a female can lay 500 eggs (Ashburner 1989).

L3 larvae used for experiments

Figure 1.1: The life cycle of *Drosophila melanogaster* raised at 25˚C. Development from the egg to the adult fly takes 9-10 days. L3 instar larvae (red arrow) used for several experiments during this thesis are present at 5 days after egg laying. Figure adapted from The Cell Cycle: Principles of Control by David O Morgan, 2007.

1.1.2 *Drosophila* embryogenesis

Drosophila embryogenesis has been characterised into different stages based on morphological changes that are occurring. The first few stages involve several nucleic cleavages which results in a multinucleate syncytial blastoderm. These nuclei migrate to the edge of the embryo where blastoderm cells form during cellularisation at stage 5. Gastrulation, a major morphogenetic movement begins at stage 6. This process changes the single layered blastoderm into the 3 layers of the germ band: ectoderm, endoderm and mesoderm. Other morphological processes which occur during embryogenesis include ventral furrow and cephalic furrow formation followed by germ band extension which forms the amniosersosa. This is a layer of flat cells which will eventually lie under the lateral epithelia of the embryo. As the cephalic furrow disappears head involution begins. Next germ band shortening takes place moving all the structures back to their original position resulting in a hole on the dorsal side of the embryo exposing the amniosersosa. In order to close this hole the lateral epithelia moves over the amniosersosa and seals at dorsal midline during a process called dorsal closure. This event will be discussed in more detailed later in the thesis. Lastly the larval structures begin to differentiate in preparation for hatching. Head involution concludes followed by gut, nervous system and tracheal formation. These morphological processes result in segmentation of the embryo and thus the hatching larva, which will have 3 thoracic segments and 8 abdominal segments. Specific adult appendages such as wings and legs then develop in the corresponding segment during pupation (Ransom 1982; Campos-Ortega 1985; Alberts et al. 1994).

1.1.3 Regulation of embryogenesis

Coordinating the morphogenetic processes that occur during segmentation of the embryo requires tight regulation of firstly maternal gene products then zygotic gene expression (Figure 1.2). Early development of the embryo is controlled by mRNAs and proteins that were laid into the egg from the mother during oogenesis. The genes that produce these mRNAs and proteins are called maternal genes and mutations within these genes result in maternal effect mutations. There are around 50 maternal genes which are involved in producing the antero-

posterior axis and mapping the framework of the embryo. The zygotic genes interpret this and build from there. Before fertilization the maternal mRNAs are specifically localised within the egg. For example *bicoid* and *nanos* mRNAs are present at the anterior and posterior ends respectively. Maternal effect mutants are missing either the anterior or posterior ends. *Nanos* mutants have no abdomen and *bicoid* mutants have no head structures.

Shortly after fertilization the maternal mRNAs are translated and the proteins defuse across the embryo to produce a concentration gradient. These gradients at the antero-posterior axis signal for zygotic expression of the gap genes during the syncytial blastoderm stage of embryogenesis. Gap genes which are mostly transcription factors are expressed in bands across the embryo. This separates the axis into unique regions depending on which gap gene is expressed. Gap gene mutants result in gaps in the embryo where several segments are missing.

After gastrulation grooves are seen across the surface of the embryo which divides it into parasegments. There are 14 parasegments which develop independently from its neighbours due to specific gene expression. The parasegments define the boundaries from which the segments of the *Drosophila* larvae are derived. One segment is made from the posterior region of one parasegment and the anterior region of the next. Pair-rule gene expression in seven stripes across the embryo coordinates the development of the parasegments. Pair-rule gene mutants have only half the number of parasegments.

The segment polarity genes are activated in response to pair-rule gene expression. They are responsible for patterning the parasegments. For example the segment polarity gene *engrailed* is expressed in the anterior region of each parasegment and activates the expression of other genes such as *hedgehog* and *wingless*. Expression of these genes at the anterior region of each parasegment signals that this will develop into the posterior region of the resultant segments. Segment polarity gene mutants have either the anterior or posterior region of a segment duplicated i.e. *engrailed* mutants have the posterior region of each segment replaced by the anterior region. Thus in the adult flies the structures such as the wing possess two anterior halves and is therefore a mirror image.

Each segment will develop into a unique adult structure. Homeotic gene expression gives each segment its own identity. Homeotic mutants result in misplacement of the adult structures for example *Antennapedia* mutants have legs on their head instead of antennae (Wolpert 2007). Since Drosophila development is the best understood of all organisms and the molecular basis underlying many pathways are understood it provides an ideal organism for the understanding of novel gene regulatory processes such as mRNA stability.

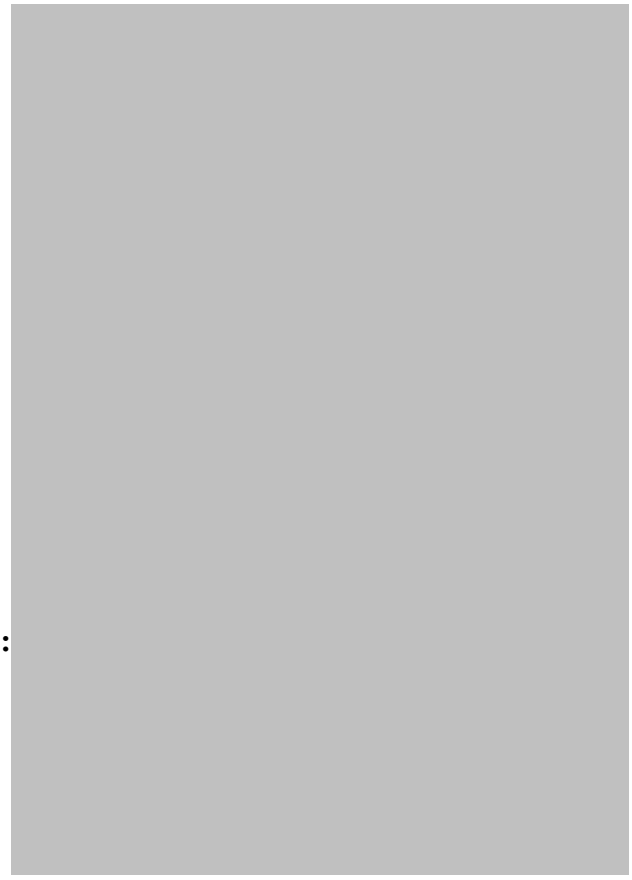

Figure 1.2: The gene expression cascade which regulates *Drosophila* body plan development during embryogenesis. Maternal effect genes produce the antero-posterior axis and map the framework of the embryo. Mutants are missing either the anterior or posterior ends. Gap genes separate the body axis into unique regions. Gap gene mutants result in gaps in the embryo where several segments are missing. Pair-rule genes are expressed in seven stripes across the embryo coordinating the development of the parasegments. Pair-rule gene mutants have only half the number of parasegments. Segment polarity genes pattern the parasegments. Segment polarity gene mutants have either the anterior or posterior region of a segment duplicated. Figure adapted from Life: the Science of Biology by William K. Purves, 1998.

1.2 RNA stability/turnover

Eukaryotic gene expression can be regulated by changes in mRNA stability (Bashirullah et al. 2001; Parker et al. 2004). Some mRNAs have a half life of several hours such as β-globin. However others have very short life spans such as those that encode growth factors (Alberts et al. 1994; Newbury 2006). Levels of these regulatory proteins must change rapidly in a cell depending on environmental cues. Unstable mRNAs often contain specific sequences within their 3' untranslated region for example AU rich sequences that target them for degradation (Barreau et al. 2005). The stability of a specific mRNA can also change in response to extracellular signals. A well documented example of this involves the transport of iron into cells. The transport of iron is tightly regulated by the degradation of the transferrin receptor mRNA. Transferrin binds the iron to transport it through the transferrin receptor into the cell. Normally the transferrin receptor mRNA is rapidly degraded. However when iron levels are low in the cell, an RNA binding protein called aconitase binds the IRE (iron responsive element) region of the mRNA blocking degradation. This leads to translation of the transferrin receptor which results in more iron transportation into the cell (Alberts et al. 1994).

In order for correct development of an organism, mRNA levels must be closely regulated. Translation and degradation of mRNAs throughout each stage of development are in a delicate balance (Coller et al. 2005; Newbury 2006). Disruption of this balance can cause severe abnormalities, diseases and cancer. Regulation of the translation of mRNAs has been extensively studied for a many number of years. Incorrect translation leading to overexpression of transcription factors such as the oncogene *c-fos* can lead to cancer (Alberts et al. 1994; Lodish et al. 2004). In contrast we are still in the early stages of understanding the regulation of the mRNA degradation pathways.

The link between mRNA degradation, translational repression and correct development is evident in the case of *Drosophila melanogaster* embryo development (Ransom 1982; Campos-Ortega 1985). Early embryo development is dependent on maternally contributed mRNA gradients which determine the anterior-posterior and dorsal-ventral axes. (Bashirullah et al. 1999; Bashirullah et

al. 2001) For example *bicoid* and *hunchback* mRNA is tethered to the anterior end of the embryo, both gradients are highest at the anterior tip and decrease towards the posterior. In contrast *nanos* mRNA is highest at the posterior end (Myers et al. 1995; Tadros et al. 2003). These gradients therefore produce protein gradients in the same pattern. Nanos has the ability to bind *hunchback* mRNA and repress its translation leading to degradation of *hunchback* at the posterior end. Embryos from mothers who have a *bicoid* null mutation lack anterior structures i.e. the head and thorax. *nanos* mutants have no abdomen. The abdomen is determined by the Gap genes which includes the gene *hunchback*. Therefore without the presence of Nanos to regulate the degradation of *hunchback* mRNA the abdomen is missing (Cooperstock et al. 1997; Lasko 1999). Therefore mRNA degradation can play a critical role in development and greater understandings of the mechanisms of this process are needed.

1.3 Degradation of mRNAs

1.3.1 Degradation in yeast – XRN1

The process of mRNA degradation, where mRNAs, are removed from the cell, is highly regulated by many different mechanisms including specific destabilising sequences, extracellular signals and environmental cues such as stress. Degradation involves the digestion of the mRNA by ribonucleases. In yeast the cytoplasmic 5'-3' exoribonuclease is Xrn1p (Hsu et al. 1993; Kim et al. 2004). This enzyme is highly conserved in eukaryotes, and include the *Drosophila* homologue *pacman* and the *C.elegans* homologue xrn-1(Stevens 1980; Kenna et al. 1993). The nuclear 5'-3' exoribonuclease is Rat1p (Kenna et al. 1993; Page et al. 1998). This is involved in nuclear RNA degradation and rRNA processing. The 3'-5' exoribonuclease activity is undertaken by a complex of nuclease proteins called the exosome (Seago et al. 2001; Parker et al. 2004). This complex has nine core subunits which form a ring structure that is thought to allow the RNA to pass through it. The exosome subunits are also highly conserved in eukaryotes. Its activity is dependent on interactions with several Ski proteins Ski2p, Ski3p, Ski8p and Ski7p (Newbury 2006). Many of these proteins are helicases that unwind the RNA to allow its entry into the ring structure of the exosome for degradation (McLaren et al. 1991; Caponigro et al. 1996).

In eukaryotes mRNAs can be degraded in three different ways shown in Figure 1.3. The first way involves 5'-3 digestion which begins with decapping of the 5' cap by the decapping enzyme (Hsu et al. 1993; Fischer et al. 2002). This enzyme is made from two subunits Dcp1p and Dcp2p (Lin et al. 2006; Lin et al. 2008). Once the 5' cap has been removed the 5' end is free for degradation by the 5'-3' exoribonuclease Xrn1p (Kim et al. 2004). The second pathway involves 3'-5' degradation that first requires the removal of the 3' poly (A) tail by de-adenylation using a complex of de-adenylase proteins including Ccr4, Pop2 and Not. The mRNA is then degraded by either the exosome or is de-capped and degraded in a 5'-3' direction by Xrn1p (McLaren et al. 1991; Parker et al. 2004). The last method of degradation in eukaryotes involves endonucleases, which cleave the mRNA at a particular sequence and allows the two fragments to be degraded by exoribonucleases; the exosome and Xrn1p (Wilusz et al. 2001; Newbury 2006). An example of this type of degradation is Nonsense-Mediated Decay (NMD). This occurs when a premature stop codon is present in the mRNA and the RNA is then cleaved near this codon and subsequently degraded (Wilusz et al. 2001; Newbury et al. 2006). Mutations in XRN1 in yeast lead to larger cell size, an increase in doubling time and defective sporulation. Growth inhibition is dependent on the C terminal and is independent of the nuclease activity of the N terminal (Long et al. 2003; Parker et al. 2004). These mutant phenotypes suggest a role for XRN1 in regulating cell growth and movement.

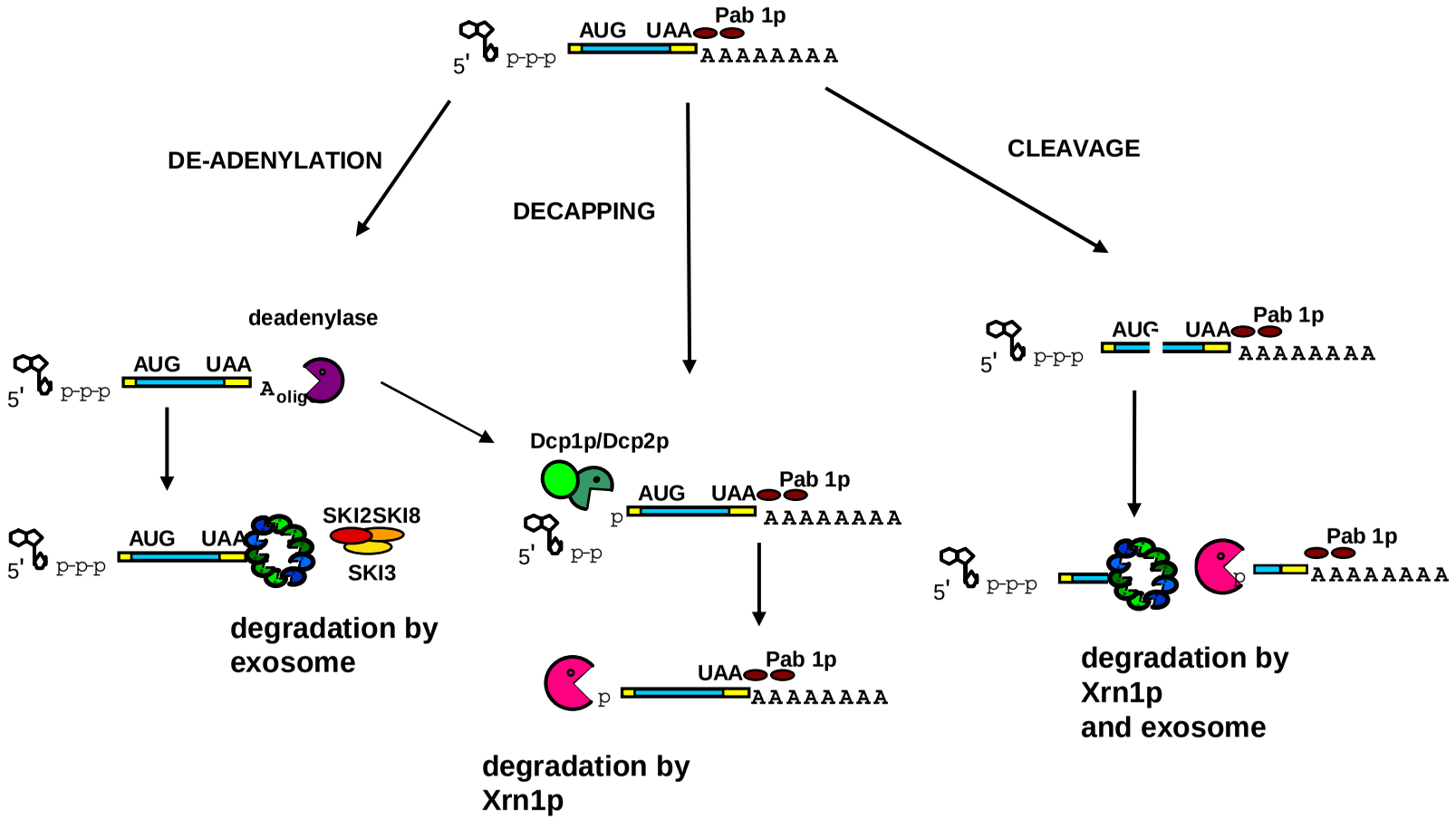

Figure 1.3: The three pathways in which mRNAs can be degraded. 1. After de-adenylation of the poly (A) tail the mRNA is degraded by the 3'-5' exosome. 2. After decapping of the 5' cap by the Dcp1/Dcp2 complex the mRNA is degraded by the 5'-3' exoribonuclease Xrn1p. 3. Endonuclease enzymes cleave the mRNA and it is then degraded by both 3'-5' and 5'-3' exoribonucleases.

1.3.2 P bodies

Recent work has shown in yeast, human, mice and *Drosophila* cells that the proteins involved in degradation are clustered together in structures called P-bodies (processing bodies) (Bashkirov et al. 1997; Ingelfinger et al. 2002). Proteins that have been shown to be present in P-bodies include Xrn1, Dcp1, Dcp2, Lsm proteins, Dhh1, Pat1 and mRNA itself (Figure 1.4) (Lin et al. 2006; Lin et al. 2008). mRNAs which have exited translation and have been targeted for degradation enter these structures where they are decapped and degraded (Wilusz et al. 2001; Sheth et al. 2006). These structures change in size and number in response to different stimulus such as stress caused by heat shock (Zabolotskaya et al. 2008). They are thought to be the site for RNA storage, where RNA remains dormant until it is either translated or degraded (Sheth et al. 2006; Parker et al. 2007). In *Drosophila* testes cells, heat shock treatment causes the P-bodies to increase in size and frequency (Zabolotskaya et al. 2008). Inhibiting 5'-3' digestion or the decapping steps in yeast leads to an increase in number and size of the P-bodies (Sheth et al. 2003; Parker et al. 2007). Having all the proteins needed for degradation together allows for a rapid response to external signals and therefore a rapid regulation of gene expression levels.

1.3.3 Degradation in mammalian cells

Although mammalian RNA degradation pathways remain poorly characterized some information is beginning to emerge. As mentioned earlier the exoribonucleases involved in yeast degradation are highly conserved. In mammalian cells the predominant degradation pathway appears to involve 3'-5' degradation of mRNA by the exosome. Human homologues of the decapping complex (Dcp2, Dcp1A and Dcp1B), the cytoplasmic 5'-3' exoribonuclease (Xrn1) and the nuclear 5'-3' exoribonuclease (Xrn2) have also been found. Cytoplasmic foci thought to be P-bodies have been seen in human HeLa cells and mouse cells. These foci are the sites for co-localisation of Dcp1A/B, Dcp2, Xrn1 and Lsm proteins (decapping enhancers) (Ingelfinger et al. 2002; Lehner et al. 2004).

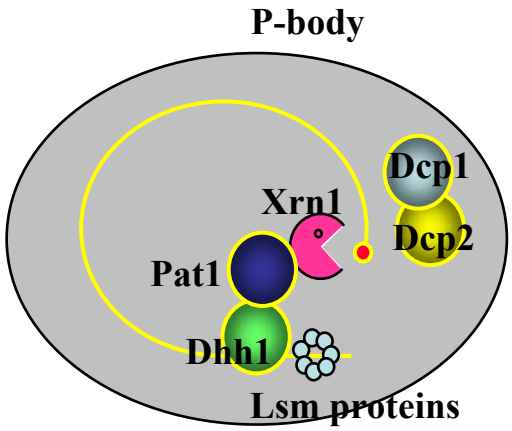

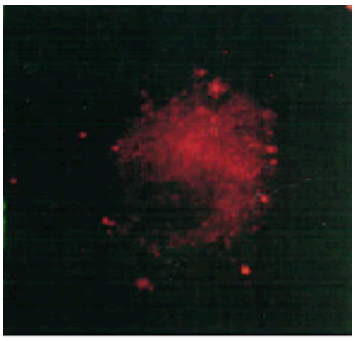

mouse Xrn1p

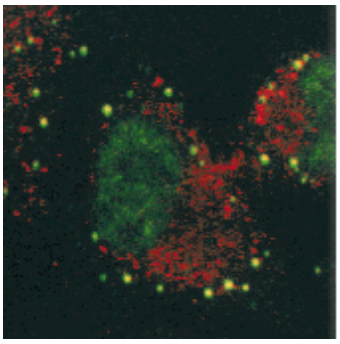

co-localisation of hLSm4 (green) with hXrn1(red) in HeLa cells

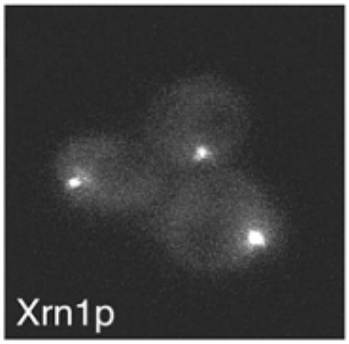

yeast Xrn1p

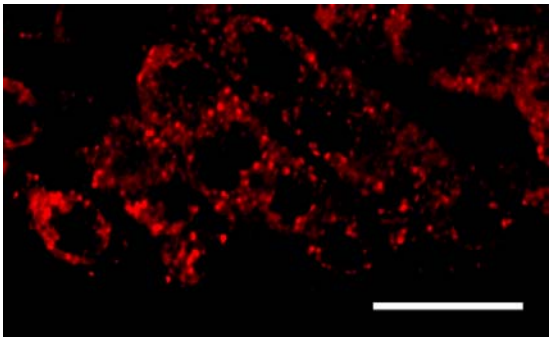

Drosophila testes *pacman*

Figure 1.4: This diagram shows the proposed structure of a P-body. These clusters are thought to be the site of degradation and have been found in the cells of many organisms. Several proteins involved in degradation have been found to be localised at these sites including Xrn1, Dcp1, Dcp2, Pat1, Dhh1 and Lsm proteins. Mouse P-body adapted from Bashkirov, 1997. Human P-body adapted from Ingelfinger et al, 2002. Yeast P-body adapted from Sheth and Parker, 2003. *Drosophila* P-body adapted from Zabolotskaya, 2008.

1.3.4 Degradation in *Drosophila* – *pacman*

The *Drosophila* Xrn1 homologue is called *pacman* and the gene sequence has 59% identity to the yeast Xrn1p and 67% identity to the mouse mXrn1p at the N terminal end (Figure 1.5) (Till et al. 1998; Chernukhin et al. 2001). The active site of the enzyme is located within this N terminal domain. Like Xrn1p in yeast *pacman* functions as a 5'-3' exoribonuclease in the cytoplasm of the cell. The *pacman* gene has also been shown to complement yeast XRN1 deletion mutations (Till et al. 1998). Maria Zabolotskaya in the Newbury lab has been researching P-bodies in *Drosophila* testis cells as mentioned in Section 1.3.2 and has shown that the *Drosophila* homologues Pacman, dDcp1, dDcp2 and Me31B (Dhh1) are all present in these structures (Zabolotskaya et al. 2008). Recent studies of nurse cells in *Drosophila* embryos have also shown the co-localisation of dDcp1, dDcp2, Me31B and Pacman in P-body like structures (Ingelfinger et al. 2002).

1.3.5 *pacman* homologues – *C. elegans*

As mentioned earlier the Xrn1p homologue in *C.elegans* is *xrn-1* which also encodes a 5'-3' exoribonuclease involved in mRNA degradation. XRN-1 was shown to be critical for the correct development of the nematode (Newbury et al. 2004). When *xrn-1* was silenced by RNA interference the worm embryos arrested at the two-fold stage having failed to correctly undergo ventral enclosure (Figure 1.6) (Williams-Masson et al. 1997; Piekny et al. 2003). During the process called ventral enclosure the epithelial cells stretch over the embryo and the two sides seal together on the ventral side (Chin-Sang et al. 2000; Simske et al. 2001). In embryos mutant for *xrn-1* a hole is present on the ventral side and when the next step of development, elongation of the embryo occurs, the internal cells 'leak' out (Newbury et al. 2004). These mutant phenotypes suggest a role for *xrn-1* in regulating cell shape changes and cell movements.

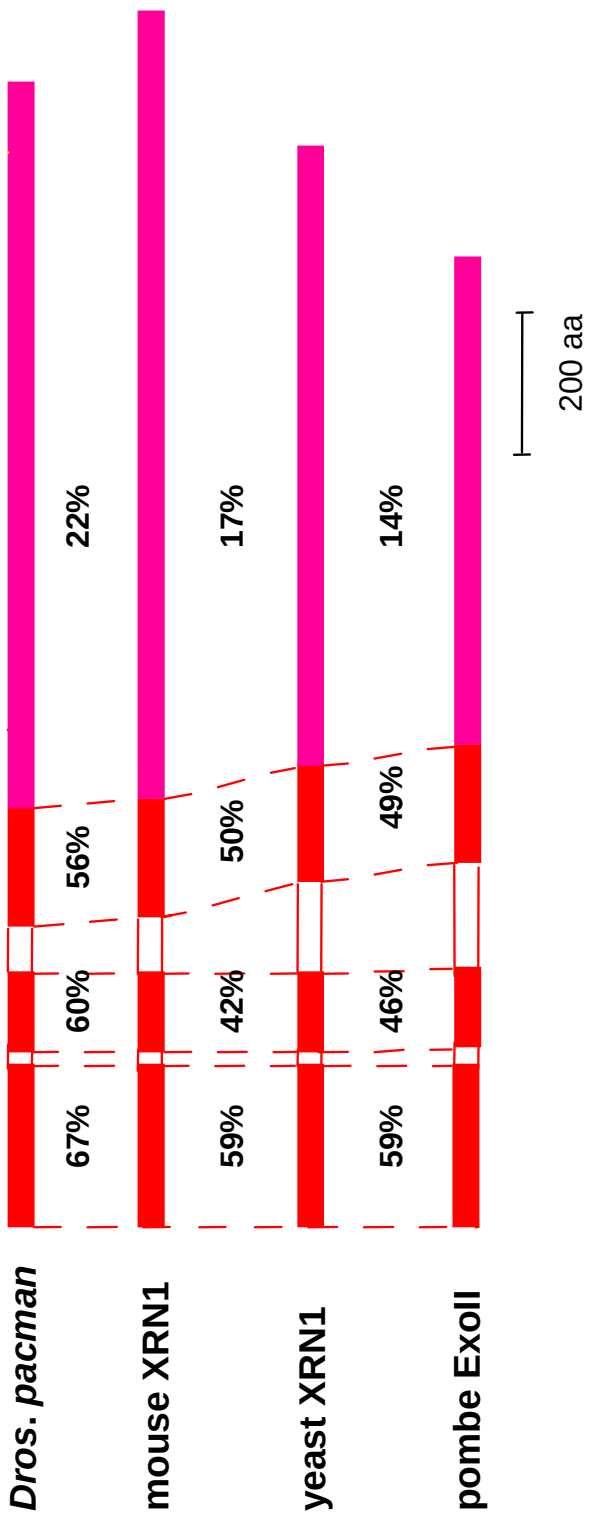

Figure 1.5: The exoribonuclease Xrn1 has highly conserved homologues. The *Drosophila* Xrn1 *pacman* has 67% sequence identity to the mouse Xrn1 and 59% sequence identity to the yeast Xrn1for the region shown. PACMAN has been shown to complement yeast XRN1 mutations.

wild-type embryos

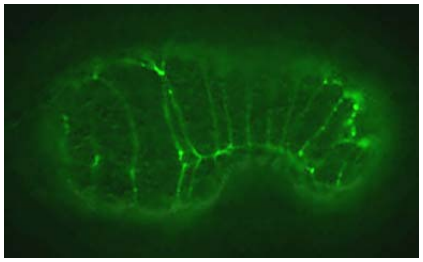

xrn-1(RNAi) embryos

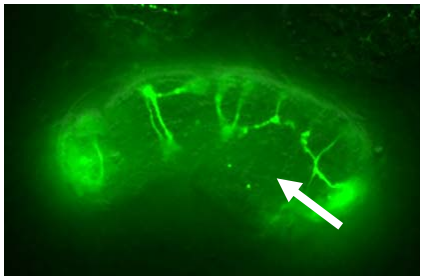

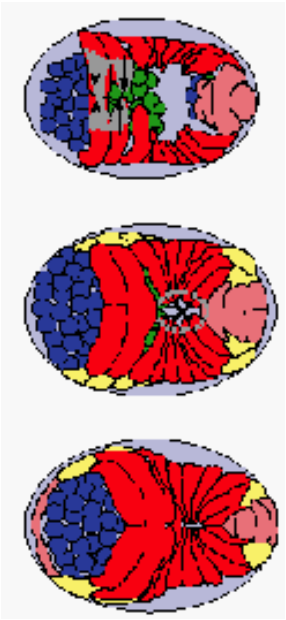

Ventral enclosure (*C.elegans*)

Figure 1.6: *C.elegans* embryos that are mutant for xrn-1 fail to correctly undergo the morphogenetic process ventral enclosure. These mutant embryos are left with a hole on the ventral side adapted from Newbury, 2004 (white arrow). The diagram on the left shows a schematic of ventral enclosure adapted from Chin-Sang, 2000.

1.4 Understanding of the function of *pacman* prior to the start of my project.

Since the discovery of the *Drosophila* xrn1 homologue *pacman* in 1998 the Newbury group has been trying to further characterize the function of *pacman*. The *pacman* locus was mapped to chromosome X at cytological location 18D1-4 which encodes a 4839bp open reading frame. A Pacman antibody was created which detected a single major band of 184kDa in size by western blotting experiments (Till et al. 1998; Grima et al. 2008).

The *pacman* gene contains the sequence CAG, repeated 9 times that encodes a polyglutamine tract near the 3'end of the coding region (Till et al. 1998; Grima et al. 2008). In *Drosophila* the majority of genes that contain these polyglutamine tracts are essential for development and often function as transcription factors or RNA binding proteins (Pinheiro et al. 2002).

1.4.1 *pacman* expression in *Drosophila*

Pacman has been shown to be differentially expressed throughout *Drosophila* development with Northern blotting experiments showing the 5.2kb *pacman* transcript in abundance at 0-8 hour embryos, 1st instar larvae and male and female adult flies in wild type strains. This was the first time that a ribonuclease had been shown to be differentially expressed throughout development (Figure 1.7) (Till et al. 1998).

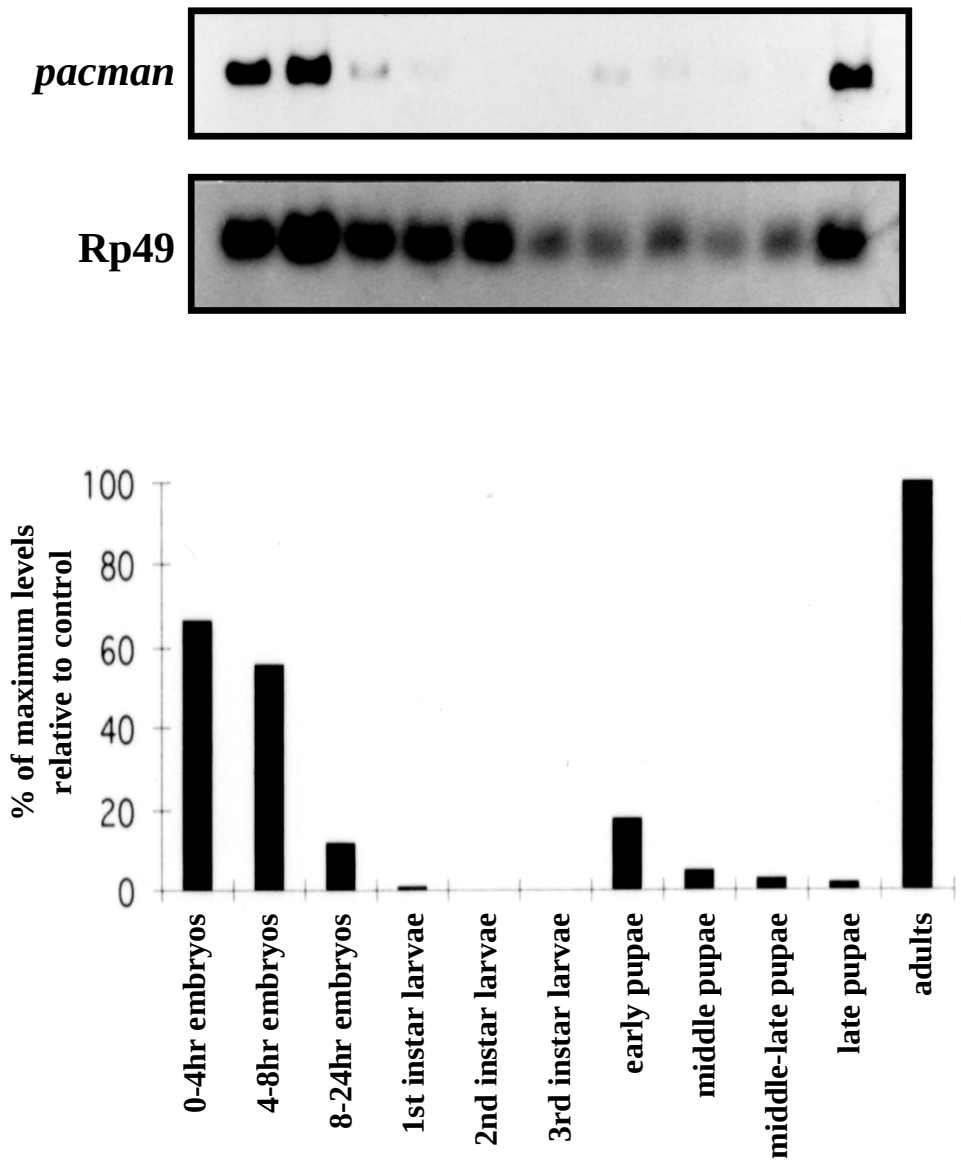

Figure 1.7: Northern blotting experiments showed that *pacman* is differentially expressed throughout *Drosophila* development. Developmental stages are 0–4-h embryos, 4–8-h embryos, 8–24-h embryos, 1st instar larvae, 2nd instar larvae, 3rd instar larvae, early pupae, mid-pupae, mid-late pupae, late pupae, adults. Data and figures adapted from Till et al, 1998.

1.4.2 The making of the *pacman* mutants

In order to further characterise the functions of *pacman*, mutant alleles were created by Dr Dom Grima using P-element excision. The P-element 3' downstream of *pacman* shown in Figure 1.8 was excised leading to deletions of the *pacman* gene at the 3' end. The P-element EP(x)1526 was 485 bp from the 3' terminus of the *pacman* coding sequence. The transposition of EP(X)1526 involved several crosses, the first of which created offspring flies carrying transposase as well as the P-element insertion. The transposition events occurred in the germline of the male offspring. These males were individually mated to females with the FM7c balancer. This cross produced females with the FM7c balancer and the transposed P-element but no transposase. This would prevent any further P-element transposition in the resultant offspring. Lastly these females were individually mated with FM7c/Y males to maintain the mutant line. Several mutant *pacman* lines were created however this project will investigate three of those mutant deletion lines known as pcm^3, pcm^5 and pcm^6 (Figure 1.8) (Grima 2002; Grima et al. 2008).

Semiquantitative RT-PCR experiments by Dr Dom Grima showed that all mutants expressed *pacman* mRNA and were therefore not null mutants. Levels of truncated *pcm* protein expression in the mutants were determined by Western blotting experiments. The *pcm* protein measures 184kDa and bands were seen on a Western blot for pcm^3 (167.7kDa) and pcm^6 (160.0kDa) male and female flies. Little or no band has been seen for pcm^5 (predicted molecular weight =149.2kDa) suggesting this mutant allele has the least *pcm* expression i.e. undetectable levels of *pacman* protein (Figure 1.9) (Grima 2002; Grima et al. 2008).

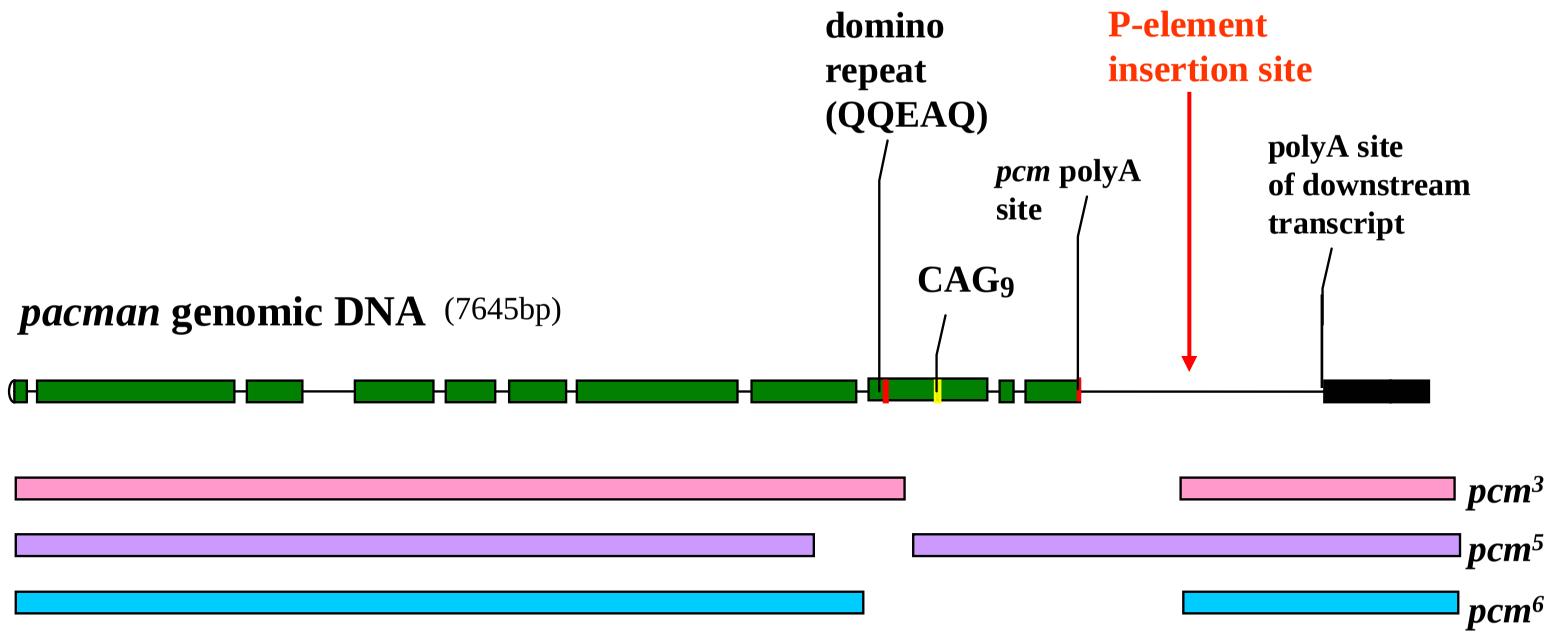

Figure 1.8: Diagram shows the *pacman* genomic DNA and the P element insertion site 3' of the gene. *Pacman* contains a polygluatmine repeat similar to those seen in the human Huntington protein. The 3' P element was excised to create the *pacman* mutants pcm^3, pcm^5 and pcm^6.

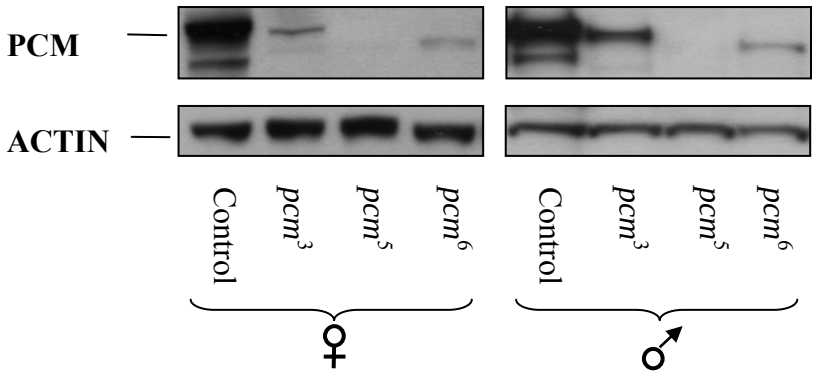

Figure 1.9: An example of a Western blotting experiment using the *pacman* antibody on extracts prepared from adult males and females flies. The *pcm* protein band can be seen for the wild type control measuring 184.5kDa, pcm^3=167.7kDa and pcm^6=160.0kDa. Normally little or no band is seen for pcm^5 (predicted molecular weight =149.2kDa). An Actin loading control is shown below (adapted from Zabolotskaya, 2008).

1.4.3 *pacman* mutant phenotypes

Several mutant phenotypes have been observed by members of the Newbury group. Firstly embryos appear to be considerably shorter than the normal length wild type embryos. This phenotype is similar to those seen in *puckered* mutants. This is a gene member of the JNK signalling pathway which will be discussed later. Embryos also undergo unusual invagination at gastrulation, which is consistent with a possible role for *pacman* in cell shape changes and cell movement (Grima 2002).

pacman mutants have reduced male fertility, this is thought to be a consequence of smaller testis in length and width and a narrowing of the tip (Roberts 2002). The *pacman* expression levels in testis of the mutants were tested by Western blotting. Results showed that pcm^3 mutants had much lower levels of *pacman* expression compared to the wild type controls and pcm^5 had undetectable levels (Zabolotskaya et al. 2008).

The mutations in *pacman* also affected female fertility as there was a decrease in the number of offspring from homozygous *pacman* females compared to hemizygous (one copy of *pcm* mutation) females. This decrease in offspring number was the result of a reduction in the number of eggs laid and also a reduction in the number of eggs hatching into larvae. In both cases pcm^5 showed the most severe mutant phenotypes, whereas pcm^3 and pcm^6 encoded weaker alleles (Roberts 2002).

These *pacman* mutant alleles were found to be temperature sensitive with mutant phenotypes being more penetrant at lower temperatures. Mutant adult flies have a smaller wing size which correlates to an overall reduction in fly size (Roberts 2002). The wings were also often blistered and dull in appearance. The mutant flies also have 'kinked' legs where abnormal bends are seen on their legs. These phenotypes had a higher penetrance in pcm^5 flies compared to pcm^3 flies and at 19˚C compared to 25˚C (Grima 2002).

pacman mutants can also have a malformed thorax suggesting a defect in thorax closure (Figure 1.10) (Grima 2002). This process occurs during larval development when the two wing imaginal discs move together and fuse. Thorax

closure is a similar morphogenetic process to ventral enclosure in *C.elegans* (Usui et al. 2000; Pastor-Pareja et al. 2004; Shen et al. 2005). Dorsal closure is another morphogenetic event that occurs during embryogenesis of *Drosophila* (Kiehart et al. 2000; Martin et al. 2003). After gastrulation a hole is present on the dorsal side of the embryo. The epithelial cells move together over the underlying amnioserosa and fuse together to seal the hole (Jacinto et al. 2002; Martin et al. 2002). Recent studies of *pacman* mutant cuticle preparations have shown that these mutants show dorsal closure defects, where the dorsal hole has completely failed to seal (Grima et al. 2008). During these processes cells are moving and changing shape which again leads to the hypothesis that *pacman* may have a role in cell movement. Both thorax closure and dorsal closure will be discussed in greater detail later in this chapter.

1.5 The link between thorax closure defects and JNK signalling mutants

Previous studies have shown other mutants with thorax closure defects similar to those seen in *pacman* mutants (Agnes et al. 1999; Zeitlinger et al. 1999; Martin-Blanco et al. 2000) (Figure 1.10). These other mutants (*kayak* and *hemipterous*) have mutations in genes of the JNK signalling pathway. This pathway has been shown to regulate thorax closure and other morphogenetic events such as dorsal closure (Ring et al. 1993; Jacinto et al. 2001). These similar mutant phenotypes lead to the conclusion that *pacman* may be genetically interacting with this pathway.

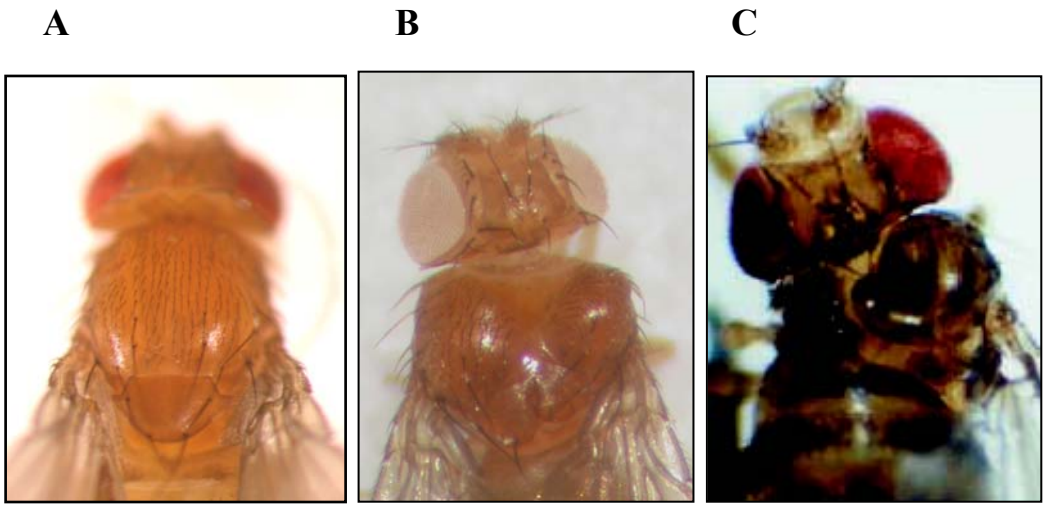

Figure 1.10: Thorax closure defects seen in *pacman* mutants and genes of the JNK signalling pathway for example *hemipterous*. Thorax defect occur when the two wing imaginal discs fail to fuse correctly during thorax closure. **A**: Wild type thorax, **B**: *pacman*^{5} mutant thorax and **C**: *hemipterous*^{1} mutant thorax (adapted from Agnes, 1999).

1.6 The JNK signalling pathway

Several recent studies have established a role for the JNK signal transduction pathway in regulating cell movements during development (Martin-Blanco et al. 1998; Martin-Blanco et al. 2001). The JNK signalling pathway consists of several protein kinases (Jun N terminal kinases) which ultimately phosphorylate transcription factors that lead to gene expression and changes in cell behaviour. These kinases are also known as stress activated protein kinases (SAPKs) because they were first identified in mammals, by their ability to phosphorylate c-Jun when activated by UV light i.e. stress. They form a subgroup of the mitogen-activated protein kinases (MAPKs) which are found in all eukaryotes. Other subgroups include the extracellular-signal-regulated kinases (ERKs) and the p38s. MAPKs are highly conserved with pathways in *Caenorhabditis elegans*, *Drosophila*, rats, mice and humans (Goberdhan et al. 1998; Stronach 2005). This high conservation through evolution has allowed model systems to be used to study the possible roles of the JNK signalling pathway.

The JNK signalling pathway is activated in a number of cell types during several different stages of the *Drosophila* life cycle. Physiological, pathological and environmental cues are known to stimulate the activation of the pathway. A particular cue will induce a particular response therefore the pathway must have evolved a way of distinguishing each cue and a way of relaying this back to the pathway. The activity of the pathway is regulated through a three step cascade involving MAPK kinase kinase, MAPK kinase and MAPK (Figure 1.11). Each step involves activation of the next kinase by phoshorylation. MAPKKKs phosphorylate MAPKKs at serine and threonine residues. These activate MAPKKs, dual specificity kinases, which in turn phosphorylate MAPKs at Thr-X-Tyr motifs. MAPKs then phosphorylate substrates, most of which are transcription factors, at serine and threonine residues (Harden 2002; Stronach 2005). How extracellular signals are linked to the activation of this three step cascade is still poorly understood.

1.6.1 Mammalian JNK

In mammals the MAPK pathways can be separated into five groups: extracellular regulated kinase1 and 2 (ERK1/2), Jun N-terminal kinase (Figure 1.12), p38, ERK3/4 and ERK5 (Bashirullah et al. 2001; Chang et al. 2001). These are complex systems were each MAPKK can be activated by more than one MAPKKK however it is assumed that each MAPKKK responds to a distinct stimuli e.g. growth factors, inflammatory response (Goberdhan et al. 1998; Xia et al. 2004). There are three JNK loci (JNK1/2/3) all of which have been knocked out in mice. The mutant mice with single mutations appear normal with no defects. However double mutants for JNK1 and JNK2 result in neural tube defects (Chang et al. 2001; Weston et al. 2002). This is consistent with the idea the JNK pathway is somehow involved in regulating development.

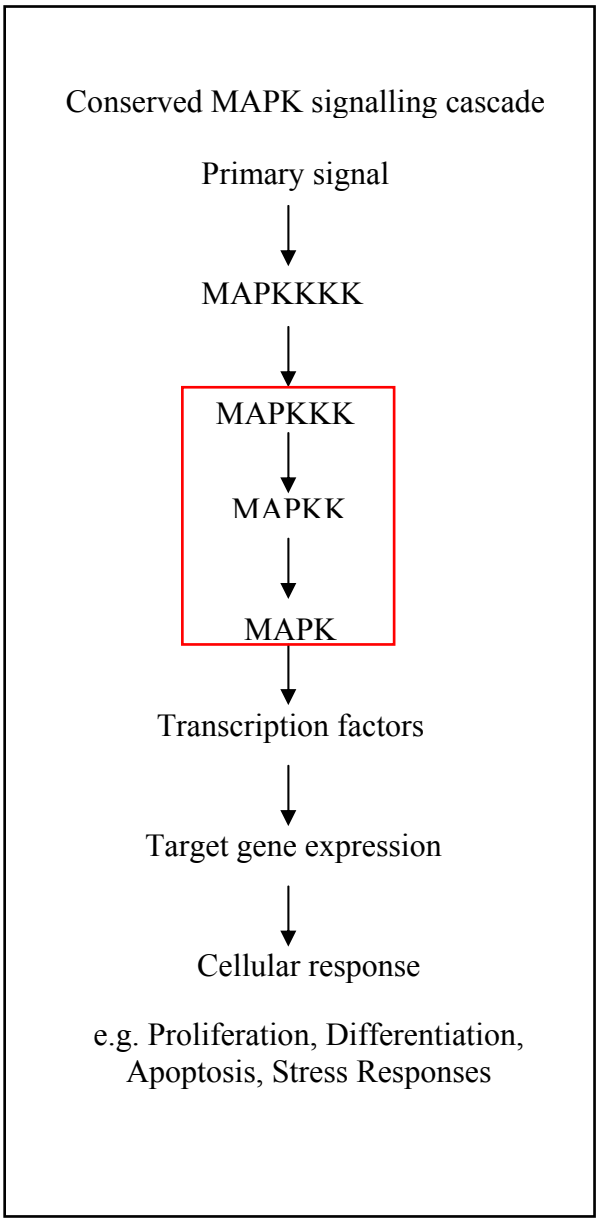

Figure 1.11: Diagram of MAP kinase signalling pathway adapted from Xia and Karin 2004. Red box highlights the three step signalling cascade.

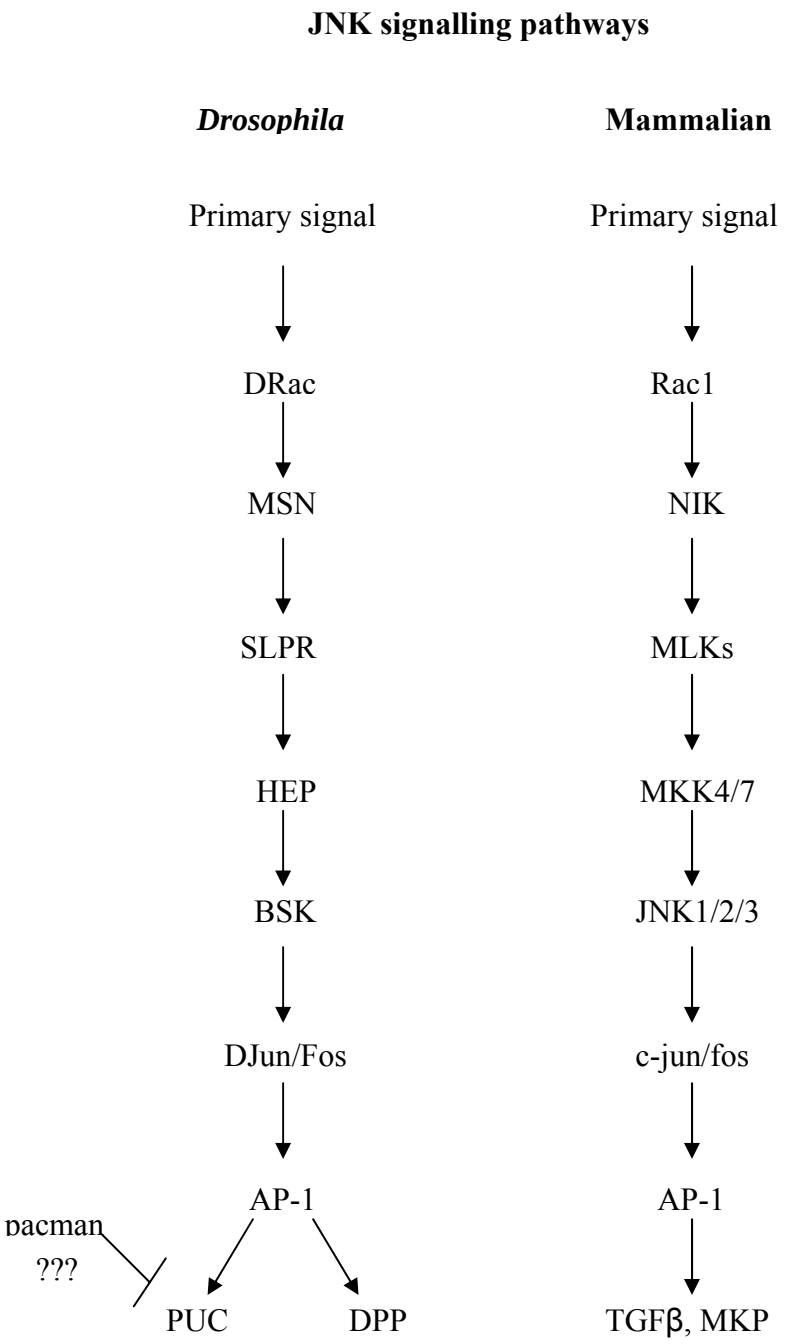

Figure 1.12: Diagram of the *Drosophila* and mammalian JNK signalling pathways adapted from Xia and Karin 2004. A possible role for *pacman* interacting with *puckered* has been added.

1.6.2 *Drosophila* JNK

In *Drosophila* there is only one JNK called DJNK which is encoded by the *basket* (*bsk*) gene (Figure 1.12) (Riesgo-Escovar et al. 1996; Goberdhan et al. 1998; Botella et al. 2001). DJNK has 70% amino acids identity to the mammalian homologue JNK with highest homology to JNK2 (Riesgo-Escovar et al. 1996). A downstream target of DJNK is the transcription factor DJUN, a homologue of the mammalian c-jun (Figure 1.12). DJUN along with another transcription factor DFOS control the localised expression of two target genes *decapentaplegic* (*dpp*) and *puckered* through AP-1 (adapter protein) activation (Figure 1.12)(Stronach 2005). Djun can form homodimers (jun:jun) or heterodimers with Dfos (jun:fos) encoded by *kayak.* Heterodimers are more stable and lead to AP-1 activation. *dpp* encodes the *Drosophila* homologue of TGFβ (transforming growth factor-β) a secreted morphogen needed during embryogenesis (Kockel et al. 2001; Ciapponi et al. 2002). *puc* encodes a MAPK phosphatase with dual specificity, which is a member of the VH-1 family. As well as being a target of the JNK signalling pathway *puckered* also acts in a negative feedback loop to downregulate the pathway through dephosphorylation of *bsk*. Therefore the expression levels of *dpp* and *puc* alter in relation to changes in *puc* levels (Ring et al. 1993; Martin-Blanco 1998).

1.6.3 Upstream activators

Upstream activators of DJNK include *hemipterous* (*hep*), *slipper* (*slpr*), *misshapen* (*msn*) and various small GTPases (Figure 1.12) (Stronach et al. 2002; Sathyanarayana et al. 2003). *bsk* is a downstream substrate of *hep*, which encodes a JNKK similar to the mammalian protein MKK7 (mouse JNK activator protein). MKK7 when expressed in *Drosophila* can rescue *hep* mutations (Glise et al. 1995; Zeitlinger et al. 1997; Harden 2002) . Connector of kinase to AP-1 (Cka) is thought to act as a scaffold protein bringing *hep*, *bsk*, *jun* and *fos* together to allow correct phosphorylation and the subsequent AP-1 activation (Harden 2002; Martin et al. 2002). *hep* is the substrate for an upstream JNKKK. The fly genome contains six JNKKKs that are capable of phosphorylating *hep*. They are *Pk92B*, *Tak1*, *Tak12*, *slpr*, *CG8789* and *Mekk1*. Each JNKKK links a distinct signal upstream to the signalling pathway downstream. These upstream signals are

produced at different stages of the *Drosophila* life cycle therefore each JNKKK is expressed at a different time (Stronach et al. 2002; Stronach 2005). For example *slpr* encodes a mixed lineage kinase MLK which is the main or only JNKKK acting during a morphological process called dorsal closure that occurs during embryogenesis (Stronach et al. 2002). *Tak1* and *Mekk1* on the other hand are not expressed during embryogenesis (Stronach 2005).

To increase specificity in the pathway even further, JNKKKs can be activated by small GTPases of the Ras superfamily, JNKKKKs like *msn* or adaptor proteins that link membrane receptors to the JNK pathway e.g. Traf (Figure 1.12). *Drosophila msn* a ste20- related kinase is a member of the germinal centre kinase (GCK) family (Su et al. 1998; Paricio et al. 1999; Su et al. 2000). Homologues include the mammalian NIK, a JNK activator and *C.elegans* mig-15. All family members contain an amino- terminal kinase domain and a carboxy-terminal regulatory domain. Both these domains are essential for JNK activation. *MSN* is required for JNK activation during dorsal closure (Su et al. 1998; Harden 2002).

1.6.4 Small GTPases

The Rho family of small GTPases are known to be involved in regulating changes in the actin cytoskeleton, focal adhesions and membrane protrusions as well as regulating upstream activators of the JNK and p38 signalling pathways (Noselli 1998). The Rho family are part of the larger Ras superfamily of GTPases. This family can be further divided into the subgroups Rac, cdc42 and Rho. The *Drosophila* genes for the Rac subgroup are *Drac1*, *Drac2* and *mtl*. The cdc42 *Drosophila* gene is *Dcdc42* and *RhoA/Rho1* is the *Drosophila* gene for the Rho subgroup. The roles of the Rho family proteins are being investigated through looking at dorsal closure during *Drosophila* development. *Drac1* makes the biggest contribution to dorsal closure, is it essential for formation and/or maintaining the cytoskeleton in the leading edge. *Drac1* has been shown to activate the JNK signalling cascade although the route by which it does is still unclear (Figure 1.12). It is possible that *Drac1* activates the cascade through direct contact with *slpr*, a JNKKK or contributes to the activation through *msn* indirectly. *Drac1* can not bind *MSN*. *Dcdc42* is thought to have two roles in dorsal closure, firstly to contribute to the formation of the leading edge cytoskeleton and

secondly and surprising to aid the breakdown of the leading edge cytoskeleton through *DPAK* at the end of dorsal closure. *RhoA* is not required for JNK activation during dorsal closure however a possible role in the assembly of the leading edge cytoskeleton at segment border cells has been suggested (Harden et al. 1996; Woolner et al. 2005).

1.7 Dorsal closure

Dorsal closure is a morphogenetic process that occurs during *Drosophila* embryogenesis. After gastrulation, when the germband retracts, a hole is left in the epidermis at the dorsal side of the embryo exposing the amnioserosa (Scuderi et al. 2005). The amnioserosa called the extraembryonic epithelium consists of approximately 200 flat cells that connect the dorsal and side of the embryo to the yolk sac (Lamka et al. 1999). DC is the process by which the hole is sealed (Figure 1.13A). Lateral epithelium from the two sides of the embryo spread over the amnioserosa and fuse at the dorsal midline (Figure 1.13B). Closure occurs through cell shape changes of the leading edge cells rather than proliferation of new cells and also through changes in shape of amnioserosal cells (Knust 1997; Jacinto et al. 2001; Martin et al. 2002).

Initiation of DC begins at stage 13 of embryogenesis about 11 hours after egg laying (Bownes 1975; Ransom 1982; Campos-Ortega 1985; Ashburner 1989). The primary signal that triggers DC is not yet known. It is more likely to be the combination of several cues that trigger initiation rather then one lone signal. Dorsalventral patterning of the lateral epithelial cells and forces generated by germband retraction are possible initiation cues (Kiehart et al. 2000; Ligoxygakis et al. 2003). These cues ultimately lead to changes in JNK signalling which in turn leads to upregulation of *puc* and *dpp* in the leading edge of the lateral epithelial. After initiation the cells of the leading edge, a single row of cells at the front of the lateral epithelial, start to elongate in a dorsalventral direction. It is followed by the stretching of more lateral cells behind the leading edge also in the dorsalventral direction. This stretching is driven by an actomyosin cable. The leading edge cells accumulate filamentous actin (F actin) and non muscle myosin heavy chain which form the actomyosin apparatus. As the actomyosin cable contracts the lateral epithelial spreads over the amnioserosa. The spreading of the

lateral epithelial is not uniform, the cells at the anterior and posterior ends begin to move together first. This movement is similar to drawing a purse string bag together therefore the force that drives this movement is often referred to as 'purse-string' activity. During this spreading filopodia and lamellipodia are seen protruding over the amnioserosa from the cells of the leading edge searching for the cells of the opposite leading edge (Jacinto et al. 2001; Harden 2002).

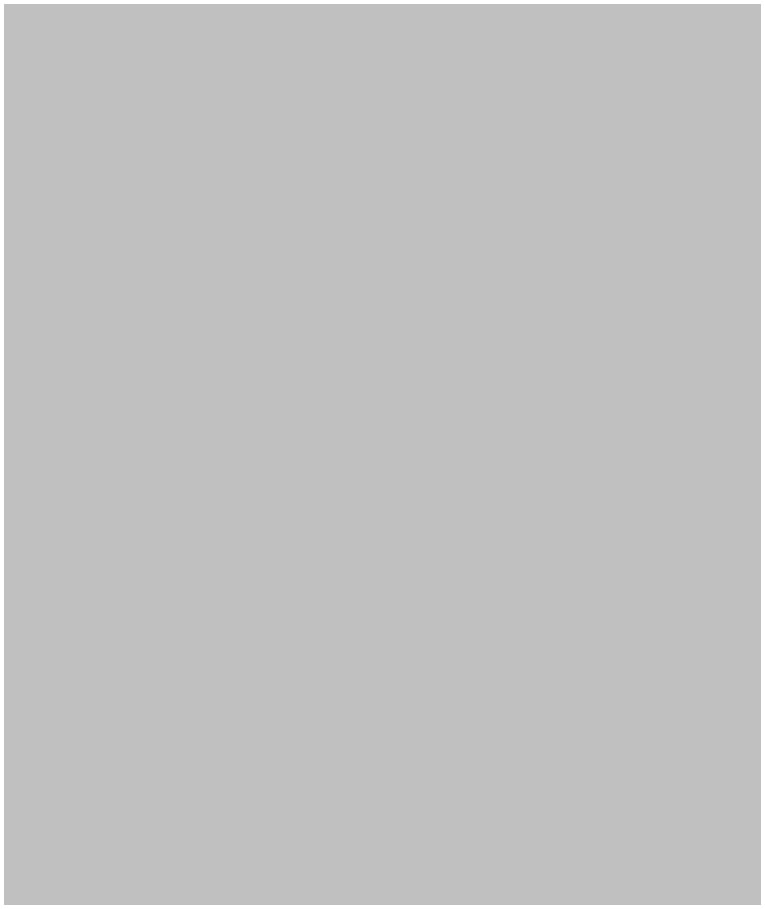

Figure 1.13: **A**: Diagram shows the dorsal hole in the *Drosophila* embryo after gastrulation and the embryo after the hole has closed. Diagram adapted from Goberdhan and Wilson 1998. **B**: Diagram shows a transverse section through the embryo during dorsal closure. The pale green cells are the amnioserosa and the darker green is the leading edge. Diagram adapted from Jacinto and Martin 2001.

1.7.1 Filopodia and lamellipodia

Filopodia are long thin bundles of parallel actin filaments that extend out from the cell surface. Lamellipodia are thin but broad actin filament projections at the edge of moving cells that are constantly changing shape. Once the moving cells of the leading edge are close enough for the filopodia protrusions to touch the zippering of the hole begins. Filopodia which are induced by *Dcdc42* play a key role in drawing the two edges together and ensuring correct cell matching so that when the hole is closed the correct segments from both sides of the embryo are aligned. In the absence of filopodia the opposing edges are misaligned (Jacinto et al. 2000). During the zippering stage, the filopodia interdigitate and then the opposite edges form mature adheren junctions (Jacinto et al. 2002; Martin et al. 2002).

1.7.2 The JNK signalling pathway and dorsal closure

As mentioned earlier the JNK signalling pathway is involved in regulating cell movements. A link between dorsal closure and the JNK signalling pathway has been established (Ring et al. 1993; Glise et al. 1995; Martin-Blanco 1998). Mutations in genes of the JNK signalling pathway lead to 'dorsal open' phenotypes, where the leading edges fail to close correctly and a hole is left in the dorsal side of the embryo. This suggests the JNK signalling pathway plays a central role in directing dorsal closure. During dorsal closure the JNK signalling pathway is upregulated in the leading edges and downregulated in the amnioserosa, resulting in localised expression of *puc* and *dpp* (Ring et al. 1993; Riesgo-Escovar et al. 1996; Reed et al. 2001). In one study using *thickveins* (*Tkv*) (the *dpp* receptor) mutants the leading edge elongates but the more lateral cells remain stationary. *dpp* appears to be required for elongation of the more lateral cells behind the leading edge cells (Glise et al. 1997). Puckered acts in a negative feedback loop downregulating the JNK signalling pathway through BSK. A possible role for Puckered would be to act as a brake at the end of dorsal closure (Ring et al. 1993; Martin-Blanco et al. 1998).

1.7.3 A possible role for *pacman* in the JNK signalling pathway

As mentioned earlier preliminary data suggests *pacman* mutant embryos have a dorsal closure defect (Grima et al. 2008). This is similar to these phenotypes seen in JNK signalling mutants (Zeitlinger et al. 1997; Martin-Blanco et al. 1998). These similar mutant phenotypes suggest a common role for the genes. The hypothesis that *pacman* interacts with the JNK signalling pathway possibly through *puckered* was suggested (Figure 1.12). If the hypothesis is true then *pacman* may also regulate other morphogenetic processes as the JNK signalling pathway does. The thorax closure defects shown earlier provide a strong argument that this is true (Grima 2002).

1.8 Thorax closure

Another example of cell sheet movement is the process of thorax closure (Figure 1.14). This occurs during *Drosophila* prepupal stages of metamorphosis when the two wing imaginal discs fuse and ultimately give rise to the adult thorax (Agnes et al. 1999; Martin-Blanco et al. 2000).

Like dorsal closure actin fibres accumulate along a row of margin cells between the columnar and peripodial epithelial. Another similarity between dorsal closure and thorax closure is the involvement of the JNK signalling pathway. *Dfos* and *puc* have been shown to be expressed in the stalk and peripodial membrane of the wing imaginal discs (Agnes et al. 1999; Zeitlinger et al. 1999). These two regions of the imaginal disc are thought to be the site at which the imaginal discs fuse together. Flies with homozygous mutations for *Dfos* or *hep* show a cleft at the dorsal midline of the thorax and bristles are abnormally parted (Zeitlinger et al. 1997; Agnes et al. 1999).

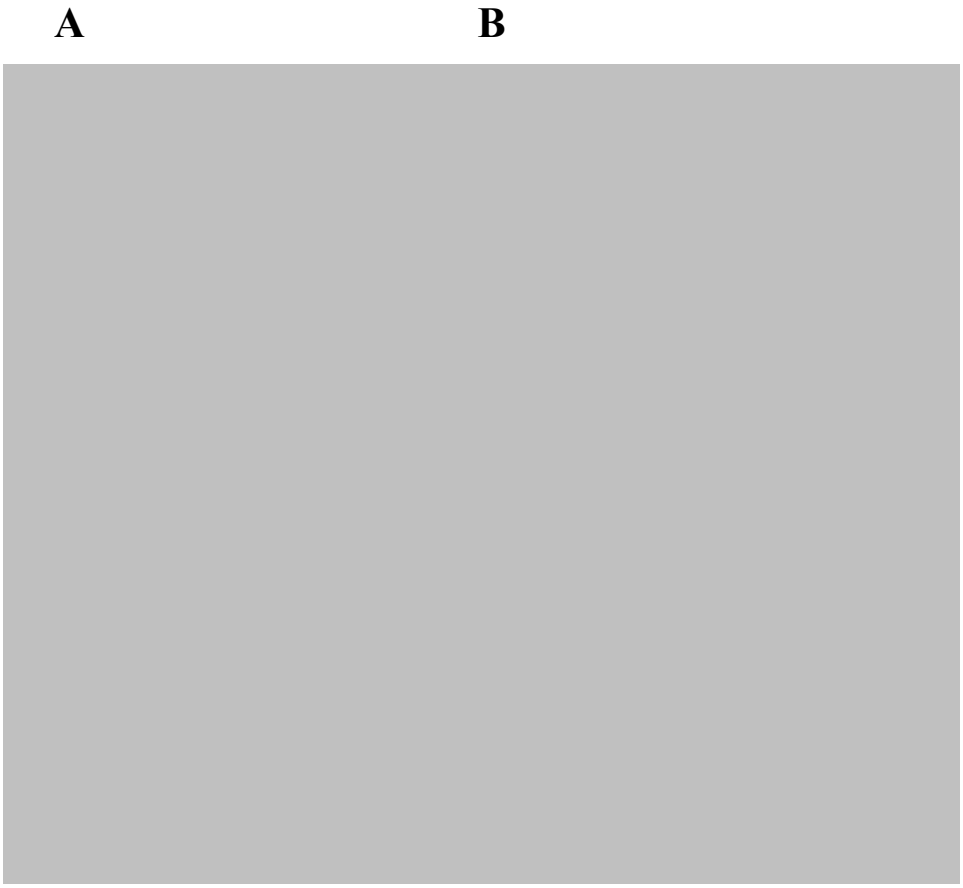

Figure 1.14: **A**: Diagram shows thorax closure during metamorphosis of *Drosophila*. Adapted from Zeitlinger and Bohmann 1999 **B**: A wing imaginal disc showing *pucLacZ* reporter expression (→) at the stalk and peripodial membrane border. Adapted from Agnes et al. 1999.

1.9 Wound healing in humans

The epithelial cell movements seen in wound healing are similar to natural tissue movements seen during development in many different species such as dorsal closure (Figure 1.15) and thorax closure in *Drosophila*, ventral enclosure in *C.elegans* and hind brain closure and neural tube formation in humans (Grose et al. 1999; Jacinto et al. 2001; Martin et al. 2004).

The skin acts as a protective barrier to the outside world. After an organism has received an injury it must rapidly re-epithelialize the wound to reduce the risk of infection and increase its chances of survival. In adult tissues, the wound is first temporarily repaired by a fibrin clot that consists of platelets embedded in a matrix of fibrin strands along with fibronectin and vitronectin. The clot has a dual function to stem the loss of blood from damaged blood vessels and to release cytokines and growth factors into the surrounding cells. These act as chemotactic signals that recruit inflammatory cells to the wound site. Neutrophils, that arrive within minutes of the injury, and macrophages clear the wound site of contaminating bacteria, cell and matrix debris by phagocytosis. Macrophages also amplify the earlier chemotactic signals by releasing more cytokines and growth factors (Martin 1997; Werner et al. 2003; Galko et al. 2004)

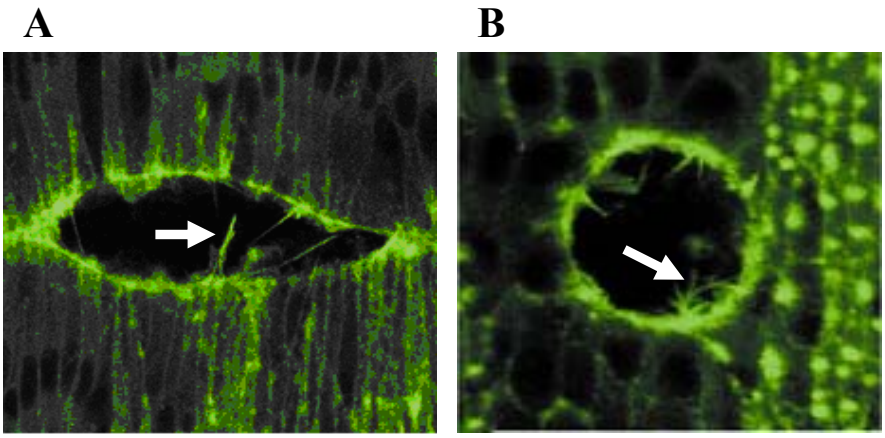

Figure 1.15: Parallels between *Drosophila* dorsal closure (A) and wound healing (B). Pictures adapted from Martin and Parkhurst 2004. Lamellipodia and filopodia (arrows) are seen extending from the leading edges of the two holes.

Adult skin comprises of an upper layer of keratinized stratified epidermis with an underlying thick layer of collagen rich dermal connective tissue (Figure 1.16). Wound healing is achieved through active movements of both layers. After the clot has formed there is a delay before the front few rows of keratinocytes, in the epidermal layer at the wound edges produce lamellipodia. Lamellipodia are thin but broad actin filament projections at the edge of moving cells that are constantly changing shape. They move the epidermis forward to cover the exposed connective tissue by altering its integrin binding. Further down fibroblasts and capillaries invade the connective tissue to form the granulation tissue. These fibroblasts when triggered by the growth factor TGF-β differentiate into myofibroblasts that can express α-smooth muscle actin which contracts and help to pull the wound edges together (Martin 1997; Jacinto et al. 2001). When lamellipodia from opposite sides of the wound are within touching distance the wound begins to seal. Wounds will normally heal in 1-2 weeks however the newly sealed epithelium is not perfect. There will be a visible scar present, which is the remains of the connective tissue. Epidermal appendages such as hair follicles or sweat glands that were damaged at the wound site will not be regenerated (Ramet et al. 2002; Galko et al. 2004).

1.9.1 Embryo wound healing

In contrast wound healing in embryos leaves no scar, they heal perfectly. This is very interesting especially since there is no inflammatory response in embryos to protect them from infection. This has become the focus of many studies; ultimately scientists want to know if adult tissue could be made to heal without leaving a scar. Over the past 15 years our knowledge of how cells move together to repair wounds has increased greatly mostly due to studies using model organisms. The mechanisms of wound healing seem to be evolutionally conserved so information gathered from model organisms can be related to humans. This could benefit many patients for example burns victims, chronic diabetes sufferers and post-surgery patients (McCluskey et al. 1995; Oehmichen 2004).

Figure 1.16: Diagram illustrating healing of a human skin wound with its fibrin clot and migrating epidermal cells. Picture adapted from Martin 1997. → shows the granulation tissue.

It is now believed that the inflammatory response in adult tissue is the cause of the scarring (Azouz et al. 2004). This is backed up by the fact that scars are first seen at the same foetal stage that the inflammatory response begins in embryos (Liechty et al. 2000). Mutant mice that are PU.1 null i.e. 'macrophageless' so they have no inflammatory response heal normally without scarring (Martin et al. 2003; Cooper et al. 2005). Therefore the inflammatory response is not essential for repair. It has been suggested that the level of growth factors such as TGF-β1 may affect the presence of a scar after wounding. As mentioned earlier the inflammatory cells recruit growth factors to the wound site so there are high levels of TGF- β1 at the wound sites of adult tissues. However it has been shown there are low levels of TGF- β1 at wound sites in embryos. This may be due to lack of inflammatory cells in embryos (Martin 1997; Martin et al. 2003; Redd et al. 2004). Antibodies that neutralise TGF- β1 are being considered as a way to reduce scarring (Wadman 2005).

Wound healing in embryos is rapid because it is driven by actin 'purse string' activity not lamellipodia. Therefore there is no time delay caused by altering integrin binding in the epidermal cells. An actomyosin cable forms at the leading edge cells around the wound within two minutes of wounding. The actomyosin apparatus consists of filamentous actin (F actin) and non muscle myosin heavy chains. As the actomyosin cable contracts the edges of the wound are drawn together bringing the attached basal lamina along too. This movement is similar to drawing a purse string bag together therefore the force that drives this movement is often referred to as 'purse-string' activity. Studies have shown that re-epithelialization fails when embryos are treated with cytochalasin D which blocks actin polymerisation. Therefore the actomyosin cable is essential for wound healing. When the wound edges are close together the cells at the leading edge produce filopodia protrusions that feel for the cells of the opposite edge. Filopodia are long thin bundles of parallel actin filaments that extend out from the cell surface. Once the moving cells of the leading edge are close enough for the filopodia protrusions to touch the zippering of the wound begins (Bement et al. 1999; Kiehart 1999; Altan et al. 2004; Martin et al. 2004).

Wound healing in embryos is not dependent on cell division; instead the wound is closed by a combination of cell shape changes and cell shuffling. In embryos as the wound closes the cells around the hole change shape and are forced out of the wound edge by the contractions of the actin cable. Hence the wound circumference gets smaller as the wound closes (Grose et al. 1999; Wood et al. 2002; Martin et al. 2004; Redd et al. 2004).

1.9.2 The role of the JNK signalling pathway in wound healing

Previous studies in both adult flies and larvae of *Drosophila* have shown that the JNK signalling pathway is involved in regulating wound healing of these tissues (Ramet et al. 2002; Galko et al. 2004). Ramet at al, 2002 used an enhancer trap fly line containing a *pucLacZ* fusion protein to determine *puc* expression by looking at β galactosidase staining. They found *puckered* gene expression was induced in epithelial cells at the leading edge of a wound (Ramet et al. 2002). This is similar to the expression patterns of *puc* during dorsal closure. They also determined that mutations in *kayak* (c-fos homologue) cause failure in wound healing and there is no *puc* expression in the cells of the leading edge of these mutants (Ramet et al. 2002). Galko et al, 2004 studied *puc* expression around the wounds of larvae using the same enhancer trap line. The β galactosidase staining and therefore the *puc* expression were seen in the nuclei of individual cells. This expression was present in a gradient emanating from the wound edge. The highest expression was seen in the cells of the leading edge and this decreased outwards to about a 5 cell diameter (Galko et al. 2004). The JNK signalling pathway is therefore activated after wounding and this pathway signals to the surrounding cells. Activation of the JNK signalling pathway leads to an increase in the expression of TGF-β which has been shown to have a role in cell movement and shape changes. Therefore it has been suggested the activation of the JNK signalling pathway after wounding induces the cells around the wound to begin changing shape and moving together to heal the wound (Sluss et al. 1996; Ramet et al. 2002; Bosch et al. 2005; Stramer et al. 2005).

1.10 A possible role for *pacman* in wound healing

As mentioned several time earlier *pacman* mutants have defects in both thorax closure and dorsal closure (Grima 2002; Grima et al. 2008). These defects suggest a role for *pacman* in regulating these events. Both these developmental processes involve cell shape changes and movements that are similar to those seen in ventral enclosure in *C.elegans*, hind brain closure and neural tube formation in humans and wound healing. Dorsal closure, thorax closure and wound healing are regulated by the JNK signalling pathway (Ring et al. 1993; Jacinto et al. 2001). Mutations in genes of the JNK signalling pathway lead to thorax and dorsal closure defects similar to those seen in *pacman* mutants (Agnes et al. 1999; Zeitlinger et al. 1999). It was therefore suggested that *pacman* may be interacting with the JNK signalling pathway to regulate both dorsal closure and thorax closure. Hence it makes sense that *pacman* also has a role in wound healing too.

1.11 The thesis aims

The aim of this project is to determine the role of *pacman,* a 5'-3' exoribonuclease, in wound healing of *Drosophila melanogaster*. The first part of the project is to determine whether *pacman* mutant flies show any wound healing phenotypes. As wound healing is regulated by the JNK signalling pathway, the hypothesis that *pacman* is interacting with this pathway specifically through *puckered* has been suggested. Therefore the next part of this project is to characterise the interactions between *pacman* and the JNK signalling pathway. Specific aims are to:

- Wound wild type control flies along with *pacman* mutant flies and those over expressing *pacman* with a scalpel on the abdomen and record their survival. This will determine whether mutations in *pacman* affect wound healing.

- In order to confirm any reduction in survival is due to a specific wound healing defect, the time at which the wild type and *pacman* mutant flies form a clot after wounding will be recorded.

- The affects of ageing and infection on the survival of wild type and *pacman* mutant flies after wounding will also be investigated.

- To determine whether *pacman* interacts with the JNK signalling pathway, *pacman* and *puckered* double mutant flies will be created.

- The survival of these double mutants after wounding will also be investigated.

- Using the *pucLacZ* reporter gene of the double mutant strain, β-galactosidase staining experiments will be performed to determine the affect of a *pacman* mutation on the JNK signalling pathway.

- Western Blotting experiments, Semi-quantitative PCR and Real-Time Quantitative PCR will be performed to quantify the changes in expression of the JNK signalling pathway in *pacman* mutant strains compared to the wild type control.

The results of these experiments will broaden our knowledge of *pacman's* role in wound healing through interactions with the JNK signalling pathway.

Chapter 2 Methods

2.1 Fly Strains

Strain Name	Genotype	Strain Information and Use	Originator
OregonR	wild type	Wild type control	David Ish-Horowicz
pcm^{3}	*pcm*^{3}/FM7c	*pacman* mutant strain: Survival Experiments	Dom Grima
pcm^{5}	*pcm*^{5}/FM7c	*pacman* mutant strain: Survival Experiments	Dom Grima
pcm^{6}	*pcm*^{6}/FM7c	*pacman* mutant strain: Survival Experiments	Dom Grima
SFN167	*pcm*^{3}/FM7i (actin-GFP)	*pacman* mutant strain with actin-GFP balancer for homozygous larvae identification: Ageing, Clotting and Infection Experiments	Melanie Sullivan
SFN164	*pcm*^{5}/FM7i (actin-GFP)	*pacman* mutant strain with actin-GFP balancer for homozygous larvae identification: Ageing, Clotting and Infection Experiments	Melanie Sullivan
SFN168	*pcm*^{6}/FM7i (actin-GFP)	*pacman* mutant strain with actin-GFP balancer for homozygous larvae identification: Ageing, Clotting and Infection Experiments	Melanie Sullivan

SFN203	*bsk*[2] cn[1] bw[1] sp[1]/CyO (actin-GFP)	*basket* mutant strain with actin-GFP balancer for homozygous larvae identification: Western Blotting Control	Melanie Sullivan
SFN209	+/Y ;; *puc*[A251]/TM6 TbSb	*puckered* mutant strain: β-galactosidase Staining control and Survival Experiments	Melanie Sullivan
SFN210	pcm^5/FM7i ;; *puc*[A251]/TM6 TbSb	*pacman*/*puckered* double mutant: β-galactosidase Staining Experiments and Survival Experiments	Melanie Sullivan
K2	P{Cas}hsK2/CyO	*pacman* overexpression strain: Survival Experiments	Kay Chong Wan

2.2 Fly husbandry

2.2.1 Fly food recipe

Recipe for 7 litres of fly food

Agar (GP)	81g
Baker's yeast	81g
Oatmeal	616g
Distilled H_2O	7000ml
Black treacle	410g
Propionic acid	40ml
Nipagin	1 spatula

The agar, baker's yeast, oatmeal and water were mixed together in a large saucepan then on a heat source brought to the boil while continuously stirring to avoid burning. This was then removed from heat and allowed to cool for 5 minutes. Next the treacle was added and the mixture was allowed to cool for a

further 10 minutes. Followed by the nipagin and propionic acid and stirred thoroughly. The food was poured in bottles/vials and covered in muslin to cool overnight. A thin layer of yeast pellets were sprinkled over the food and then foam bungs were used to cap the bottles/vials. These were stored at 4˚C until needed.

2.2.2 Apple/ grape juice plates

Agar	11g
Distilled H_2O	300ml
Sucrose	5g
Apple/grape Juice	50ml

The agar and water were mixed then heated to dissolve the agar. The sucrose and apple/grape juice was then added and reheated to dissolve all the sugar. This mixture was allowed to cool for 10 minutes and then poured into 2” plastic Petri dishes.

2.2.3 Stock maintenance

Flies were bred in bottles containing the above fly food at 25˚C and 19˚C. Every Friday new bottles for all strains were made. Bottles made within the last 2 weeks were kept for use and older ones were discarded. Crosses and virgin collections were stored in vials. These were changed each week and discarded after 2 weeks. Fly strain SFN210 was weak and prone to dying out suddenly so this stock was kept in both bottles and vials to prevent lose of the whole strain.

2.3 Virgin collection

Virgins were collected following the protocol outlined in (Ashburner 1989)

2.4 Larval Collection

2.4.1 Collection

For several experiments L3 stage larvae were required. During the L3 larval stage the larvae move out of the food and up the sides of their container in preparation for pupation. Using tweezers the L3 larvae were picked from the sides of the cultures and placed on grape juice plates ready for separating by genotype.

2.4.2 GFP actin cross

Homozygous pacman larvae are required for several experiments. Three new fly strains were created containing an actin-GFP balancer chromosome to allow distinction between the different genotypes. Cross is shown in Chapter 3 Figure 3.1. Typically 10 individual crosses were set up with at least 2 ♂and 2 virgin ♀ per vial but ideally 5 of each sex per vial depending on availability.

2.4.3 Fluorescence Collection

Using the Leica MZ16F microscope with a long pass- autofluorescence GFP filter, homozygous and heterozygous larvae can be differentiated.

pcm/FM7i → **Fluorescent** *pcm*/*pcm* → Non fluorescent

FM7i/Y → **Fluorescent** *pcm*/Y → Non fluorescent

2.5 Embryo Collection

2.5.1 Egg laying

To collect embryos, 2-3 bottles of the desired strain were tipped into 1 empty bottle (no fly food). An apple/grape juice plate containing a small blob of fresh yeast paste on its centre was taped over the mouth of the bottle and labeled with the date and time. The flies were left to lay at 25˚C for 3 hours then they were removed and embryos were aged for the appropriate time.

2.5.2 Dechorionation

To remove the outer chorion (egg envelope), embryos were transferred to egg baskets (2" Petri dish with their bottom removed and replaced with nitex membrane glued using chloroform) and soaked in bleach for several mins then washed with water.

2.5.3 Fluorescence Collection

Using the same procedure as 2.4.3, embryos were separated into different genotypes. To collect the embryos required, 10µl of methanol was added to a microcentrifuge tube. A paintbrush was used to lift the embryos from the egg basket and dispersed into the methanol. Finally methanol was removed using a Pasteur pipette and samples were stored at -70˚C.

2.6 Survival Experiments

Approximately twenty 3-5 day old ♀ flies for each strain were collected and anaesthetized using CO_2. Half the flies for each strain were wounded using a scalpel on the ventral side of the abdomen, being careful not to cut into underlying tissue. Wounded flies were then placed in food vials and allowed to recover. Unwounded flies were placed into a separate vial. Flies that did not wake up after wounding were discarded. The number of flies surviving was then recorded every

3 hours e.g. 9am, 12am, 3 pm and 6pm. This was repeated everyday until all mutant wounded flies were dead.

2.7 Clotting Experiments

Approximately five 3-5 day old ♀ flies for each strain were collected. Flies were wounded on the abdomen as above. The time at which the clot starts to form around the wound was recorded.

2.8 Infection experiments

Thirty 3-5 day old ♀ flies for each strain were collected. Ten flies were left unwounded, ten were wounded as above with sterile scalpel blades and ten were wounded with blades dipped in *E.coli* strain DH1 pellet. The number of flies surviving was then recorded every 3 hours e.g. 9am, 12am, 3 pm and 6pm. This was repeated everyday until all mutant wounded flies were dead.

2.8.1 Preparation of the *E.coli* strain DH1

DH1 was prepared from a frozen sample kept at -70˚C. This was spread on agar plates and left overnight in a 37˚C incubator. The next day individual colonies (normally 4) were picked and added to separate 5ml universals of LB broth. The universal lids were sellotaped on. The universals were then placed in an orbital shaker (Heidolph Unimax 1010) overnight at 37˚C. The following day 2ml of the *E.coli*/broth mix was added to an eppendorf and spun down in a centrifuge at 14000 rpm for 2 mins to produce a pellet of *E.coli*. The supernatant was discarded. This was repeated until all the mix had been spun down and pelleted. The *E.coli* pellets and agar plates were stored at 4˚C and reused for up to 1 week.

2.9 Ageing experiments

Wild type bottles were emptied and then flies were collected at the required number of days. Approximately twenty ♀ flies for each age 9, 7, 5, 3 and 1 day old flies were collected and anaesthetized using CO_2. Half the flies for each strain were wounded using a scalpel on the ventral side of the abdomen, being careful not to cut into underlying tissue. Wounded flies were then placed in food vials and allowed to recover. Unwounded flies were placed into a separate vial. Flies that did not wake up after wounding were discarded. The number of flies surviving was then recorded every 3 hours e.g. 9am, 12am, 3 pm and 6pm. This was repeated everyday until all wounded flies were dead.

2.10 Creating new strains through genetic crosses

Firstly new bottle of the required strains were set up at 25˚C on Friday to allow virgins to hatch 10 days later on Monday. Parents were tipped off after 5 days. Virgin females and males of the appropriate genotypes were collected and stored at 19˚C. On the following Friday the crosses were set up using 5♀ and 5♂ (at least 3♀ and 3♂) per vial. Up to 10 vials were prepared. Parents were tipped off after 5 days. 10 days later on the Monday either the stable stock (Finished outcome) or the next lot of require genotypes will be hatching. Subsequent crosses were repeated as above.

2.11 β Galactosidase Staining Experiments

2.11.1 Fly Staining Experiments

Approximately ten 3-5 day old ♀ flies for each strain were collected. Half the flies were wounded using the Method in 2.6. Flies were then allowed to heal for 4 hours (Galko et al. 2004). All flies were fixed on ice in 1ml 1xPBS with 100µl of glutaraldehyde for 10 mins. Flies were then washed on ice in approximately 600µl of 1xPBS for 10 mins. This was repeated 4/5 times. Flies were added to 1 ml of pre-incubated staining solution (Recipe: see 2.11.5) to which 50µl of 0.8% Xgal (Sigma) was added and incubated at 37˚C for the desired time e.g. 5 hours.

Staining solution was washed away with 1xPBS and this was repeated 4/5 times. Flies were photographed on a Nikon SMZ800 microscope using a Nikon DN100 camera.

2.11.2 Larval Staining Experiments

Approximately ten L3 larvae for each strain were collected. Half the larvae were wounded on the ventral side between denticle belts A3 and A4 using a 0.1mm needle. Larvae were allowed to heal for 4 hours (Galko et al. 2004). After healing larvae were dissected open in chilled Ringer's solution (Recipe: 2.11.5) on the opposite side from the wound to allow staining solution through the cuticle. Larvae were fixed, washed and stained as above. They were then incubated at 37˚C overnight then wash as above. Before mounting, larvae insides are scraped out to leave only the cuticle. Cuticles are mounted on a coverslip in 20% ethanol in glycerol. Samples were photographed on a Zeiss Axioplan microscope.

2.11.3 Wing imaginal disc staining experiments

L3 larvae were dissected in Ringer's solution using size 5 Dumont forceps (Agar). The larvae were held at approximately one third of its length from the interior end and at the base of the mouth hooks with forceps and then pulled apart. This allows the imaginal discs along with the brain to be removed intact. The imaginal discs were then collected and fixed on ice in 1ml 1xPBS with 100µl of glutaraldehyde for 10 minutes as before. The fix was removed using a 200µl pipette and 600µl of clean PBS is used for washing. This is repeated 4/5 times as above. After washing, the imaginal discs were transferred to 1ml of pre-incubated staining solution using a specially designed mouth pipette. This was followed by adding 50µl of 0.8% Xgal and then incubation at 37˚C overnight. The next day the staining solution was washed using 600µl of PBS 4/5 times. Imaginal discs were mounted on a coverslip in 20% ethanol in glycerol. Samples were photographed on a Zeiss Axioplan microscope.

2.11.4 Designing the imaginal disc mouth pipette

During the imaginal disc staining experiments the imaginal discs were moved between 1xPBS and the glutaraldehyde fix. The discs are very small so a specially adapted mouth pipette was created. The tip of a Pasteur pipette was heated in a Bunsen burner and then stretched to narrow the width of the pipette. This stretched region was then snapped to produce a new narrow tip slightly larger than the width of a wing imaginal disc. The new adapted Pastuer pipette was inserted into one end of some plastic tubing approximately 1m in length. In the other end a 1000µl pipette tip was inserted as a mouth piece. Imaginal discs were sucked into the Pastuer pipette using the mouth piece. To disperse the discs the user blew through the mouth piece.

2.11.5 Staining Reagents

Staining Solution (Ramet et al. 2002):

$K_4Fe(CN)_6$	5mM
$K_3Fe(CN)_6$	5mM
NaCl	150mM
$MgCl_2$	1mM
NaH_2PO_4	10mM
Na_2HPO_4	10mM
Xgal	0.4% (added later)

Wash:

1xPBS 1 sachet of PBS (Sigma) in 1000ml

Fix:

100µl of Glutaraldehyde (Sigma) in 1000µl of 1xPBS

Mount:

20% ethanol in glycerol

Ringer's Solution:

NaCl	9mM
KCl	3mM
$CaCl_2$	3mM

pH 7.2

2.12 Western Blotting

2.12.1 Larval preparation

Ten homozygous (or heterozygous) L3 larvae for each strain were collected and snap frozen. Samples were homogenized in eppendorf tubes using Sigma polypropylene pestles in 150ml of 2xSDS loading buffer then placed at 100˚C for 7 mins. They were then centrifuged for 5 mins at top speed. The supernatant was transferred into a new eppendorf tube. The new tube was then centrifuged for a further 5 mins at top speed. The supernatant was removed to a new tube.

2.12.2 Western Technique

10µl of the above samples were loaded on a Nupage 10% Bis Tris precast gel (Invitrogen) along with 1 lane containing Pre-stained protein marker. Unused sample was stored at -70˚C. The gel was run in Running Buffer for 1hour 15mins at 150V (Invitrogen X Cell Surelock Novex Mini Cell). Proteins were transferred to Millipore Immobilon P Transfer Membrane for 1hour at 100V (400mA) in Transfer Buffer (BioRad Mini Transblot Cell). The membrane was washed on a rocking platform (Heidolph Unimax 1010) in Blocking Solution for 1hour. The membrane was washed briefly in 1x PBS-Tween protein side up then probed for protein using the primary antibody (Dilutions: 2.12.4) overnight on the rocking platform at 4˚C. This was followed by 4x 10minute washes of the membrane on the rocker in Wash Buffer. The membrane was then probed with the secondary antibody (Dilutions: 2.12.4) for 1 hour at room temperature on the rocker. This was again followed by 4x 10 minute washes with Wash Buffer then 2x 10 minute washes with 1x PBS-Tween. The membrane was covered with the ECL Chemiluminescent solutions for 1 minute and exposed to Super RX Fuji Medical

X ray Film for the desired time then developed using the x-ograph Compact X2 machine.

2.12.3 Western reagents

2x SDS loading buffer:

Tris pH6.8	250mM
SDS	4%
Glycerol	10%
Bromophenol blue	0.006%
Mercaptoethanol	2% (added later)
Protease cocktail inhibitors	2% (added later)

1x Running Buffer:

Dilute 20x Tris acetate in distilled H_20

Transfer Buffer:

Tris	25mM
Glycine	190mM
Methanol	20%

Blocking Solution:

10x PBS	1 Sachet
Tween 20	0.1%
Marvel	5%

Wash Buffer:

5x PBS	1 Sachet
Tween 20	0.5%
Marvel	2.5%

1x PBS-Tween:

1x PBS	1 Sachet
Tween 20	1%

Chemiluminescent Solutions:

ECL Chemiluminescent kit (Amersham)

ECL Advance Chemiluminescent kit (Amersham)

2.12.4 Antibody Dilutions

Pacman Antibody:

1˚ Ab	P3 Anti Pacman (Newbury Lab) 1:2000
2˚ Ab	Monoclonal Anti Rabbit Peroxidase (Sigma) 1:80000
Exposure time	5-15mins ECL

Actin Antibody:

1˚ Ab	Monoclonal Mouse Anti Clone 4 (ICN Biomed) 1:10000
2˚ Ab	Goat Anti Mouse Peroxidase (Sigma) 1:80000
Exposure Time	1-5mins ECL, 1-10secs ECL Advance

Sigma β-Galactosidase Antibody:

1˚ Ab	Monoclonal Anti β-Galactosidase Mouse 1:5000, 1:1000
2˚ Ab	Goat Anti Mouse Peroxidase (Sigma) 1:80000
Exposure Time	1sec ECL Advance

Cell Signalling Technology c-Jun Antibodies:

c-Jun

1˚ Ab	Monoclonal c-Jun Rabbit 1:5000
2˚ Ab	Monoclonal Anti Rabbit Peroxidase 1:80000
Exposure Time	40-55mins ECL

pJun73

1˚ Ab	Polyclonal Phospho c-Jun (Ser73) Rabbit 1:5000
2˚ Ab	Monoclonal Anti Rabbit Peroxidase 1:80000
Exposure Time	40mins ECL

pJun63

1˚ Ab	Polyclonal Phospho c-Jun (Ser63) 1:5000
2˚ Ab	Monoclonal Anti Rabbit Peroxidase 1:80000
Exposure Time	40mins ECL

JNK Antibodies:

Santa Cruz Biotechnology JNK

1˚ Ab	Phospho JNK Mouse Monoclonal IgG 1:1000
2˚ Ab	Goat Anti Mouse Peroxidase 1:5000

Dilutions from ((Ramet et al. 2002))

Exposure Time	10-15mins ECL

Cell Signalling Technology JNK

1˚ Ab	Phospho SAPK/JNK Monoclonal Rabbit 1:1000
2˚ Ab	Monoclonal Anti Rabbit Peroxidase 1:80000
Exposure Time	27-30mins ECL

Promega JNK

1˚ Ab	Anti Active JNK pAntibody 1:1000
2˚ Ab	Monoclonal Anti Rabbit Peroxidase 1:80000
Exposure Time	27-45mins ECL

Sigma JNK

1˚ Ab	Monoclonal Anti JNK mouse IgG 1:5000
2˚ Ab	Goat Anti Mouse Peroxidase 1:80000
Exposure Time	30secs-1min ECL Advance

2.13 Polymerase Chain Reaction

All PCR reactions were carried out on a Gene Amp PCR system 2400 (Perkin Elmer) Thermal cycler. Details of specific programs used are outlined below.

2.13.1 PCR to check for the presence of the *pacman* mutations in the new *pacman* mutant flies carrying the FM7i GFP-Actin balancer chromosome

DNA preparation:
10 homozygous ♀ flies for each *pacman* mutant (round white eyes) and the wild type control were collected in eppendorf tubes then snap frozen in liquid nitrogen. The flies were homogenised in 200µl of REB lysis Buffer using Sigma polypropylene pestles. Another 300µl of REB lysis Buffer was then added to each eppendorf tube.

Phenol/Chloroform Purification:
500µl of Phenol/Chloroform was added to each tube and mixed by shaking for 2 minutes. This was centrifuged at 14.5 rpm for 5 minutes. As much of the top clear layer as possible is removed and transferred to a new eppendorf tube being careful to avoid the surface layer and the interface of fatty tissue. This new solution is made up to 500µl using RNase free water. Then another 500µl of Phenol/Chloroform are added, centrifuged for 5 minutes and the top layer removed. This is repeated until the interface layer has become clear. The extraction is repeated one final time with only Chloroform.

Ethanol Precipitation:
The top layer from the Chloroform extraction is removed and transferred to a new eppendorf tube. 1ml of Absolute Ethanol and 40µl of 3M Sodium Acetate is added to the eppendorf tube. The tubes are shaken well and the DNA becomes visible (white, Stringy). These are then centrifuged for 10 minutes at 14.5 rpm. A pellet will be visible at the bottom of the eppendorf tube. As much ethanol as possible is removed. Another 1ml of Absolute Ethanol is added and centrifuged

for 5 minutes at 14.5 rpm. Again the ethanol is removed. The pellet is left to dry under a lamp for 10 minutes. The pellet was then resuspended in 50µl RNase free water and can be stored at -20˚C.

RNase Treatment:

RNase free water	15µl
NEB2 Buffer	5µl
1mg/ml RNase A (Ambion)	5µl
DNA sample	25µl

These above solutions were mixed well in a fresh eppendorf tube and incubated at 37˚C for 30 minutes. 300µl of RNase free water was added to each tube and another Phenol/Chloroform extraction was performed as before. 1ml of Absolute Ethanol and 40µl of 3M Sodium Acetate was added and mixed by inversion. The tubes were placed at -70˚C for 20 minutes then centrifuged for 10 minutes at 14.5 rpm. The ethanol was removed without disturbing the pellet and another 1ml of ethanol was added. This was centrifuged for 5 minutes at 14.5 rpm and the ethanol removed as before. The pellet was left to dry under a lamp and then 50µl of RNase free water was used to resuspend the pellet. These tubes can be stored at -20˚C.

PCR reaction using Jes1 and Big1 primers (Sequences in appendices):

1x Master Mix 50µl reaction

RNase free water	29.5µl
10x PCR Buffer (Qiagen)	5µl
Qiagen Q Solution	10µl
1nM dNTPs	1µl
Jes1/Big1 primer mix	2µl
Taq DNA Polymerase (Qiagen)	0.5µl
DNA template sample	2µl

The above master mix was prepared on ice and mixed thoroughly. This was aliquoted (48µl) into individual PCR tubes for each DNA sample. The 2µl DNA

sample was added to each tube. The tubes were then placed in the PCR thermal cycler which was programmed with the following thermal cycle.

Initial Denaturation	5mins	94˚C	
Denaturation	30secs	94˚C	40 cycles
Annealing	1min	55˚C	
Extension	4mins	65˚C	
Final Extension	5mins	65˚C	

Gel Electrophoresis:

10µl of each PCR reactions plus 2µl of Loading Buffer (Sigma) were loaded on a 2% agarose (Sigma) gel (5µl Ethidium Bromide per 50ml) in 1x TBE Buffer along with 10µl of 1kb ladder (Biolabs). The gel was run at 60V for 2 hours. The bands were visualised using a GeneFlash Syngene Bio Imaging.

2.13.2 PCR to check for the presence of the *pacman* mutations in the new *pacman* and *puckered* double mutant flies

Single-fly DNA preparation:

Individual flies were collected in an eppendorf tube and placed at -20˚C for 10 minutes. The following fly genotypes were collected: pcm^{5}/Y ;; puc^{A251}/ TM6 TbSb, FM7i/Y ;; puc^{A251}/TM6 TbSb and wild type flies. Each fly was mashed using a pipette tip in 50µl of Squishing Buffer for 5-10 seconds. The tubes were incubated at 37˚C for 30 minutes then 95˚C for 1-2 minutes to deactivate the Proteinase K. This mixture can be added directly to the PCR reaction as DNA template. Store at -20˚C.

Squishing Buffer:

Tris-Cl pH 8.2	10nM
EDTA	1nM
NaCl	25nM
Proteinase K	200µg/ml

PCR reaction using *pcm*^{5} primers (Sequences in appendices):

1x Master Mix 50µl reaction	
RNase free water	40.9µl
10x Red Taq Buffer (Sigma)	5µl
Primer *pcm*^{5} Forward	0.1µl
Primer *pcm*^{5} Reverse	0.1µl
dNTPs 25nM	0.4µl
Red Taq Polymerase (Sig	2.5µl
DNA Template	1µl

The above master mix was prepared on ice and mixed thoroughly. This was aliquoted (49µl) into individual PCR tubes for each DNA sample. The 1µl DNA sample was added to each tube. The tubes were then placed in the PCR thermal cycler which was programmed with the following thermal cycle.

Initial Denaturation	2mins	95˚C	
Denaturation	30secs	95˚C	35 cycles
Annealing	30secs	55˚C	
Extension	1min 30secs	72˚C	
Final Extension	7mins	72˚C	

Gel Electrophoresis:

10µl of each PCR reactions plus 2µl of Loading Buffer (Sigma) were loaded on a 2% agarose (Sigma) gel (5µl Ethidium Bromide per 50ml) in 1x TBE Buffer along with 10µl of 1kb ladder. The gel was run at 100V for 45 minutes. The bands were visualised using a Gel Doc UV transluminator.

2.13.3 PCR to check for the presence of the *pucLacZ* reporter gene in the new *pacman* and *puckered* double mutant flies

DNA samples were prepared using the single-fly DNA preparation technique outlined in Method 2.13.2. The PCR reaction master mix and the thermal cycle were also the same as Method 2.13.2. Primers used were mellacZ forward and mellacZ reverse whose sequences are outlined in the appendices.

Gel Electrophoresis:

10µl of each PCR reactions plus 2µl of Loading Buffer (Sigma) were loaded on a 1% agarose (Sigma) gel (5µl Ethidium Bromide per 50ml) in 1x TBE Buffer along with 10µl of 1kb ladder. The gel was run at 100V for 45 minutes. The bands were visualised using a GeneFlash Syngene Bio Imaging.

2.14 Semi-Quantitative PCR

2.14.1 RNA extraction

10 homozygous L3 larvae were collected for the *pacman* mutants and the wild type control, placed in an eppendorf and snap frozen in liquid nitrogen. RNA extraction was performed using the Qiagen RNeasy Mini Kit and QIAshredder according to the manufacture's instructions (Page 39-44 starting at step 3b). 600µl of RLT Buffer is added to the starting tissue. The RNA is eluted in 100µl of RNase free water. Samples stored at -70˚C.

2.14.2 DNase Treatment of RNA samples

The RNA samples were DNase treated with the Ambion DNA-free kit following the manufacture's instructions (Page 6-7). Samples stored at -70˚C.

2.14.3 Reverse Transcription of total RNA to cDNA

cDNA was produced from the DNase treated total RNA using the Invitrogen Superscript III Reverse Transcriptase. The maximum volume of RNA 8µl is added to each reaction per PCR tube.

RNA	8µl
Oligo DT	1µl (Invitrogen)
RetroScript dNTPs	4µl (Ambion)

This mixture was heated at 65˚C for 5 minutes then incubated on ice for at least 1 minute. The contents were centrifuged briefly then the following was added:

5x First Strand Buffer	4µl
0.1M DTT	1µl
RNase Out recombinant RNase Inhibitor	1µl (Promega)
Superscript III Reverse Transcriptase	1µl

The mixture was spin down to collect the contents then incubated in the Gene Amp PCR system 2400 (Perkin Elmer) Thermal cycler at 50˚C for 1hour followed by 70˚C for 15minutes. Samples stored at -70˚C.

2.14.4 Semi-quantitative PCR reaction using *puckered* and *rp49* primer sets

Primer sequences are outlined in the appendices.

Primer Master Mix:

RNase free water	30µl
*puc*F	5µl
*puc*R	5µl
*rp49*F	5µl
*rp49*R	5µl

1x Master Mix 50µl Reaction:

RNase free water	39.1µl
10x PCR Buffer	5µl
25mM dNTP mix	0.4µl
Jumpstart Red Taq	2.5µl (Sigma)
Primer master Mix	1µl
cDNA	2µl

The mixture was gently mixed. PCR reaction carried out in the Gene Amp PCR system 2400 (Perkin Elmer) Thermal cycler.

Initial Denaturation	1min	94˚C	
Denaturation	30secs	94˚C	35 cycles
Annealing	30secs	55˚C	
Extension	1min	72˚C	
Final Extension	1min	72˚C	

2.14.5 Removal of the PCR reactions samples for quantification

Samples were removed from the reaction at the end of every second cycle starting from as early as Cycle 14. Sample sizes varied from 6µl to 16µl. These samples (5µl or 15µl) were run on a 1.5% agarose gel at 100V for 45 minutes. There was no need for Loading Buffer as the Jumpstart Red Taq Polymerase already contains this. The bands were visualised on the GeneFlash Syngene Bio Imaging.

2.15 Real-Time Two Step Quantitative PCR

RNA extraction and DNase treatment for Real-Time Two Step Quantitative PCR was the same as Methods 2.14.1 and 2.14.2 for Semi-Quantitative PCR.

2.15.1 Quantification of RNA samples

1µl of RNA is diluted in 49µl of RNase free water. The absorbance of the samples was measured in a spectrophotometer at 260nm (A260) and 280nm (A280). The purity of the RNA can be estimated from the A260/A280 ratio. A ratio of 1.5-2 is fairly pure. The concentration of the RNA sample was given as µg/ml. This concentration for each RNA sample was used to calculate the volume to be added to each Reverse Transcriptase reaction. Therefore producing approximately equal concentrations of cDNA in each sample after the Reverse Transcriptase.

2.15.2 Reverse Transcription of total RNA to cDNA

Different volumes of RNA sample were added to each reaction for each strain. Roughly 1.5µg of total RNA was present in each Reverse Transcription reaction. Reverse Transcription performed using Invitrogen Superscript III Reverse Transcriptase according to Method 2.14.3.

2.15.3 Real-Time Quantitative PCR reaction using *puckered* and *rp49* primer sets

Real-Time Quantitative PCR was performed using the Qiagen Quantitect SYBR Green PCR kit following the manufacture's instructions (Page 11-13)

1x Master Mix 50µl Reaction:

SYBR Green	25µl
Primer mix	5µl
cDNA	2µl
RNase free water	18µl

3µM stock concentrations of primer mix were produced. Primer sequences are outlined in the appendices. The standard dilutions were produced by a serial dilution from wild type cDNA. Master Mixes for each primer set were produced in two separate eppendorf tubes. These were firstly aliquoted in individual tubes for each different set of triplicates then aliquoted again into 3 separate PCR tubes for each triplicate. PCR reaction carried out in the Stratagene Mx3000P Quantitative PCR machine.

Initial Denaturation	15mins	95˚C	
Denaturation	15secs	94˚C	45 cycles
Annealing	30secs	55˚C	
Extension	30secs	72˚C	
Disassociation	1min	95˚C	
	30secs	55˚C	
	30secs	95˚C	

2.15.4 PCR to check for the *puckered* and *rp49* primers used for Real-Time Two Step Quantitative PCR

Wild type cDNA sample produced by Method 2.15.2 was used to check the *puckered* and *rp49* primers only produce one PCR product each. Primer sequences are outlined in appendices.

1x Master Mix 50µl Reaction:

RNase free water	39.1µl
10x PCR Buffer	5µl
25mM dNTP mix	0.4µl
Taq Polymerase	2.5µl
Primer mix	1µl
cDNA	2µl

PCR carried out in the Gene Amp PCR system 2400 (Perkin Elmer) Thermal cycler.

Initial Denaturation	5mins	94˚C	
Denaturation	30secs	94˚C	40 cycles
Annealing	1min	56˚C	
Extension	30secs	65˚C	
Final Extension	5mins	65˚C	

Gel Electrophoresis:

10µl of each PCR reactions plus 2µl of Loading Buffer (Sigma) were loaded on a 1.5% agarose (Sigma) gel (5µl Ethidium Bromide per 50ml) in 1x TBE Buffer along with 10µl of 100bp ladder. The gel was run at 100V for 45 minutes. The bands were visualised using a GeneFlash Syngene Bio Imaging.

2.15.5 Primer Matrix

A primer matrix was performed to optimize the concentrations used for each primer forward and reverse within the primer set. This was performed following the instructions in the appendix of the Stratagene manual: Introduction to Quantitative PCR (Stratagene 2006). 50nM, 100nM, 300nM, 600nM and 900nM concentrations of forward and reverse primers were tested against each other for both *puckered* and *rp49* primer sets. The primer concentration combination that gave the lowest Ct value was selected for each primer set.

Chapter 3 Pacman affects survival after wounding

The aim of this thesis is to characterize the role *pacman* may play in regulating wound healing and determine whether this is due to interactions with the JNK signalling pathway which is known to mediate wound healing and epithelial cell sheet movements (Martin-Blanco et al. 1998; Agnes et al. 1999; Noselli et al. 1999). Previous studies have shown that *pacman* mutants have a defect in thorax closure during larval development (Grima 2002). These *pacman* mutant thorax phenotypes are similar to those seem in flies who are mutant for a gene of the JNK signalling pathway (Figure 1.10) (Agnes et al. 1999; Zeitlinger et al. 1999; Martin-Blanco et al. 2000). Therefore *pacman* may interact with the JNK signalling pathway to regulate cell sheeting sealing processes such as thorax closure, dorsal closure and wound healing. The starting hypothesis is that this interaction with the JNK signalling pathway may be through the degradation of the *puckered* mRNA by Pacman (Figure 1.12). This chapter focuses on determining whether mutations in the *pacman* gene lead to defects in wound healing. Subsequent chapters focus on characterizing the interaction between *pacman* and the JNK pathway.

3.1 Confirmation of mutations in the *pacman* gene.

In order to determine the function of the *Drosophila* gene *pacman* in wound healing, it was necessary to create mutants. This was previously accomplished in our lab by Dr Dom Grima using P-element excision. A P-element 3' downstream of *pacman* was excised causing deletions of the *pacman* gene at the 3' end. The P-element EP(x)1526 was 485 bp from the 3' terminus of the *pacman* coding sequence. The transposition of EP(X)1526 involved several crosses, the first of which created offspring flies carrying transposase as well as the P-element insertion. The germline of the male offspring possessed the transposition events. These males were individually mated to females with the FM7c balancer. This

cross produced females with the FM7c balancer and the transposed P-element but no transposase. This would prevent any further recombination in the resultant offspring. Lastly these females were individually mated with FM7c/Y males to maintain the mutant line. This project involves 3 of those mutant deletion lines known as pcm^3, pcm^5 and pcm^6. These mutant alleles were originally balanced over FM7c, a female sterile X chromosome with a co-dominant Bar marker, to allow the individual genotypes to be separated. However this balancer did not allow for characterisation of the larvae into separate genotypes. Since several of the experiments in thesis focus around larvae, a new strain of *pcm* mutant balanced over FM7i were created. The FM7i balancer contains sequences encoding Green Fluorescent Protein (GFP) fused to the actin promoter. When present in the genotype this actin-GFP fusion causes the flies/larvae to glow green under fluorescent light. Therefore using the new strains it was possible to pick *pcm* homozygous larvae for the experiments because these genotypes contain no FM7i balancer and do not glow under the fluorescent light. The schematic of this cross is shown in Figure 3.1 and Section 2.4.2 of the methods outlines the steps taken to achieve this. Method 2.4.3 demonstrates the phenotypes of each genotype of the FM7i cross.

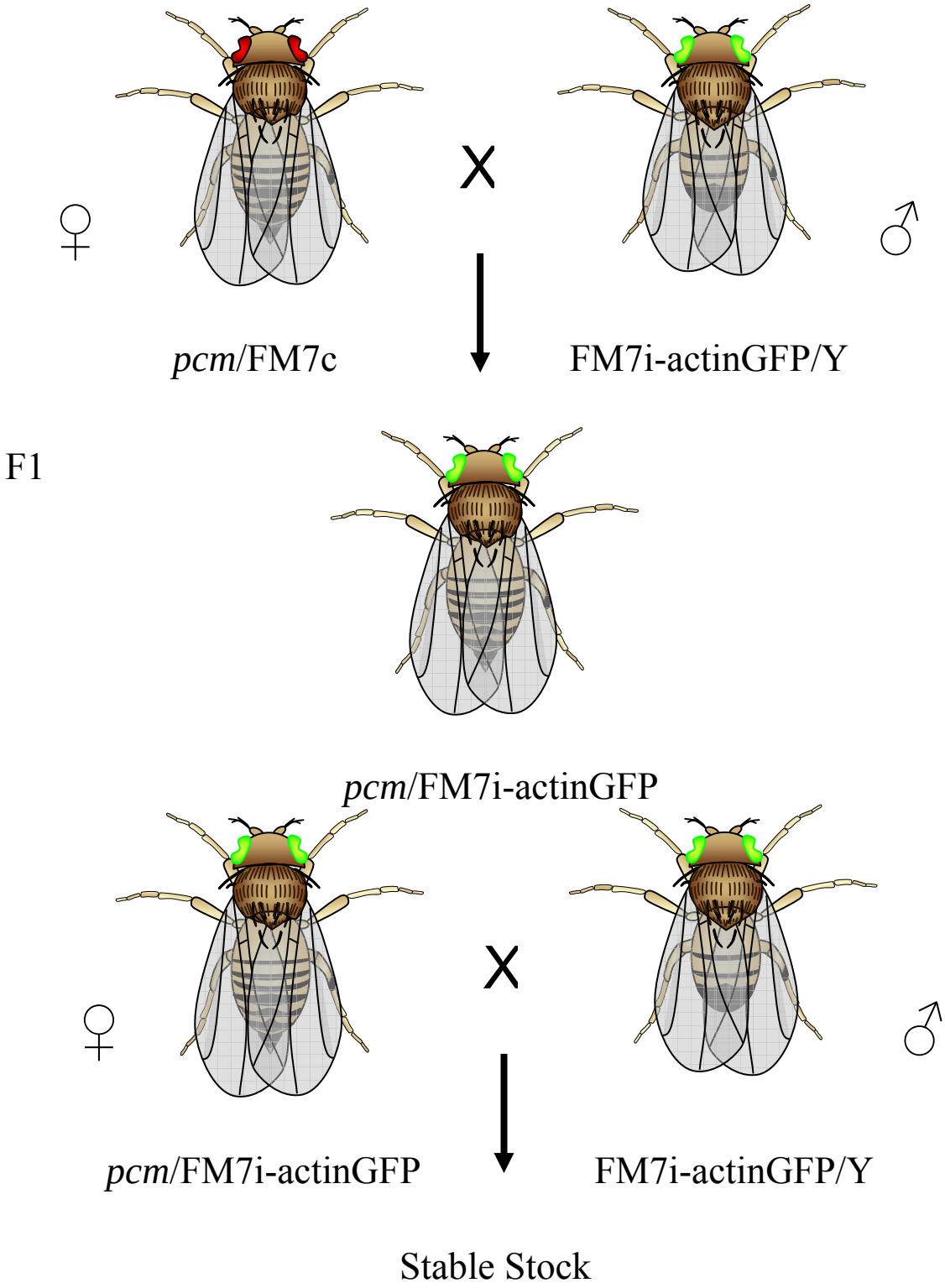

Figure 3.1: Schematic of the cross to replace FM7c balancer with FM7i-actinGFP. The green eyes symbolize the flies carrying the FM7i balancer. *pcm* represents any *pacman* mutation.

To confirm that these new mutants (from now on referred to as *pcm*^{3}, *pcm*^{5}, and *pcm*^{6}) still contained the *pcm* deletions, PCR was performed using primers on either side of the deletion. These amplify the 3' region of *pcm* from exon 8 to exon 11 and extend downstream past the location of the original P-element insertion. Figure 3.2 shows the locations of the Jes1 and Big1 primers and the deleted regions for each mutant. The sequences of these primers (Jes1 and Big1) are shown in Appendix 1. The wild type (OregonR) amplicon is 3324bp in length. The amplicon sizes for *pcm*^{3}, *pcm*^{5} and *pcm*^{6} are 1803bp, 2808bp and 1540bp respectively (Figure 3.3). Therefore the size of the deletion in *pcm*^{3} is 1521bp, for *pcm*^{5} it is 516bp and lastly for *pcm*^{6} 1784bp. These results show *pcm*^{5} has the smallest deletion and *pcm*^{6} the largest; this is consistent with previous research in the Newbury group. Therefore these new strains still contain the *pacman* deletions.

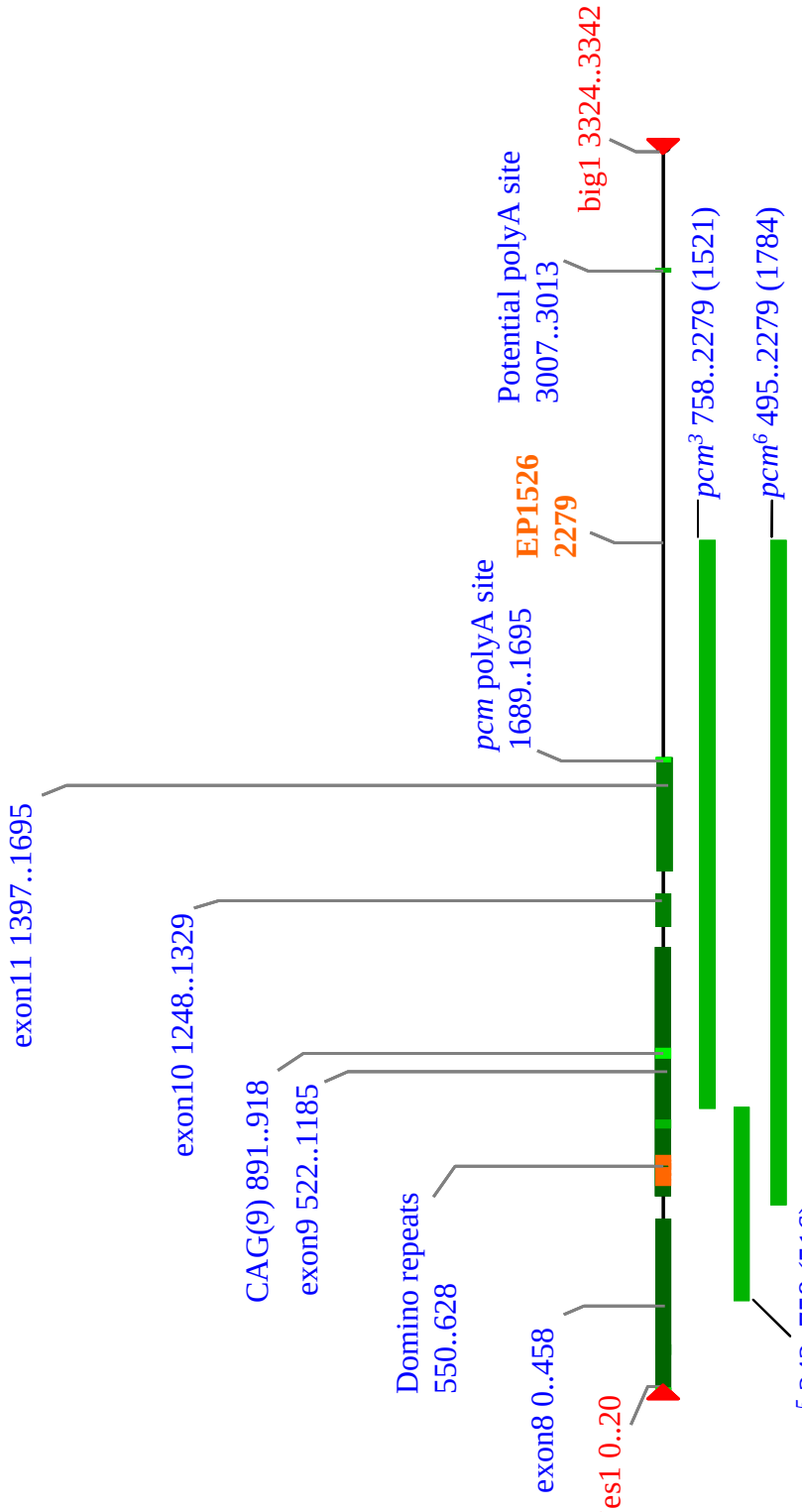

Figure 3.2: Diagram showing the 3' end of the *pacman* gene showing the intron/exon structure as well as the site of the transposon used to make the *pacman* mutations (EP1526). Exons are marked by dark green boxes and deletions are marked in light green. Jes1 and Big1 primer locations are given by red arrows (Grima, 2002).

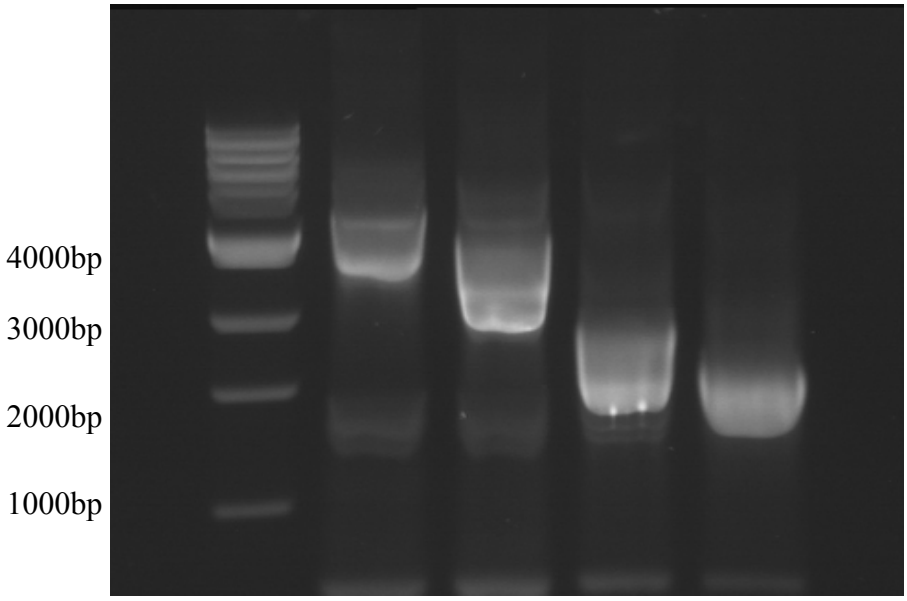

Figure 3.3: PCR to determine whether the *pacman* mutants still contain the *pacman* deletions. Sizes of fragments expected are 2808bp, 1803bp and 1540bp for pcm^5, pcm^3 and pcm^6 alleles respectively. Marker used is 1kb ladder.

3.2 Survival experiments

As mentioned earlier in the introduction adult *pcm* mutants show a thorax closure defect. These thorax defects are similar to those seen in JNK signalling mutants. Previous studies have linked the JNK signalling pathway to several morphogenetic processes during development such as *Drosophila* dorsal closure and thorax closure as well as wounding healing which involves similar cell movements. A hypothesis linking the JNK signalling pathway and *pacman* was proposed due to the similarities of the thorax defects seem in both sets of mutants. This hypothesis suggests that *pacman* regulates the JNK signalling pathway through interactions with *puckered* possibly by degradation of its mRNA (Figure 1.12). Since the JNK signalling pathway mediates wound healing, this directed the Newbury group to investigate a possible role for *pacman* in wound healing through its interactions with the JNK signalling pathway.

The first experiment was to determine whether homozygous *pcm* mutants survive as well as wild type flies after wounding. These survival experiments involved wounding the flies on the abdomen and then recording the number of flies still alive at particular time points. This was performed at two temperatures 25˚C and 19˚C because our *pcm* mutants are temperature sensitive in that the phenotypes are more severe when flies are raised at lower temperatures. Female flies were used as they are larger and easier to wound on the abdomen. Flies between 3 and 5 days old were also selected for use since Elizabeth King, a summer student in the Newbury lab had shown that the age of the fly affects survival after wounding, Experimental methods outlined in Method 2.6. Briefly, the method involved anaesthetising female flies with CO_2 and then making a small incision on the ventral side of the abdomen using a small scalpel blade (Figure 3.4). Care was taken not to cut into the underlying tissue. This method was found to be most reproducible; other wounding methods such as using a small pair of dissecting scissors (Ramet et al. 2002) were tried but found to be less successful. Practice sessions were undertaken in order to perfect the wounding technique prior to the actual experiments. After wounding, the flies were placed in a food vial to recover. Flies that did not wake up were discarded. Less than 2% of all flies wounded failed to recover.

Figure 3.4: Wounding of a wild type fly on the abdomen with a scalpel. Picture taken by Chris Jones.

Figure 3.5 shows the combined survival data for each *pacman* mutant compared to the wild type control for both temperatures (19˚C pcm^3 n = 4, x = 40, pcm^5 n = 6, x = 40 and pcm^6 n = 4, x = 40)(25˚C pcm^3 n = 3, x = 40, pcm^5 n = 5, x = 40 and pcm^6 n = 4, x = 40 where n represents total number of experiments and x represents the total number of flies used). The average percentage of survival for each time point is shown. The error bars represent the standard error between the experiments at each time point. For the unwounded flies these error bars tend to be small showing that this pattern of survival is frequent. At later time points the survival of the unwounded flies appears to be more variable producing larger error bars. This is consistent with survival in nature i.e. survival of the fittest. Older flies are more fragile resulting in the possibility of damaged wings and a tendency to get stuck in their food causing death. This is investigated later in the thesis during the ageing experiments. The error bars of the wounded flies are larger, this may suggest there is some variability in the wound technique even though great care was taken to treat each sample the same. A more consistent wound procedure may involve an automated device such as a laser wounding.

As expected for both wild type and mutant flies, unwounded flies survive longer than wounded flies. For each *pcm* mutant the wounded flies survive less well than the wild type wounded flies. In the case of pcm^3 and pcm^5 the error bars appear to show a small difference in survival of the unwounded wild type flies compared to the unwounded mutants. This suggests *pacman* alleles pcm^3 and pcm^5 confer a disadvantage to survival even before other factors such as inflicting wounds are taken into account. However the difference in survival between the wounded mutant flies and the wounded control appears to be greater which may suggest an additional phenotype i.e. defective wound healing caused by this mutation.

Looking at the graphs as a whole the decrease in survival of the wounded *pacman* mutants compared to the wounded wild type flies appears to be more prominent at 19˚C. The error bars at this temperature show a larger significant difference in survival between the wounded mutants and wounded wild type flies than at 25˚C. This is certainly the case for pcm^5 and pcm^6 however for pcm^3 there does not appear to be a significant difference in survival between the mutant and the control at time points 48 and 72 hours.

A clot forms over exposed tissue after wounding to prevent loss of blood (hemolymph) and bacteria entering the wound, causing infection. Normally the clot begins to form around 20-30 minutes after wounding (Ramet et al. 2002; Galko et al. 2004). All of the graphs show no significant difference in survival between the wounded wild type and wounded mutant flies at either temperature before 3 hours. Therefore it is unlikely that *pacman* mutations cause a defect in clot formation resulting in the reduced survival seen. This will be discussed in greater detail later in this chapter during the clotting experiments.

Previous studies by Ramet et al and Galko et al have shown that *Drosophila* wounds heal within 24 hours of the wound infliction. At 19˚C there is a significant difference in survival between each wounded *pacman* mutant and the wounded wild type flies at the 24 hour time point. At 25˚C this is also true for the survival of pcm^3 and pcm^5 wounded flies. Survival of the wounded pcm^6 flies does not appear to be significantly different from the survival of the wounded wild type flies suggesting pcm^6 allele is the mildest for this phenotype. These results are consistent with earlier studies by Dr Dom Grima showing *pacman* mutants are temperature sensitive and that mutant phenotypes are more severe at lower temperatures (Grima 2002).

Once again, when comparing the survival of wounded flies with the unwounded flies the significant differences of the wounded flies (at the 24 hour time point) are greater than the significant differences seen at the same time point for the unwounded flies. This additional reduction in survival seen in the wounded mutant flies is likely to be due to a defect in wound healing which should be complete by the 24 hours. Mutations in *pacman* may result in failure of wound healing at the later stages such as the final sealing of the epithelial tissues since earlier time points show no significant difference in survival between the wounded mutant and wild type flies.

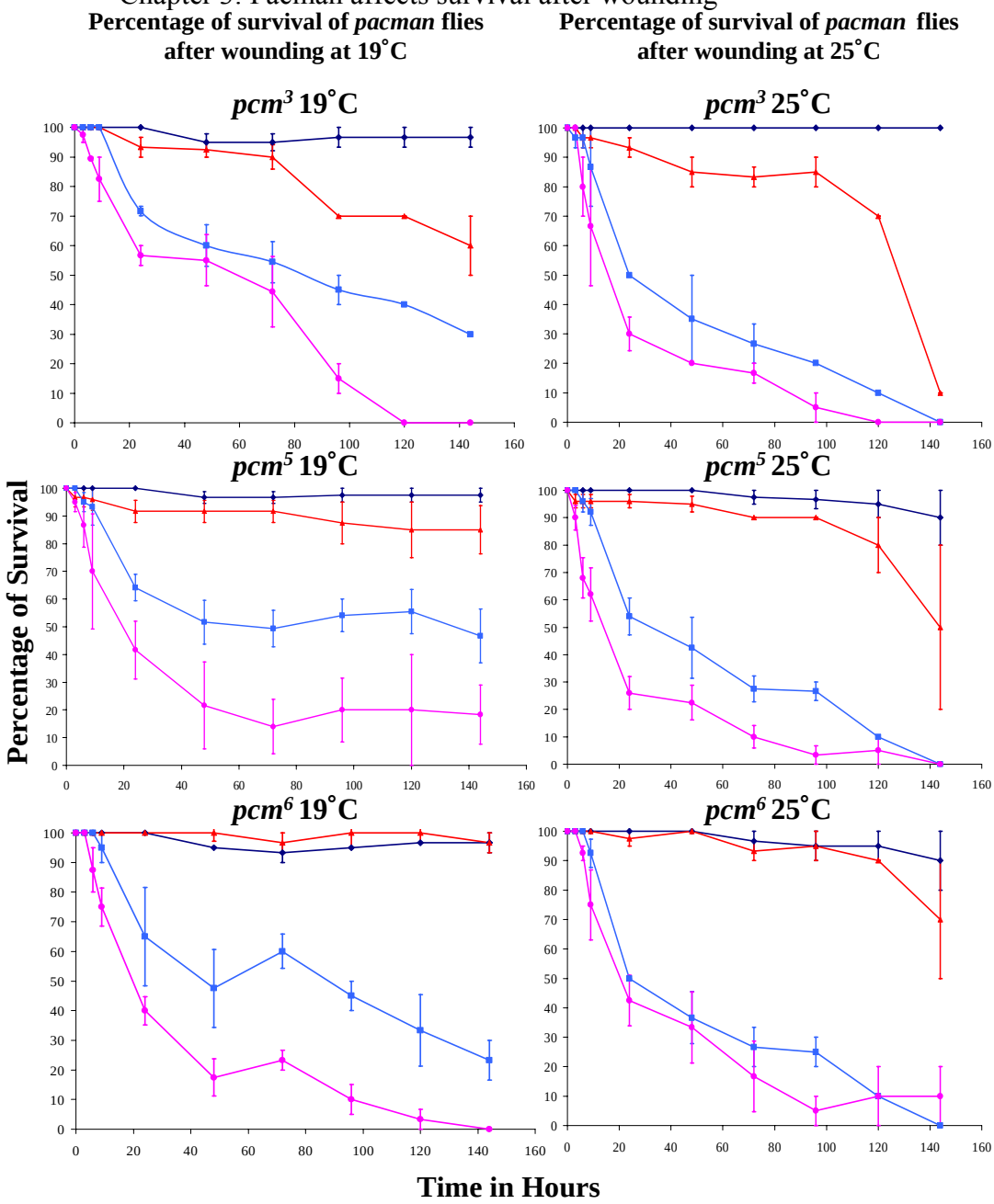

Figure 3.5: The combined survival data for each *pacman* mutant compared to the wild type control for both temperatures (19˚C pcm^3 n = 4, x = 40, pcm^5 n = 6, x = 40 and pcm^6 n = 4, x = 40)(25˚C pcm^3 n = 3, x = 40, pcm^5 n = 5, x = 40 and pcm^6 n = 4, x = 40). The average percentage of survival for each time point is shown. The error bars represent the standard error between the experiments at each time point. Key: W.T. unwounded, W.T. wounded, *pcm* unwounded and *pcm* wounded.

To analyse the data further the average half lives of the wounded flies were calculated. This is the time at which 50% of the flies have died. This data is displayed as histograms in Figure 3.6. At 19˚C the standard errors show there is a significant difference between the half life survival times of the wild type control flies compared to the three mutant *pcm* strains. At 25˚C there is a similar trend of half life survival. There appears to be significant difference between the half life survival times of the wild type control and pcm^3 and pcm^5 mutant flies. However there is no significant difference between half life survival times of the wild type and pcm^6 mutant flies. Again this highlights the temperature sensitivity of the *pacman* mutants showing pcm^6 is the mildest allele and therefore has the least severe wound healing phenotype.

At 25˚C the half lives for all three mutants are around 20 hours after wounding. It is interesting that nearly half the flies are dead around the time at which wound healing should be complete. If mutations in *pacman* prevent completion of wound healing this may account for the high mortality seen at this time point. At 19˚C the half lives are slightly higher between 20 and 40 hours after wounding. *Drosophila* development is known to slow down at lower temperatures. The initial increase in survival of the *pacman* mutants seen at this temperature compared to their survival at 25˚C may be explained if wound healing progresses slower at 19˚C. Therefore the mutants do not die until the later stages of wound healing which may occur several hours after those at 25˚C.

These results are consistent with the previous survival analysis (Figure 3.5) and support the hypothesis that *pacman* mutations cause a wound healing defect which results in reduced survival after wounding. A possible role for Pacman during wound healing may be through interactions with the JNK signalling pathway which has been shown to mediate wound healing (Ramet et al. 2002).

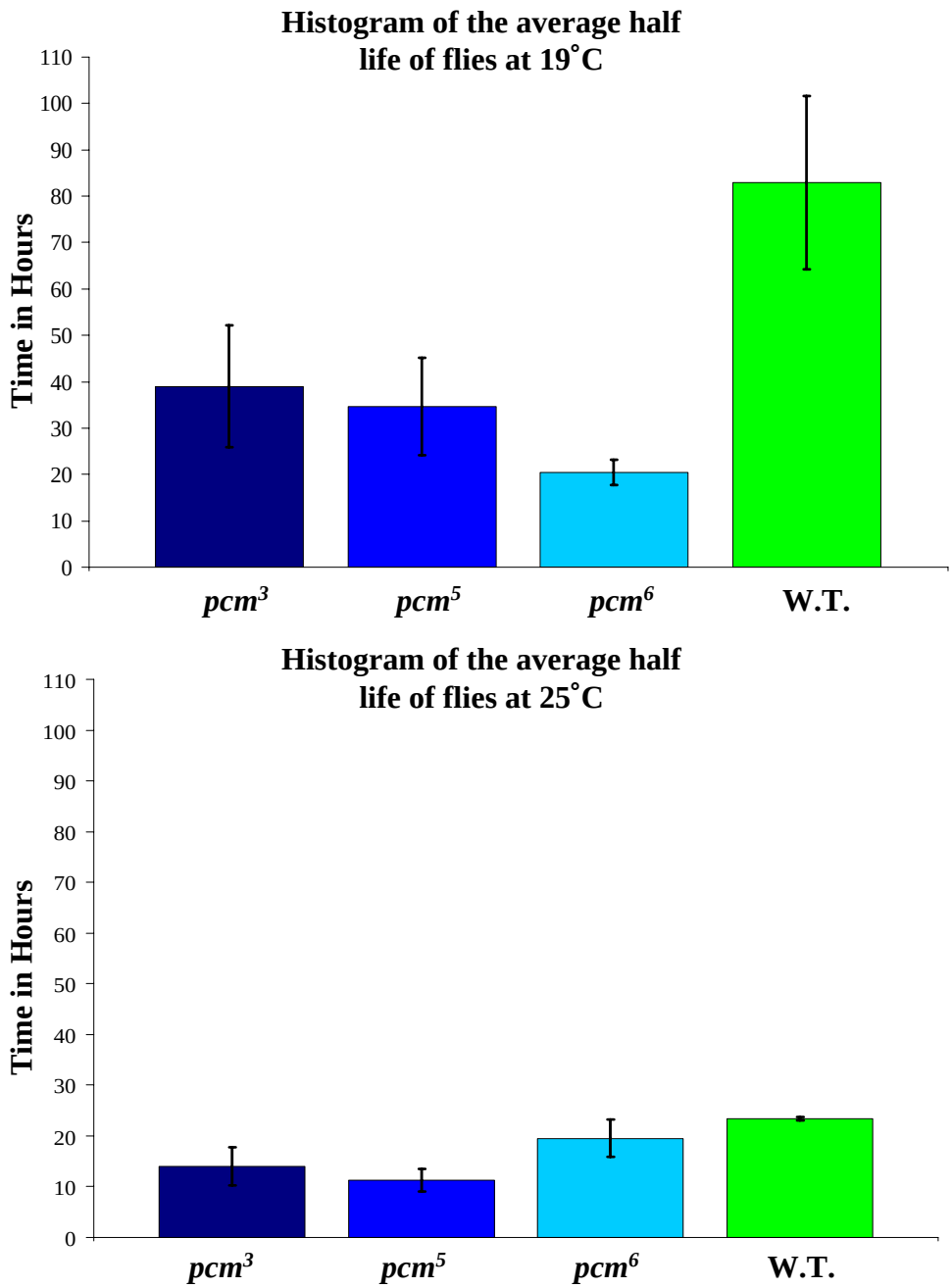

Figure 3.6: Histograms showing the average half life of survival of flies after wounding at both 19˚C and 25˚C temperatures. Error bars represent the standard error. (19˚C *pcm*^{3} n = 4, x = 40, *pcm*^{5} n = 6, x = 40 and *pcm*^{6} n = 4, x = 40)(25˚C *pcm*^{3} n = 3, x = 40, *pcm*^{5} n = 5, x = 40 and *pcm*^{6} n = 4, x = 40)

3.3 Survival of flies over-expressing *pacman* after wounding

It is now known that deletions in the *pacman* gene can lead to reduced survival of these mutant flies after wounding in comparison to wild type flies survival after wounding. Would overexpression of *pacman* have an effect on survival of these flies? Since mutations in *pacman* resulted in lower survival after wounding, presumably because the epithelial sheet sealing process is compromised, could increased levels of *pacman* promote wound healing. Would an increase in *pacman* expression lead to more rapid wound healing? To test this, a strain that expresses an extra copy of *pacman* cDNA under the control of a leaky heat shock promoter was used. This stock was constructed by Kay Wan, who generated a transgenic fly stock expressing a cDNA copy of *pacman* on chromosome 2 under the control of the heat-shock promoter. Kay showed that *pacman* was over-expressed in these flies both at the RNA and protein level. She also showed that expression of *pacman* cDNA was leaky in that it expressed low levels of Pacman at 25˚C without heat-shock and that this expression rescued the phenotypes of the *pacman* mutant even without heat-shock (Wan 2003). Survival experiments as outlined in Section 3.2 were undertaken using homozygous K2, P{Cas}hsK2/ P{Cas}hsK2 (ectopically expressing Pacman) and wild type flies at 25˚C. The survival of the wounded flies in previous experiments was shown to be variable. This was possibly due to an inconsistent wounding technique. In order to reduce the variability, the survival experiment technique was adapted. Fly stocks used for these survival experiments were grown in uncrowded cultures therefore these flies will be bigger and healthier. Hopefully this means any reduction or increase in survival seen for these flies will be due to the infliction of a wound rather than outside influences.

Figure 3.7 shows the combined data for all the *pacman* overexpression survival experiments at 25˚C (n = 12, x = 40). The average percentage of survival for each time point is shown. The error bars represent the standard error between the experiments at each time point. As seen in the previous survival experiments with *pcm* deletion mutants, the unwounded flies survive better than the wounded flies for both strains. There appears to be little or no difference in survival between the

unwounded wild type control and unwounded *pacman* overexpression flies across the time points. There is no significant difference in survival between the wounded *pacman* overexpression and wildtype flies before 3 hours which is consistent with the *pacman* mutant survival experiments. Therefore it was unlikely the reduced survival of the *pacman* overexpression wounded flies is due to a clotting defect. At 24 hours the time at which *Drosophila* wound healing should be complete there is a small but significant difference between the survival of *pacman* overexpression wounded flies and the survival of the wounded wild type flies. This data suggests that overexpression of *pacman* does not promote rapid wound healing and is instead detrimental to survival after wounding.

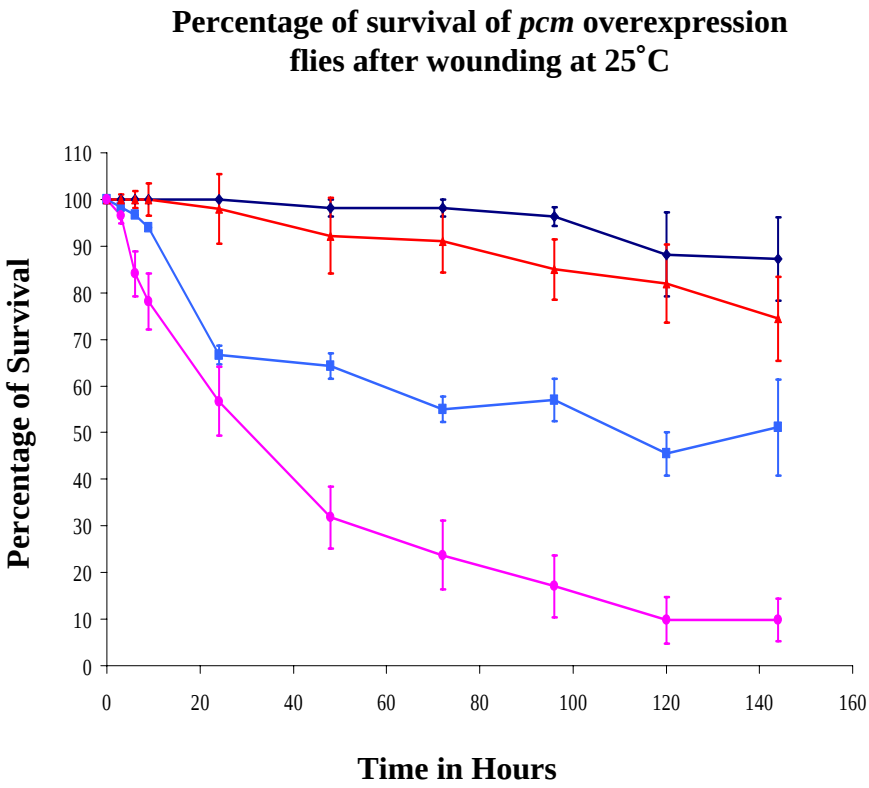

Figure 3.7: The combined data for all the *pacman* overexpression survival experiments compared against wild type survival at 25˚C (n = 12, x = 40). The average percentage of survival for each time point is shown. The error bars represent the standard error between the experiments at each time point.. Key: W.T. unwounded, W.T. wounded, *pcm* overexpression unwounded and *pcm* overexpression wounded.

The average survival half lives after wounding were calculated for *pacman* overexpression and wild type flies and displayed in the histograms in Figure 3.8. The standard errors show that there is a significant difference between the survival of wild type flies and the *pacman* overexpression flies. These flies do not survive as well as the wild type flies after wounding. These results are consistent with those seen in the survival graphs in Figure 3.7 that overexpression of *pacman* reduces survival after wounding.

Interestingly during these survival experiments the time at which half of the wild type and *pacman* overexpression wounded flies are dead is several hours later than the half lives of the flies wounded in the previous experiments. This could be due to the use of flies taken from uncrowded cultures. In this case their survival may not be hindered by external factors such as fly size to wound ratio and general health.

These survival experiments have shown that overexpression of *pacman* also results in a significant reduction in survival of these flies after wounding. When these results are combined with the previous survival experiments of Section 3.2 they suggest that only the correct amount of *pacman* expression, no more or no less will allow successful wound healing in *Drosophila*.

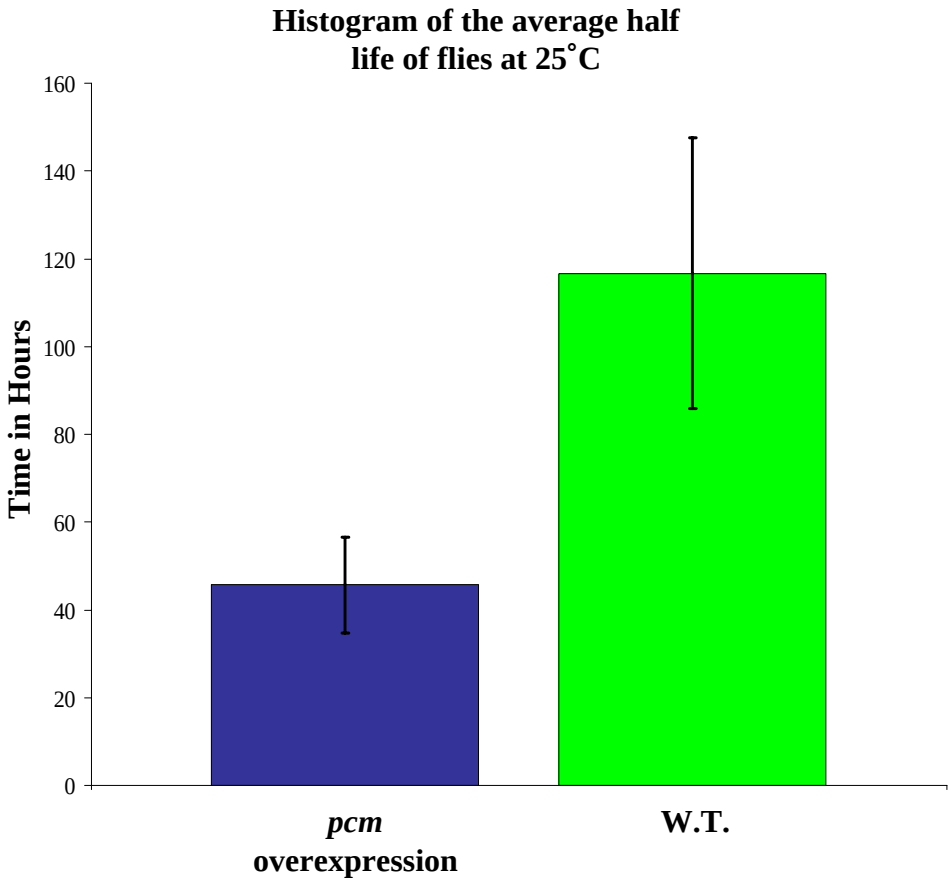

Figure 3.8: Average half lives for overexpression of *pacman* survival compared to wild type survival at 25˚C. Error bars represent the standard errors. (n = 12, x = 40)

3.4 Ageing experiments

There are several previous studies that have shown a link between reduced wound healing ability and increasing age (DeVeale et al. 2004; Gosain et al. 2004). As previously mentioned in section 3.2, Elizabeth King, a summer student in the Newbury lab, had briefly investigated whether the age of the wounded fly affects the wound healing response. She found that 3-5 day old flies survive the longest after wounding. These age related survival experiments were repeated to investigate survival after wounding of wild type flies of different ages at 25˚C. The data from these previous experiments was not combined with this new data. The flies were aged to 1, 3, 5, 7 and 9 day old, then wounded as before and the number of flies surviving recorded every 3 hours (Method 2.9).

Figure 3.9 shows the combined survival data from all the experiments for each fly age individually (n = 4, x = 100). The average percentage of survival for each time point is shown. The error bars represent the standard error between the experiments at each time point. For each age the wounded flies survive less successfully then the unwounded flies. As expected this reduction in survival after wounding is significant. Although this significance for 3 and 5 day old flies does not appear to be great, which confirms Elizabeth King's findings that 3-5 day old flies survive best after wounding. Interestingly 9 and 1day old flies have the biggest significant difference in survival after wounding. When comparing the survival of the wounded 3, 5 and 7 day old flies to the survival of the unwounded flies a significant reduction is seen 9 hours after wounding. This is consistent with the survival of wounded wild type flies in earlier *pacman* and *pacman* overexpression survival experiments. Therefore these flies are unlikely to be dying from defective clot formation. For 9 and 1 day old flies this significant reduction in survival begins straight after wounding.

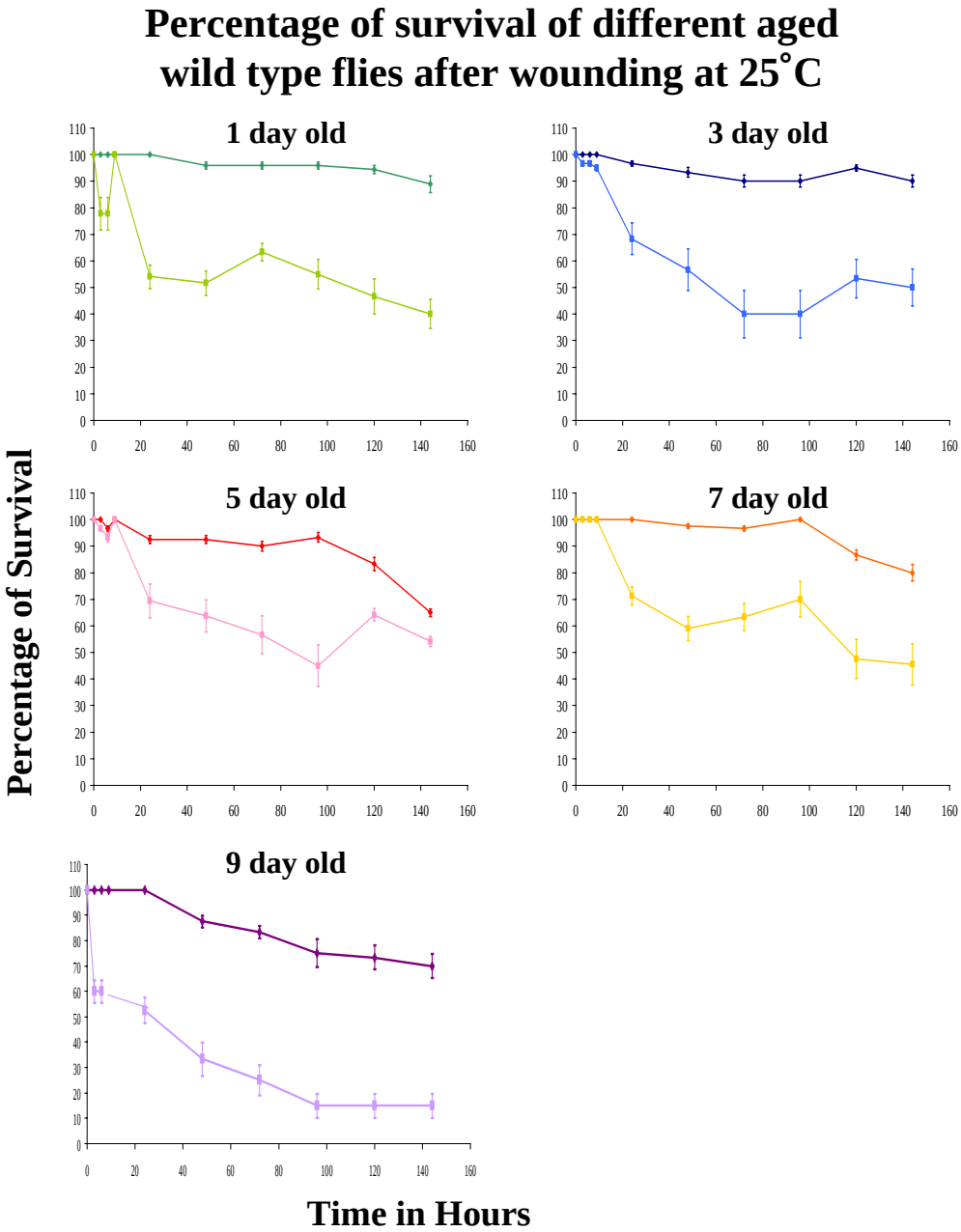

Figure 3.9: The combined survival data from all the ageing experiments for each fly age individually (n = 4, x = 100) at 25˚C. The average percentage of survival for each time point is shown. The error bars represent the standard error between the experiments at each time point. Key: 1 day unwounded, 1 day wounded, 3 day unwounded, 3 day wounded, 5 day unwounded, 5 day wounded, 7 day unwounded, 7 day wounded, 9 day unwounded and 9 day wounded.

Figure 3.10 A shows the combined data from all ageing experiments together in one survival graph. The average percentage of survival for each time point is shown. Figure 3.10 B shows the combined survival data from all the ageing experiments for only the wounded flies. The average percentage of survival for each time point is shown. The error bars represent the standard error between the experiments at each time point. These graphs allow comparison of the survival of the different wild type ages after wounding. As expected all unwounded wild type ages survive better than the wounded flies. The survival of wounded flies differs across the different ages of the flies. At the 24 hour time point, the time at which wound healing is complete in *Drosophila* the wounded wild type flies of ages 3, 5 and 7 days survival the best. The average percentage of flies surviving at 24 hours after wounding for the 9 and 1 day old flies is lower. The error bars show no significant difference in survival after wounding between the 3, 5 and 7 day old flies. There is also no significant difference in survival after wounding between the 9 and 1 day old flies. However there appears to be a significant reduction in survival after wounding of the 9 and 1 day old flies compared to the survival of the wounded 3, 5 and 7 day old flies. These results suggest that the overall wound healing process is impaired in younger and older flies. This may include both clot formation and epithelial closure.

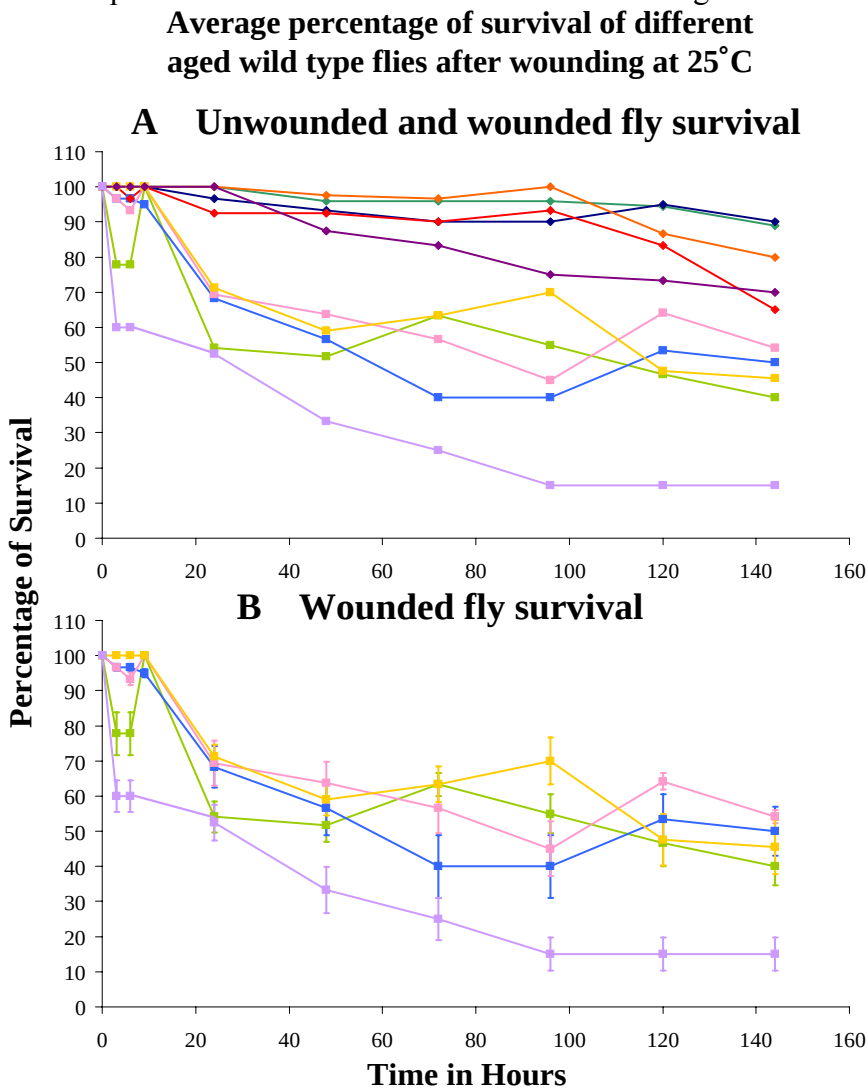

Figure 3.10: A) The combined survival data for unwounded and wounded of all ages from all ageing experiments at 25˚C. B) The combined survival data from all the ageing experiments for only the wounded flies at 25˚C. The average percentage of survival for each time point is shown. The error bars represent the standard error between the experiments at each time point. These graphs allow comparison of the survival of the different wild type ages after wounding. Key: 1 day unwounded, 1 day wounded, 3 day unwounded, 3 day wounded, 5 day unwounded, 5 day wounded, 7 day unwounded, 7 day wounded, 9 day unwounded and 9 day wounded.

The average half life i.e. the time at which half the flies are still alive across the experiments were calculated for the different fly ages and displayed in Figure 3.11. The histogram shows that again the 3 day and 5 day flies survive the longest after wounding and the more extreme ages 9 and 1 day old flies are not so successful. Interestingly the half life of the wounded 7 day old flies is less than that of the 1 day old flies. Taken with the survival graphs this suggests that the 7 day old flies survive the wound infliction better than the 1 day old flies but as they age further during the experiments they are more likely to die than the 1 day old flies. This is confirmed by the faster deaths of the 9 day old unwounded flies compared to the other ages of unwounded flies shown in figure 3.10 A.

The reduced survival after wounding of the 9 and 1 day old flies suggest wound healing is slower or unsuccessful in these flies, which leads to an early death. This is consistent with previous studies determining the affects of ageing on human wound healing (Pajulo et al. 2000; Gosain et al. 2004). The first recorded literature linking age to impaired wound healing in humans was almost 100 years ago. Several changes take place in human skin during ageing including dryness, wrinkling, sagging, roughness, flattening of the dermal-epidermal junction, disorganized collagen and decreased fibroblasts and macrophages i.e. decreased immune response. These factors and others are thought to delay healing in human aged skin after wounding (DeVeale et al. 2004; Gosain et al. 2004). This delay leads to chronic wounds and death. A delay in wound healing is likely the reason for the reduced survive seen in older wild type wounded flies.

A previous study has shown that age also affects wound healing in children. Like aged skin in humans where decreased levels of fibroblasts and macrophages are thought to play a role in impaired wounding healing, it has been shown that the inflammatory response may play a part in wound healing of young children. Migration of inflammatory cells to the site of a wound is thought to contribute to the onset of wound repair. As a child ages there are changes in the pattern of the immune response to the infliction of a wound. The migration of the immune cells to the wound site of young children appears delayed (Pajulo et al. 2000). This could results in lag before wound healing begins. Thus explaining why very young children are susceptible to infections. The reduced survival of the 1 day

wounded flies may be explained by a delay in the onset of wound healing due to late migration of the inflammatory cells in young flies. Overall these ageing experiments performed in *Drosophila* could be an excellent model for understanding the effect of ageing on human wound healing.

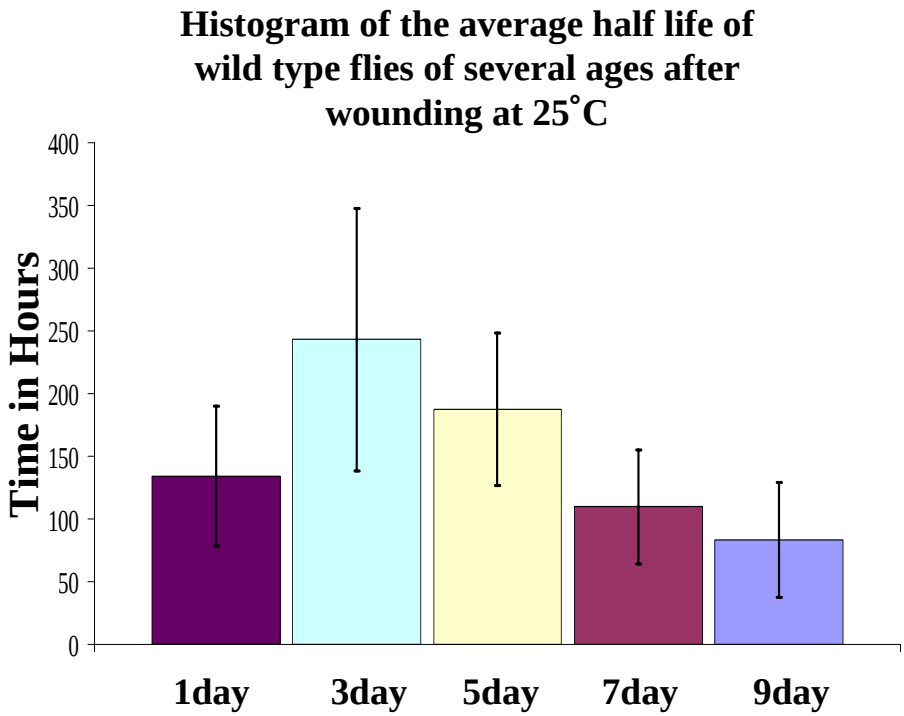

Figure 3.11: Histogram showing the average half life of wild type flies of several ages after wounding at 25˚C (N = 4). Error bars represent the standard error.

3.5 Clotting experiments

It was previously shown that deletions in the *pacman* gene can lead to reduced survival after wounding, which has lead to the conclusion that *pcm* mutants have a defect in wound healing. To confirm that the flies are dying quicker due to this defect and not just an overall reduction of metabolic processes, clotting experiments were performed. The signalling pathway that controls the clotting process is separate and distinct from the wound healing pathway, the JNK signalling pathway. After a wound is inflicted, a clot forms around the entry point. In *Drosophila* this begins to occur around 20-30 minutes after wounding. Firstly a clear fluid is secreted to plug the wound and then after some time melanin builds up forming the scab (Martin 1997; Martin et al. 2004; Wood et al. 2006). Little is known about the clotting system in *Drosophila*. However hemolymph (the insect version of a blood stream) coagulation in most insects appears to involve cellular and circulating immune components which are activated upon wounding (Theopold et al. 2002; Theopold et al. 2004). So far studies of *Drosophila* clotting have shown that hemolectin is the most abundant clot protein. Hemolectin mutant larvae show clotting defects (Scherfer et al. 2004; Babcock et al. 2008). The recently discovered gene *fondue* encodes another major hemolymph protein required for efficient clotting in *Drosophila*. Knockout mutants of *fondue* lead to reduced activity of larval hemolymph (Scherfer et al. 2006).

During the clotting experiments homozygous *pcm* mutants and wild type flies were wounded as before then the time at which the clot started to form was recorded (Method 2.7). The time at which the edges of the wound started to turn black as pictured in Figure 3.12 was taken as a marker for the onset of clot formation.

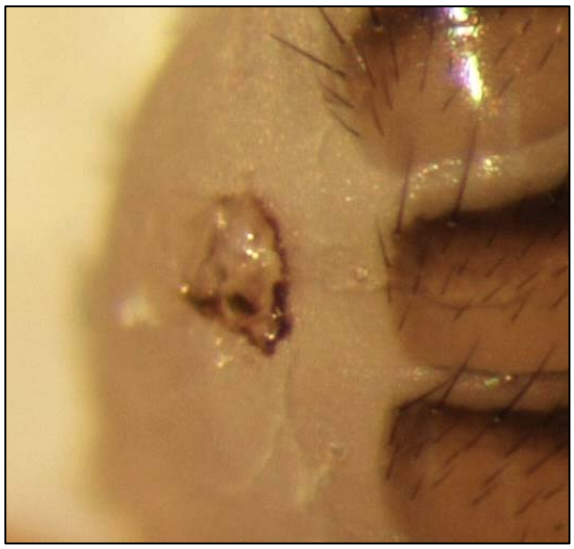

Figure 3.12: Picture shows the melanin clot forming round a wound on a wild type adult fly. Flies are wounded using scalpel on the abdomen. Clot begins to form between 20-30 minutes after wounding.

The average clotting times were calculated for each strain for two temperatures 19˚C (n = 2, x = 20) and 25˚C (n = 6, x = 20). This data was displayed as histograms in Figure 3.13. This data confirms that clotting begins between 20-30 minutes after wounding in wild type and *pacman* mutant flies as expected. The standard errors show there is no significant difference between the average clotting times of the wild type and *pcm* mutants flies at either 19˚C or 25˚C. To confirm this result a one way ANOVA statistical analysis test was performed. The P values for the ANOVA test confirm there is no significant difference between the clotting times of the wild type and *pacman* mutant flies after wounding at 19˚C (P = 0.832) or 25˚C (P = 0.431). These results are consistent with the *pacman* survival experiments which suggested there was no significant difference in survival between the mutants and wild type wounded flies at the time of clot formation i.e. before 3 hours. Overall the results from the clotting experiments and *pacman* survival experiments suggest the reduction in survival seen in the previous experiments is due to a specific defect in wound healing possibly through an interaction with the JNK signalling pathway.

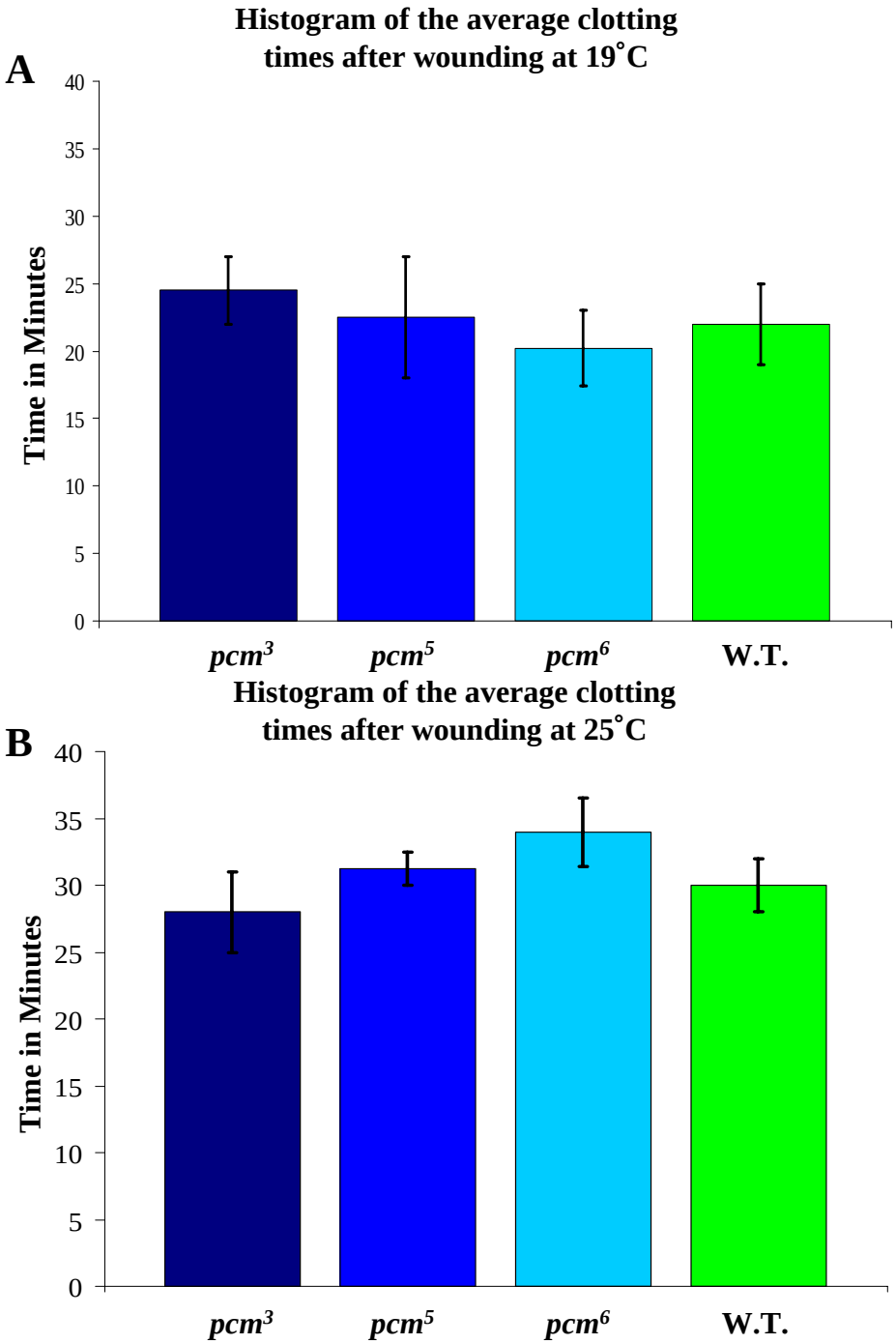

Figure 3.13: Graph A is a histogram showing the average clotting times after wounding at 19˚C (n=2) One Way ANOVA $F_{3,4}$=0.29 P=0.832. Graph B shows the average clotting times after wounding at 25˚C (n=6) One Way ANOVA $F_{13,30}$=0.95 P=0.431. Error bars represent the standard error. Clotting times for both temperatures show no significant difference between the wildtype and *pacman* mutant flies.

3.6 How does infection effect survival after wounding?

A possible reason for the reduced survival of *pacman* mutants after wounding is that they are more susceptible to infection. Metozoans such as *Drosophila* possess only innate immunity, which is essential in the fight against microbial infection. They do not produce specific antibodies to an invading antigen seen in the adaptive immunity of higher organisms including mammals. In humans innate immunity is considered the first line of defence to eliminate microbes and prevent infection. This form of immunity recognises groups of invading pathogens through specific markers on their surface such as lipopolysaccharides and peptidoglycans and then launches a counter attack. This involves the production of antimicrobial peptides (AMP), opsonisation (antibodies) and melanization (clotting) to kill or isolate the pathogens (Boutros et al. 2002; Jasper et al. 2002). Recent studies in *Drosophila* have shown two pathways that are activated and regulate the immune responses after invasion from pathogens. The toll/$NF_{kappa}\beta$ pathway regulates the response to gram positive bacteria and fungal infections whereas the Imd/Relish pathway regulates the response to gram negative bacteria infections. The Imd/Relish pathway is most likely to be activated in the infected flies of the subsequent survival experiments as *E.coli* is a gram negative bacteria (Boutros et al. 2002; Jasper et al. 2002). Boutros et al performed gene expression profiling after bacterial infection using microarrays. It was found that after invasion other signalling pathways are also activated including the JNK signalling pathway (Boutros et al. 2002). This highlights a link between microbial response and the cytoskeletal rearrangements regulated by JNK signalling during wound healing. If infection also induces the JNK signalling pathway that may suggest that flies with both an infection and an inflicted wound will have a higher level of expression which in turn may lead to better wound healing and therefore will survive better than flies with sterile wounds.

The scalpel used in previous survival experiments was used for all flies without sterilisation so it is possible the flies were infected with bacteria during the wounding process. To determine whether infection is playing a role in the reduced survival seen in *pacman* mutants the previous survival experiments were repeated

with the same fly strains homozygous *pcm*^{3}, *pcm*^{5}, *pcm*^{6} and the wild type control. However this time they were stabbed with a different sterile scalpel for each fly or with a scalpel whose tip was coated in bacteria to try and deliberately infect each wound. For sterile wounds, a new scalpel tip was sterilized by autoclaving for each fly. The bacteria used for infection were the *E.coli* strain DH1which was prepared as described in Method 2.8.1. At the end of these experiments more data was required therefore Chris Jones, a fellow PhD student in the Newbury lab repeated this infection two more times. The data for these experiments were combined before analysis (n=4, x = 120). These experiments were only performed at 25˚C as collection of the required number of homozygous *pacman* mutant flies at 19˚C was problematic due to reduced numbers of homozygous flies hatching.

After wounding the flies on the abdomen with a sterile scalpel or a scalpel coated with *E.coli* the number of flies surviving was recorded every three hours (Method 2.8). Like the *pacman* deletion survival experiments previously described in section 3.2, the combined survival data from all experiments for unwounded, sterile wounded and infected wounded flies for each *pacman* mutant and the wild type control were displayed as survival curves (Figure 3.14). The average percentage of survival for each time point is shown. The error bars represent the standard error between the experiments at each time point. These survival curves show that for all the strains the sterile and infected wounded flies survive less well than the unwounded flies. This reduction in survival is significant including at the time point 24 hours after wounding. Thus there is a significant reduction in survival of the sterile wounded and infected wounded flies for each strain at the time which wound healing should be complete. This result is consistent with the previous *pacman* mutant survival experiments. The sterile wounded flies for each strain survive significantly better than the infected wounded flies. For each strain there is no significant difference between the survival of the sterile wounded and the infected wounded flies before 3 hours. Therefore, as in original *pacman* survival experiments in section 3.2, the clot formation process does not appear to be impaired. Of the infected wounded flies the wild type flies seem to survive the best because their survival and the survival of the sterile wounded wild type flies are the closest. The infected wounded *pcm*^{3} flies show the biggest reduction in survival compared to the sterile wounded *pcm*^{3} flies. This data corroborates the

previous hypothesis that mutations in *pacman* cause reduced survival of these flies due to a defect in wound healing. It is likely the infected wounded flies die faster than the sterile wounded flies due to the added complication of the immune response during the wound healing process.

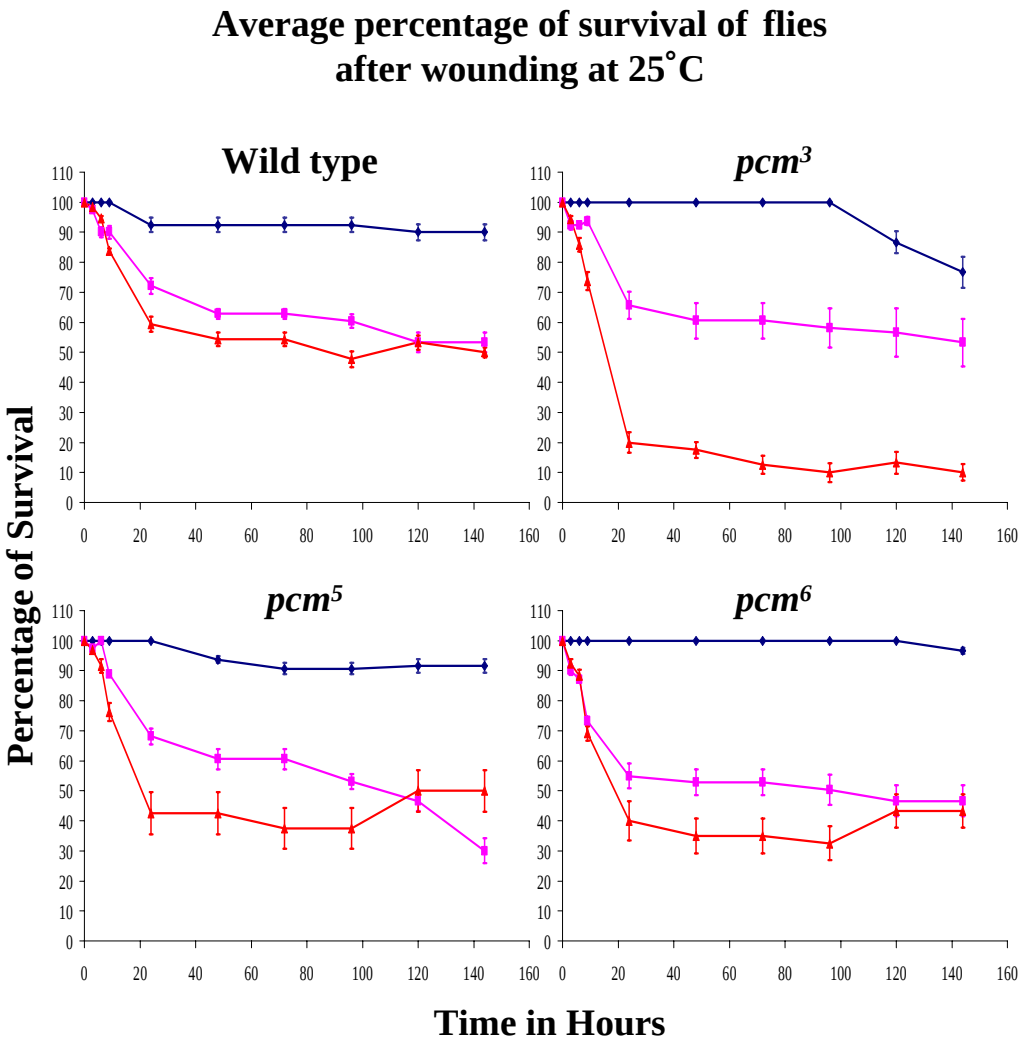

Figure 3.14: The combined survival data from all experiments for unwounded, sterile wounded and infected wounded flies for each *pacman* mutant and the wild type control at 25˚C (n=4, x = 120). The average percentage of survival for each time point is shown. The error bars represent the standard error between the experiments at each time point. Key: unwounded, Sterile wounded and infected wounded.

For each strain the average half life i.e. the time at which half the flies are still alive across the experiments was calculated for sterile and infected wounding. This data was displayed in the histogram in Figure 3.15. The error bars represent the standard error. This histogram shows there is a survival trend for the wild type control, pcm^3 and pcm^6 flies. The results seem to suggest the sterile wounded flies survive better than the infected flies. The error bars show this reduction in survival of the infected wounded wild type, pcm^3 and pcm^6 is significant when compared to the survival of the sterile wounded flies. This is consistent with the survival curves in Figure 3.14. For pcm^5 flies at the half life time point the infected flies appear to survive slightly better than the sterile ones however the error bars show this change is not significant. This result is inconsistent with the previous survival curves.

Overall the sterile wounded flies appear to survive significantly better than the infected wounded flies. This may suggest a role for *pacman* in regulating the immune response after wounding Although as mentioned early a link between the JNK signalling pathway and the innate immune response this already been established therefore *pacman* may affect innate immunity through its interactions with the JNK signalling pathway (Boutros et al. 2002; Jasper et al. 2002).. Alternatively *pacman* mutants show a defect in wound healing and when infection is also present at the wound site the healing process is compromised further possibly slowing wound healing leading to more deaths. This seems a likely scenario since infected wounded wild type flies also show this reduction in survive. If it is a *pacman* mutation in the infected wounded flies that is causing the reduction in survival through defective wound healing and immune response then we would expect the survival of the infected and sterile wounded wild type flies to be the same.

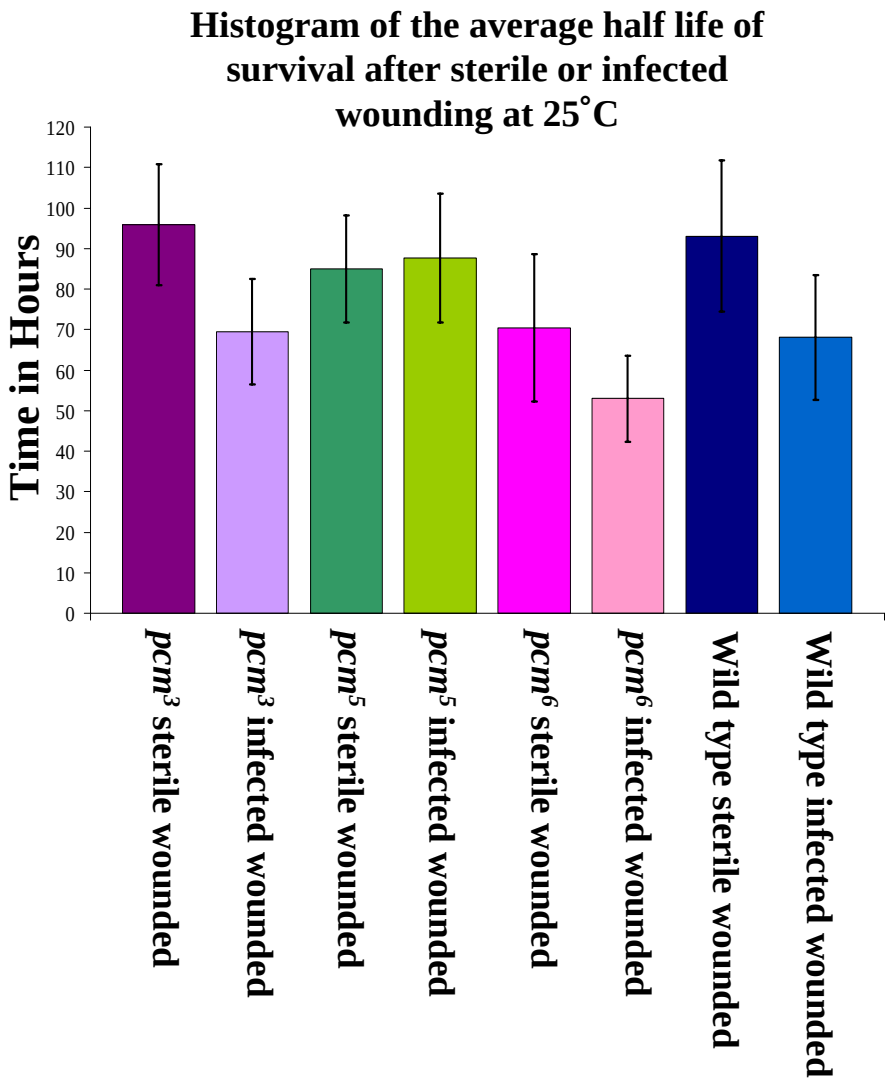

Figure 3.15: Histogram showing the average half life of survival of wild type and *pacman* mutant flies after sterile or infected wounding at 25˚C (n = 4). Error bars represent the standard error.

3.7 Chapter Conclusions

Previous work by Dr D. Grima in the Newbury lab has shown that mutations in *pacman* cause defects in thorax closure (Grima 2002). Thorax closure is a morphogenetic process that occurs during larval development which is regulated by the JNK signalling pathway. These defective thorax phenotypes are similar to those seen in JNK signalling mutants such as *hep1*. These phenotypes suggest a role for *pacman* within the JNK signalling pathway. This pathway also regulates others cell sheet sealing mechanisms such as dorsal closure in *Drosophila* embryos, hind brain closure in mammals and wound healing. Therefore a possible role for *pacman* in wound healing was investigated using survival experiments. These experiments showed that at 19˚C pcm^3, pcm^5 and pcm^6 mutant flies survive significantly less well than the wild type control after wounding at the 24 hour time point. Studies have shown that wound healing in *Drosophila* is complete by this time (Ramet et al. 2002; Galko et al. 2004). At 25˚C pcm^3 and pcm^5 were also shown to survive significantly less well than the wild type after wounding at this same time point. pcm^6 also does not survive as well as the wild type flies after wounding however this difference is not significant. This shows the temperature sensitivity of the *pacman* mutants. Thus pcm^6 is the mildest allele and its mutant phenotypes are less severe at higher temperatures. Before 3 hours there is no significant difference between the survival of the *pacman* mutants and the wild type flies after wounding. This suggests that clot formation in these flies is normal and it is not a defect in clotting that is hindering survival. Overall these results are consistent with the hypothesis that *pacman* mediates wound healing. Whether *pacman* regulates wound healing through a possible interaction with the JNK signalling pathway is investigated in the following chapters.

Survival experiments have shown mutations in *pacman* reduce survival after wounding. Further survival experiments were performed comparing survival of wild type and *pacman* overexpression mutant flies after wounding. These experiments showed a significant reduction in survival for flies which overexpress *pacman* compared to the wild type control after wounding at the 24 hour time point. Again there is no significant difference in survival between the wounded

pacman overexpression flies and the wounded wild type flies before 3 hours. Therefore overexpressing *pacman* does not appear to affect clot formation after wounding. These results suggest the correct amount of *pacman* expression is essential for wound healing. More or less Pacman will lead to defective wound healing and possibly death.

Previously in human studies initiation of wound healing has been shown to be delayed in aged tissue, in individuals of 65 years and older (DeVeale et al. 2004; Gosain et al. 2004) and in young children, whose inflammatory response changes with age (Pajulo et al. 2000). Would age have a similar affect on wound healing in *Drosophila*? Survival experiments on wild type flies of different ages were performed. These showed a significant reduction in survival of the 9 and 1 day old flies 24 hours after wounding compared to the other ages. Therefore age does affect wound healing in *Drosophila* and this is probably due to a delay in the initiation of wound healing similar to that seen in older and younger human tissue. This result is very interesting and suggests *Drosophila* would be an excellent model for wounding and ageing studies.

After a wound is inflicted, a clot forms over the exposed tissue to protect the wound from pathogens. Could the reduced survival after wounding seen in the *pacman* mutant flies be due to a defect in clot formation? Clotting experiments showed that there is no significant difference between the times at which a clot forms in *pacman* mutant flies compared to the wild type control flies at 19˚C or 25˚C. Therefore the reduced survival seen in the *pacman* mutant flies is a specific wound healing defect and not an overall reduction in metabolic processes.

A link between the innate immune response and the JNK signalling pathway after wounding has been established (Boutros et al. 2002; Jasper et al. 2002). What affect does infection have on the survival of the *pacman* mutant flies after wounding? Flies that are deliberately infected with a scalpel coated in bacteria during wounding do not survive as well as the flies wounded with a sterile scalpel. This reduction in survival is significant for all 3 *pacman* mutants and the wild type control. The added complication of the immune response may hinder the wound healing process increasing the death rate of the infected wounded flies.

Interestingly at 24 hours after wound infliction the significant difference in survival between the sterile wounded and the infected wounded wild type flies is smaller than the difference seen for the *pacman* mutants. This may suggest a role for *pacman* in regulating the innate immune response however this could be due to its interactions with the JNK signalling pathway which is activated upon infection (Boutros et al. 2002).

Overall the results of this chapter have shown that *pacman* mutants have a specific wound healing defect. This defect suggests a role for *pacman* in the JNK signalling pathway. One possible hypothesis under further investigation in the next chapter is that Pacman regulates the JNK signalling pathway by degradation of the phosphatase *puckered* mRNA.

Chapter 4 Pacman affects the JNK pathway, JNK affects epithelial sheet sealing and wound healing

In the previous results chapter, survival experiments have shown that mutations in *pacman* reduce the survival times of these flies after wounding. After performing control clotting experiments it was concluded that *pacman* has a role in wound healing of *Drosophila melanogaster*. The next step was to determine the means by which *pacman* affects wound healing.

The Jun N-terminal Kinase (JNK) signalling pathway has been shown to have a role in wound healing (Figure 4.1)(Altan et al. 2004). In *Drosophila,* mutations within genes of this pathway cause defects in epithelial sheet sealing leading to incorrect wound healing, dorsal closure and thoracic closure (Ring et al. 1993; Noselli et al. 1999; Ramet et al. 2002; Galko et al. 2004). In mice and more than likely humans, mutations again affect wound healing and can lead to defects in eyelid closure in mice (Martin et al. 1992; Chang et al. 2001; Weston et al. 2002). Dorsal closure, thoracic closure, ventral enclosure and eyelid closure are all morphogenetic processes that occur during development. The cell movements involved in all these processes and wound healing also are the same. It has been shown that the JNK signalling pathway regulates these cell movements. The JNK signalling pathway appears to play a subtle role in regulating ventral enclosure. The genes of this pathway are not essential for epithelial closure in *C.elegans* (Chin-Sang et al. 2000).

Both the model organisms *Drosophila melanogaster* and *C.elegans* have been used by the Newbury group to research the role of *pacman*/*xrn1.* Previously the group has shown that mutations in the *C.elegans pacman* homologue *xrn1* have defects in ventral enclosure and that *Drosophila* mutants have thoracic closure

defects (Grima 2002; Newbury et al. 2004). There is also some evidence that in *Drosophila, pacman* mutants have defects in dorsal closure (Grima et al. 2008). These similar mutant phenotypes suggest that *pacman* may target a mRNA within the JNK signalling pathway.

Both models process a cytoplasmic exoribonuclease and they undergo morphogenetic epithelial sheet sealing so why chose to study *pacman*/*xrn1* in *Drosophila* rather than *C.elegans*? The benefits of *Drosophila* as a model organism for research are discussed in chapter 1. These advantages include fast generation time, cheap to breed and maintain, simple genome, balancer chromosomes and P-elements. *C.elegans* are also cheap and fast to breed and they can be frozen for storage. They have a simple genome with 6 chromosomes and the whole nematode processes only 959 cells. *C.elegans* are a great candidate for RNAi (interference), a form of directed mutagenesis which allows a target gene to be silenced by feeding the worms bacteria expressing double stranded target gene RNA. This allows for the function of the target gene to be assessed. The JNK signalling pathway does not play an essential role in ventral enclosure, the *C.elegans* version of epithelial sheet sealing. Thus the JNK signalling pathway may not regulate wound healing in *C.elegans.* Therefore for studying the interactions between *pacman* and the JNK signalling pathway and how they may regulate wound healing *Drosophila melanogaster* is the model of choice.

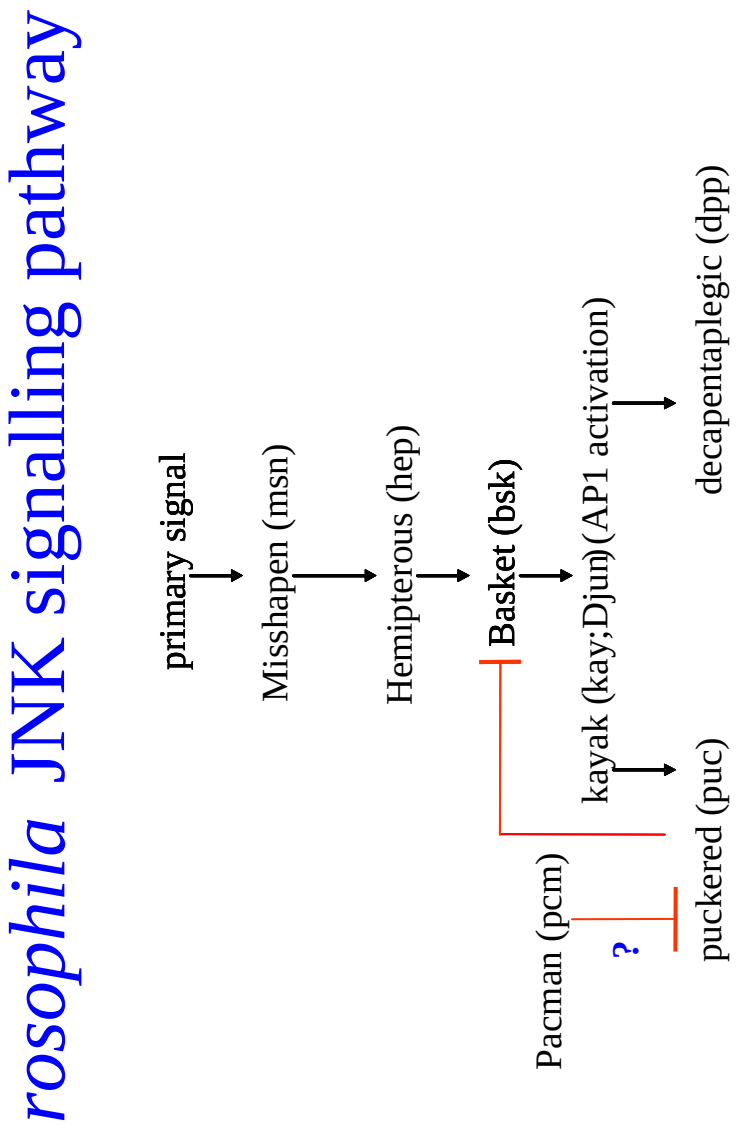

Figure 4.1: The *Drosophila* JNK signalling pathway and a possible role for *pacman* within this pathway (**?**).

4.1 Genetic interactions between *pacman* and *puckered*

The easiest way to start to test this hypothesis was to look for a genetic interaction between *pacman* and *puckered*. If this occurred flies which carried *pacman* and *puckered* mutations would exhibit phenotypes not seen in either single mutant alone. To investigate this potential interaction a new double mutant fly strain was created containing both the *pacman* mutation (pcm^5) and a mutant *puckered* allele (Figure 4.2). *puckered* is a member of the JNK signalling pathway. The gene encodes a phosphatase that acts in a negative feedback loop to downregulate the *Drosophila* JNK, *basket*. The *puckered* allele puc^{A251} was created by a P-element insertion into the second intron of the *puckered* gene and is homozygous lethal (Martin-Blanco et al. 1998). The P-element insertion contains the *E.coli* LacZ sequence, this means LacZ expression i.e. β galactosidase staining can be observed under the control of the *puckered* promoter. This function of the double mutants is discussed later in the chapter.

Creating this new strain was highly problematic, there are several generations involved and the flies needed for the cross are in few numbers due to high lethality. For the first attempt the *pucLacZ* allele was balanced over TM6 Hu Tb, this means the heterozygous *pucLacZ* flies will have humeral and tubby phenotypes. When flies are humeral the bristles at the "shoulder" area of the thorax are all the same length instead of 2 longer ones and the rest shorter. This is a notoriously difficult balancer to pick out and the resultant cross was not correct due to wrongly selected parents. Several other failed attempts resulted in death of the offspring needed and unsuccessful crosses resulting in no offspring at all. Finally the balancer was changed from TM6 Hu Tb exchanging the humeral phenotype to tubby (TM6b Tb Sb). Heterozygous *pucLacZ* will now be recognized by the presence of Tubby and Stubble. Stubble means all the bristles of the fly are short and this is much easier to visualize. The tubby phenotype has the advantage that pupae and larvae carrying this mutation can be distinguished. The balancer was successfully exchanged using the cross outlined in Figure 4.2. The *pacman* gene in this new cross is balanced over FM7i-actinGFP, which was

described earlier in chapter 3, to allow homozygous *pacman* larvae and potentially homozygous *puckered* to be picked for experiments. This strain is referred to by SFN210 (pcm^5/pcm^5 ;; puc^{A251}/TM6bTbSb) A control strain carrying only the *pucLacZ* insertion was created (Figure 4.3) and will be used for comparison in later experiments. The control strain is referred to as SFN209.

1a

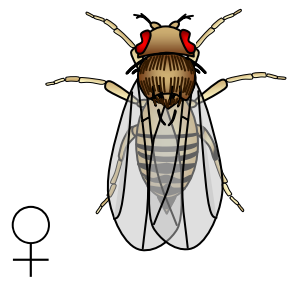

X

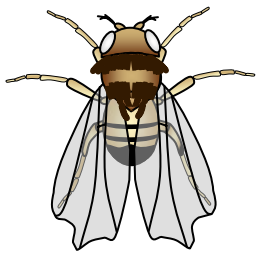

♀

♂

pcm/FM7i ;; +/+

w/Y ;;

Tm3Ser/Tm6TbSb

F1

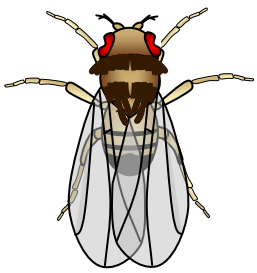

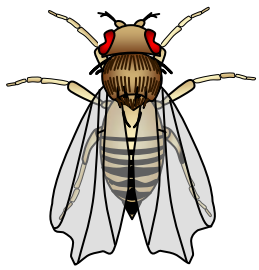

FM7i/Y ;; Tm6TbSb/+

FM7i/w ;; Tm3Ser/+

2a

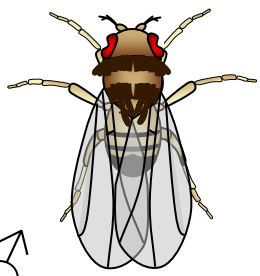

X

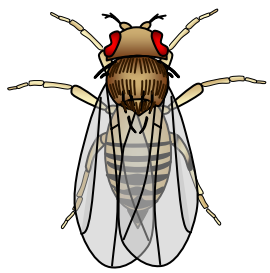

♂

♀

FM7i/Y ;; Tm6TbSb/+

pcm/FM7i ;; +/+

F1

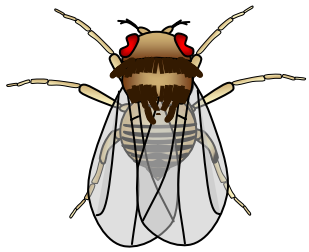

pcm/FM7i ;; Tm6TbSb/+

2b

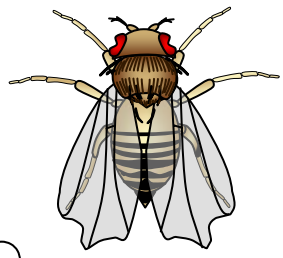

X

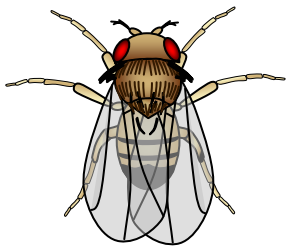

♀ ♂

FM7i/w ;; Tm3Ser/+

F1

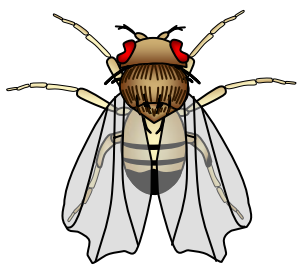

FM7i/Y ;; puc^{A251}/ Tm3Ser

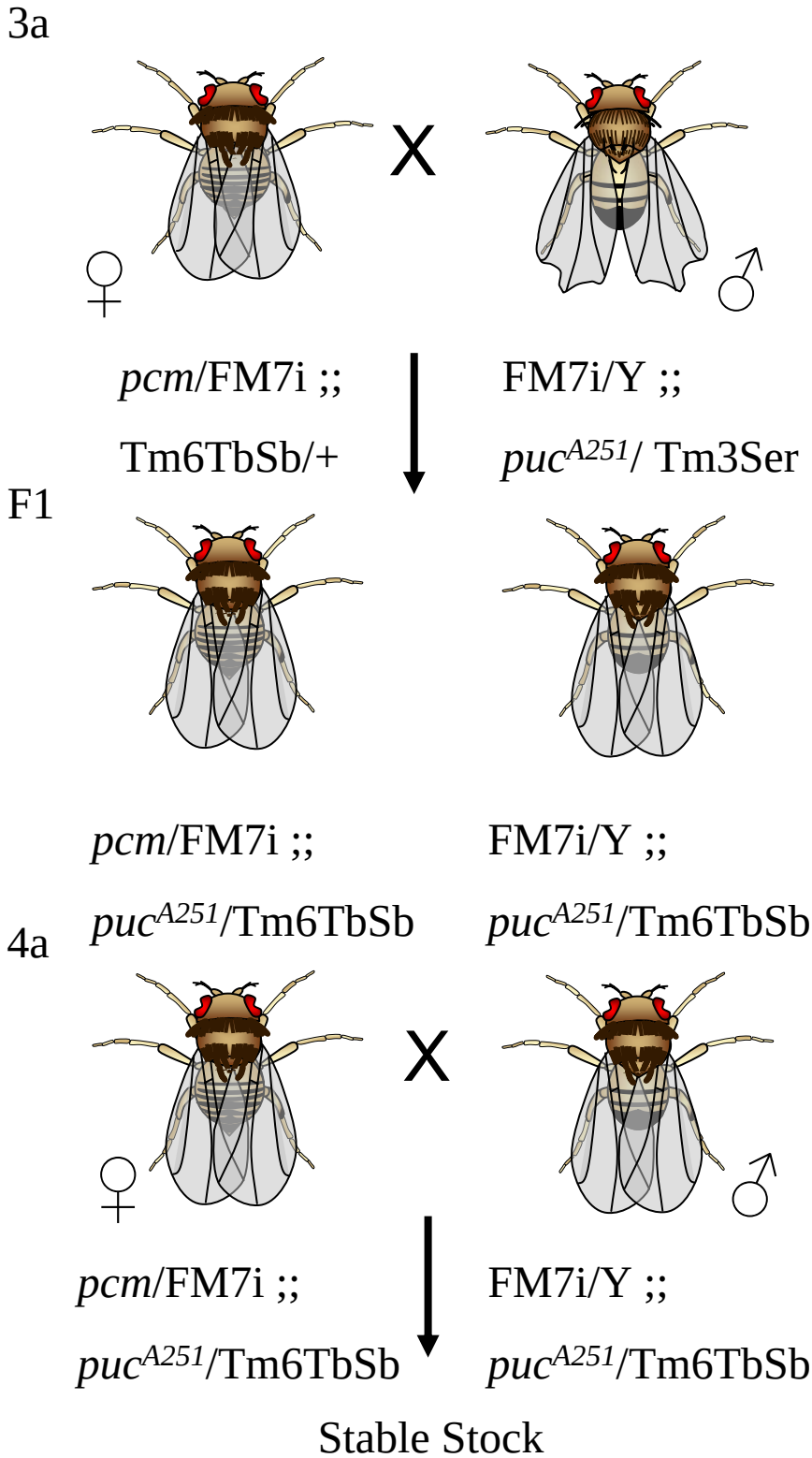

Figure 4.2: The schematic for the cross producing the *pacman puckered* double fly strain.

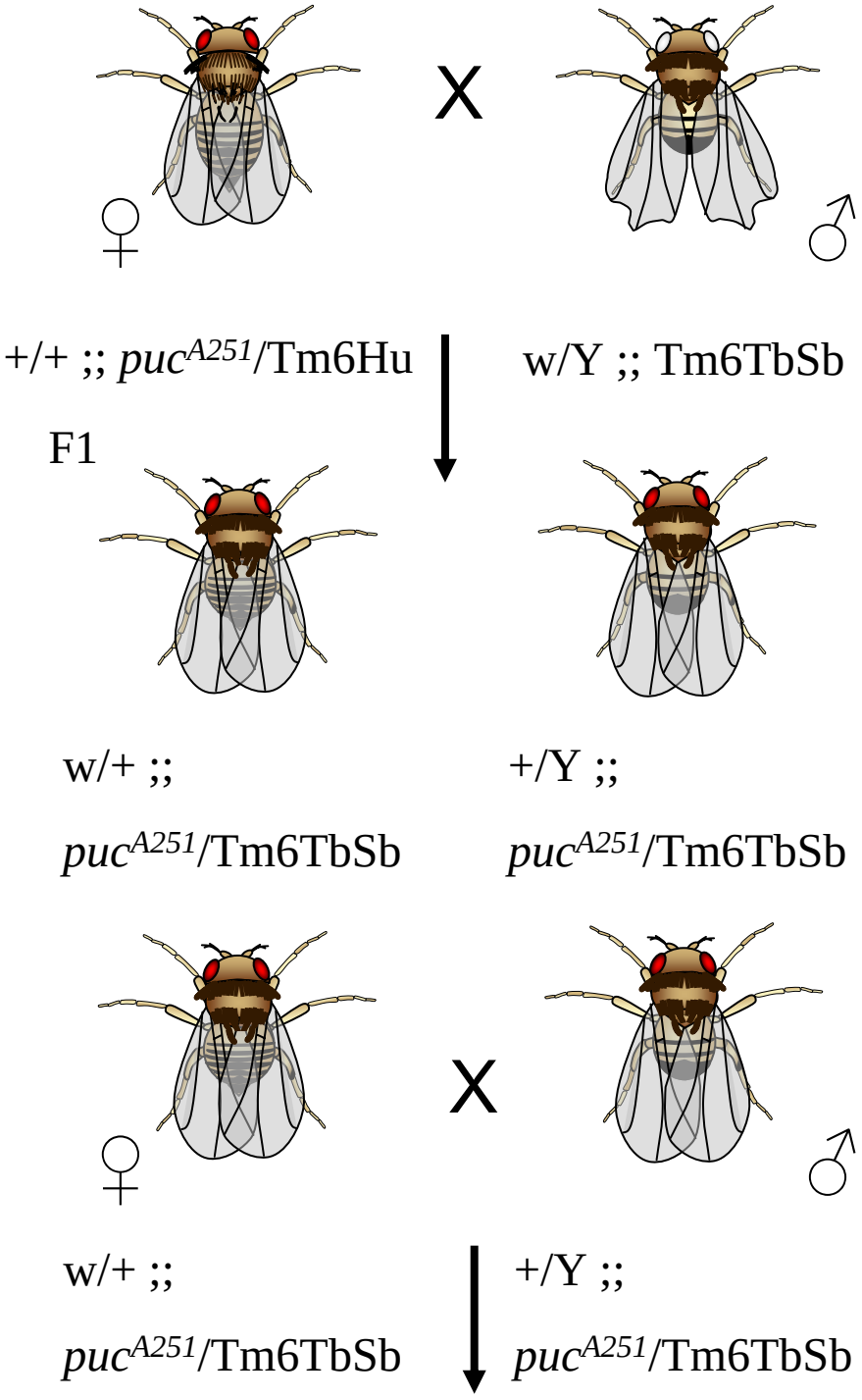

Figure 4.3: The schematic for the cross producing a *puckered* single mutant flies containing only the *puckered* mutation. This will act as the control strain for the *pacman puckered* double mutant strain.

4.2 Phenotypes of the *pacman* and *puckered* double mutant

To test the hypothesis that *pacman* might genetically interact with *puckered*, searches for unique mutant phenotypes associated with these flies carrying both these mutations were made. No heterozygous *pucLacZ* flies were present in the double mutant strain. Therefore the *puckered* mutation is still homozygous lethal and thus the mutation in *pacman* does not rescue the *puckered* lethality. These observations highlighted two phenotypes unique to the double mutant and not present in either of the single mutant strains. Both phenotypes were only seen in flies homozygous for *pacman* and heterozygous for *puckered* i.e. females pcm^5/pcm^5;; *pucLacZ*/TM6bTbSb and males pcm^5/Y;; *pucLacZ*/TM6bTbSb. These phenotypes were "curled" wings and a "bald" patch on the thorax at the dorsal midline (Figure 4.4). The penetrance for "curled wings" in both males and females increases when the temperature is increased from 19˚C to 25˚C. For the "bald" patches this is also true for males however females seem to decrease slightly (Table 4.1). This is usual as normally the severity of temperature sensitive mutant phenotypes increase at lower temperatures which is the case for the *pacman* mutant wound healing phenotype investigated in chapter 3. However for the curled wings and bald patches in homozygous pcm^5/heterozygous *puckered* flies the penetrance increases at the higher 25˚C temperature. Both curled wings and bald patches are developmental phenotypes. Therefore maybe the faster development of *Drosophila* at 25˚C might play a part in the penetrance of these phenotypes.

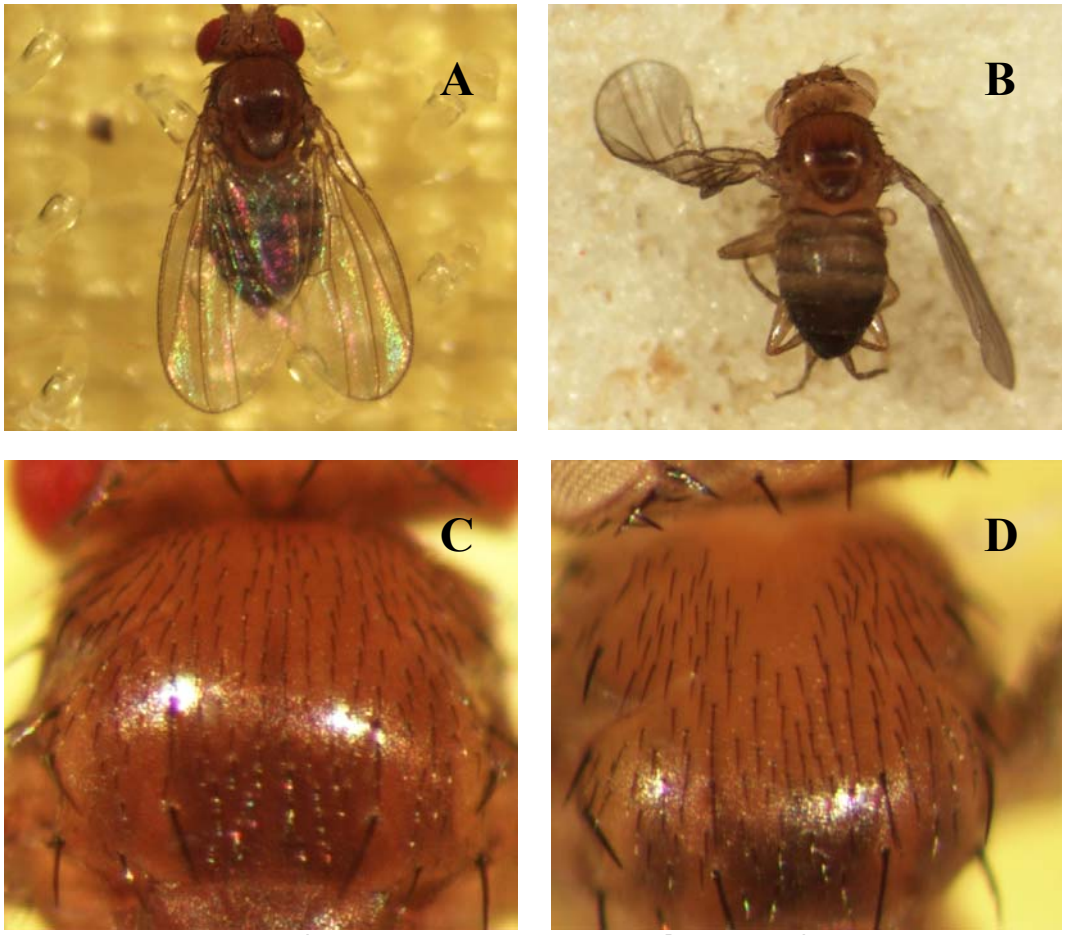

Figure 4.4: *pacman puckered* double mutant phenotypes. Curled wings and bald patches are only seen in the *pacman*/*puckered* double mutant. B and D show the mutant phenotypes of the *pacman* and *puckered* double mutants. A and C show the wings and thorax of the heterozygous *puckered* control flies. *pacman/puckered* flies n = 159 for 19˚C and n = 169 for 25˚C

	Temperature 19˚C		Temperature 25˚C	
Phenotype	**Females**	**Males**	**Females**	**Males**
Curled wings	40%	20.8%	85.1%	42.1%
Bald patches	70%	58.3%	66.6%	94.7%

Table 4.1: Table shows the penetrance of adult *pacman/puckered* double mutant phenotypes in both males and females for both temperatures 19˚C and 25˚C. n = 159 for 19˚C and n = 169 for 25˚C

To determine the viability of these double mutants in comparison to the *pacman* mutants the following crosses were instigated:

1. *pcm*/FM7i ;; *puc*/TM6bTbSb X *pcm*/Y ;; *puc*/TM6bTbSb
2. *pcm*/FM7i X *pcm*/Y

The number of flies hatching for each genotype was calculated. The data shows there is a reduction in viability of the pcm^5/pcm^5;; *pucLacZ*/TM6bTbSb and pcm^5/Y;; *pucLacZ*/TM6bTbSb flies compared to the *pcm*/*pcm* and *pcm*/Y flies. The unique phenotypes along with the reduction in viability show that there is a genetic interaction between *pacman* and *puckered*. Therefore *pacman* may have a role in regulating the JNK signalling pathway. The hypothesis that *pacman* is interacting with the JNK pathway by inhibiting *puckered* was proposed (Figure 4.1 blue question mark). The obvious method of inhibition would be *pacman* is degrading *puckered* RNA, which therefore leads to translational repression and reduced gene expression. The remaining thesis concentrates on characterizing the interaction between *pacman* and the JNK signalling pathway.

4.3 Confirmation that the double mutant strain still contains the *pacman* mutant

Before beginning to investigate the role of *pacman* in the JNK pathway using the double mutant flies, confirmation that the new strain still contains the *pacman* mutation was required. PCR was performed using primers specific for the pcm^5 mutation (Method 2.13.2 Appendix 2). The results confirm the presence of the *pacman* mutation in double mutant flies but not in the wild type or single *puckered* mutant flies (Figure 4.5).

4.4 Confirmation of the LacZ insert

It was also confirmed that this new strain still contained the *puckered* mutant allele. PCR looking for the presence of the LacZ construct was undertaken (Method 2.13.3). This sequence is foreign to the *Drosophila* so a band will only

be seen when the *puc*LacZ insertion is present. From the gel it can be seen that the wild type control flies do not contain the *puc*LacZ insertion. However the SFN210 double mutants (pcm^5/pcm^5;; puc^{A251}/TM6TbSb) and their control SFN209 (+/+ *or* *w*/+ ;; puc^{A251}/TM6TbSb) both contain the insertion which means the *puckered* mutation is still present in both these strains (Figure 4.6). Further experiments can now be performed with these flies.

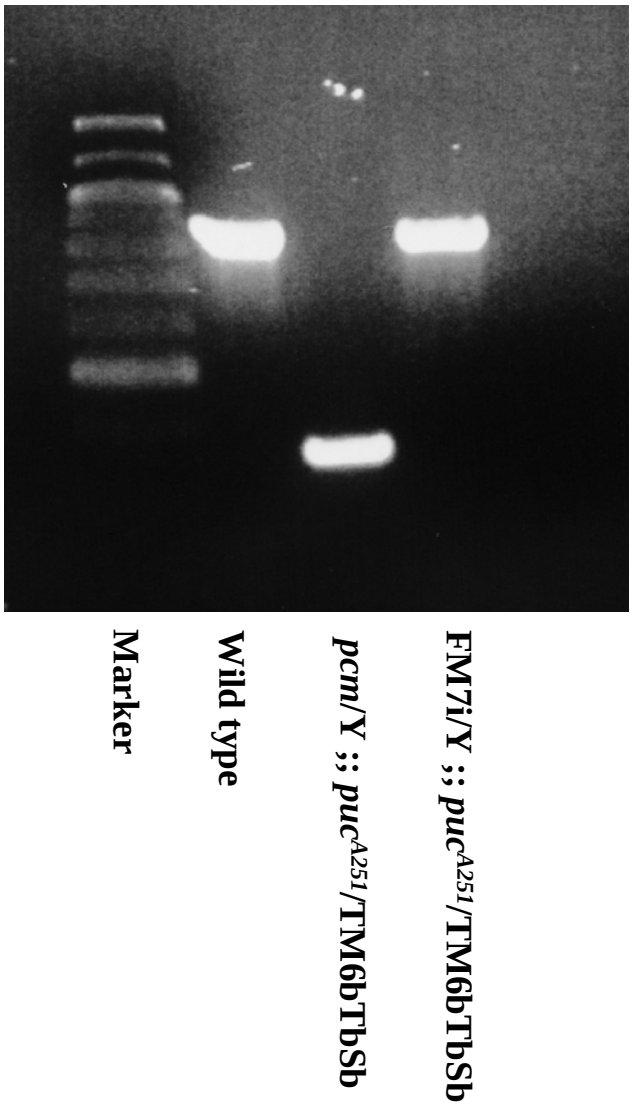

Figure 4.5: PCR to confirm that the *pacman puckered* double mutants still contain the *pacman* mutation. Marker = 1kb
Wild type band: 867bp

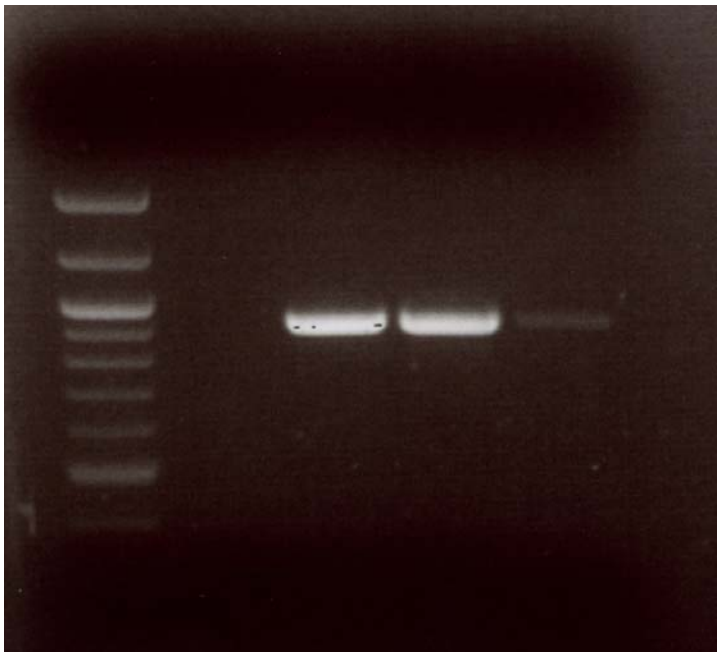

Figure 4.6: PCR to confirm that the *puc*LacZ insertion is still present in the new double mutant strains. The LacZ primers used are outlined in Appendix 3. Product size 925bp. Marker = 100bp,

4.5 Wounding of the *pacman* and *puckered* double mutant

To determine whether having mutations for both *pacman* and *puckered* affects wound healing, further survival experiments were performed like those in Section 3.2. The aim was to determine whether having both mutations would be further detrimental to survival or would there be a rescue affect. Flies were wounded as stated before in Method 2.6. Wild type and SFN209 (+/+ *or* *w*/+ ;; puc^{A251}/TM6TbSb) were used as controls. Figure 4.7 shows the survival curves of the unwounded and wounded wild type, *puckered* single mutant (+/+ *or* *w*/+ ;; puc^{A251}/TM6TbSb) and *pacman puckered* double mutant (pcm^{5}/pcm^{5};; puc^{A251}/TM6TbSb) flies at 25˚C (n = 10, x = 60). The unwounded flies survive better than the wounded flies. This is consistent with previous survival experiment results. The *pacman puckered* double mutant appears to survive the longest with the wild type control flies surviving the least time. At the 24 hour time point there is a significant increase in survival of wounded *pacman*/*puckered* double mutants (SFN210) and the wounded *puckered* single mutants (SFN209) compared to the survival of the wounded wild type control flies. However there does not appear to be a significant difference between the survival of the wounded double (pcm^{5}/pcm^{5};; puc^{A251}/TM6TbSb) and single mutants (+/+ *or* *w*/+ ;; puc^{A251}/TM6TbSb). This may suggests the *pacman*/*puckered* double mutants are more efficient at wound healing. At 3 hours after wounding there is no significant difference in survival between the strains therefore it is unlikely the deaths are due to a clot formation defect. The average half lives were calculated for each strain (Figure 4.8). This is the time at which half the flies are dead. The standard errors on the histogram show that the double mutants survive significantly better than both the wild type control and the flies carrying only one copy of the wild type *puckered* gene. This is consistent with the survival curve in Figure 4.7. These results suggest mutations in *puckered* not only restore the *pacman* mutant wound healing phenotype but result in better wound healing than wild type flies. This is therefore an extremely significant result.

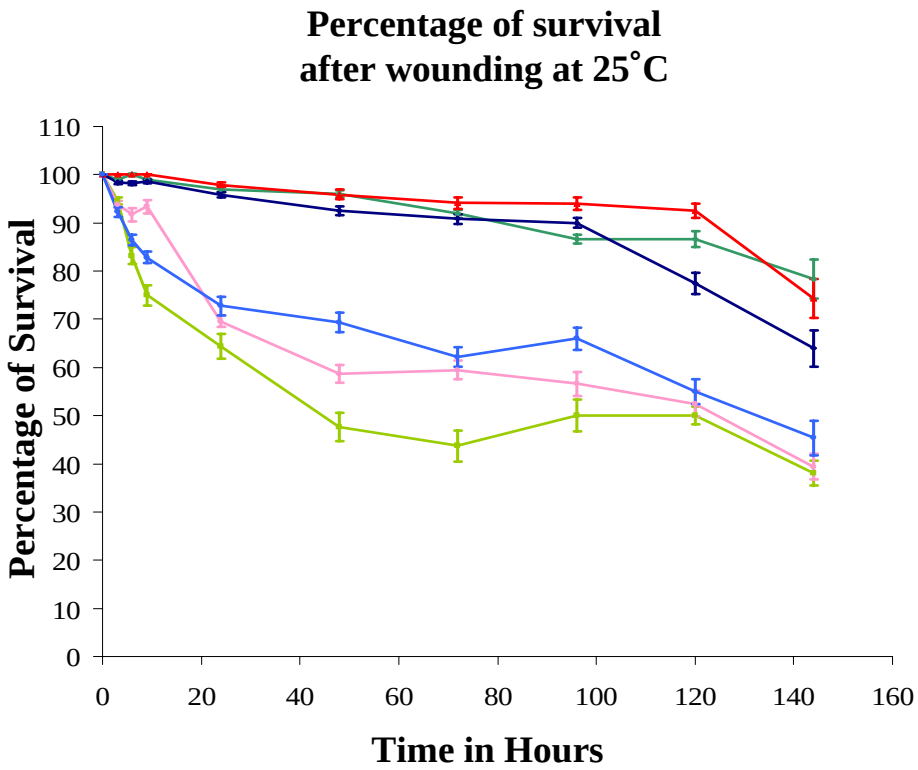

Figure 4.7: The combined survival data for the unwounded and wounded wild type, *puckered* single mutant (*+/+ or w/+ ;; puc*^{A251}/TM6TbSb) and *pacman puckered* double mutant (*pcm*^{5}/*pcm*^{5};; *puc*^{A251}/TM6TbSb) flies at 25˚C (n = 10, x = 60) The average percentage of survival for each time point is shown. The error bars represent the standard error between the experiments at each time point. Key: Wild type unwounded, Wild type wounded, *pcm*^{5}/*pcm*^{5};; *puc*^{A251}/TM6TbSb unwounded, *pcm*^{5}/*pcm*^{5};; *puc*^{A251}/TM6TbSb wounded, *+/+ or w/+ ;; puc*^{A251}*/TM6TbSb* unwounded and *+/+ or w/+ ;; puc*^{A251}*/TM6TbSb* wounded.

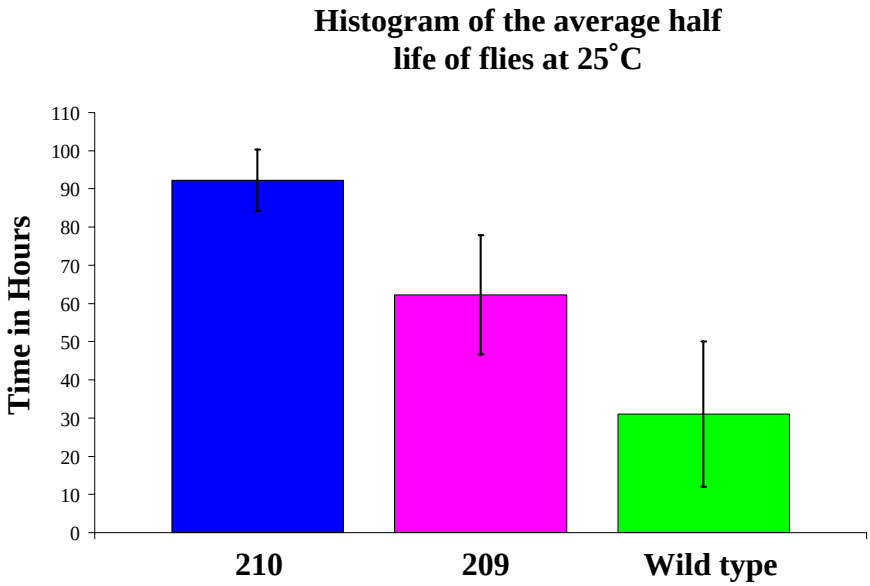

Figure 4.8: Histograms showing the average half life of survival of flies after wounding at 25˚C comparing *pacman puckered* double mutants SFN210 (*pcm*^{5}/*pcm*^{5};; *puc*^{A251}/TM6TbSb), *puckered* single mutants SFN209 (+/+ *or* *w*/+ *;; puc*^{A251}/TM6TbSb) and the wild type control flies. (n = 10, x = 60) Error bars represent the standard error.

4.6 β galactosidase staining of the *pacman* and *puckered* double mutant

A useful application of the *puc*LacZ insertion is the use of the lacZ sequence as a marker for *puckered* expression. The LacZ sequence is inserted downstream of the *puckered* promoter therefore the expression of LacZ mimics that of the *puckered* protein. To observe the LacZ expression and therefore the *puckered* expression, β galactosidase staining experiments can be used. The substrate Xgal is added to the β galactosidase staining solution. β galactosidase which is produced by LacZ expression breaks down the Xgal to produce galactose and 5-bromo-4-chloro-3-hydroxyindole. 5-bromo-4-chloro-3-hydroxyindole is oxidized into 5,5'-dibromo-4,4'-dichloro-indigo, an insoluble blue product. Therefore blue is seen at the location of the β galactosidase. The blue staining ultimately shows the expression levels and whereabouts of the JNK signalling pathway activity. The *puc*LacZ insertion has been used for this type of staining experiment by previous groups. Galko and Krasnow showed in 2004 that the JNK signalling pathway is abundantly expressed in the cells surrounding a larval wound after 4 hours of healing (Galko et al. 2004). In addition similar results were obtained in adult flies with JNK signalling expression observed at 6 hours after healing (Ramet et al. 2002).

β galactosidase staining experiments were preformed to determine where the puckered-lacZ fusion and the JNK signalling pathway are expressed after wounding in control and *pacman* mutant flies and larvae to determine whether there is a difference in expression levels when *pacman* is mutant.

4.6.1 β galactosidase staining of flies

Flies were used to optimize the experimental technique as these are easier to collect and wound. To observe *puckered* expression after wounding in flies the following genotypes were collected:

1. *pcm*/*pcm* ;; *puc*LacZ/Tm6bTbSb (homozygous *pacman* mutants)
2. +/+ ;; *puc*LacZ/Tm6bTbSb (control flies – no *pacman* mutation)

These flies were wounded as previously detailed for survival experiments and then allowed to heal for 4 hours (Galko et al. 2004). The technique for fly staining is outlined in method 2.11.1. The flies were left in the staining solution for 5 hours. This experiment was performed with several different incubation times. An incubation time of 5 hours was chosen for further experiments because there was obvious staining present, however the flies were not over stained which was the case in longer incubation times.

The results show that the wild type control flies do not stain when exposed to Xgal as expected (Figure 4.9). Staining is observed around the wounds of both the SFN210 (pcm^5/pcm^5;; puc^{A251}/TM6TbSb) and SFN209 (+/+ or w/+ *;;* puc^{A251}/TM6TbSb) flies (Figure 4.9). This suggests that *puckered* and therefore the JNK signalling pathway is expressed near the wound edge. This is consistent with previous findings by other groups (Ramet et al. 2002; Galko et al. 2004).

The aim of the staining experiments were to determine whether the expression levels of the JNK signalling pathway after wounding change when *pacman* is mutant. Comparing the SFN209 (+/+ or w/+ *;;* puc^{A251}/TM6TbSb) control flies which are wild type for *pacman* to the SFN210 (pcm^5/pcm^5;; puc^{A251}/TM6TbSb) flies which are homozygous *pacman* mutant should reveal this.

The β galactosidase staining appears as a faint ‘smudge’ around the wound edge showing the *pucLacZ* fusion protein is expressed here. This expression diffuses across the surrounding cells decreasing in the cells further from the wound (Figure 4.9). In order to quantify the *pucLacZ* expression for each mutant, a simple scoring method was applied to the staining (no staining: -, low staining: +, medium staining: ++ and high staining: +++). Although the above pictures in Figure 4.9 suggest there is an increase in staining around the wound edge of SFN210 (pcm^5/pcm^5;; puc^{A251}/TM6TbSb) (n = 9) flies when compared to SFN209 (+/+ or w/+ *;;* puc^{A251}/TM6TbSb) (n = 11) overall the scoring system suggested this increase is minimal.

In conclusion the β galactosidase staining experiments using fly tissue has shown *pucLacZ* expression and thus JNK signalling levels appear to be similar for both SFN210 (pcm^5/pcm^5;; puc^{A251}/TM6TbSb) and SFN209 (+/+ or w/+ ;; puc^{A251}/TM6TbSb) flies after wounding. Although the aim of this experiment, to quantify the *pucLacZ* and therefore the JNK signalling expression was not possible when using adult fly tissue, a number of positive outcomes have resulted. For example using adult fly tissue has allowed the development of this technique and the scoring system. To further develop this experimental technique new tissue types were examined.

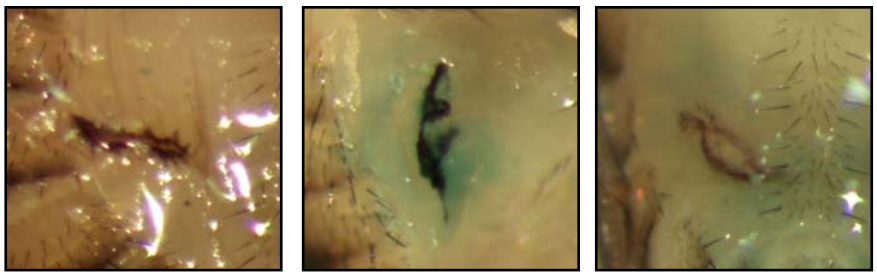

Figure 4.9: Fly strains wild type, SFN210 (pcm^5/pcm^5;; puc^{A251}/TM6TbSb) (n = 9) and SFN209 (+/+ *or* *w*/+ *;;* puc^{A251}/TM6TbSb) (n = 11) showing *puckered* expression patterns around a wound after 4 hours of healing. β galactosidase which is produced by LacZ expression breaks down the Xgal to produce galactose and 5-bromo-4-chloro-3-hydroxyindole. 5-bromo-4-chloro-3-hydroxyindole is oxidized into 5,5'-dibromo-4,4'-dichloro-indigo, an insoluble blue product. Therefore blue is seen at the location of the β galactosidase. This shows where the *puckered*LacZ fusion protein is produced after wounding.

4.6.2 β galactosidase staining of larvae

An earlier study investigating the expression patterns of the JNK signalling pathway after wounding in larvae, have shown staining in the nuclei of individual cells around the wound edge (Galko et al. 2004). In order to quantify the differences in JNK expression levels between the strains β galactosidase staining experiments using larvae were conducted. The idea was to count the number of cells away from the wound that the staining appeared. The further the staining spreads the more upregulated the JNK signalling pathway is after wounding for that strain.

The same genotypes were required for the larval staining as before in the fly staining experiments. When collecting the SFN209 (+/+ or w/+ *;;* puc^{A251}/TM6TbSb) control any larvae were picked as they are all the same genotype. For the SFN210 flies, homozygous *pacman* larvae (pcm^5/pcm^5;; puc^{A251}/TM6TbSb) were required. In order to pick these larvae the FM7i-ActinGFP balancer chromosome properties outlined in Method 2.4.2 and Section 3.1 were used. Larvae with genotypes containing the FM7i-actinGFP balancer are easily detected because they glow green under the fluorescence microscope. Homozygous *pacman* larvae do not contain the FM7i-actinGFP balancer and therefore will not glow green. They are instead an orange colour which is the result of auto-fluorescence from their gut.

Larval staining experiments were conducted as described in Method 2.11.2. To allow the staining solution to enter the thick cuticle of the larvae, a small cut was inflicted on the opposite side from the wound after the healing time. Also larvae were incubated overnight in staining solution as oppose to 5 hours for flies to maximize the resulting stain.

Initial control experiments looked encouraging, as the previously described nuclei staining (Galko et al. 2004) can be seen in Figure 4.10 with SFN209 (+/+ or w/+ *;;* puc^{A251}/TM6TbSb) larvae. Specific endogenous β galactosidase activity can also be seen in the gut which is protruding from the cut needed to allow the

staining solution to enter the cuticle. This did not allow for clear pictures so an alternative plan was designed. Larvae were dissected open after the overnight incubation in the staining solution. This required cutting the larvae completely open down the opposite side from the original wound and then scraping out all the internal organs. This meant only the cuticle was left and this was mounted on a coverslip.

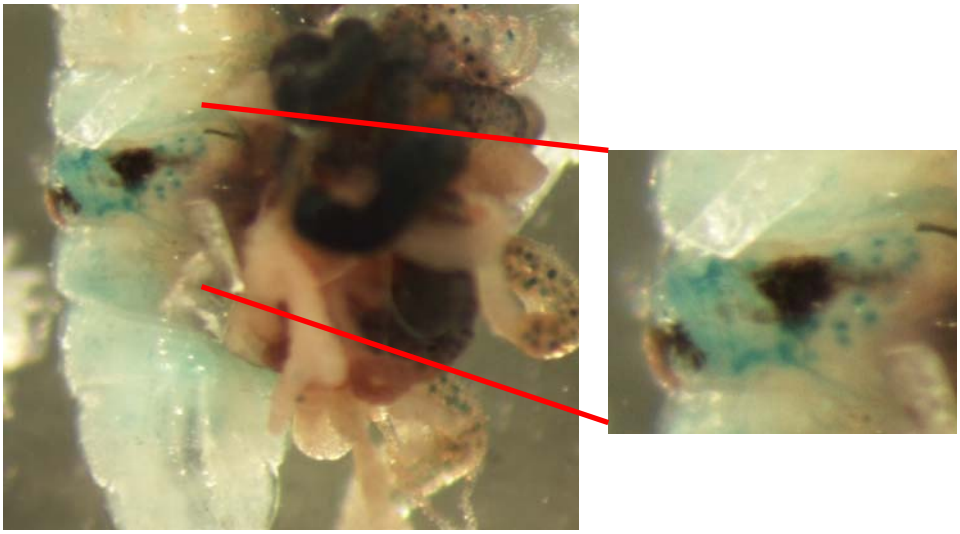

Figure 4.10: Control β galactosidase staining experiment using SFN209 (+/+ or w/+ *;; puc*^{A251}/TM6TbSb) flies. Individual cell nuclei can be seen stained blue (enlarged area). The larval gut can be seen protruding from the cut on the side of the larvae.

Using the revised dissection technique nuclei staining can be seen (Figure 4.11) for both the control (+/+ or w/+ *;; puc*^{A251}/TM6TbSb) and double mutant larvae (*pcm*^{5}/*pcm*^{5};; *puc*^{A251}/TM6TbSb). Figure 4.11 shows examples of the best staining pictures for each strain. It was observed that the majority of the samples had very little or no nuclei staining. More often the staining was seen as a 'smudge' around the wound similar to those staining patterns seen in the adult flies. By applying the scoring system developed using adult flies the results suggest slightly more staining around the wounds of the double mutants. Therefore more *pucLacZ* expression in *pacman* mutants may suggest a mutation in *pacman* leads to an increase in JNK signalling at the wound site. Further quantification of β galactosidase staining in *pacman* mutants is required to confirm this hypothesis. Although fly and larval tissue were helpful for developing the earlier steps of the technique, these tissues did not allow for accurate quantification therefore a new approach was required.

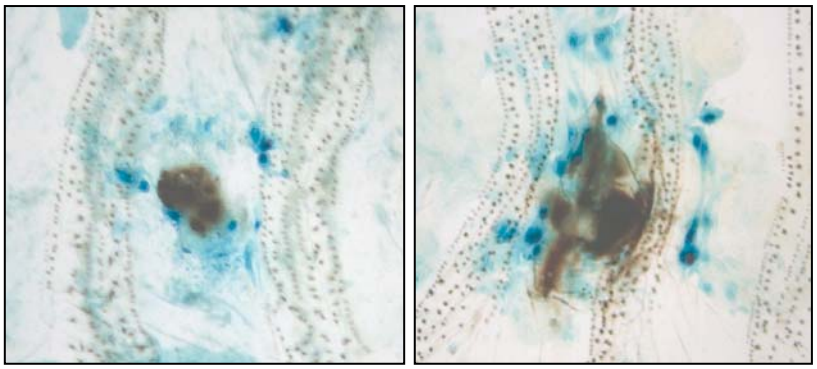

SFN209 **SFN210**

Figure 4.11: Photos of larval β galactosidase staining for SFN209 single *puckered* mutant control (+/+ or w/+ *;; puc*^{A251}/TM6TbSb) and SFN210 *pacman/puckered* double mutant (*pcm*^{5}/*pcm*^{5};; *puc*^{A251}/TM6TbSb) cuticles. Blue stain shows β galactosidase expression which indicates where the JNK signalling pathway is expressed after wounding. Black mark is the clot formed at the wound site.

4.6.3 β galactosidase staining of wing imaginal discs

Previous attempts to visualise the expression levels of the JNK signalling pathway in *pacman* mutants using *puc*LacZ induced β galactosidase staining prove inconclusive. The next step was to observe and quantify an example of the natural expression of the JNK signalling pathway. During larval development the morphogenetic process thorax closure occurs, this involves the fusing of the two wing imaginal discs. This process requires the cells near the top of the disc to spread together and fuse (Agnes et al. 1999; Zeitlinger et al. 1999). Imaginal discs are found only at the larval stage, they are small sacs of cells that go on to produce the adult structures during morphogenesis such as wings, legs, halters and eyes. A study by Agnes et al in 1999 showed that the JNK signalling pathway is required for the correct morphogenesis of the imaginal discs. *Puckered* is expressed in cells at the dorsal side of wing, leg, haltere and eye imaginal discs. The exact location of the cells expressing *puc* is the border between the peripodial and columnar epithelia (Figure 4.12) (Agnes et al. 1999).

Previous studies (Figure 4.12) have shown *puckered* is naturally expressed in imaginal discs (Agnes et al. 1999) therefore the expression patterns of *puckered* in *pacman* mutant strain imaginal discs were investigated. Wing imaginal discs were chosen as the tissue type since they are the largest imaginal disc and therefore the easiest to dissect. It is also known that *pacman* mutations affect thorax closure of which the wing imaginal discs play a role.

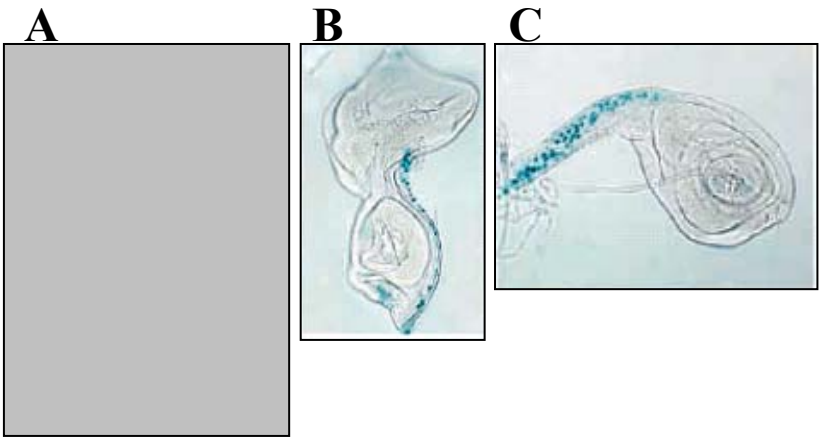

Figure 4.12: Pictures show *puckered* expression in imaginal discs using LacZ staining of the enhancer trap puc^{E69}. Adapted from Agnes et al, 1999. Imaginal discs: **A** = wing disc, **B** = haltere disc and **C** = leg disc.

The same genotypes of larvae were collected for imaginal disc staining as those for the larval staining i.e. control SFN209 (+/+ or w/+ *;; puc*^{A251}/TM6TbSb) larvae (wild type for *pacman* and heterozygous for *puc*LacZ) (n = 52) and SFN210 (*pcm*^{5}/*pcm*^{5};; *puc*^{A251}/TM6TbSb) larvae (homozygous *pacman* and heterozygous *puc*LacZ) (n = 43). The technique for the wing disc dissection is outlined in Method 2.11.3. The discs were incubated overnight as this time was convenient and it did not lead to any over staining. The wing discs were photographed on the Zeiss Axioplan microscope using a 10x plan-neofluar objective. Using the programme AxioVision Release 4.6 an outline was drawn around the perimeter of the disc and perimeter length, the area of the disc and the blue density within the disc were among the data calculated.

β galactosidase staining can be seen at the peripodial epithelium of the SFN210 (*pcm*^{5}/*pcm*^{5};; *puc*^{A251}/TM6TbSb) and SFN209 (+/+ or w/+ *;; puc*^{A251}/TM6TbSb) wing imaginal discs (Figure 4.13). Thus *puckered* and the JNK signalling pathway are naturally expressed at this region of the disc which is consistent with previous data (Agnes et al. 1999).

Wild type	210	209
	pcm^{5}/*pcm*^{5};;	+/+ or w/+ ;;
	puc^{A251}/TM6TbSb	*puc*^{A251}/TM6TbSb

Figure 4.13: β galactosidase staining of the wing imaginal discs of SFN210 (*pcm*^{5}/*pcm*^{5};; *puc*^{A251}/TM6TbSb) and SFN209 (+/+ or w/+ ;; *puc*^{A251}/TM6TbSb) compared to wild type flies. Wild type flies do not carry the *puc*LacZ enhancer trap therefore show no staining. The blue stain for SFN210 and 209 shows the expression patterns of LacZ under the control of an enhancer trap *puc*^{A251}. Therefore the blue stain relates directly to the expression of *puckered* and the JNK signalling pathway in the wing imaginal discs.

At first glance it is difficult to determine whether there is a difference in quantity of staining between the wing imaginal discs of the two strains. To determine whether a mutation in *pacman* effects the expression levels of *puckered* and the JNK signalling pathway, the mean blue density was compared within the wing imaginal discs for SFN210 (pcm^5/pcm^5;; puc^{A251}/TM6TbSb) and SFN209 (+/+ or w/+ ;; puc^{A251}/TM6TbSb). This was performed by capturing the images on a Zeiss Axioplan microscope, drawing around each disc and then using the Axiovision programme to measure the amount of blue colour within each imaginal disc. The wing disc area was also calculated. For each strain the average blue density was calculated (Table 4.2) and displayed in a histogram (Figure 4.14 Graph 1). The histogram shows an increase in the levels of β galactosidase staining in SFN209 imaginal discs compared to SFN210 discs. This could suggest a decrease in *pucLacZ* expression and therefore the JNK signalling pathway in *pacman* mutants.

Interestingly another observation resulting from the staining experiments is shown in the second histogram of Figure 4.14 Graph 2. When the average areas of the imaginal discs for wild type, SFN210 and SFN209 were compared (Table 4.2), SFN210 (pcm^5/pcm^5;; puc^{A251}/TM6TbSb) larvae were shown to have smaller wing imaginal discs. This is consistent with previous findings by Carol Roberts in the Newbury group which showed *pacman* mutant adult flies have smaller wings. This reduction in average area for SFN210 could account for the decreased average blue density seen within these discs. This could suggest an additional role for *pacman* in the development of the imaginal disc at an earlier stage than thorax closer, possibly a role in cell growth and movement during the development of the imaginal discs.

Graph 1

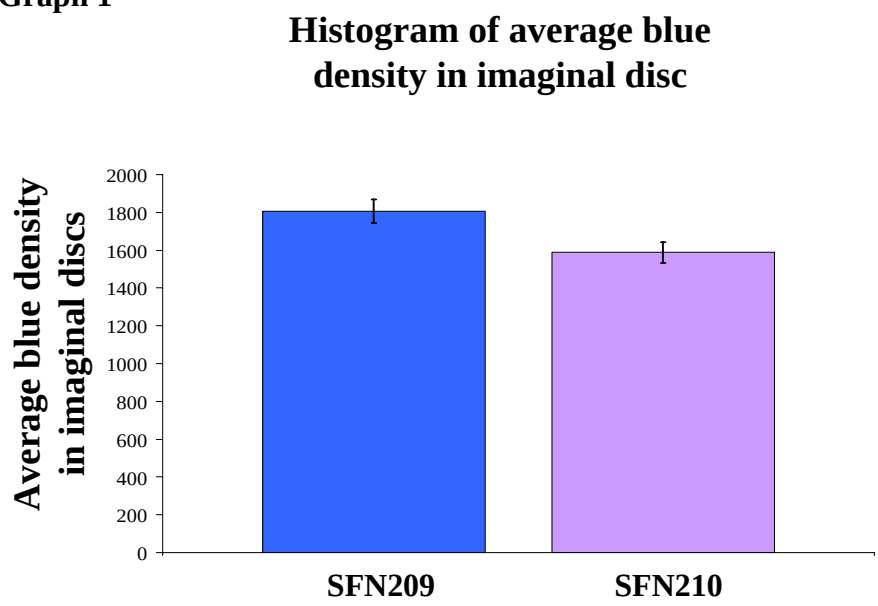

Graph 2

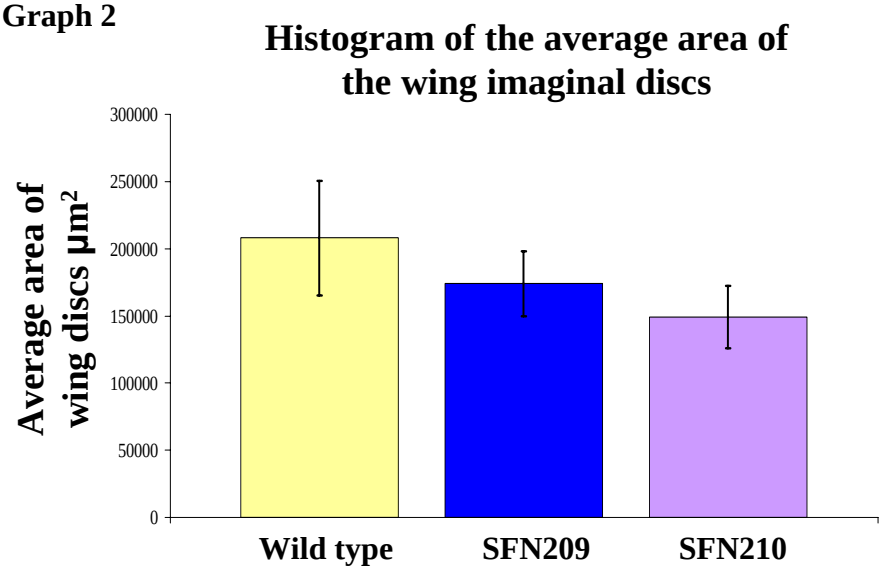

Figure 4.14: Graph 1 compares the average blue density in imaginal discs for SFN209 (+/+ or w/+ *;; puc*^{A251}/TM6TbSb) and SFN210 (*pcm*^{5}/*pcm*^{5};; *puc*^{A251}/TM6TbSb). (One Way ANOVA $F_{1,74} = 0.18$, $P = 0.674$) Graph 2 compares the average area of imaginal discs for wild type, SFN209 (+/+ or w/+ *;;* *puc*^{A251}/TM6TbSb) and SFN210 (*pcm*^{5}/*pcm*^{5};; *puc*^{A251}/TM6TbSb). All error bars represent the standard errors. Wild type n = 24, SFN209 n = 52 and SFN210 n = 43. (One Way ANOVA $F_{2,83} = 4.79$, $P = 0.0111$)

	SFN209	**SFN210**
Average blue density	1805.735	1588.56
Average Area	174091.4375 μm^2	149279 μm^2
Average density when imaginal discs are the same size	1548.372	1588.56

Table 4.2: Table shows SFN209 (+/+ or w/+ *;;* puc^{A251}/TM6TbSb) and SFN210 (pcm^5/pcm^5;; *pucA251*/TM6TbSb) imaginal disc values for the average blue density, average area of imaginal disc and average blue density when the imaginal discs are considered the same size. Area measured in μm^2 and blue density measured in grey units using the AxioVision Release 4.6 computer programme. SFN209 (+/+ or w/+ *;;* $puc^{A251/}$TM6TbSb) n = 52 and SFN210 (pcm^5/pcm^5;; puc^{A251}/TM6TbSb) n = 43.

The histograms in Figure 4.14 show that there is more than one variable when comparing the wing imaginal discs for SFN210 (*pcm*^{5}/*pcm*^{5};; *puc*^{A251}/TM6TbSb) and SFN209 (+/+ or w/+ *;; puc*^{A251}/TM6TbSb). In order to make a direct comparison a variable must be eliminated. When comparing the β galactosidase staining in the SFN210 and SFN209 imaginal discs the average areas must be normalized i.e. the same for both strains. Therefore the ratio of the average areas was calculated. Using this ratio the normalized average blue density for each strain was evaluated (Table 4.2).

This data displayed in the histogram in Figure 4.15 correlates with earlier staining experiments, there is an increase in β galactosidase staining in SFN210 (*pcm*^{5}/*pcm*^{5};; *puc*^{A251}/TM6TbSb) larvae and imaginal discs. It is interesting that these imaginal discs are smaller but still have more β galactosidase staining than the SFN209 (+/+ or w/+ *;; puc*^{A251}/TM6TbSb) imaginal discs. These β galactosidase staining results suggest there is increase in the expression of *puckered* when *pacman* is mutated. The *pucLacZ* transgene is a transcriptional reporter for the expression of the JNK signalling pathway therefore this also suggests an increase in the expression of the JNK signalling pathway. This is not consistent with the hypothesis that Pacman degrades *puckered* mRNA. If this were true in *pacman* mutants there would be more Puckered which would act through the negative feedback loop to downregulate the JNK signalling pathway. However the JNK signalling pathway appears to be upregulated in *pacman* mutants suggesting a possible role for *pacman* in inhibiting the pathway.

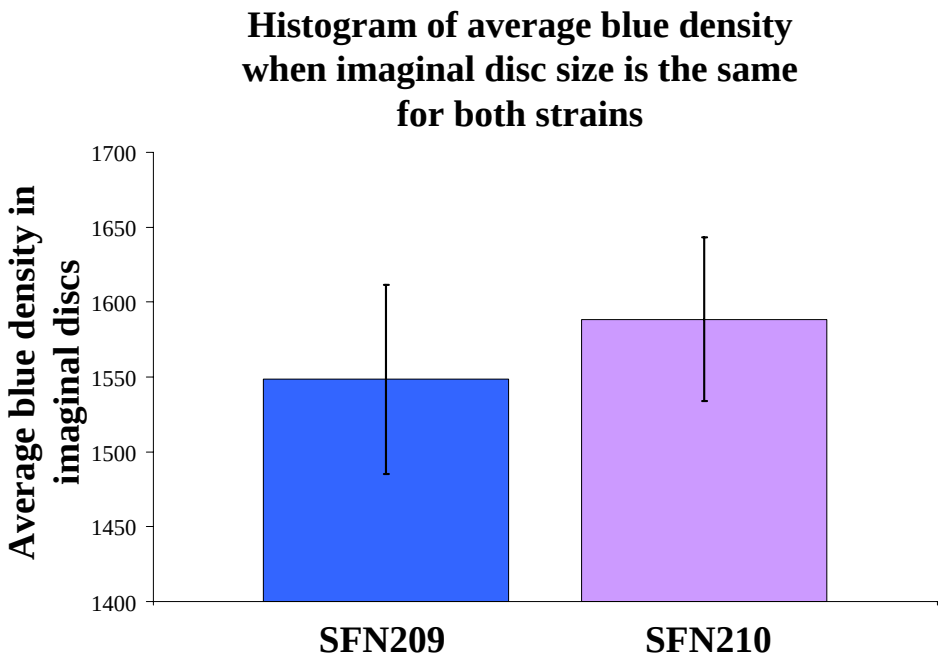

Figure 4.15: The average blue density when the imaginal discs for each strain are the same size. All error bars represent the standard errors. SFN209 (+/+ or w/+ ;; puc^{A251}/TM6TbSb) n = 52 and SFN210 (pcm^5/pcm^5;; puc^{A251}/TM6TbSb) n = 43.

4.7 Chapter Conclusions

The creation of the *pacman puckered* double mutants resulted in unique mutant phenotypes which suggest a genetic interaction between *pacman* and *puckered* and therefore also the JNK signalling pathway. Wounding of the *pacman puckered* double mutants showed these flies survive significantly better than the wild type control at 25˚C. This suggests a mutation in *puckered* can rescue the wound healing defects seen in *pacman* mutant flies. It would be interesting to see if overexpressing *pacman* with the *puckered* mutation could rescue the mutant phenotypes of curled wings and bald patch seen in the *pacman* and *puckered* double mutant. This could be possible future work. Since flies overexpressing *pacman* still show a reduction in survival after wounding it would be predicted that overexpressing *pacman* with a *puckered* mutation would rescue the curled wings and bald patch phenotypes.

If Pacman down regulates the JNK signalling pathway through degradation of *puckered* mRNA then *pacman* mutants will have more *puckered* mRNA which could lead to the reduction in survival of these flies after wounding (Section 3.2). In the *pacman puckered* double mutants there is presumably no increase in *puckered* therefore no reduction in survival. Therefore this result is consistent with the hypothesis (Figure 4.1) that Pacman degrades *puckered* mRNA to regulate the JNK signalling pathway.

Alternatively, *pacman* may be enhancing the longevity phenotype of the *puckered* heterozygotes. Previously heterozygous *puckered* mutants have been shown to live longer (Wang et al. 2003; Wang et al. 2005). What is being measured in these experiments is actually survival rather than wound healing itself. Therefore if survival is independent of wound healing then the *pacman puckered* double mutants could be surviving for longer even if their wounds are not healing so well. In this case the unwounded double and single mutants both heterozygous for the *puckered* mutation would be expected to survive better than the wild type. This is consistent with the results in this thesis. It is therefore possible that the

properties of the *puckered* heterozygotes can explain the increased survival of the wounded flies. Further experiments are needed to confirm this conclusion.

To further characterize the genetic interaction between *pacman* and *puckered* β galactosidase staining experiments in flies, larvae and imaginal discs were performed. The β galactosidase staining experiments have once again confirmed a genetic interaction between *pacman* and *puckered* and hence the JNK signalling pathway which was first observed by looking at the phenotypes of the double mutant cross. The results suggest that there is an increase in expression of the JNK signalling pathway when *pacman* is mutated. This is not consistent with the proposed hypothesis that Pacman regulates the pathway by degrading *puckered* mRNA. If the hypothesis were true and Pacman degrades *puckered* mRNA then in *pacman* mutants we would expect the expression of the JNK signalling pathway to decrease due to more Puckered acting on the negative feedback loop to downregulate the pathway. The results suggest a role for Pacman in inhibiting the JNK signalling pathway. Therefore it is possible that Pacman may target the mRNA(s) of another gene(s) of the pathway or an upstream activator which leads to downregulation of the JNK pathway. The next step is therefore to quantify the changes in expression of the JNK signalling pathway when *pacman* is mutated.

Chapter 5 Effects of *pacman* mutations on the JNK signalling pathway.

In the previous two chapters it has been shown that *pacman* mutations reduce survival after wounding and that *pacman* genetically interacts with *puckered*, a member of the JNK signalling pathway. This pathway was shown to have a slight increase in expression levels during larval development in *pacman* mutants. This increase in expression levels was also seen when the JNK expression was induced by wounding and seems to imply that *pacman's* normal role is to have an inhibiting effect on the JNK signalling pathway (Chapter 4). The previous hypothesis that Pacman degrades *puckered* mRNA does not stand true after β-galactosidase staining experiments showed the JNK signalling pathway increases in *pacman* mutants. Therefore the alternative hypothesis was put forward that *pacman* degrades the mRNA of another gene member of the JNK signalling pathway or an upstream activator. This final results chapter concentrates on quantifying the changes in expression levels of the JNK signalling pathway in *pacman* mutants compared to the levels in control flies that are wild type for *pacman*.

5.1 Western Blotting experiments

5.1.1 Optimization of the Western blotting technique for larval tissue type

Western Blotting experiments were used to examine the expression levels of proteins encoded by the JNK signalling pathway. Previously in the Newbury group Western blotting experiments were used to show the levels of the truncated *pacman* protein produced in pcm^3, pcm^5 and pcm^6 mutants (Grima 2002). The *pcm* protein has a molecular mass of 184.5kDa. Bands were seen on a Western blot for pcm^3 and pcm^6 at size 167.7kDa and 160.0kDa respectively. Little or no band has been seen for pcm^5 (149.2kDa) suggesting this mutant allele has the least *pcm* expression (Figure 1.9) (Zabolotskaya et al. 2008).

Chapter 5: Effects of *pacman* mutations on the JNK signalling pathway

To correspond with previous chapters the following experiments were performed using larvae. Previous experiments in the lab (by Dr. Dominic Grima) had shown that female flies carrying 1 copy of the mutated *pacman* gene had thorax closure defects, most likely resulting from perturbations in the JNK signalling pathway (Grima 2002). As explained earlier thorax closure starts during L3 larval development, therefore there is a natural increase in JNK signalling during this stage. If *pacman* affects the JNK signalling pathway, an effect on this natural increase in JNK signalling would be expected. The new *pacman* mutant strains outlined in chapter 3 were used to distinguish homozygous *pacman* mutants from heterozygous. The *pacman* mutations in these strains are balanced over FM7i which contains the Green Fluorescent Protein sequence fused to Actin. Therefore *pacman* homo- or hemizygotes, which do not carry this balancer chromosome, can be distinguished by their lack of fluorescence. Homozygous *pcm* L3 larvae were used for all Western blotting experiments and were collected using the Leica MZ16F fluorecence microscope with a long pass- autofluorescence GFP filter as described in Method 2.4.3. The experimental design was modified for larvae and each step of the fly Western blotting technique was optimized.

The first stage of optimization was deciding how much tissue to use as a starting product. In previous fly Westerns 10 whole flies were homogenized in 150µl of loading buffer. Therefore 10 larvae in the same volume of loading buffer was adopted as a starting volume. This resulted in a solution covered in a layer of fatty tissue. This solution was centrifuged twice rather than once to allow for extra removal of fatty produce. Several different volumes of loading buffer 40µl, 100µl, 150µl and 200µl were tested to see which gives the clearest bands at the end (Figure 5.1). The final volume utilized was 150µl as this was enough solution to homogenize the sample and also gave a good clear band during visualization.

The next issue to tackle was the electrophoresis step. 10% Bis-Tris gels (Invitrogen) were used to run the samples since this allowed for a good spread of the middle protein sizes which included the 45kDa band of the loading control Actin. Each gel was run for 1hr and 15mins.

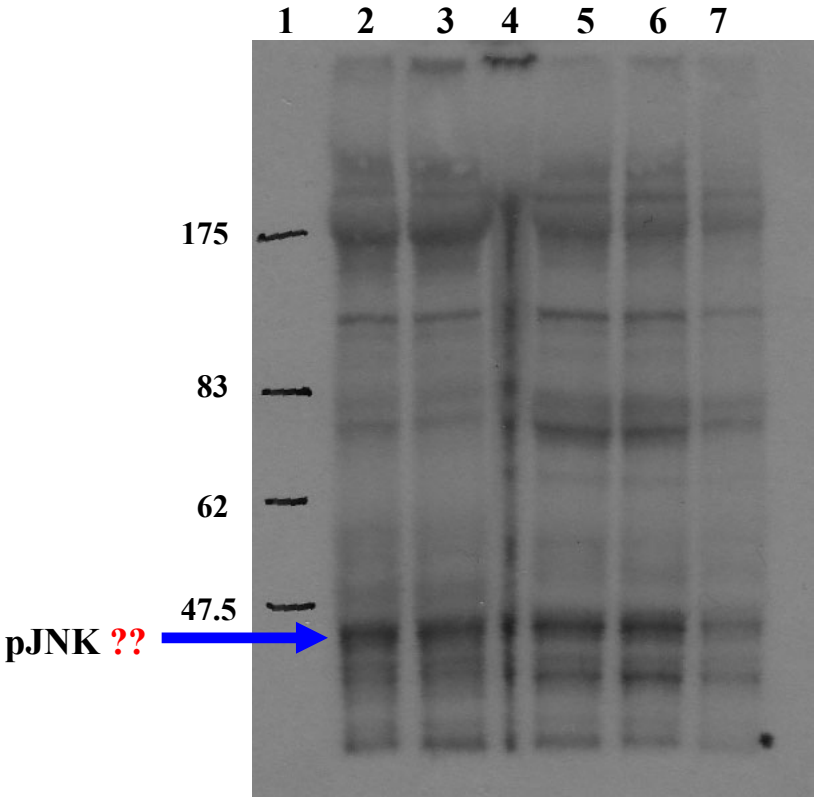

Figure 5.1: Western Blotting experiment to test different volumes of loading buffer used to homogenise samples of 10 larvae. Antibody used pJNK (G7) from Santa Cruz Biotechnology. Lanes: **1** is the prestained protein marker. **2** and **3** are wild type fly samples each containing 10 flies in 150µl of loading buffer. **4-7** contain 10 larvae samples homogenised in different volumes of loading buffer (40µl, 100µl, 150µl and 200µl respectively). → represents the pJNK band of 46-54kDa. The sample containing 40µl was smeared suggesting this volume is too small for correct homogenisation.

All the primary antibodies used for the Western blotting experiments needed overnight incubations. This meant changing the gel transfer procedure as this is normally performed overnight. All Western blotting experiment gels were transferred for 1hr at 100V to allow for the overnight primary incubation. The use of Amersham ECL™ Advance Western Blotting Detection Kit was implemented during the course of the Western blotting experiments. This kit is 10 times more sensitive than the normal ECL detection kit and allowed detection even at low antibody concentrations. This was used for several of the antibodies which cut the film exposure time for example from 45mins to 1min for the anti-JNK antibody from Sigma. Another adaptation to the original technique involved the secondary antibody dilutions. Secondary antibodies were initially used at 1:5000 however this resulted in background on the film. Thus the dilution was changed to match the secondary for the Actin antibody which was 1:80000. This modified Western blotting technique for larvae is outlined in Method 2.12. Antibody dilutions and film exposure times for each antibody are described in each relevant chapter section. During the Western blotting experiments to detect JNK and c-Jun protein levels there was an issue of possible cross reactivity between the Actin, JNK and c-Jun antibodies. These proteins are all between 45-55kDa in size. To prevent cross reactivity of these antibodies 2 separate gels were ran together. Each gel had the same samples and underwent the same conditions except one was washed in Actin antibody and the other in JNK or c-Jun antibody.

5.1.2 Western Blotting experiments using the anti-β-galactosidase antibody

A simple way to measure the activity of the JNK signalling pathway would be Western blotting experiments using an anti-β-galactosidase antibody with the new *pacman*/*puckered* double mutant flies. The monoclonal anti-β-galactosidase antibody reacts specifically with *E.coli* β-galactosidase expressed by the LacZ gene. The intent was to use this as an indicator of the expression of the fusion protein containing *puckered*. As described in chapter 4 pcm^5/pcm^5;; puc^{A251}/TM6TbSb double mutants carry one copy of a *pucLacZ* fusion protein. Therefore the expression of the *pucLacZ* would show the expression levels of the

JNK signalling pathway. A Western blotting experiment was set up using SFN210 homozygous *pcm*, heterozygous *puc* larvae (pcm^5/pcm^5;; puc^{A251}/TM6TbSb), SFN209 heterozygous *puc* larvae (+/+ or w/+ *;;* puc^{A251}/TM6TbSb) and wild type larvae. No band should be present in the wild type lane as this strain does not contain the LacZ gene. SFN209 and SFN210 should both have bands around 120kDa (LacZ 116kDa and ~ 10 kDa of *puckered* fragment) because they do contain the LacZ gene and hopefully they would be a difference in band intensity to indicate different expression levels of the JNK signalling pathway between larvae that are wild type or mutant for *pacman*.

The Western procedure was described in Method 2.12. The antibody dilutions for anti-β-galactosidase started at 1:5000 for the primary and 1:80000 for the secondary (anti mouse IgG alkaline phosphatase). Actin was used as a loading control, the dilutions for this antibody were as described in Method 2.12.4. Using the described dilutions no bands were seen even after 45mins of exposure to the ECL solution. Next the primary antibody was diluted 1:1000 and the ECL Advance Detection Kit used. The results were not as expected (Figure 5.2). Several bands were seen in all 3 lanes however there did not seem to be any that were only present in the lanes for SFN209 (+/+ or w/+ *;;* puc^{A251}/TM6TbSb) and SFN210 (pcm^5/pcm^5;; puc^{A251}/TM6TbSb) or any that corresponded with the β-galactosidase protein size.

These results, several bands in all the lanes, suggest that the antibody is not specific. This antibody has not been used in *Drosophila* before and was unfortunately not suitable for this use. The anti-β-galactosidase Western blotting experiments allowed the further development of the Western blotting technique using larvae to measure the JNK signalling pathway expression levels. Following these results the focus of the Western blotting experiments was altered to measure the JNK signalling expression levels directly by using an antibody specific to a member of the pathway itself. The results for the rest of this section detail the challenges in finding the best antibodies to measure the JNK signalling expression.

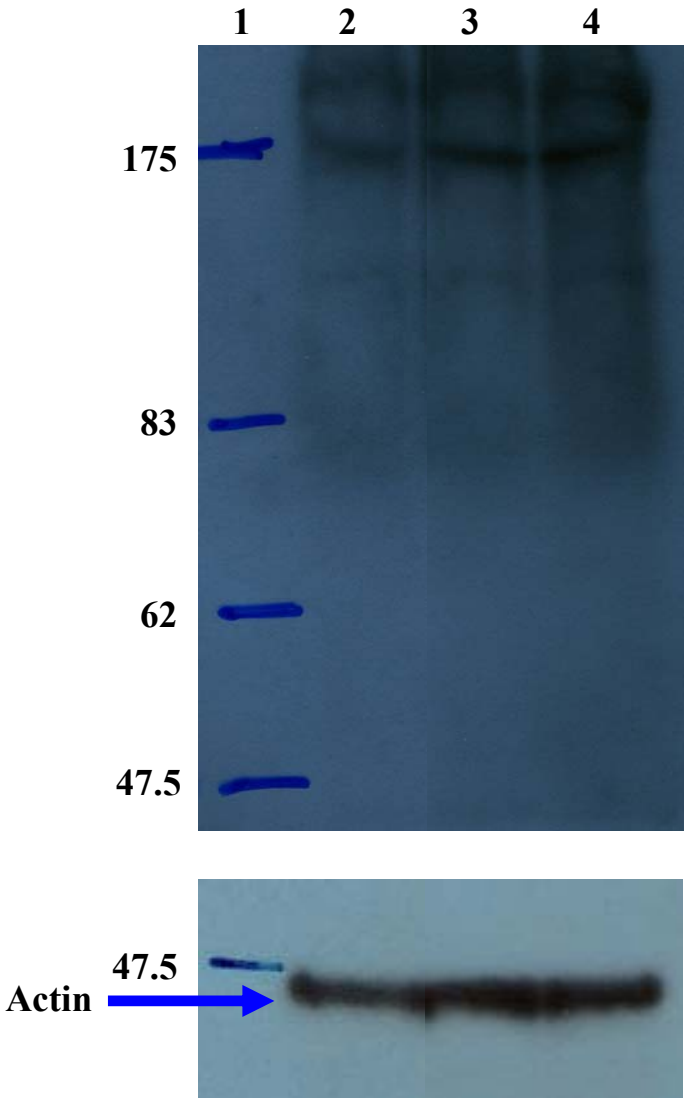

Figure 5.2: Western Blotting experiment using anti-β-galactosidase antibody to quantify the level of *pucLacZ* fusion protein expression and therefore JNK signalling expression in *pacman* mutants. Lanes: **1** = prestained protein marker, **2** = wild type larvae, **3** = 209 heterozygous *puc* larvae (containing the *pucLacZ* fusion protein) and **4** = 210 homozygous *pcm,* heterozygous *puc* larvae (containing the *pucLacZ* fusion protein). Several bands are seen but none seem to correspond to the *pucLacZ* protein size (~120kDa). The loading control actin is shown below at 45kDa.

5.1.3 Western Blotting experiments using c-Jun, pJun63 and pJun73 antibodies

In order to measure the expression levels of the JNK signalling pathway in *pacman* mutants, Western blotting experiments were performed using antibodies to a protein encoded by a gene of the pathway. Ideally an antibody to Puckered would be best as the hypothesis is that Pacman is interacting with Puckered. However no commercial Puckered antibody is available. Antibodies to alternative proteins encoded by other genes in the JNK signalling pathway were purchased. The first gene investigated was *DJun*, this encodes a transcription factor which forms a dimer with another transcription factor D-FOS producing the AP-1 complex (Kockel et al. 2001; Ciapponi et al. 2002). *DJun* is the *Drosophila* homologue of the mammalian *c-jun*. This complex regulates the expression of *puckered* and *decapentaplegic* (Stronach 2005). The transcriptional activity of c-Jun is regulated by phosphorylation at Ser63 and Ser73. A phospho-plus c-Jun antibody kit was available from NEB which can be used to detect the phosphorylation status of c-Jun and therefore the activation of the JNK signalling pathway. The kit contains monoclonal IgG anti c-Jun, polyclonal IgG anti phospho c-Jun (Ser63) and polyclonal IgG anti phospho c-Jun (Ser73). The c-Jun antibody detects total c-Jun protein levels regardless of phosphorylation state, un-phosphorylated c-Jun (43kDa) and phosphorylated c-Jun (48kDa). Both anti phospho c-Jun Ser73 and Ser63 detect the phosphorylated c-Jun (48kDa). These antibodies were produced against the human form of c-Jun and had not before been tested in *Drosophila*. In these Western blotting experiments the level of phosphorylated c-Jun will correlate to the level of expression of the JNK signalling pathway. The monoclonal anti c-Jun in this case is used as a control.

As outlined earlier these Western blotting experiments were performed using larvae with the following genotypes: homozygous and heterozygous SFN164 (pcm^5), SFN167 (pcm^3), SFN168 (pcm^6) and a wild type control. The Western blotting technique was as described in Method 2.12. Antibody dilutions for all three primary antibodies were 1:5000 and the secondary antibody anti rabbit peroxidase was 1:80000. Antibody incubations were overnight for the primary

antibodies and 1 hour for the secondary antibody. Separate gels were used to avoid cross reactivity between the antibodies.

A band was expected around 47-50 kDa in size for each antibody. Figure 5.3 has an example blot for each antibody (c-Jun n = 3, pc-Jun73 and pc-Jun63 n = 2). Several bands were present including a band of around 48kDa is seen for all strains for each antibody. In order to quantify these bands the 2nd membrane was probed with an antibody to a loading control, Actin. Actin is used as a reference of how much protein is present in each sample.

Measurements of the intensity of the DJun and Actin bands were taken. The amount of DJun i.e. the expression level of DJun, for each strain was then calculated as a ratio of the amount of Actin present in the sample. These values for each strain were highly variable and when the average expression level for each was calculated and displayed in a histogram some of the standard errors were large (Figure 5.4). We would expect the average expression levels to be roughly the same for each antibody i.e. the levels all decrease or increase in *pacman* mutants compared to wild type larvae. The anti c-Jun measures total c-Jun protein levels so these values may be slightly higher than the pc-Jun73 and pc-Jun63 measurements. When the histograms are examined there doesn't appear to be a consistent trend of average expression levels for each strain across the different antibody types.

As mentioned earlier the c-Jun antibody kit was designed using a peptide from the human c-Jun sequence. This may explain the inconsistency of the antibody in the *Drosophila* larvae in that it may not be very specific and could be binding to other proteins. At this stage it was decided to discontinue the use of this kit and find an alternative gene of the JNK signalling pathway to target. Although this kit did not allow for actual quantification of the JNK signalling pathway expression levels it did allow further optimization of the Western blotting procedure needed.

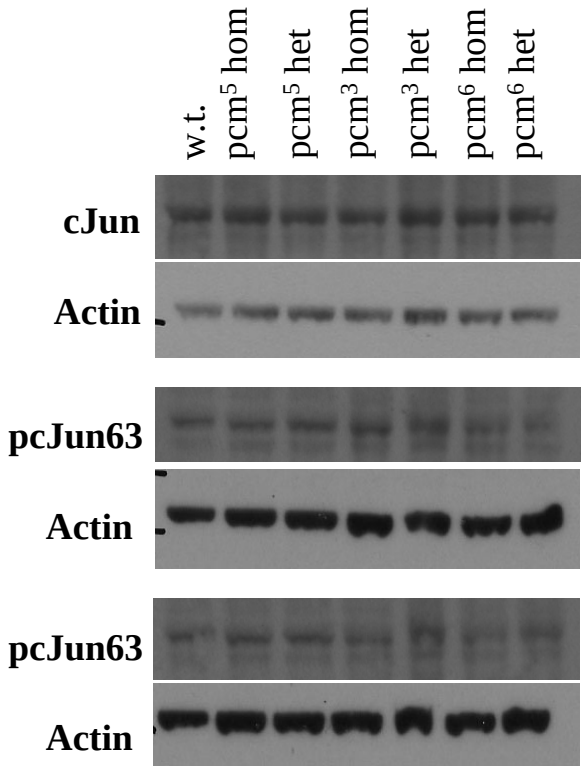

Figure 5.3: Western blotting experiments to determine the levels of the JNK signalling pathway using antibodies cJun, phospho cJun63 and phospho cJun73 from Cell Signalling Technology. Bands of between 47-50 kDa are expected for these antibodies. Actin is the loading control and has a band size of 45kDa. (c-Jun n = 3, pc-Jun73 and pc-Jun63 n = 2).

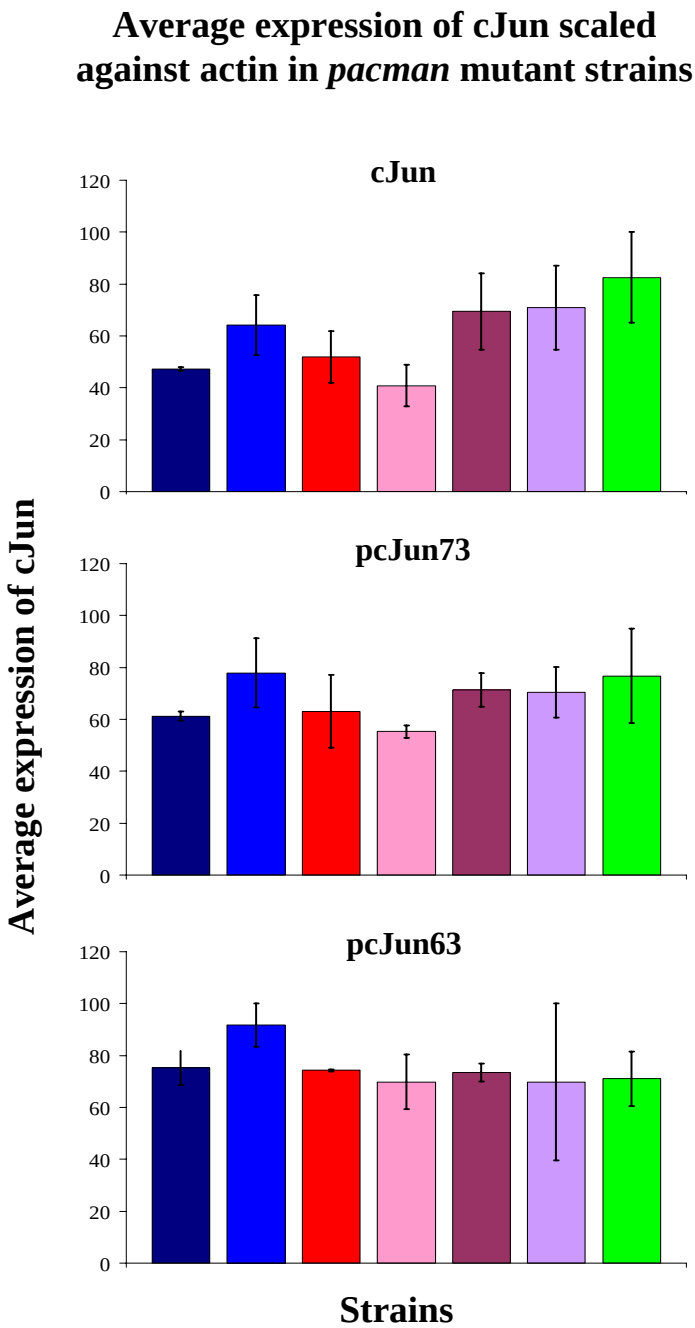

Figure 5.4: Histograms showing the average expression levels of cJun, pcJun73 and pcJun63 (Cell Signalling Technology) scaled against Actin in *pacman* mutants compared to wild type larvae. Error bars represent the standard error. Key: pcm^3 homozygous, pcm^3 heterozygous, pcm^5 homozygous, pcm^5 heterozygous, pcm^6 homozygous, pcm^6 heterozygous and wild type larvae. cJun n = 3, pcJun73 and pcJun63 n = 2.

5.1.4 Western Blotting experiments using the phosphorylated JNK antibody

In this section the search for a suitable antibody to a gene of the JNK signalling pathway continued. Several antibodies were tested and eliminated from use due to poor specificity in *Drosophila.* There were many commercially available antibodies to the human form of JNK/c-Jun N-terminal kinase (MAPK) thus this seemed like a sensible next step. The *Drosophila* homologue of JNK is the gene *basket*. This gene encodes a kinase that phosphorylates and activates the *c-Jun*/*cFos* AP-1 complex. The *Drosophila* homologues of the AP-1 complex components are DJun and Kayak. *basket* itself is activated by diphosphorylation at two sites Thr^{181} and Tyr^{183} by the kinase *hemipterous* (JNKK). These sites correspond to Thr^{183} and Tyr^{185} for the human form of JNK. JNK/Basket is also involved in the negative feedback loop of the JNK pathway. The phosphatase Puckered dephosphorylates Basket i.e. deactivates, leading to a reduction in expression of the JNK pathway (Ring et al. 1993; Glise et al. 1997; Martin-Blanco 1997; Martin-Blanco 1998; Noselli et al. 1999; Xia et al. 2004; McEwen et al. 2005). Western blotting experiments showing JNK signalling pathway expression in wounded *Drosophila* epidermis were attempted by Ramet at al. They used anti JNK antibodies from Santa Cruz Biotechnology and Promega (Ramet et al. 2002). The human isoforms JNK1, JNK2 and JNK3 produce band sizes of 46kDa, 54kDa and 49kDa respectively during Western blotting. Therefore a *basket* band in *Drosophila* Western blotting experiments is expected between these sizes. Flybase, a useful reference tool for *Drosophila* researchers suggests a BASKET band size of 49kDa. Separate gels were used to avoid cross reactivity between the JNK antibodies and the Actin antibody.

The first JNK antibody used for Western blotting experiments was from Santa Cruz Biotechnology, pJNK (G7), a monoclonal IgG antibody derived from mouse. This antibody detects the human, mouse, and rat forms of JNK1, JNK2 and JNK3 when they are diphosphorylated at sites Thr^{183} and Tyr^{185}. Antibody dilutions were used as stated in Ramet et al. These were 1:1000 for the primary antibody and 1:5000 for the secondary antibody which in this case was goat anti-

mouse IgG peroxidase (Sigma). Western blotting technique as outlined in Method 2.12. Film was exposed to the normal ECL mix for 10mins. Figure 5.1 and 5.5 show examples of Western blotting experiments using this antibody. Several dark bands are seen including one around the expected human JNK1 band size of 46kDa. However this suggests the Santa Cruz JNK antibody is not specific in *Drosophila*. This was also the case with the c-Jun antibodies.

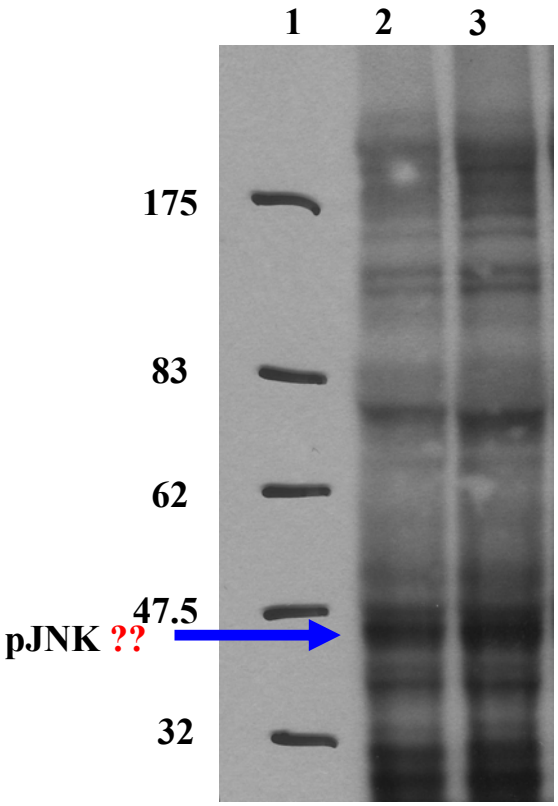

Figure 5.5: Western blotting experiment using the pJNK (G7) Santa Cruz Biotechnology antibody to quantify the expression level of the JNK signalling pathway. Lane **1** contains the prestained protein marker, **2** and **3** contain wild type samples. Several dark bands are seen including one around the expected band size 46kDa.

Alternative JNK antibodies antiACTIVE JNK from Promega and phospho SAPK/JNK from Cell Signalling Technology were received as free samples and tested. AntiACTIVE JNK is a polyclonal antibody derived from rabbit which detects the dually phosphorylated active form of JNK. Phospho SAPK/JNK is a monoclonal antibody derived from rabbit which detects levels of JNK only when both Thr^{183} and Tyr^{185} are phosphorylated. This antibody has been used for Western blotting experiments previously in human, mouse, rat and hamster.

The suggested antibody dilutions were followed for the Western blotting experiments. Promega recommended 1:5000 for the primary antibody and Cell Signalling technology recommended 1:1000. A 1:80000 dilution was used for the secondary antibody which was monoclonal anti rabbit peroxidase. Figure 5.6 shows the comparison between the two antibodies. After 27mins of exposure to the ECL mix no bands are seen at the expected JNK band size. After 30mins of exposure bands are seen at the correct size 46kDa for the human JNK1 in both antibodies. However neither antibody is particularly clear and several other bands are present as well. Again these additional bands are probably due to the reduced specificity of these antibodies in *Drosophila*.

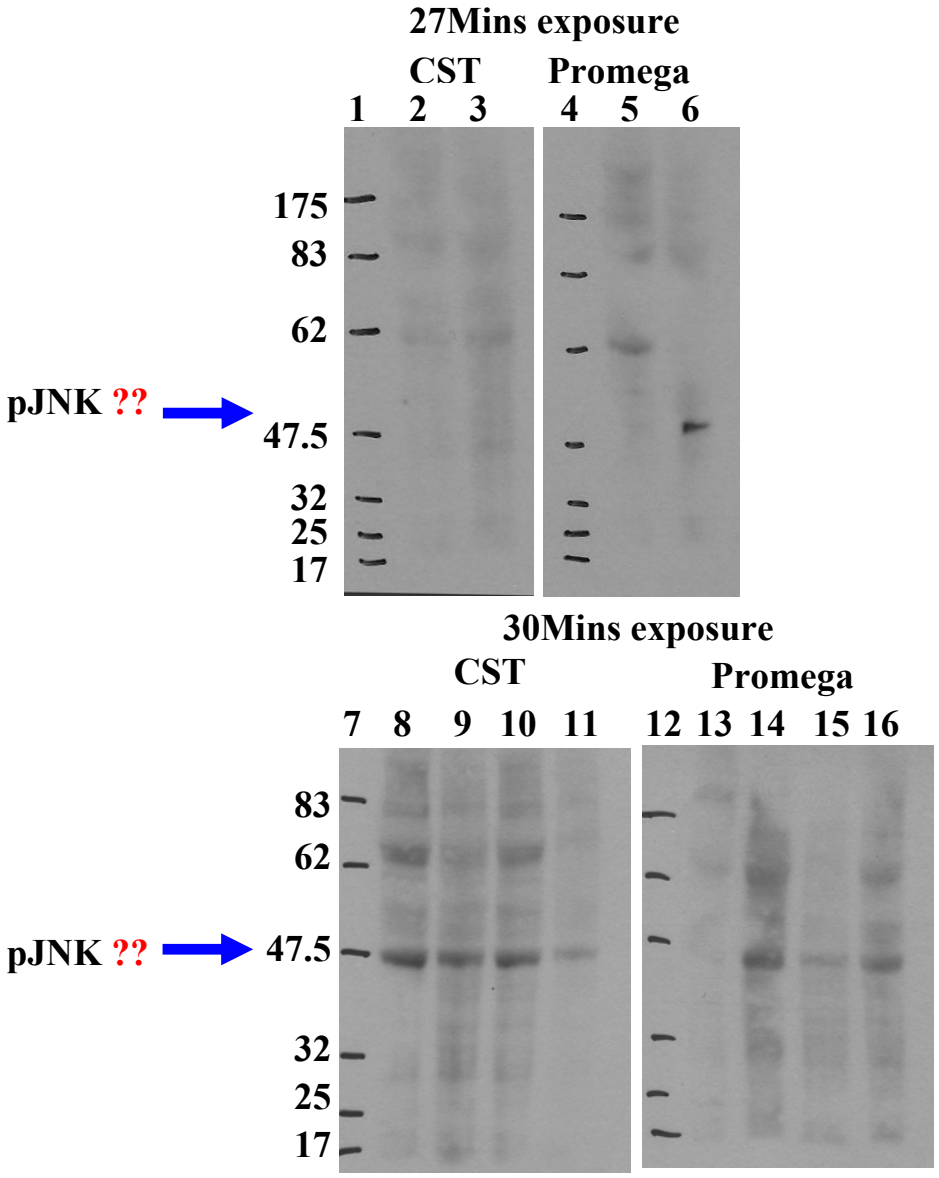

Figure 5.6: Western blotting experiments comparing the Promega and Cell Signalling Technology JNK antibodies. Almost No bands are seen at the expected JNK band size after 27mins of exposure to the ECL kit. After 30mins exposure bands are seen at ~46kDa for both antibodies. Lanes: **1**,**4**,**7** and **12** are prestained protein marker, **2**,**3**,**5**,**6**,**8**,**9**,**13** and **14** are all wild type larvae samples and **10**,**11**,**15** and **16** are homozygous pcm^5 larvae samples.

The next JNK antibody tested was monoclonal Anti-JNK produced by Sigma. This antibody was derived in mice and reacts specifically with the activated diphosphorylated form of JNK. Using this antibody a band size of ~54kDa is expected for JNK during Western blotting experiments. This would be closer in size to the human isoform JNK2. For these experiments the primary antibody was used at a 1:5000 dilution followed by the secondary at 1:80000. Actin was used as a loading control and the antibody dilutions were as outlined on Method 2.12. Using the Normal ECL detection kit the film need at least 45mins of exposure before bands were seen. Therefore the advanced ECL detection kit mentioned early in Section 5.1.1 was utilized. Film exposure times were cut to 1min and sometimes as little as 30 seconds were required. When developing the Actin Western blotting experiments, the original ECL kit was used as the advanced kit resulted in overexposure.

The Sigma anti-JNK antibody produced very good results. Several bands were seen similar to those for the previous antibodies however a band around the expected BASKET size 49kDa was present and this band was darker than any of the others. This result was encouraging and it was decided to settle on using this Sigma antibody to complete the Western blotting experiments. Interestingly a band is seen at this size 49kDa in lane 6 (Figure 5.6) for the Promega antiACTIVE JNK antibody on the Western blot exposed for 27 minutes. The manufacturer suggested this antibody would have a band size of 46/47kDa for this antibody. Promega's antiACTIVE JNK was eliminated from the Western blotting technique due to reduced specificity in *Drosophila* but this antibody may have nevertheless have been detecting the correct band in *Drosophila*. Further Western blotting experiments using antiACTIVE JNK could be performed to investigate this.

As mentioned in previous chapters *pacman* mutants are temperature sensitive. Several mutant phenotypes are more severe at lower temperatures, for example dull wings. Due to this the Western blotting experiments were performed using larvae reared at both 19˚C and 25˚C. The strains of larvae used for this experiment were homozygous pcm^3, pcm^5 and pcm^6 and wild type. Figure 5.7 shows an example Western using the anti-JNK antibody from Sigma for both temperatures.

As mentioned earlier a darker band is present slightly above the 47kDa marker which is consistent with this being pJNK.

These experiments were repeated several times for each temperature (n = 5 for both temperatures). Measurements of the intensity of the pJNK and Actin bands were then taken. As explained earlier in Section 5.1.3 for c-Jun Western blotting analysis, the expression level of pJNK (Basket), for each strain was then calculated as a ratio of the amount of Actin present in the sample. Average expression levels for each strain were then calculated and the data displayed in histograms (Figure 5.8 and 5.9).

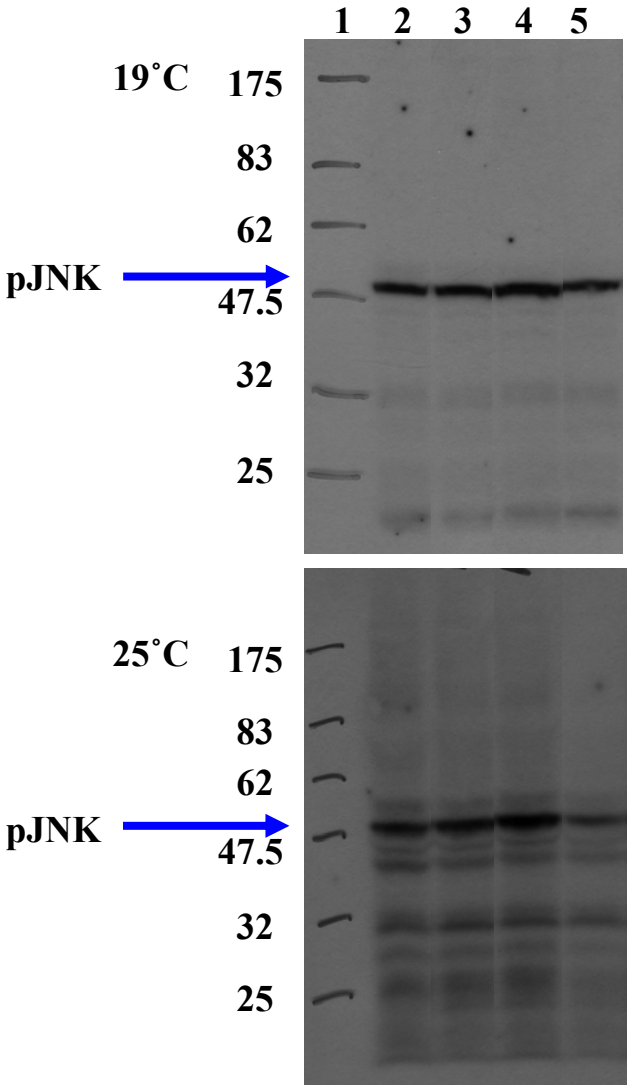

Figure 5.7: Western Blotting experiments using the anti-JNK antibody from Sigma for larvae reared at 19˚C and 25˚C. Several bands are seen. However the band that corresponds to pJNK at ~47kDa (→) is darker than the rest.
Lanes: **1** = prestained protein marker, **2** = wild type larvae samples,
3 = homozygous *pcm*^{5}, **4** = homozygous *pcm*^{3} and **5** = homozygous *pcm*^{6}.

The histogram in Figure 5.8 for Western blotting experiments at 19˚C shows pcm^3, pcm^5 and pcm^6 larvae all have increased expression of *basket* thus also the JNK signalling pathway when compared to expression in the wild type larvae. Unfortunately the standard errors show this increase is not significant at 19˚C. The histogram in Figure 5.9 for Western blotting experiments at 25˚C shows the same increase in expression of *basket* for all three mutant strains. The standard errors at 25˚C show this increase is significant for pcm^3 mutants but not quite pcm^5 or pcm^6.

Overall the Western blotting experiments using anti-JNK antibody has shown an increase in *basket* (pJNK) expression and therefore an increase in JNK signalling in homozygous *pacman* mutants compared to the wild type strain at both temperatures. This increase in JNK signalling expression in *pacman* mutants seen in the Western Blotting experiments is consistent with those found in chapter 4 where β-galactosidase staining experiments showed a slight increase in expression of the *puckered* lacZ reporter expression, which measures activity of the JNK pathway. Therefore this data shows that JNK signalling increases during larval development and after wound healing in *pacman* mutant larvae compared to the wild type strain.

5.1.5 Control to check the specificity of the anti-JNK antibody

The Western blotting experiments using anti-JNK antibody from Sigma detailed in Section 5.1.4 appeared to successfully show an increase in the JNK signalling pathway in *pacman* mutants compared to wild type larvae. An additional control showing the anti-JNK antibody was specific and therefore binding the correct antigen i.e. pJNK would support and validate this previous result. A *basket* null fly strain was purchased from the Bloomington stock centre. The *basket* mutation in this strain caused embryonic lethality at the dorsal closure stage (Riesgo-Escovar et al. 1996). Dorsal closure occurs at stage 13 around 11 hours after the egg is laid.

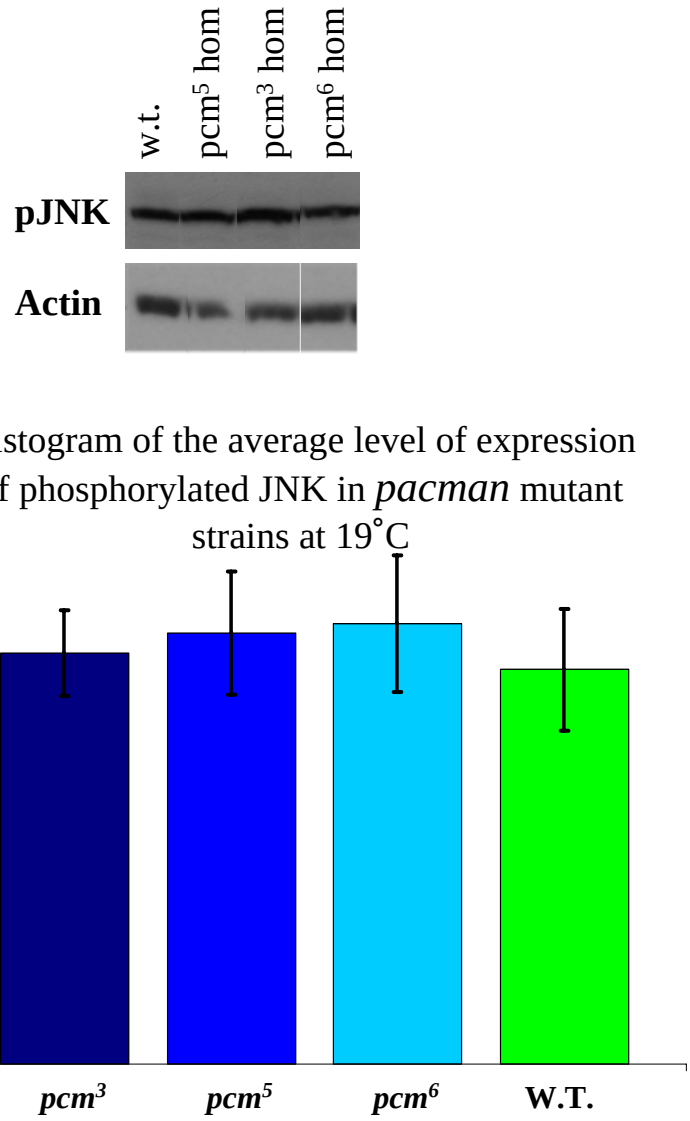

Figure 5.8: Western Blotting experiment using anti-JNK antibody from Sigma on *pacman* mutant larvae reared at 19˚C. Actin used as loading control. Histogram showing the average level of expression of JNK (*basket*) in homozygous pcm^3, pcm^5 and pcm^6 mutant larvae at 19˚C compared to wild type larvae (n = 5). Error bars represent the standard error. (One Way ANOVA $F_{3,16} = 0.12$, $P = 0.947$)

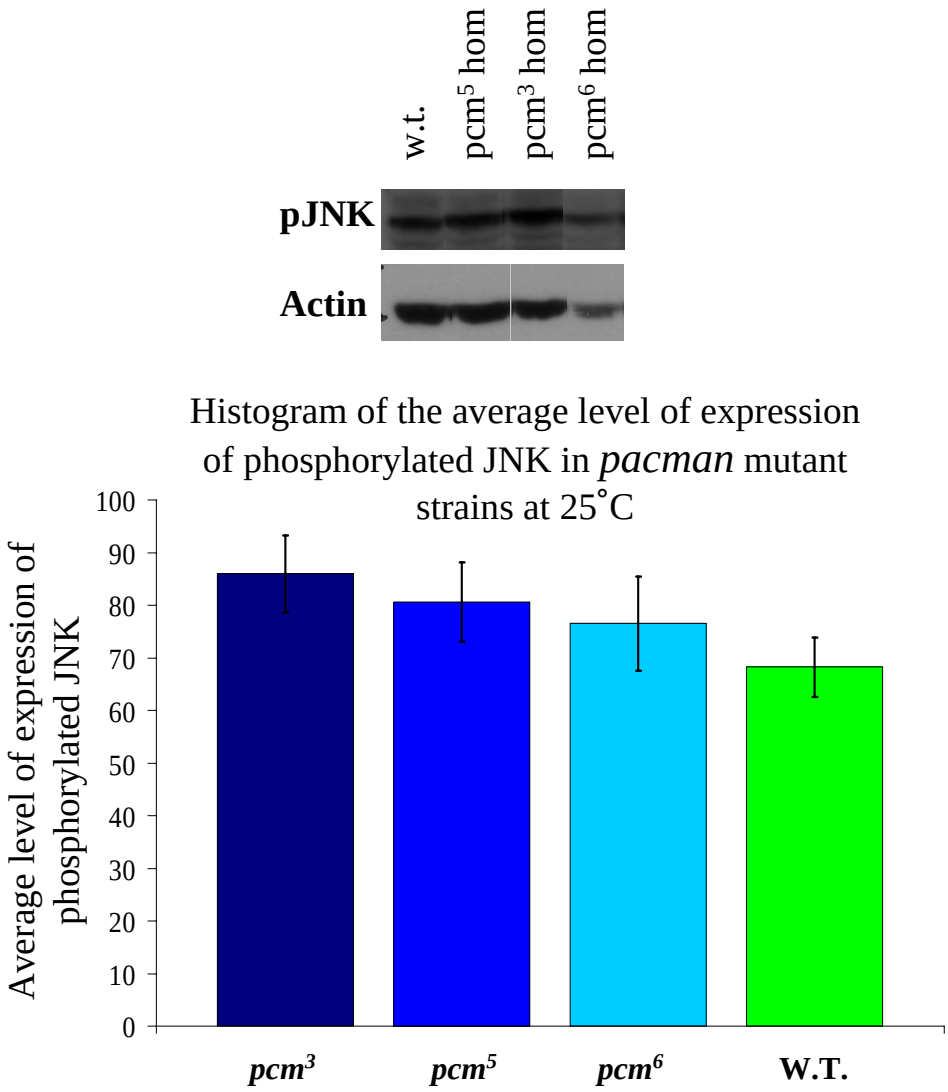

Figure 5.9: Western Blotting experiment using anti-JNK antibody from Sigma on *pacman* mutant larvae reared at 25˚C. Actin used as loading control. Histogram showing the average level of expression of JNK (*basket*) in homozygous pcm^3, pcm^5 and pcm^6 mutant larvae at 25˚C compared to wild type larvae (n = 5). Error bars represent the standard error. (One Way ANOVA $F_{3,16} = 1.00$, P = 0.4.16)

Due to the embryonic lethality, this strain is heterozygous for the null *basket* mutation and is balanced over the balancer 2nd chromosome CyO which includes the dominant marker gene Curly (*bsk*^{2}/CyO). In order to collect homozygous *bsk* mutant embryos a new fly strain was created where the *bsk*^{2} mutation was balanced over the visible marker gene Curly carrying GFP under the control of the Actin promoter ("green balancer"). Then homozygous mutant *bsk*^{2} embryos could be collected using a fluorescent dissecting microscope in similar experiments to those for selecting homozygous *pcm* mutants (Section 3.1). Figure 5.10 shows the schematic for this cross. Using the Leica MZ16F fluorescence microscope with a GFP long pass filter, embryos that are homozygous for *bsk* can be collected because they do not possess the CyO-ActinGFP balancer and therefore will not fluoresce.

The time at which to collect the homozygous *bsk*^{2} embryos was essential as too late in development and the embryos will die at the dorsal closure stage and too early and the maternal contribution will affect the results of the experiment. The early development of the *Drosophila* embryo is controlled by maternal mRNAs and proteins provided by the mother during oogenesis known as the maternal contribution. No RNA synthesis has been seen in the embryo before stage 4 when the Syncitial Blastoderm is established. This occurs around 2 and a half hours after the embryos is laid (Bownes 1975; Ransom 1982; Campos-Ortega 1985). In order to collect embryos before they enter dorsal closure and die and after the maternal contribution has diminished flies were allowed to lay eggs at 25˚C for 3 hours (normally 2-5pm), these eggs were then placed at 19˚C overnight to develop as outlined in Method 2.5.1. Development at 19˚C takes almost twice the time of development at 25˚C (Ashburner 1989). The following morning (around 10am) these embryos were dechorionated (Method 2.5.2) in preparation for separating out the homozygous *bsk* mutants using the fluorescence microscope. Following this procedure the embryos should be around 8-10 hours old.

Unfortunately any attempts to collect homozygous *bsk* mutant embryos were unsuccessful. Therefore Western blotting experiments to confirm whether the anti-JNK antibody is specific for JNK in *Drosophila* could not be performed. This is probably due to a problem with the *bsk* strain. Future investigations could test

the new *bsk* strain for the presence of the bsk^2 allele by PCR or by examination of "cuticle preps" to determine whether the dorsal closure phenotype was present.

Although it was not possible to confirm that the anti-JNK antibody from Sigma is binding to JNK (*basket*) in *Drosophila* using the negative control of the *bsk* null mutants, it is highly likely that this antibody is specific. The band seen in the Western blotting experiments is around the correct size 46-54kDa and a band was seen at this size in all four JNK antibodies tested. In addition, it was the major band seen on the Western blot.

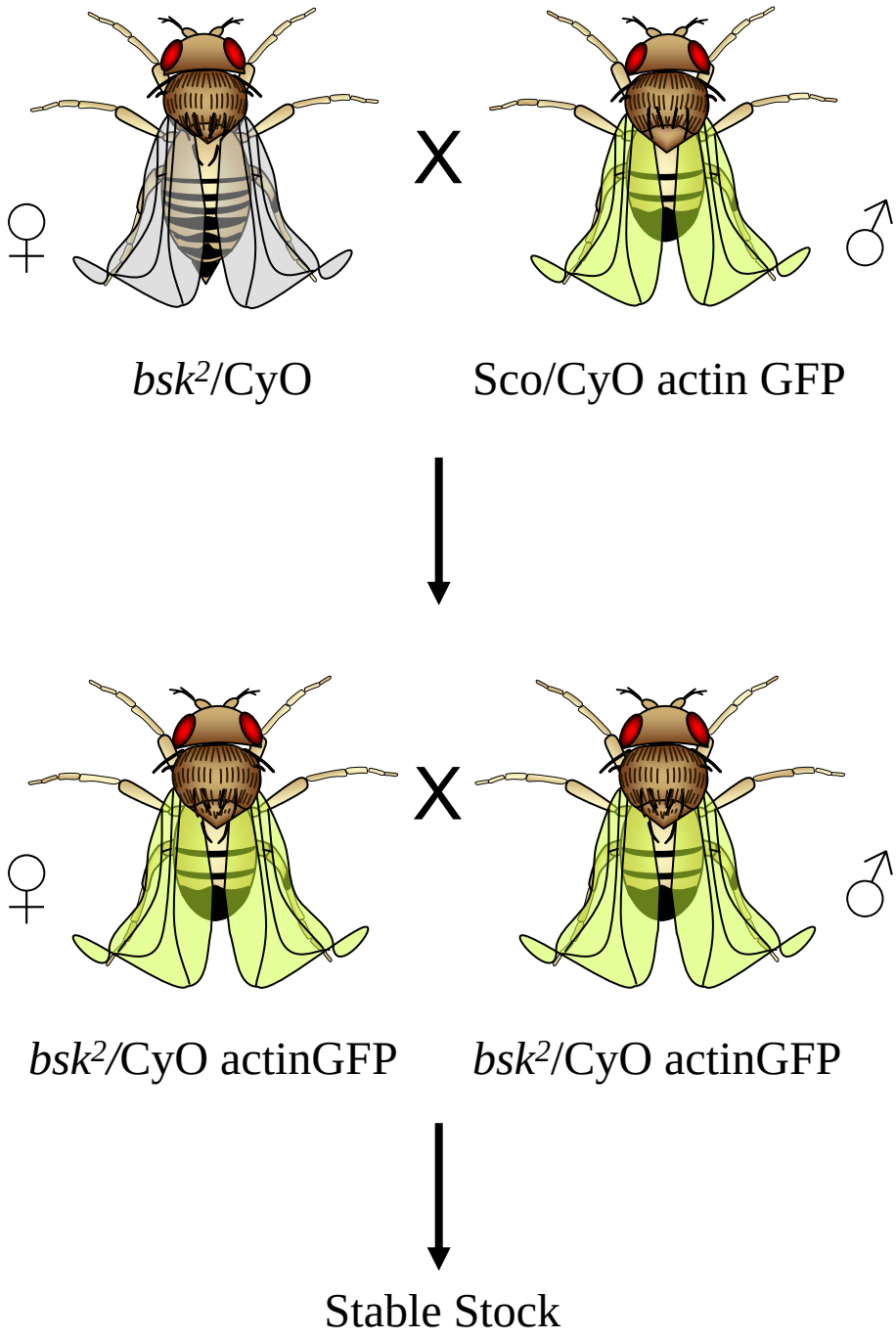

Figure 5.10: Schematic to create a fly strain containing the *basket* null mutation balanced over a "green balancer" chromosome. Green wings represent the fluorescent properties of the curly-actin GFP fusion.

5.1.6 Western Blotting experiments to check for the presence of the 2 forms of phosphorylated JNK

Previous Western blotting experiments by Kirchner et al used JNK antibodies to measure the level of expression of *bsk* in several mutant flies including flw^{1}/Y; puc^{A251}. *flw* (flapwing) encodes a serine/threonine protein phosphatase which regulated non-muscle myosin activity. Levels of *bsk* were shown to increase in the presence of the flw^{1}/puc^{A251} double mutant. Kirchner et al also noticed the presence of a second band near the 47kDa marker. They suggested this was the inactive monophosphorylated form of JNK (Kirchner et al. 2007). The antibodies used in this study were pJNK (G7) from Santa Cruz Biotechnology and antiACTIVE JNK from Promega. To separate the monophosphorylated and diphosphorylated JNK bands the electrophoresis was ran at a low voltage (60V) for several hours.

Both these antibodies were used during the fore mentioned Western blotting experiments but no monophosphorylated JNK band was present. It was decided to check the anti-JNK antibody from Sigma for the presence of this band. The protocol outlined in Kirchner et al was followed and electrophoresis gels were ran for 6 hours at 60V. Figure 11 shows the results of the Western blotting experiment (Kirchner et al. 2007). No second band corresponding to the monophosphorylated JNK is seen after the extended electrophoresis stage of the Western blotting experiments. Therefore the JNK band seen on previous Western blotting experiments corresponds to the diphosphorylated form of the activated JNK.

During this thesis a Western blotting technique to determine the interactions between *pacman* and the JNK signalling pathway was developed. This involved testing several antibodies before settling on the Sigma Anti-JNK antibody which produced clear bands on the Western Blots which when measured revealed that *basket* expression and therefore the JNK signalling pathway increases in the all three *pacman* mutants compared to the wild type control. However these changes were not quite significant which is not surprising as the expression of the JNK signalling pathway is more than likely only localized to a few tissues in larvae.

This means when looking at the larvae as a whole any changes that occur in the *pacman* mutants are probably relatively small. Future Western Blotting experiments could be performed using wing imaginal discs. The JNK signalling pathway is activated in these discs during larval development and the β-galactosidase staining experiments of chapter 4 have already shown that the expression of the JNK signalling pathway increases in *pacman* mutant wing imaginal discs compared to wild type discs.

5.2 Semi-quantitative PCR

The previous two results chapters have shown that *pacman* genetically interacts with *puckered*, a phosphatase in the JNK signalling pathway. The aim of this chapter was to quantify the changes in expression levels of the JNK signalling pathway when *pacman* is mutant. Western blotting experiments and β-galactosidase staining experiments have established that the expression level of the phosphorylated Bsk protein increases in *pacman* mutant when compared to a wild type control.

To quantify this increase in expression, the levels of mRNA for the gene *puckered* in *pacman* mutants compared to the wild type control were examined. Semi-quantitative PCR was used as a starting method to measure the level of *puckered* mRNA in *pacman* mutants (Marone et al. 2001; Bustin 2002). This technique requires less starting material than Northern blotting and is easy and fast to run without the need for radioactivity. Semi-quantitative PCR can be used to compare the amount of product produced from different primer sets at the same cycle number and then determine the relative abundance of the mRNA for a particular gene of interest. When using specific *puckered* primers in a PCR reaction, the amount of *puckered* template (cDNA) will directly relate to the amount of mRNA present in the sample i.e. the expression level of *puckered* and therefore the JNK signalling pathway.

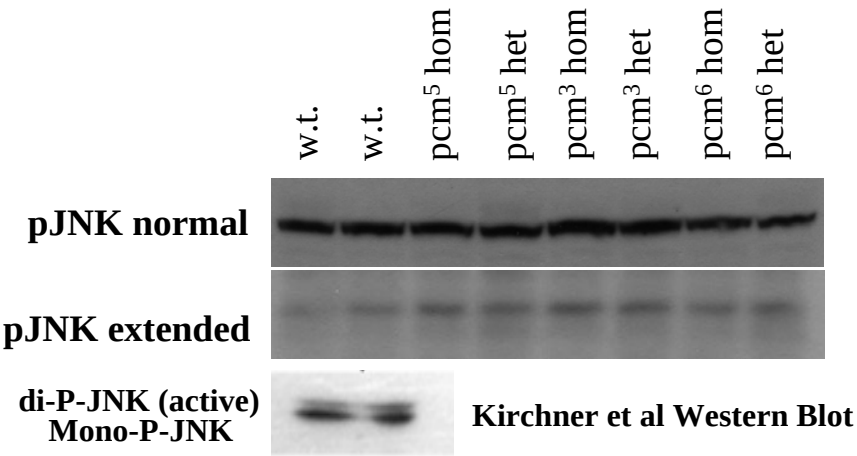

Figure 5.11: Western blotting experiments comparing the effect of different electrophoresis times and voltages on JNK bands. Kirchner et al, 2007 Western Blot of *flw*^{1}/Y ;; *puc*^{A251}/+ mutants show both di and mono phosphorylated JNK bands using pJNK (G7) from Santa Cruz Biotechnology. Both normal and extended Western Blots show only one band at the correct size for JNK (49kDa). Therefore the Sigma Anti-JNK antibody detests only the diphosphorylated form of JNK.

Semi-quantitative PCR relies on the fact that during a PCR reaction the amount of target DNA will amplify each cycle. If a small sample of the PCR mix is taken after each cycle this increase in target DNA can then be visualised on an agarose gel. The intensity of the band on the gel will directly correlate to the amount of target DNA present at that stage of the PCR. By measuring the intensities at different PCR cycles and plotting a line graph of these values, the amount of target DNA present in different samples can be calculated and compared. In order to compensate for differences in the total amount of RNA due to sample size, a control probe is used. This control is normally a housekeeping gene whose mRNA expression is constant throughout the sample. For these semi-quantitative PCR the gene *rp49*, which encodes a ribosomal protein was used. Ultimately the intention was to calculate the amount of *puckered* mRNA relative to the amount of *rp49* mRNA present in the sample.

For the semi-quantitative PCR experiments total mRNA was extracted from 10 L3 larvae from the following strains: the wild type control and homozygous pcm^3, pcm^5 and pcm^6 using the RNeasy Kit (Qiagen). This produced between 150-500ng/µl total RNA. This RNA was used as a template to sequence cDNA by reverse transcriptase (RT) PCR performed using the superscript III kit (Invitrogen). Following RT-PCR the newly synthesised cDNA was probed in a second PCR reaction with specific primers for *puckered* and *rp49*. The *puckered* and *rp49* primers were previously designed by Dr Steve Hebbes using primer3 Appendix 4. They produce amplicons of 241bp and 121bp in size respectively. The amount of *puckered* and *rp49* transcripts will amplify exponentially per cycle of the PCR reaction. 6µl samples were taken from the PCR reaction mix after cycle 18 and every second cycle onwards until cycle 35. These samples were ran on a 1.5% agarose gel for 45mins at 100V. Figure 5.12 shows the visualised bands of *puckered* and *rp49* for pcm^3, pcm^5, pcm^6 and wild type larvae. The bands were seen to become brighter as the cycle numbers increase and *rp49* expression is visible at an earlier cycle than *puckered* as expected for a housekeeping gene. The intensity of the band for each cycle was measure using NIHimage. These intensities increased each cycle and the values for each strain were plotted in a line graph (Figure 5.13). There appears to be a difference in expression of *puckered* between wild type, pcm^3 and pcm^5 larvae. For each of these strains the

rp49 expression is visible at cycle 18 but *puckered* is visible at cycle 24 for wild type and cycle 26 for pcm^3 and pcm^5. These results would suggest a decrease in the expression levels of *puckered* and therefore the JNK signalling pathway in *pacman* mutants. This is inconsistent with previous results in the β galactosidase staining and Western Blotting experiments. However the intensities of *puckered*, the gene of interest should be normalised to the internal control, the housekeeping gene *rp49* before the changes in expression levels between strains can be compared. Therefore this initial result may be misleading.

In order to calculate the levels of *puckered* expression relative to *rp49* expression for each strain it is important to complete the PCR reaction in the linear exponential stage for each gene. In the Figure 5.13 we can see that the *rp49* reaction has began to plateau for each strain. The PCR reaction was repeated and this time 6µl samples were taken from cycle 14 onwards. Hopefully this will result in both genes being at the exponential at the same cycle.

Unfortunately these earlier bands were not seen on the agarose gel suggesting the level of expression of each gene is too low to be visualised. PCR were repeated again with a larger starting volume i.e. 100µl instead of 50µl and this time taking bigger samples 16µl from cycle 14 to 24. Again no bands were seen for cycles 14 to 24. At this point in the Semi Quantitative PCR experiments there was no way of calculating the expression levels of *puckered* in relation to the *rp49* for each strain. Our lab was in the process of moving location and at our new institute there would be access to a Real Time Quantitative PCR machine. Therefore the decision to conclude this set of experiments was made and to begin Quantitative PCR in our new laboratory. However these semi quantitative PCR experiments allowed the design and optimization of the basic PCR steps before they were applied to the Real Time quantitative PCR in the next section.

If the semi quantitative PCR experiments were to continue the next step would have been to alter the primer concentrations of the gene of interest and the control i.e. increase the concentration of *puckered* primers and reduce the concentration of *rp49* primers. This should result in lower levels of expression of the control and hopefully both genes will be in the exponential stage from cycle 18 onwards.

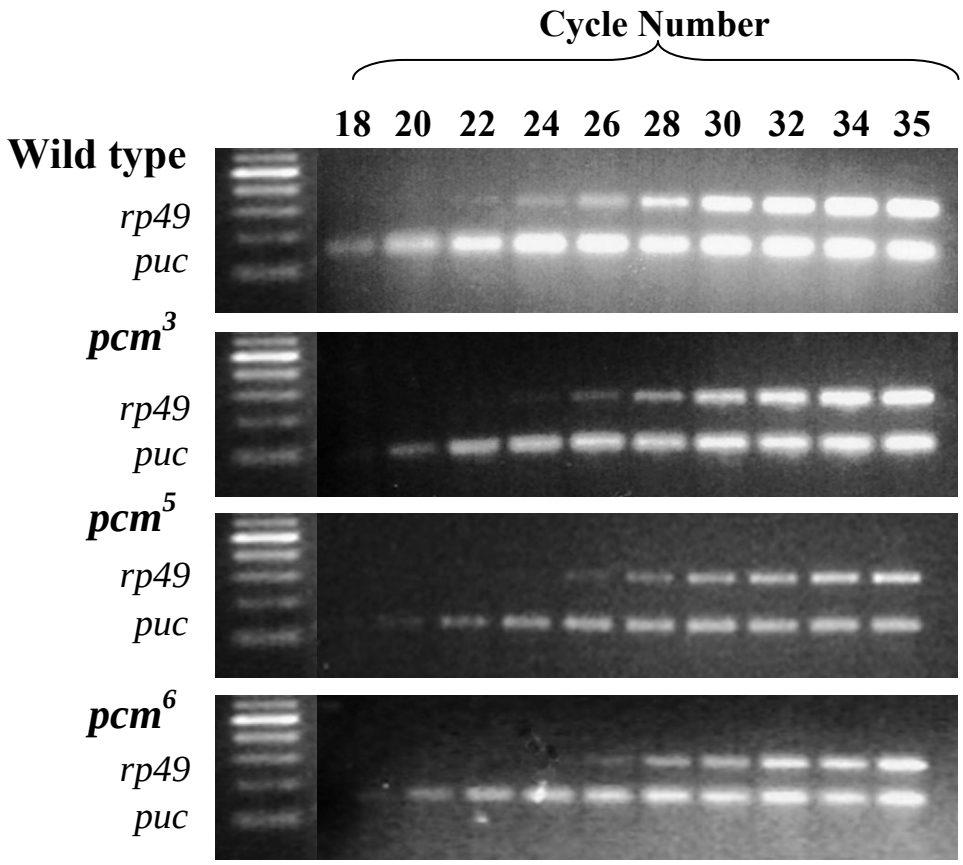

Figure 5.12: Electrophoresis gels produced from Semi-Quantitative PCR using *puckered* and *rp49* primers sets to quantify *puckered* mRNA levels in wild type, pcm^3, pcm^5 and pcm^6 larvae. Bands intensify as the cycle numbers increase. Marker: 100bp ladder.

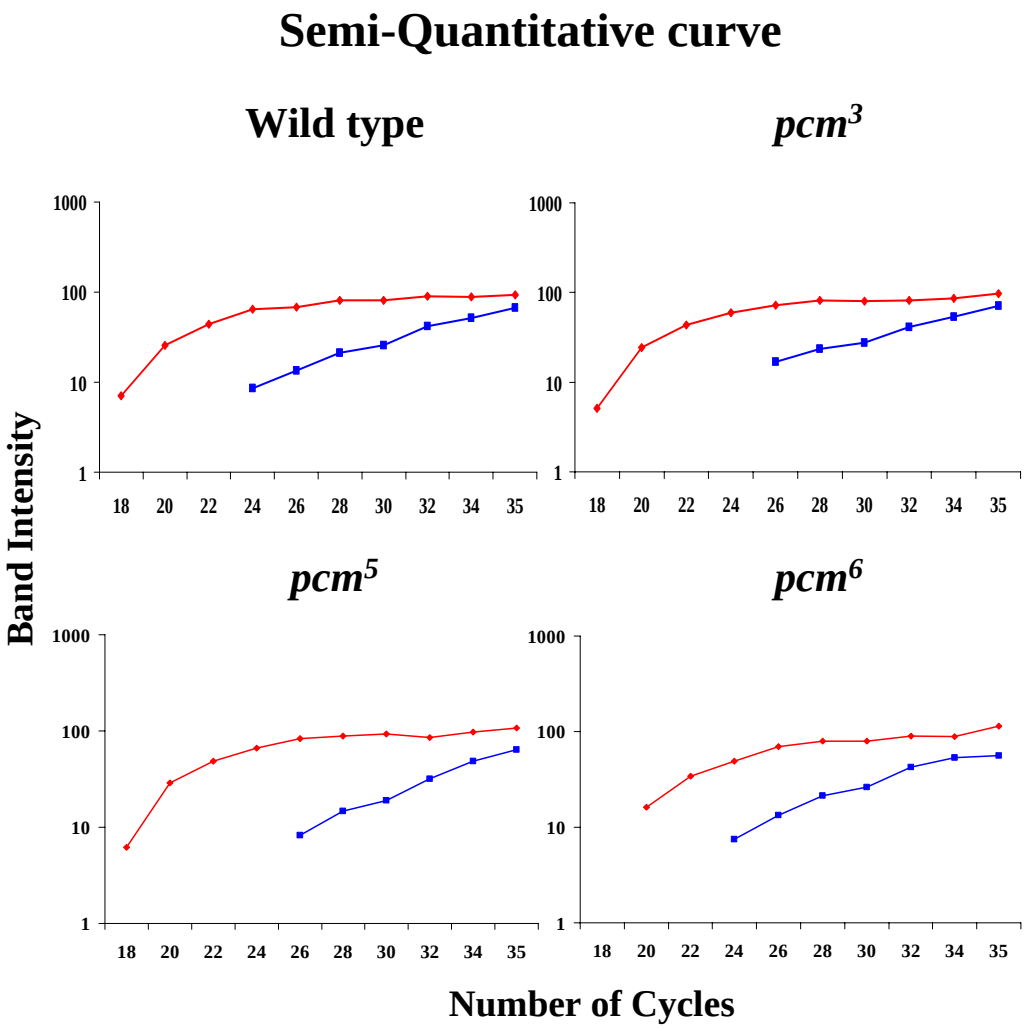

Figure 5.13: Graphs showing the increasing intensities of the Semi-Quantitative PCR bands produced using *puckered* and *rp49* primer sets for wild type, *pcm*^{3}, *pcm*^{5} and *pcm*^{6} larvae. Key: *rp49* and *puckered*.

5.3 Real-Time Two Step Quantitative PCR

Quantitative PCR follows the same principle as Semi Quantitative PCR in the last Section 5.2 (Bustin 2002; Radonic, 2004; Stratagene 2006). The amount of *puckered* template (cDNA) will directly relate to the amount of mRNA present in the sample i.e. the expression level of *puckered* and therefore the JNK signalling pathway. It was intended to quantify the increase in expression of *puckered* by looking at the levels of mRNA (expression) for the gene *puckered* in *pacman* mutants compared to the wild type control.

As before in Semi-Quantitative PCR, when quantifying cDNA target gene expression, the RNA must first be reverse transcribed into cDNA using oligo dT primers with Superscript III (Invitrogen) and treated with DNase1 to remove any genomic DNA contamination. A sample of this newly synthesized cDNA (no more than 10% of the reaction volume) is then transferred to another eppendorf where real-time PCR takes place.

It is important to perform the QPCR with equal amounts of cDNA for each sample so we can then directly compare them. If we began the reaction with different cDNA levels then we are bound to have different levels at the end of the reaction which would complicate interpretation of the results. There are two ways to ensure the reactions start equally for each sample: firstly the concentration of the RNA sample can be measured and appropriate volumes can be added to the RT reaction to produce similar concentration of cDNA in all the samples or the cDNA can be measured after the RTPCR and the appropriate volume for each sample then added to the QPCR reaction. The concentration of the RNA samples before RTPCR was measured using a spectrophotometer. This enabled calculation of the volume of RNA from each sample to be added to the RT PCR reaction to allow equal volumes of cDNA to be produced. This meant the same volume of cDNA could then be added to all the samples in the QPCR reaction.

For the Real-Time Quantitative PCR experiments Quantitect SYBR Green PCR mix (Qiagen) was used. This kit contains the fluorescent dye SYBR Green 1

which binds any double stranded DNA molecules and emits a fluorescent signal upon binding (Figure 5.14). The QPCR machine measures this signal during the exponential phase of each amplification cycle and this directly relates to the amount of target product present at that cycle. The first cycle at which the QPCR machine can detect the fluorescence as being greater than the background is called the Ct or threshold cycle. The QPCR machine used for these experiments is the Stratagene Mx3000P. This machine can determine the Ct for each sample individually by comparing unknown samples to a standard curve dilution series that is ran at the same time.

The aim of these Real Time Quantitative PCR experiments was to measure the levels of a RNA encoded by the *puckered* gene (unknown) in samples compared to a calibator, the wild type control. This type of QPCR is referred to as Relative or Comparative Quantification. The wild type calibator is used as the baseline for the expression of *puckered*. The differences in Ct values between the unknown samples and the wild type are expressed as fold changes i.e. up or down regulation. The samples are also normalised using a gene of constant expression in all the samples i.e. the housekeeping gene *rp49*. Using a normalizer allowed for the control of differences in RNA isolation and efficiency of reverse transcription between samples.

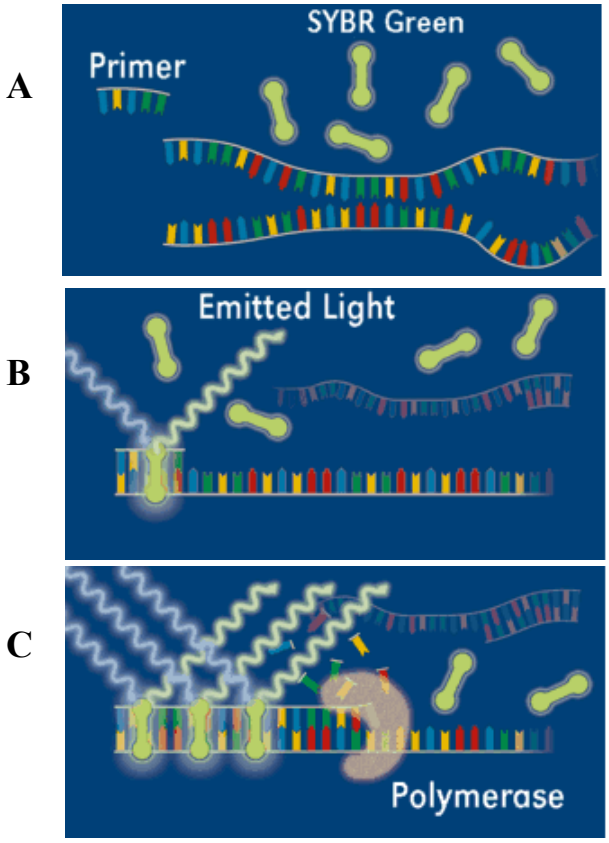

Figure 5.14: SYBR Green binding to double stranded DNA. A: At the beginning of amplification the unbound dye molecules weakly fluoresce, producing a minimal background fluorescence signal which is subtracted during computer analysis. After annealing of the primers, a few dye molecules can bind to the double strand. B: DNA binding results in a dramatic increase of the SYBR GreenI molecules to emit light upon excitation. C: During elongation, more and more dye molecules bind to the newly synthesized DNA. This is measured by the Stratagene Mx3000P Quantitative PCR machine. (Picture adapted from: www.gene-quantification.de/chemistry.html)

5.3.1 Designing the Real-Time Quantitative PCR primers

The success of a set of Quantitative PCR experiments relies heavily on good primer design. Primers must be highly specific otherwise primer dimers or non specific DNA binding would lead to untrue Ct values as a result of the non-specificity of the SYBR Green 1 binding of double stranded DNA. When designing primers for QPCR there are many programmes available to help such as primer3 mentioned earlier in Section 5.2. The sequence of the gene of interest and normaliser is uploaded into the programme and the parameters required for the primers listed. The parameters that are essential when designing primers for Quantitative PCR using the Stratagene Mx3000P machine and the Roche Applied Science Lightcycler machine are outlined in Table 5.1.

QPCR machine	**Stratagene Mx3000P**			**Roche Applied Science Lightcycler**	
Condition under review	Min	max	optimal	Min	max
Primer Tm (melting Temperature)	58	60	59	58	60
Primer GC content	45	55	50	50	60
Primer length	18	22	20	18	20
Amplicon Tm	75	85			
Amplicon Length	50	150		100	150

Table 5.1: The parameters required for designing primers for Quantitative PCR for the Stratagene Mx3000P and Roche Applied Science Lightcycler PCR machines.

To prevent detection of sequences from genomic DNA, the primers are normally designed to span an exon-exon boundary. If this is not possible a DNAse treatment is required before the reverse transcription step. For QPCR experiments it is important to keep the amplicon length relatively short, this helps to increase the efficiency of the PCR amplification. When using SYBR green 1 the amplicon size should be between 100 and 400bp to allow for more double stranded DNA which the SYBR green can bind to and produce more fluorescence. Other general rules for primer design include: the melting temperatures of the forward and reverse primers should be within 2˚C of each other and there should be no more than two G or Cs in the last five bases of the primer sequence.

Previously Dr Maria Zabolotskaya, another member of the Newbury group had designed *puckered* and *rp49* primers in the hope of performing QPCR using the Roche Lightcycler machine when the laboratory was based at Newcastle University. Unfortunately she never performed these experiments so the decision was taken to test her primers during these QPCR experiments using the Stratagene machine at Sussex University. Maria used the Lightcycler probe design software version 1.0 by Roche Applied Science to design the *puckered* and *rp49* primer sets. The sequences for the primer sets Dpuc3, Dpuc4, Drp491 and Drp492 are detailed in Appendix 5. A basic PCR confirmed these primer sets only amplified one PCR product (Figure 5.15). The primer sets Dpuc3 and Drp491 were therefore chosen for the initial QPCR experiments. The next step was to optimize the primer conditions to produce successful QPCR experiments.

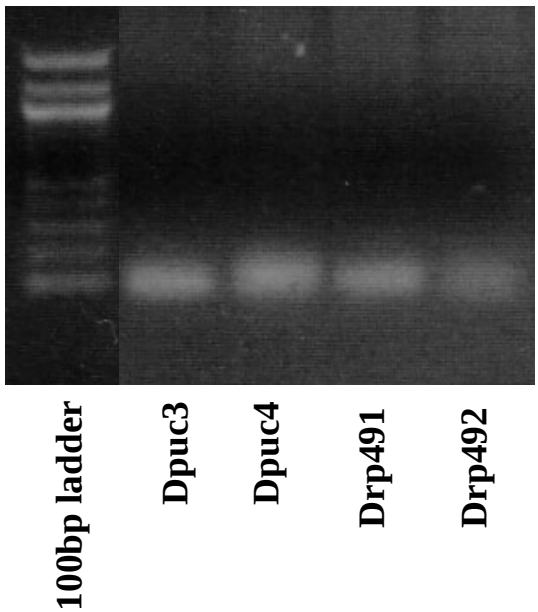

Figure 5.15: PCR to confirm the *puckered* and *rp49* primer sets used for Quantitative PCR only amplify 1 PCR product each. Amplicon Size: Dpuc3= 141bp , Dpuc4= 136bp , Drp491= 141bp and Drp492= 113bp .

5.3.2 Primer optimization

As mentioned in the previous section, the success of QPCR experiments relies heavily on having the correct primer conditions. If the primers produce more than one products or primer-dimers, the Ct values for the experimental samples will be altered and this will give misleading data.

In order to avoid primer-dimers when using SYBR green 1 which would lead to false fluorescence, low primer concentrations between 50-300nM are used. A primer matrix (titration) can be performed to optimize the forward and reverse primer concentrations. This was performed for the *puckered* and *rp49* primers. It involved comparing several different concentrations of forward and reverse primers with each other. The concentrations used were 50nM, 100nM, 300nM, 600nM and 900nM. The protocol for this matrix is outlined in Method 2.15.5. The Ct values for the primer concentrations were compared. The lowest Ct value is considered the most desirable primer mix. The data produced from this primer matrix is shown in Table 5.2. Forward and reverse primer concentration mix of 900nM for both gave the lowest Ct value for both primer sets. It is also important to look at the disassociation (melting) curves for the different primer concentration mixes to confirm that they only produce one product.

The disassociation analysis is performed at the end of the QPCR reaction for each sample to determine whether there was any contamination in that sample or if there were any primer-dimers produced. This involves melting all the products of the PCR amplification by heating them at 95˚C for 1minute. They are then allowed to anneal at 55˚C for 30 seconds. This is followed by a gradual increase in temperature until the reaction reaches 95˚C. A measurement of fluorescence is taken after each temperature increase. This data is displayed in two graphs; firstly Raw Fluorescence signal (R) against temperature which shows a decrease in fluorescence as the temperature increases and normally has a rapid decline at one temperature for all samples per primer set that represents the target amplicon melting temperature. The negative derivative of the Raw Fluorescence signal (-R'(T)) is then plotted against the temperature. This data results in a peak which

represents the melting temperature of the PCR products. An optimized PCR reaction will contain only one peak for the target amplicon. Every peak in the curve represents a specific product is melting. If other peaks are seem on the graph then the PCR reaction is contaminated i.e. something else other than the target amplicon is being amplified. For these QPCR experiments the melting temperature and therefore the peak should be between 80˚C and 90˚C. A peak at a lower temperature would suggest primer-dimers or contamination. Primer-dimers are often seen in the NTC (no template controls) especially if the primer concentrations are high. It is acceptable to see a small amount of primer-dimers in the NTC only. However if this same peak is seem in the experimental samples then the Ct values are not accurate and further optimization of the primer concentrations is needed. A peak of lower or higher temperatures than the amplicon that is not in the NTC would suggest non specific primer binding and again these Ct values are not accurate.

The primer matrix experiment showed that a concentration of 900nM for forward and reverse primers concentrations gave the best Ct values. A QPCR standard curve was performed to test these concentrations. Although no Primer-dimers had been seen during the primer matrix, they were seen when running the standard curves for the NTC of both primers sets. Primer-dimers were also seen for one point on the standard curve for the *puckered* primers. This suggests the concentration 900nM is too high resulting in incorrect binding of the primers. The standard curves were repeated with 600nM primer concentrations and again primer-dimers were seen. The concentrations ultimately used were 300nM for the forward and reverse primers of both primer sets because no primer-dimers, contamination or non specific primer binding were seen in the any of the standard curve samples.

5.3.3 Quantitative PCR controls

As with all PCR experiments no template controls (NTC) are essential to determine the master mix is not contaminated. As well as running NTC during the QPCR experiments NRT (no reverse transcriptase) samples were also ran. These samples also act as a control. Instead of water in the NTC the NRT samples

contain the pure extracted RNA which has not undergone reverse transcription into cDNA. This controls for contamination that may have occurred during the RTPCR step.

5.3.4 Determining the dilutions for the standard curve

The standard dilutions used to calculate the Ct values, are of known concentrations of the control template, in this case wild type larvae cDNA. After amplification of the dilutions, a standard curve is generated by plotting the log of the initial template copy number against the Ct for each dilution. This should generate a straight line known as the standard curve. The standard curve in these QPCR had 4 (the minimum) or 5 points and each concentration was run in triplicate. The standard curve for each primer set should cover the range of concentrations being analysed. This takes some guess work to begin with. The starting dilutions were Neat cDNA, 1/10, 1/100 and 1/1000 for both primer sets. However this was too concentrated for the *rp49* primer set as this gene is expressed in higher levels than the *puckered* gene. This was also too dilute for the *puckered* as this gene is expressed in low levels when using whole larvae. Ultimately the dilutions used were Neat cDNA, 1/5, 1/10, 1/50 and 1/100 for *puckered* and 1/10, 1/100, 1/1000 and 1/10000 for *rp49*. The cDNA for the experimental samples for both primer sets were diluted. The *rp49* primers were diluted to 1/1000 and the *puckered* primers were diluted to 1/10. This results in the Ct values for the *rp49* and *puckered* primer sets to be similar allowing comparison between them. This can be seen in Figure 5.16 Graph B, the Ct values for *rp49* and *puckered* are within 10 cycles of each other. Without this dilution of the *rp49* experimental samples their Ct values would be much lower than the *puckered* samples due to the higher level of expression of the housekeeping gene. This also allowed the Ct values for experimental samples for each primer set to lie on the line of their standard curve.

Primer Concentrations (nM)	***Puckered* Ct value**	***Rp49* Ct value**
R100-F100	No Ct	No Ct
R100-F300	No Ct	No Ct
R100-F600	No Ct	43.77
R100-F900	No Ct	No Ct
R300-F100	44.67	44.38
R300-F300	33.74	35.8
R300-F600	27.89	35.06
R300-F900	30.46	34.08
R600-F100	36.74	34.61
R600-F300	27.15	29.03
R600-F600	26.55	28.35
R600-F900	26.32	28.22
R900-F100	32.42	34.69
R900-F300	27.08	28.32
R900-F600	26.23	27.36
R900-F900	24.87	26.93

Table 5.2: The Ct values resulting from a primer matrix testing different concentrations of forward and reverse primers during Quantitative PCR. R=reverse primer and F=forward primer. The red Ct values are the lowest for each primer set.

In the case of Comparative Quantification the standard curve is used to check the amplification efficiency of the reaction and does not need to be ran each experiment. The efficiency determines the overall performance of the QPCR. An efficiency of 100% implies a perfect doubling of template each cycle. Therefore the amount of product should theoretically increase from 1 to 2, 4, 8, 18, 32 etc. Ideally the efficiency should be between 90% and 110% producing standard curves with a slope between -3.1 and -3.6. Otherwise the reaction is somehow inhibited possibly due to incorrect primer concentrations, formation of primer dimers, inconsistent pipette technique or an inhibitor during cDNA preparation. The Rsq value (R^2 or Pearson Correlation Coefficient) represents the fit of all the data (including the experimental samples) to the standard curve. This value can be affected by the accuracy of the dilutions. If the data lies perfectly on the standard curve the Rsq value is 1.00. An Rsq value of 0.985 and above is acceptable. Values lower than 0.985 represent a reduction in sensitivity of detection. It is important to maintain sensitivity when working with samples that have low expression levels.

For Comparative Quantification, multiple standard curves are ran in order to confirm the efficiency is reproducible. The efficiencies should be within 5% of each other. 8 curves for the *rp49* primer set and 7 curves for the *puckered* primer set were ran. Unfortunately the efficiencies were not between 90% and 110% and there was more than 5% between them. The average efficiency was 71.9% for *rp49* and 71.5% for *puckered*. These efficiencies suggest a flaw in the experiments. This could be due to primer-dimers, inappropriate primer concentrations or inaccurate pipetting. The average Rsq values were 0.999 for *rp49* and 0.935 for *puckered*. These results are very good so it's unlikely the low efficiencies are due to pipetting errors. When the NTC (no template control) and NRT (no reverse transcriptase control) were observed no primer-dimers were seen, as was the case for all the experimental samples. Therefore primer-dimers are not the cause of the disappointing efficiencies. This led to the conclusion that the primers were to blame. As mentioned in the previous Section 5.3.1 an attempt to optimize the primer concentrations using a primer matrix was performed. The results of this matrix were confusing as the primer concentrations with the lowest

Ct values (900nM for both forward and reverse primer sets) gave primer-dimers in the standard curve samples, which lead to a lower efficiency.

The Quantitect SYBR green kit was nearly depleted and there was no money or time to purchase another batch. Therefore the decision to go ahead with the experiments was taken despite these low efficiencies, probably due to unsuitable primer concentrations or even the primers themselves. The results would at least give a clue as to the effect of *pacman* mutations on *puckered* expression levels compared to wild type flies and would hopefully be consistent with the previous data i.e. the *puckered* expression increases in *pacman* mutants. The computer programme used by the Mx3000P QPCR machine is called MxPro. This programme has a Comparative Quantitative PCR setting which allows the average efficiencies of the standard curves to be applied to all your experimental data over several experiments. This means the results at the end which compare the Relative Quantity (dR) of each *pacman* mutant compared to the wild type take the actual efficiencies into account and don't assume they are perfect at 100%. The data for the final QPCR experiments is discussed in the next section.

5.3.5 Quantitative PCR experiments show *puckered* expression increases in *pacman* mutants compared to the wild type control

As mentioned in the last section the SYBR green kit was depleted during the long process of optimising the QPCR experiments. The efficiencies of the standard curves performed were not ideal. However it was decided that it was worth trying the QPCR with the experimental samples because the comparative QPCR programme allows the entry of the average efficiency of the reaction. This would therefore take the reduced efficiency into account when calculating the relative quantities of *puckered* expression in the *pacman* mutants compared to the wild type control.

The QPCR experiments involved comparing 2 biological replicates which each had 2 technical replicates. Biological replicates are 2 separate RNA samples for each strain. The strains used were homozygous pcm^3, pcm^5 and pcm^6 and the wild type control. The RNA sample consisted of 10 L3 larvae. Technical replicates are

2 different cDNA samples produced from the same RNA sample. The protocol to set up the QPCR experiment was detailed in Method 2.15. Within an experiment each sample is ran in triplicate to account for pipetting errors.

Each QPCR produces an amplification and disassociation graph along with the standard curve and the relative quantity graph. Several amplification graphs for one QPCR are shown in Figure 5.16. All the graphs have a blue (*puckered*) and red (*rp49*) horizontal line which represents the fluorescence threshold for each primer set. This line determines the Ct values for each sample. Graph A shows all the samples together. The triplicates are treated collectively by the MxPro programme and an average of the 3 for each sample is displayed in the graph. Graph B shows only the experimental samples, we can see that the curves create 2 groups. These groups are the samples for *puckered* and *rp49* separated by their Ct values. As expected *rp49* has the lowest Ct values because this gene is expressed in higher levels throughout each sample. *puckered* expression is lower in the samples and therefore has higher Ct values i.e. it takes longer to produce a detectable level of fluorescence hence there is less double stranded DNA being produced. The JNK signalling pathway is therefore expressed at lower levels perhaps because *puckered* expression is localized to specific areas such as the wing imaginal disc rather than being expressed throughout the larvae as for *rp49* (as discussed in chapter 4). This localized expression probably leads to the lower levels of expression of *puckered* compared to *rp49*. Graph C is used as a control to check that no Ct values are present for the NTC and NRT samples hence no DNA is being amplified in these samples.

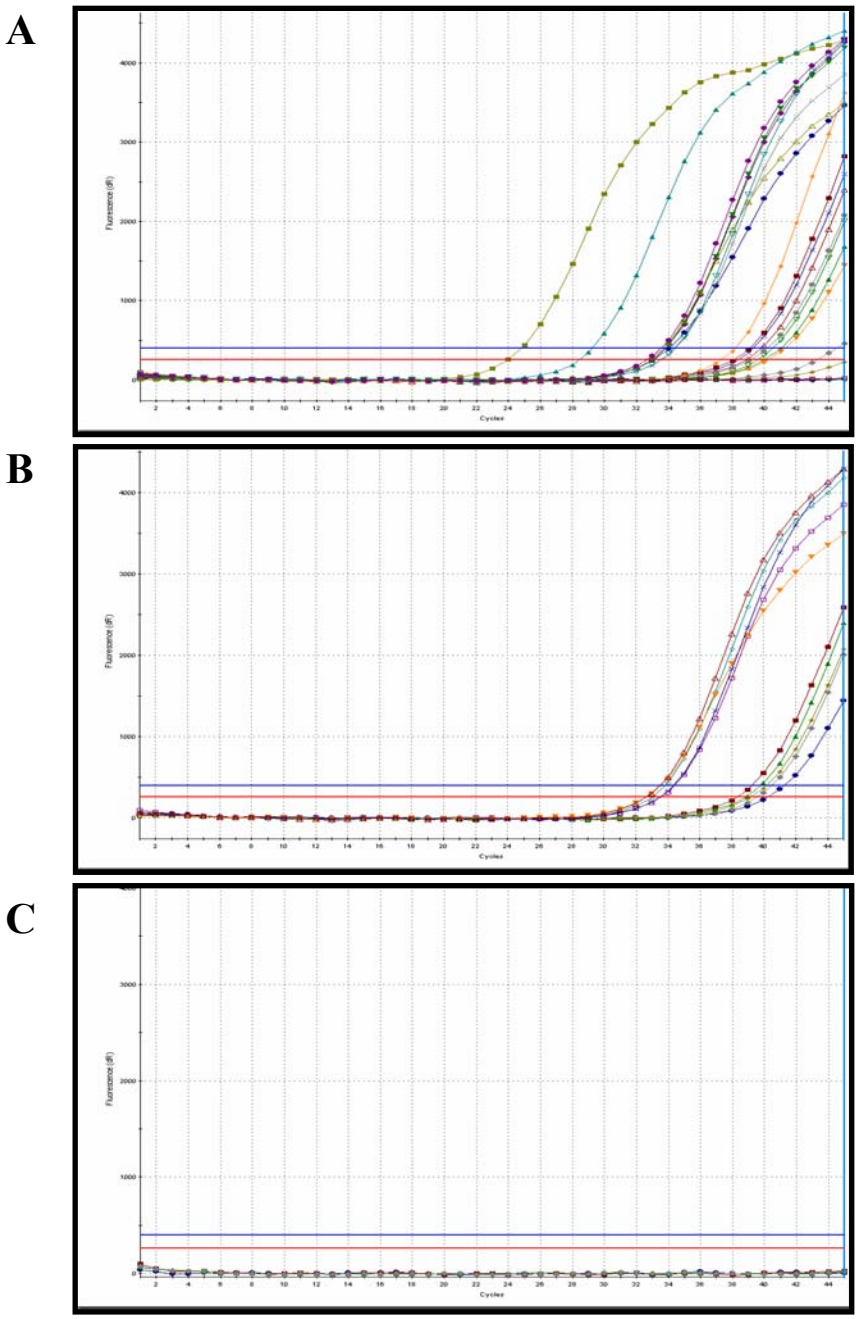

Figure 5.16: Amplification graphs from a Quantitative PCR experiment produced by the MxPro programme on the Stratagene Mx3000P. The Blue line represents the fluorescence threshold for the *puckered* primer set. The red line represents the same for the *rp49* primer set. Graph **A** shows the amplification curves for all the samples. Graph **B** shows the curves for the experimental samples alone. Graph **C** shows only the no template control and no reverse transcriptase control samples. No amplification is seen in these samples showing that no contamination is present.

After checking the samples are being amplified during the QPCR reaction the disassociation curves were observed to determine whether the samples are clean. They were checked for contamination and primer-dimers. The disassociation curve for the same QPCR as above is shown in Figure 5.17. Graph A displays the raw fluorescence data against the temperature. The sharp decrease at the end of the curve represents the melting of the PCR amplicon. Graph B, C and D shows the negative derivative of the fluorescence data against the temperature. Graph B shows all the QPCR samples. Graph C shows only the curves for the experimental samples. There is only one peak per sample and therefore no contamination. However there are two temperature peaks which correspond to the different amplicon sizes produced by the primer sets. Graph D confirms that there are no primer-dimers seen in either the NTC or NRT controls.

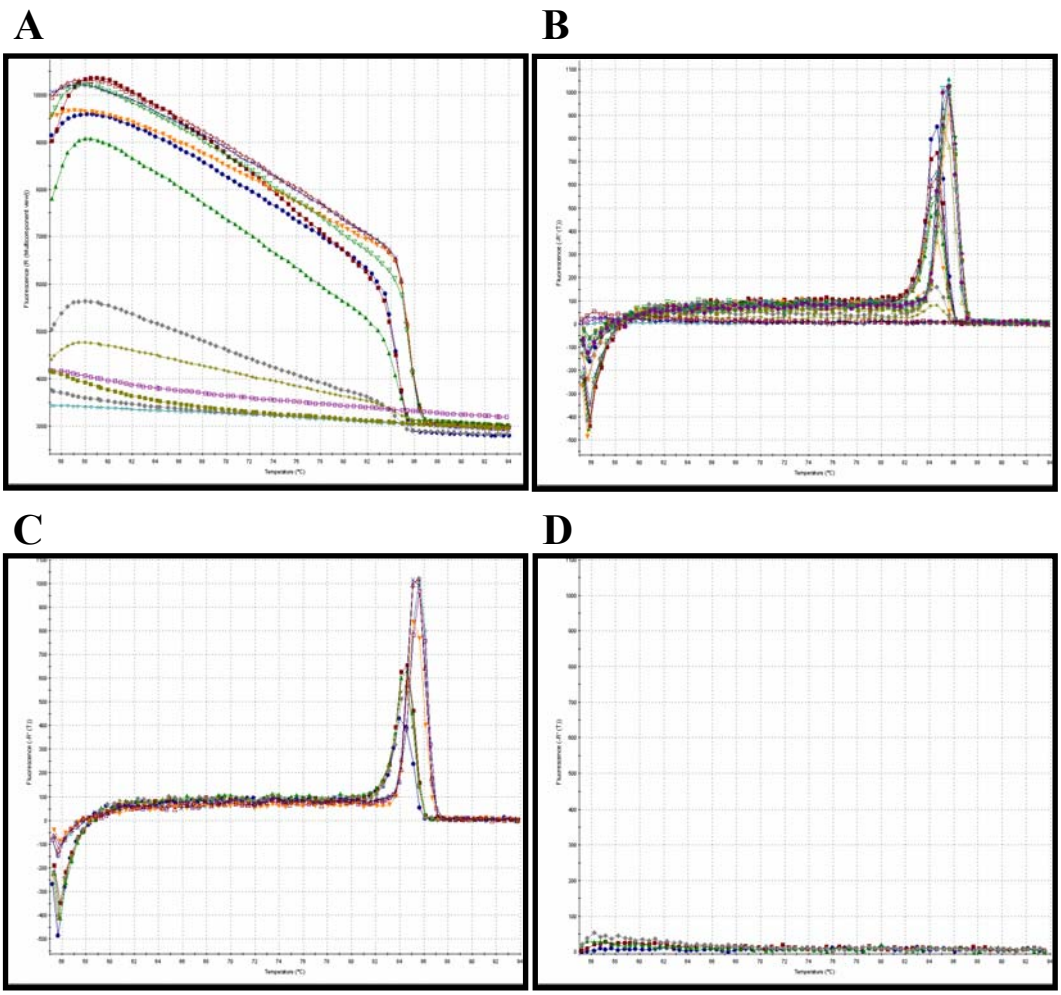

Figure 5.17: Disassociation graphs from a Quantitative PCR experiment produced by the MxPro programme on the Stratagene Mx3000P. Graph **A** shows the raw fluorescence data for all the samples resulting from a disassociation step. Graphs **B**, **C** and **D** show the negative derivative of the fluorescence data. Graph **B** displayed the disassociation curves for all the samples. Graph **C** shows only the experimental data. There is only one peak per primer set. Graph **D** shows the curves for the no template control and no reverse transcriptase control samples. There are no peaks present therefore the primers do not form dimers and there is only one binding set per primer set.

The next section of data to review is the standard curve of each primer set. As explained earlier this reveals the efficiency of the QPCR reaction which can be affected by contamination, incorrect primer concentrations and primer-dimers. Figure 5.18 shows an example of a standard curve from the same Quantitative PCR experiment as above. The standard curve for the *rp49* primer set is the red line and the blue line is the curve of the *puckered* primer set. The standard dilutions described earlier in Section 5.3.4 were neat cDNA, 1/5, 1/10, 1/50 and 1/100 for the *puckered* primers and 1/10, 1/100, 1/1000 and 1/10000 for *rp49* primers. The standards were produced using cDNA from a wild type L3 larvae RNA sample. The table shows the Rsq and efficiency values for standard curve of each primer set. The Rsq value for *rp49* is perfect at 1.000 and for *puckered* the Rsq value is 0.987. Both these values are within the acceptable Rsq Value range which means the Ct values for all the experimental samples fit well on the standard curve. Low Rsq values suggest pipetting errors have occurred. It was concluded that the pipetting for this experiment was accurate. The efficiency values are less encouraging at 46.4% for *puckered* and 67.5% for *rp49*. However as explained earlier the average efficiencies from all the standard curves can be entered into the MxPro programme. The programme uses these values to compensate for differences between the gene of interest (*puckered*) and the normaliser (*rp49*) when calculating the relative quantity of the *puckered* in the *pacman* mutants compared to the calibrator (wild type) sample.

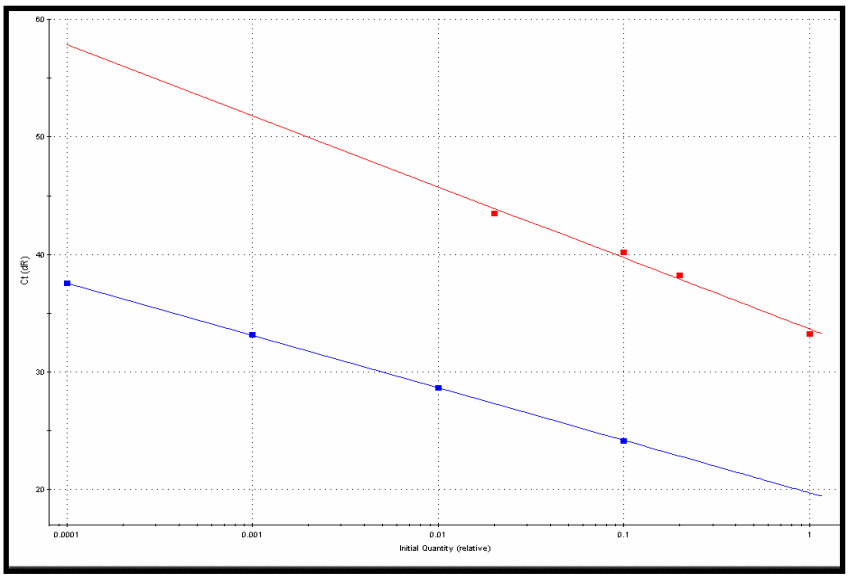

Primer Set	Rsq Value	Efficiency
puckered	0.987	46.4%
rp49	1.000	67.5%

Figure 5.18: An example of a standard curve from a Quantitative PCR experiment. The standard dilutions were neat cDNA, 1/5, 1/10, 1/50 and 1/100 for *puckered* primers and 1/10, 1/100, 1/1000 and 1/10000 for *rp49* primers. The standards were produced using cDNA from a wild type L3 larvae RNA sample. The table shows the Rsq and efficiency values for standard curve of each primer set.

The final graph produced by the MxPro programme to be analysed for each QPCR experiment is the Relative Quantity chart. This data shows the quantity of *puckered* expression in the *pacman* mutants in relation to the wild type calibrator. All samples have been normalized by the housekeeping gene *rp49.* Figure 5.19 displays the Relative Quantity data in two ways. In graph A the wild type sample has the value of 1 i.e. this is the baseline quantity. The *pacman* mutants all have values greater than 1. This means that *puckered* expression is increased in *pacman* mutants compared to the wild type control. Graph B displays the same data but as fold changes. The wild type calibrator is given the value of zero and the mutants are either above or below the zero line. In this case the mutants are above the line showing an increase in *puckered* expression in the pacman mutants. Both graphs show that pcm^5 has the biggest increase in *puckered* expression followed by pcm^3 then pcm^6. The error bars are calculated by the MxPro programme during the QPCR. The error bars on both graphs reflect the deviation in the triplicates. This means the error bars are derived from the error bars on the Cts and these error bars on the Cts are derived from the error bars on each fluorescence measurement at each cycle, and include estimates of the imprecision of the normalizer.

As mentioned earlier, two biological replicates each with 2 technical replicates were performed resulting in four QPCR experiments used to quantify the changes in *puckered* expression in the *pacman* mutants relative to the expression in the wild type control. The analysis began by calculating the average Rsq and efficiencies for all the standard curve data. Table 5.3 details these average values for each primer set.

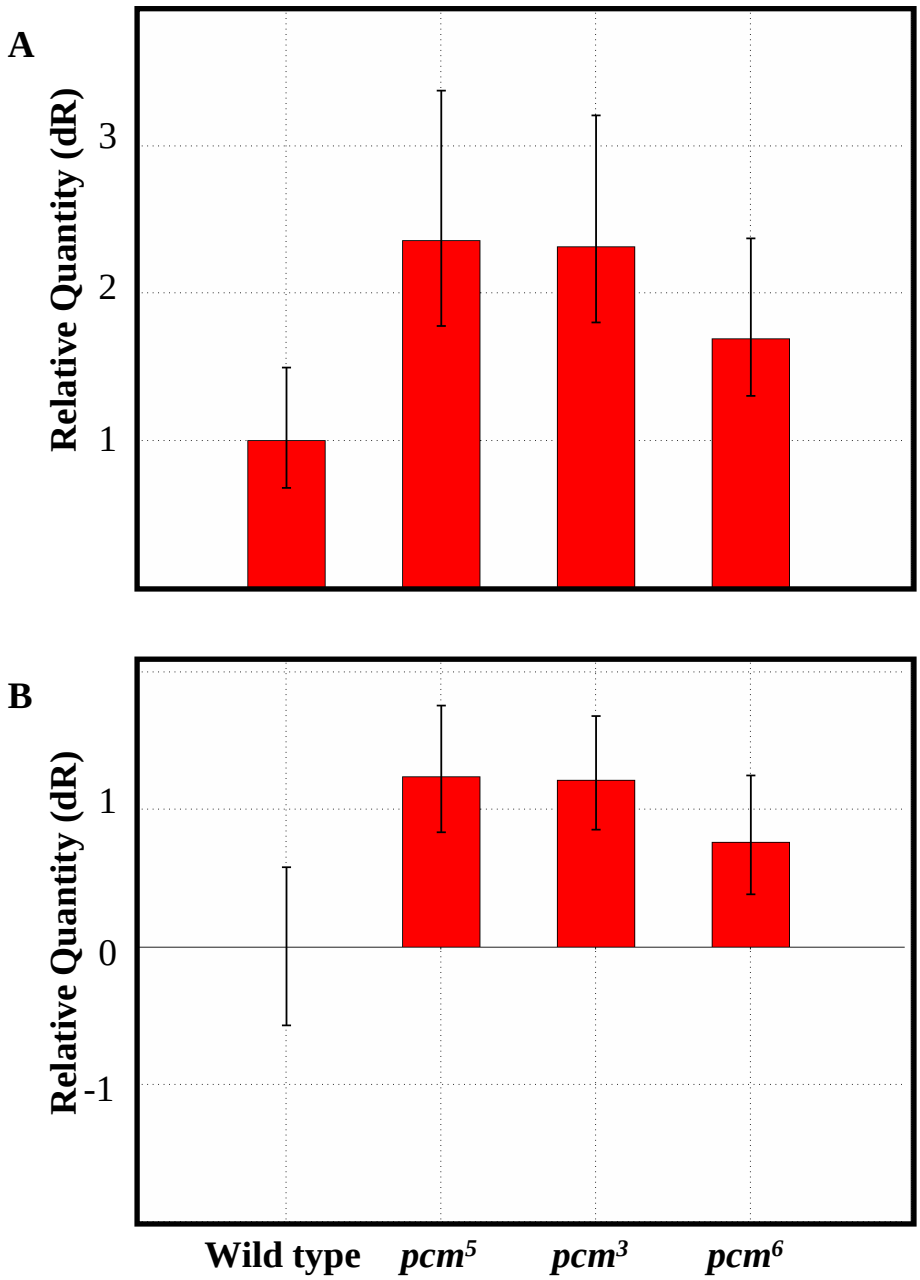

Figure 5.19: Bar graph **A** shows the relative quantity (dR) of *puckered* expression for each *pacman* mutant in relation to the wild type control. The wild type control has a dR value of 1. Graph **B** shows the same data as fold changes. Wild type has a dR value of 0 and the mutants are displayed as fold increase. The error bars reflect the deviation in the replicates for each sample.

Primer Set	Number of QPCR experiments	Average Rsq Value	Rsq Standard Deviation	Average Efficiency Value	Efficiency Standard Deviation
puckered	7	0.935	0.08	71.5%	29.4%
rp49	8	0.999	0.0007	71.9%	12.6%

Table 5.3: The average Rsq and Efficiency values were calculated for all the standard curves performed. This data shows the accuracy of the QPCR experiments. The number of standard curves produced for *puckered* n = 7 and *rp49* n = 8. The standard deviation represents the variation in the data from the average value.

The average Rsq values for both primer sets are very good and the standard deviations are very small. They are above or close to the recommend value of 0.985 which suggests the pipette technique for all samples was very accurate. During the set up of the QPCR the master mix solution was kept consistent and together for as long as possible for each primer set. The master mix was aliquoted into further tubes for each set of triplicates where the cDNA sample was added. This was aliquoted a further step into the QPCR tubes for each triplicate. This kept the triplicates the same and this is confirmed by the high Rsq values.
The average efficiencies for *puckered* and *rp49* were 71.5% and 71.9% respectively. These results are disappointing as they are below the recommended values of 90% to 110%. However as mentioned earlier when calculating the Relative Quantity (dR) using Comparative QPCR the average efficiency can be added to the MxPro programme and this is taken into account when the dR values are calculated. Ideally when adding the average efficiency to the comparative QPCR the values should be within 5% of each other. Unfortunately this was not the case with these experimental values which had standard deviations of 28.4% for *puckered* and 12.6% for *rp49*. These large deviations suggest that the primer sets are not fully optimized. There were no primer-dimers or contamination seen in any of the disassociation curves so these deviations are probably due to unsuitable primer concentrations. As mentioned previously a primer matrix was performed but the results were confusing. If more time was available optimization of the QPCR experiments with a second *puckered* and *rp49* primer sets (Dpuc4 and Drp492) produced by Dr Maria Zabolotskaya would be recommended.

The analysis of the final four QPCR experiments was continued by producing a graph of the average Relative Quantities (dR). Figure 5.20 shows that pcm^5 has the greatest increase in *puckered* expression with a value of 1.7925 compared to the wild type control's value of 1. This represents an increase of approximately 79% on the wild type value. This is followed by pcm^6 with a value of 1.6275 and an increase of approximately 63%. pcm^3 has the smallest increase with a value of 1.3985 and an increase of approximately 40%. The standard errors were calculated and they show this increase for all three *pacman* mutants is significant. Chi Squared analysis between the Wild type and each individual *pacman* mutant confirms a significant difference in the Relative Quantity of *puckered* mRNA for

pcm^{5} and *pcm*^{6} mutants from the Wild type control. The difference in Relative Quantities of *puckered* mRNA between the Wild type control and *pcm*^{3} is almost significant. These results are consistent with the Western Blotting expression of Section 5.1.4 and the β-galactosidase staining experiments of Section 4.6.3, which both show an increase in the JNK signalling pathway expression in the *pacman* mutants compared to the wild type control.

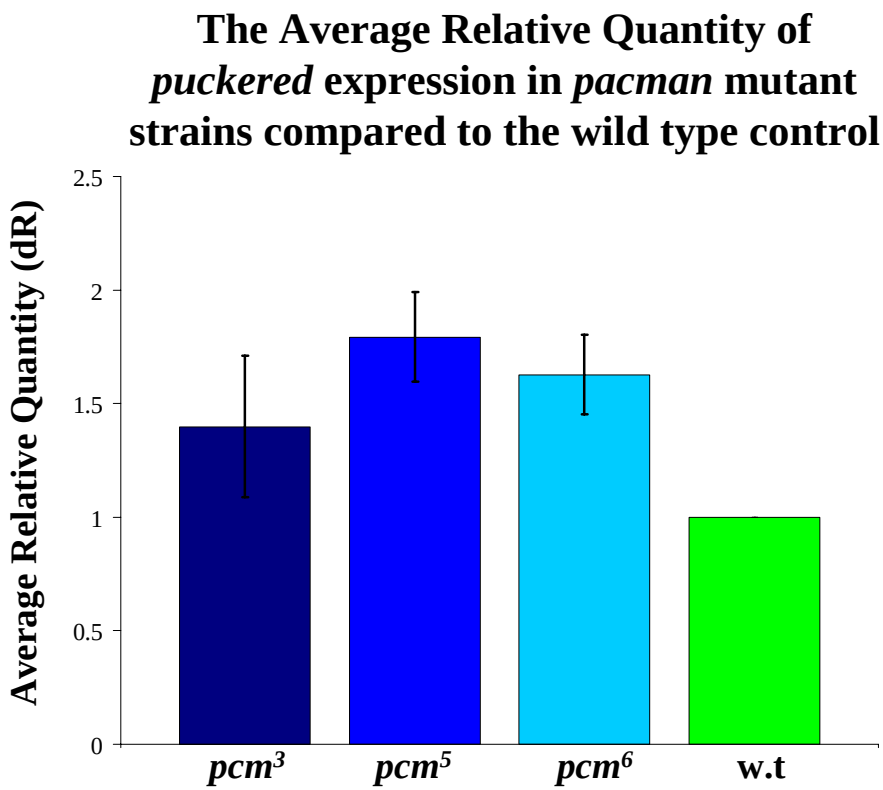

Figure 5.20: The average Relative Quantity of *puckered* expression. The three *pacman* mutants pcm^3, pcm^5 and pcm^6 are compared to the wild type control. The error bars represent the standard error. Chi squared analysis comparing wild type Relative Quantity to each individual mutant: pcm^3 P=0.080, pcm^5 P= 0.002 and pcm^6 P= 0.013. (n = 4)

5.4 Chapter Conclusions

In chapter 4, β-galactosidase staining experiments of flies, larvae and imaginal discs showed an increase in the level of expression of *pucLacZ* reporter gene in homozygous *pacman* mutants compared to the wild type control. This shows an increase in JNK activity in these mutants. During this chapter the investigation of the effects that *pacman* mutations have on the JNK signalling pathway continued. This investigation began by measuring the level of specific proteins of the JNK signalling pathway by Western Blotting. As mention in Section 5.1 several antibodies to the proteins produced by the genes *c-Jun* and *bsk* (JNK) were tested. Many of these antibodies were unspecific and produced Western Blots with many bands. Eventually an antibody with high specificity against BSK was found (from Sigma). After running the Western Blotting experiment the intensity of the bands for the three homozygous mutants and the wild type control were measured. Histograms of the average *bsk* expression scaled against the loading control Actin were produced for experiments at both 19˚C and 25˚C. These histograms show that the homozygous *pacman* mutants have more *bsk* protein expression and therefore are likely to have more JNK signalling expression than the wild type control. Unfortunately this increase did not appear to be significant. However these experiments do confirm the earlier data from the β-galactosidase staining experiments that the JNK signalling pathway is expressed at a higher level in the *pacman* mutants then the wild type control.

The next step in the investigation was to quantify the changes in the JNK signalling expression that are seen in the *pacman* mutants. Semi-Quantitative PCR was attempted to measure the expression of *puckered* normalized by the expression of the gene *rp49* in *pacman* mutants in relation to a wild type calibrator (control). This proved to be rather difficult because in order to quantify the changes between the strains, the PCR reaction must finish when both genes are in the linear exponential stage of the reaction. Due to the higher levels of expression of the *rp49* gene then the *puckered* gene this was not the case for these semi quantitative PCR experiments. Ideally the primer concentrations of *rp49* could be diluted to allow the reaction to run slower hopefully resulting in a similar

reaction time to *puckered*. It was not possible to normalize the *puckered* expression using the *rp49* expression therefore, as it stands, very little information can be taken from the Semi Quantitative PCR. However these experiments did outline that *rp49* expression is greater than *puckered* and this information could be used when optimising the Real Time Quantitative PCR experiments.

Finally Real Time Quantitative PCR experiments to quantify the changes in *puckered* expression and therefore JNK signalling expression in the *pacman* mutants in relation to the wild type control were undertaken. The *puckered* expression was normalized by the expression of a housekeeping gene *rp49* which is evenly expressed throughout all the samples. The accuracy of the QPCR experiments relies on optimising several procedures most importantly the primer conditions. These QPCR experiments have satisfactory Rsq values which imply the pipetting technique is accurate. However the efficiencies of these QPCR are lower than the recommend value. This suggests the primer conditions still need some optimization. Most likely the primer concentrations or even the primers themselves need to be adapted. Ideally the primer optimizations would continue until the efficiencies are between 90% and 110% but in this case both time and amount of SYBR green kit were a limiting factor. Therefore the QPCR experiments were undertaken using the average efficiencies in order to get an idea of the quantities of *puckered* expressed in the *pacman* mutants when related to the wild type control.

The average relative quantities of *puckered* expression in the *pacman* mutants relative to the wild type control for these Real Time Quantitative PCR experiments revealed that all three *pacman* mutants have an increase in *puckered* expression compared to the wild type control. pcm^5 has the greatest increase in *puckered* expression with an average Relative Quantity value of 1.7925 compared to the wild type value of 1 (P=0.002). This is followed by pcm^6 (P=0.013) and then pcm^3 (P=0.080) which has the smallest increase above the wild type. These results are encouraging however further QPCR experiments possibly with new primer sets would be advisable to confirm the quantities seem for the *pacman* mutants.

Overall the results from the Quantitative PCR, Western Blotting and β-galactosidase staining experiments suggest that a mutation in *pacman* leads to an increase in the expression of the *puckered* mRNA, phosphorylated Basket and therefore implies an increase in JNK signalling pathway expression. The following questions become apparent: How does this mutation lead to an increase in JNK signalling? And what member of the JNK signalling pathway does *pacman* interact with? The next chapter draws all the data together to form some conclusions and will attempt to suggest answers to the above questions.

Chapter 6 Conclusions

A common misconception when studying proteins that act as exoribonucleases is that their sole function is to work away in the background cleaning up the excess mRNA produced by transcription (Long et al. 2003; Coller et al. 2005; Parker et al. 2007). This indiscriminate exoribonuclease activity is no doubt one of the main functions of exoribonucleases, however previous studies in the Newbury lab which created *pacman* mutants by P-element excision have shown that at least in the case of the *Drosophila* exoribonuclease Pacman, this protein may have specific effects on particular mRNAs. This function involves specific and regulated spatial and temporal interactions with a signalling pathway during several developmental processes. This function may involve Pacman's exoribonuclease activity or it may represent a novel function of Pacman. Dr Steve Hebbes, a member of the Newbury group created a Pacman exoribonuclease "dead" mutant strain. This was achieved by site directed mutagenesis of the magnesium binding domain at the active site. A UAS construct containing this mutation was transformed into flies using embryo microinjection. Expressing this construct at roughly wild type levels fails to rescue the pcm^5 mutant phenotypes. This suggests the *pacman* mutant phenotypes are caused by the loss of Pacman exoribonuclease activity. A similar construct expressing a wild type copy of the *pacman* gene successfully rescued the pcm^5 mutation. The aim of this thesis was to investigate this secondary function of Pacman, its interaction with the JNK signalling pathway and determine whether through this function *pacman* has a role in wound healing.

6.1 Summary of the thesis results

6.1.1 Mutations in *pacman* result in reduce survival of flies after wounding

Previous studies have shown that mutations in *pacman* cause mutant phenotypes that are similar to those seen as a consequence of mutations in genes of the JNK signalling pathway. These mutant phenotypes such as defective thorax closure

suggest a specific role for *pacman* in epithelial sheet sealing. The JNK signalling pathway has been shown to regulate many morphogenetic and developmental processes involving cell movements including thorax closure. The similarities in mutant phenotypes between JNK signalling and *pacman* mutants suggested a genetic interaction between them. The JNK signalling pathway plays a role in epithelial sheet sealing during wound healing. If *pacman* interacts with the JNK signalling pathway during its role in cell movement we would expect to see a mutant wound healing phenotype in *pacman* mutant flies.

This is the rationale for the survival experiments which compared the survival of 3 *pacman* mutants (pcm^3, pcm^5 and pcm^6) with a wild type control after wounding with a scalpel on the abdomen. These survival experiments showed that at 19˚C the wild type control survives significantly longer than the *pacman* mutants for the time point 24 hours after wounding. Wound healing in *Drosophila* is completed by 24 hours so these results suggests the mutants have a defect in wound healing leading to premature death (Ramet et al. 2002; Galko et al. 2004). At 25˚C the *pacman* show a similar trend in survival. There is a significant decrease in survival after wounding of pcm^3 and pcm^5 mutants flies compared to the wild type. The pcm^6 mutant flies survival also appears to decrease compared to the wild type however this difference is not significant. Previously the *pacman* mutants have been shown to be temperature sensitive i.e. some mutant phenotypes are less severe at higher temperatures so these results are hardly surprising. The survival of *pacman* overexpression mutants were also compared to the wild type control. These *pacman* overexpression flies contain a transgene that expresses a cDNA copy of *pacman* under the control of the heat-shock promoter. The heat shock promoter was shown to be leaky so no heat shock treatment was required to activate the transgene expression. At 25˚C *pacman* overexpression mutants were shown to have a significant reduction in survival compared to the wild type control. This suggests the correct amount of *pacman* is critical for survival, too little or too much results in reduced survival. These results together confirm the hypothesis that *pacman* has a role on wound healing. Of course these results pose the questions:

1. How do we know the results are due to a specific defect in wound healing?
2. Could these results be due to an overall reduction in the metabolic processes that contribute to healing?

In order to answer these questions the clotting response of the *pacman* mutants after a wound is inflicted was examined. The time at which the clot starts to form after the wound is inflicted was recorded for pcm^3, pcm^5, pcm^6 and the wild type control. Clot formation occurs between 20-30 minutes after wounding in *Drosophila* (Ramet et al. 2002; Galko et al. 2004). There was no difference in clot formation times between the 3 *pacman* mutant strains and the wild type control. Therefore the reduced survival seen previously in the survival experiments is likely to be due to a specific defect in wound healing. Pacman seems to have a role in wound healing possibly through interactions with the JNK signalling pathway which will be discussed later in this chapter.

6.1.2 The age of the *Drosophila* fly affects wound healing

Interestingly, experiments to determine the affect of ageing on the survival of wounded wild type flies have shown the 3, 5 and 7 day old flies survive the longest after wounding. On the other hand there is a significant reduction in survival of the old (9day) and young (1day) flies 24 hours after wounding suggesting their wound healing is impaired or possibly slow to be activated. These results are consistent with human wound healing where older patients are slow to heal and therefore have higher incidents of chronic wounds and resultant deaths. This is extremely interesting as in humans the immune response of older patients has been implicated as a factor for chronic wounds and death as a result of imperfect wound healing. The immune response to wound infliction in young children has been shown to change with age. This may explain why young children are susceptible to infections. The innate immune response to wounding in *Drosophila* may also change with age which could explain why increased numbers of young flies die after wounding. Further studies of the immune response and wound healing signalling pathways at different ages would be invaluable. Overall these results suggest *Drosophila* would be an ideal model for wound healing and ageing studies.

6.1.3 The effect of infection on wound healing of *pacman* mutant flies

The effects infection may have on wound healing of the *pacman* mutants was investigated. The innate immune response is activated in *Drosophila* on detection of an attacking microbe. Depending on the type of microbe: fungal, gram negative or gram positive either one of two possible pathways Imd/Relish or Toll/$NF_{kappa}\beta$ will be activated. Expression of the JNK signalling pathway i.e. activation of wound healing has been shown to be intrinsically linked to the innate immune response.

Survival experiments were performed using the wild type control and the 3 *pacman* mutants which were either wounded with a sterile scalpel or one coated in *E.coli*. These experiments showed that the sterile wounded flies for each strain survived significantly better than the infected wounded flies 24 hours after wounding. The extra reduction in survival seen in the flies which were infected is probably due to the additional complication of the immune response on top of the wound healing response.

6.1.4 *pacman* genetically interactions with the JNK signalling pathway member *puckered*

Several different survival experiments have shown that *pacman* mutations result in reduced survival times after wounding suggesting a defect in wound healing. Since the JNK signalling pathway is known to regulate cell movements during wound healing it seemed a sensible conclusion that Pacman's role in wound healing may be linked to this pathway. To test this hypothesis a new fly strain was created possessing both a *pacman* and *puckered* mutation (pcm^{5}/FM7i ;; puc^{A251}/Tm6 TbSb). This double mutant strain had a unique adult phenotype, Bald patches, not seen in either single mutant strain. Bald patches were seen on the thorax of the double mutants at high penetrance suggesting they have a defect in thorax closure similar to those seen in JNK signalling mutants hep^{1} and pcm^{3}/Df(1)JA27 mutants. Df(1)JA27 is a large deficiency which maps to the X chromosome region containing the *pacman* gene. Therefore pcm^{3}/Df(1)JA27 flies

will only possess the mutant copy of the *pacman* gene making any mutant phenotypes more severe. The unique bald patch phenotype suggests a genetic interaction between *pacman* and *puckered* i.e. the JNK signalling pathway. Survival experiments wounding double mutant flies showed that these flies survive significantly better than the wild type. The wounded single *puckered* mutant flies also show a significant increase in survival compared to the wild type wounded flies. There is significant difference in the survival of the wounded double and single mutant flies. This result suggests mutations in *puckered* can restore the *pacman* mutant wound healing phenotype. Previous studies have shown that heterozygote *puckered* mutations increases the longevity of these flies (Wang et al. 2003; Wang et al. 2005). Therefore the increased survival seen in the *pacman puckered* double mutants may be a result of the single copy of the *puckered* mutation rather than a measure of more efficient wound healing. Experiments such as Electron Microscopy of the wound site or live fluorescent imaging of wound healing may help to understand this survival phenotype.

6.1.5 β-galactosidase staining experiments of the *pacman* and *puckered* mutants suggest the JNK signalling pathway expression is upregulated in *pacman* mutants

The *puckered* mutation of the double mutant strain was created by inserting the *E.coli* LacZ gene sequence downstream of the *puckered* promoter. This means the LacZ sequence can be used as marker for *puckered* transcriptional activation. Expression of the LacZ produces β-galactosidase, this breaks down the substrate Xgal and one of these products produce a blue stain which can be visualised. The blue stain represents the location of the *puckered* expression.
β-galactosidase staining experiments using the wild type control (+/+ ;; *pucLacZ*/Tm6 TbSb) and the pcm^5 mutant (pcm^5/pcm^5 ;; *pucLacZ*/Tm6 TbSb) in flies and larvae hinted that the *puckered* expression levels were higher in the double mutant than the wild type after wounding i.e. the JNK signalling expression levels were higher. However the staining in these experiments was difficult to quantify therefore a scoring system was applied to the fly and larvae staining. The JNK signalling pathway is naturally activated during thorax closure in the *Drosophila* larvae therefore wing imaginal discs which form the thorax

were used for β-galactosidase staining experiments. The β-galactosidase staining experiments of wing imaginal discs also showed that *puckered* expression increases in *pacman* mutants compared to the wild type control. This staining of the imaginal discs was quantified using the Zeiss Axioplan microscope and AxioVision Release 4.6 programme. The double mutants have smaller imaginal discs then the wild type control or the single *puckered* mutant but they contained more β-galactosidase staining i.e. more *puckered* expression although this difference does not appear to be significant.

This lead to the hypothesis that Pacman may be involved in regulating the JNK signalling pathway through degradation of the *puckered* mRNA. Therefore when *pacman* is mutant the levels of *puckered* mRNA would increase leading to more *puckered* protein; and through the negative feedback loop this would reduce the level of phosphorylated Basket (Figure 6.1).

Drosophila JNK signalling pathway: Hypothesis 1

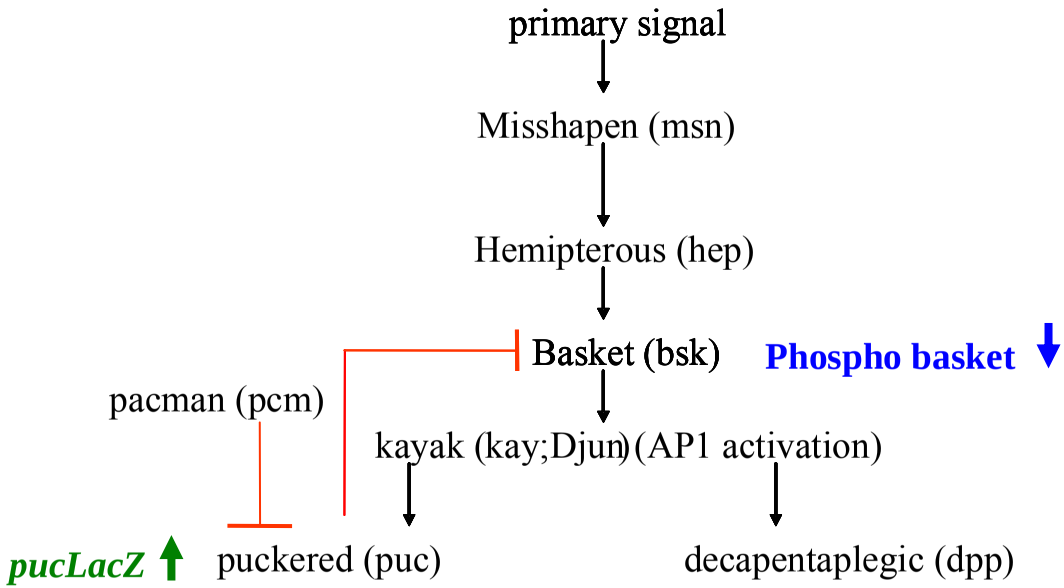

Figure 6.1: Hypothesis 1:- Possible role for *pacman* degrading *puckered* mRNA and therefore regulating the JNK signalling pathway. β-galactosidase staining experiments showed *pucLacZ* expression increases in *pacman* mutants (green). This hypothesis would lead to a reduction in phosphorylated Basket (blue).

6.1.6 Western Blotting experiments show phosphorylated *basket* (JNK) increases in *pacman* mutants

The unique bald patch phenotype of the *pacman* and *puckered* double mutant showed a genetic interaction between *pacman* and the JNK signalling pathway. This strain was used for β-galactosidase staining experiments which hinted at an increase in JNK signalling in *pacman* mutant flies. To further quantify the increase in expression of the JNK signalling pathway in *pacman* mutants, Western Blotting experiments were performed using anti phospho JNK. This detected an increase in phosphorylated *basket* (JNK) in the *pacman* mutants. This is consistent with the β-galactosidase staining experiments where both show an upregulation of the JNK signalling pathway in *pacman* mutant flies compared to the wild type control (although in the β-galactosidase staining this increase does not appear to be significant). This increase in phosphorylated Basket would lead to increased activation of the AP-1 complex leading to higher levels of transcription of *puckered* mRNA and more Puckered expression. However this is not consistent with the hypothesis suggested in Section 6.1.5 that Pacman regulates the JNK signalling pathway by degrading *puckered* mRNA. A new hypothesis was put forward that *pacman* regulates the JNK signalling pathway through degradation of an RNA encoded by gene member positioned above *basket* in the pathway (Figure 6.2). If this was the case then mutations in *pacman* would lead to an increase in the levels of phosphorylated *basket*, *puckered* mRNA and *pucLacZ* expression would increase. Phosphorylated *basket* and *pucLacZ* expression have both been shown to increase in *pacman* mutants. To test this, the level of *puckered* mRNA was investigated by Real-Time Quantitative PCR.

Drosophila JNK signalling pathway: Hypothesis 2

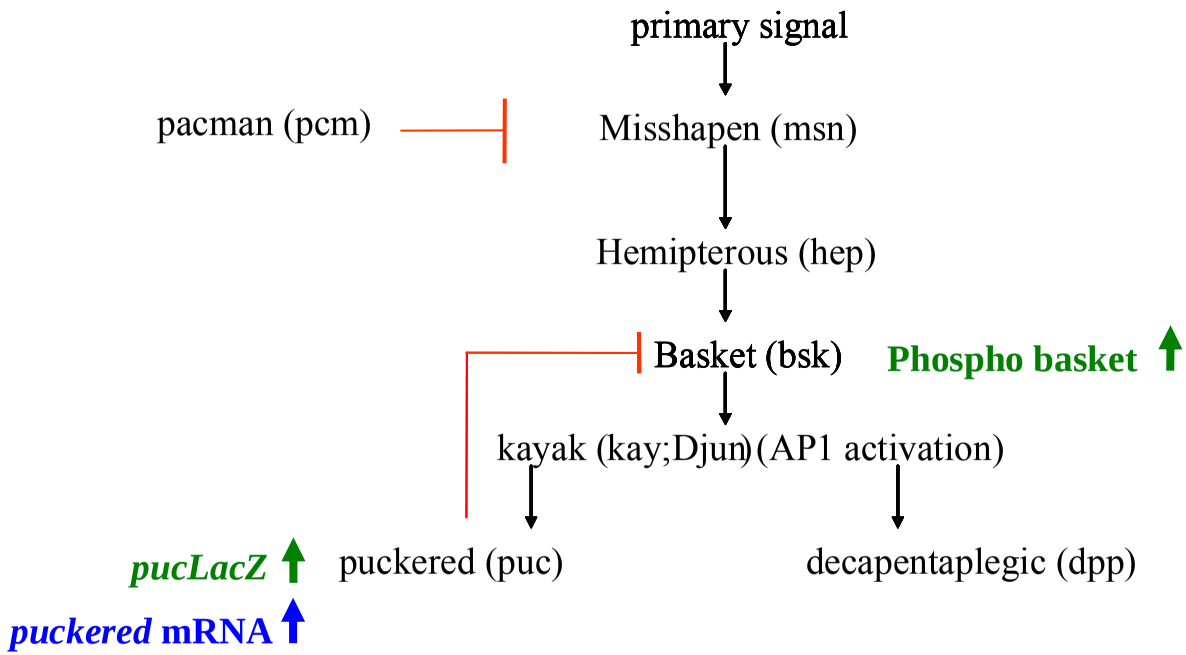

Figure 6.2: Hypothesis 2:- Possible role for *pacman* degrading mRNA of JNK signalling pathway member above *basket* and therefore regulating the JNK signalling pathway. β-galactosidase staining experiments showed *pucLacZ* expression increases in *pacman* mutants and Western Blotting experiments showed phospho Basket increases in *pacman* mutants (green). This hypothesis would lead to an increase in *puckered* mRNA (blue).

6.1.7 Real-Time Quantitative PCR shows the level of *puckered* mRNA increases in *pacman* mutants

Real-Time Quantitative PCR was performed on the wild type control, pcm^3, pcm^5 and pcm^6 larvae using *puckered* and *rp49* primer sets. This measures the levels of *puckered* and *rp49* cDNA in each sample. The cDNA was produced by Reverse Transcriptase PCR from a total RNA sample. The level of cDNA directly relates to the level of mRNA in the sample. A housekeeping gene in this case *rp49* which has a constant level of expression in every sample acts as the normaliser. The wild type control is the calibrator and the level of *puckered* mRNA in each *pacman* mutant is compared to this calibrator. Unfortunately the PCR reactions were not completely optimized probably as a result of unsuitable primer sets. However the Quantitative PCR experiments did suggest increased levels of *puckered* mRNA in all three *pacman* mutants compared to the wild type control. pcm^5 was shown to have a 79% increase in *puckered* expression compared to the wild type strain. pcm^6 has a 63% increase compared to wild type and the increase seen in pcm^3 flies was 40%. This increase in *puckered* expression in the pcm^5 and pcm^6 flies was shown to be significant. This result is consistent with hypothesis 2 that Pacman degrades the mRNA of a gene member of the JNK signalling pathway upstream of *basket*.

6.1.8 Discussion of the thesis results

Overall the results show that expression of the JNK signalling pathway increases when *pacman* is mutated. This was shown by an increase in phosphorylated Basket in the mutants compared to the wild type control detected through Western Blotting experiments, an increase in *puckered* mRNA levels in *pacman* mutants measured by Real-Time Quantitative PCR and an increase in *pucLacZ* expression and therefore *puckered* by β-galactosidase staining experiments (Figure 6.3). These results imply a role for Pacman in the inhibitation/repression of the JNK signalling pathway most likely by degradation through its exoribonuclease function. This degradation will be specifically timed and located to repress the JNK pathway where it is needed. Pacman may repress the pathway through

degradation of several JNK gene members or through degradation of a mRNA encoding for a protein which interacts directly with the JNK signalling pathway. There is evidence that Pacman degrades mRNA encoding a protein TAK1 which has been shown to be an upstream activator of the JNK signalling pathway (Mihaly et al. 2001). Recent microarray data from the Newbury lab generated using *Drosophila* testes have shown that *tak1* mRNA is unregulated in pcm^5 mutants. Using semi-quantitative RT-PCR, Dr. Maria Zabolotskaya has demonstrated that *tak1* mRNA is upregulated 2-fold in pcm^5 mutants. This would be consistent with a role for Pacman in repressing the JNK signalling pathway i.e. Pacman normally degrades *tak1* mRNA and the concomitant decrease in TAK1 protein reduces activation of the JNK signalling pathway. The effect of *pacman* mutations on *tak1* and the JNK pathway result is also being followed up in 3rd instar larvae by a PhD student in the Newbury lab, Chris Jones, who is using Taqman quantitative RT-PCR to accurately determine the levels of these mRNAs in *pacman* mutants.

Overview of thesis results

In *pacman* mutants:

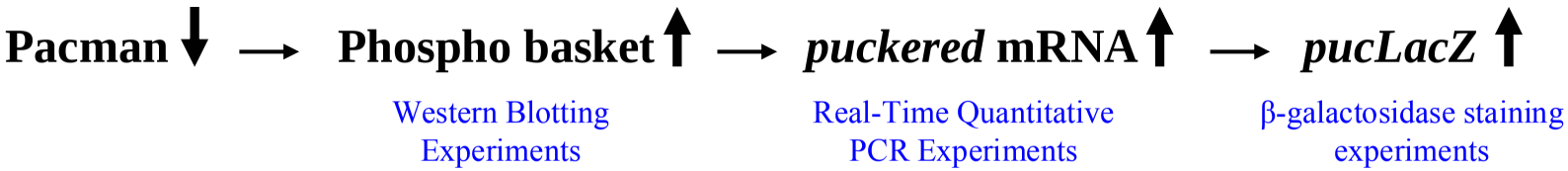

Figure 6.3: Overview of the thesis results. In *pacman* mutants there is less Pacman which leads to increased levels of phosphorylated Basket shown by Western Blotting (blue). There is also increased levels of *puckered* mRNA shown by Real-Time Quantitative PCR and lastly β-galactosidase staining experiments showed an increase in levels of the reporter transgene *pucLacZ* suggesting an increase in *puckered* expression (blue). Overall the results show an increase in expression levels of the JNK signalling pathway in *pacman* mutants suggesting a role for *pacman* in JNK signalling inhibition/repression.

6.2 A possible role for Pacman in wound healing of *Drosophila melanogaster*

During this thesis survival experiments have confirmed *pacman* plays a role in wound healing. Crossing *pacman* and *puckered* mutants flies showed that *pacman* interacts genetically with *puckered* which itself regulates wound healing in *Drosophila*. Pacman was shown to inhibit JNK signalling as *pacman* mutations lead to increased levels of transcriptional activation of this pathway. Thus Pacman's role in wound healing is most likely the repression of the JNK signalling pathway. This leads to the question: Where at the wound site may Pacman interact and repress the JNK signalling pathway?

Several previous studies have shown that the JNK signalling pathway is upregulated at the leading edge of the wound (Reed et al. 2001; Ramet et al. 2002; Galko et al. 2004). Increased *puckered* and *decapentaplegic* expression has been seen at this location. This increase in JNK signalling creates a JNK signalling gradient between the HIGH expression of the leading edge and the LOW expression of the exposed connective tissue. This JNK signalling gradient acts as a signal for focal adhesion junctions and the actomyosin cable to form which leads to the moving together of the wound. These conditions are similar to those seen at the leading edge of the lateral epithelial cells of the dorsal hole and the amnioserosa at dorsal closure in *Drosophila* embryos. It is unlikely that Pacman's role is at the leading edge of either the wound or the dorsal hole as JNK signalling is upregulated and not repressed at these locations.

Recent immunohistochemistry experiments using the Pacman antibody on *Drosophila* embryos undergoing dorsal closure (performed by Dr. Dominic Grima) have revealed Pacman localisation in possible P-body sites in the amnioserosa. This would be consistent with Pacman repressing the JNK signalling pathway in the amnioserosa to produce LOW JNK expression and create a gradient across the dorsal hole boundary. This hypothesis is strengthened by results generated by a undergraduate student in the Newbury lab, Steven Nottley, who has shown that downregulation of Pacman in the amnioserosa results in

complete lethality. A possible location for Pacman repression of the JNK signalling pathway during wound healing would be the connective tissue where JNK signalling expression is LOW to allow the gradient to form (Figure 6.4).

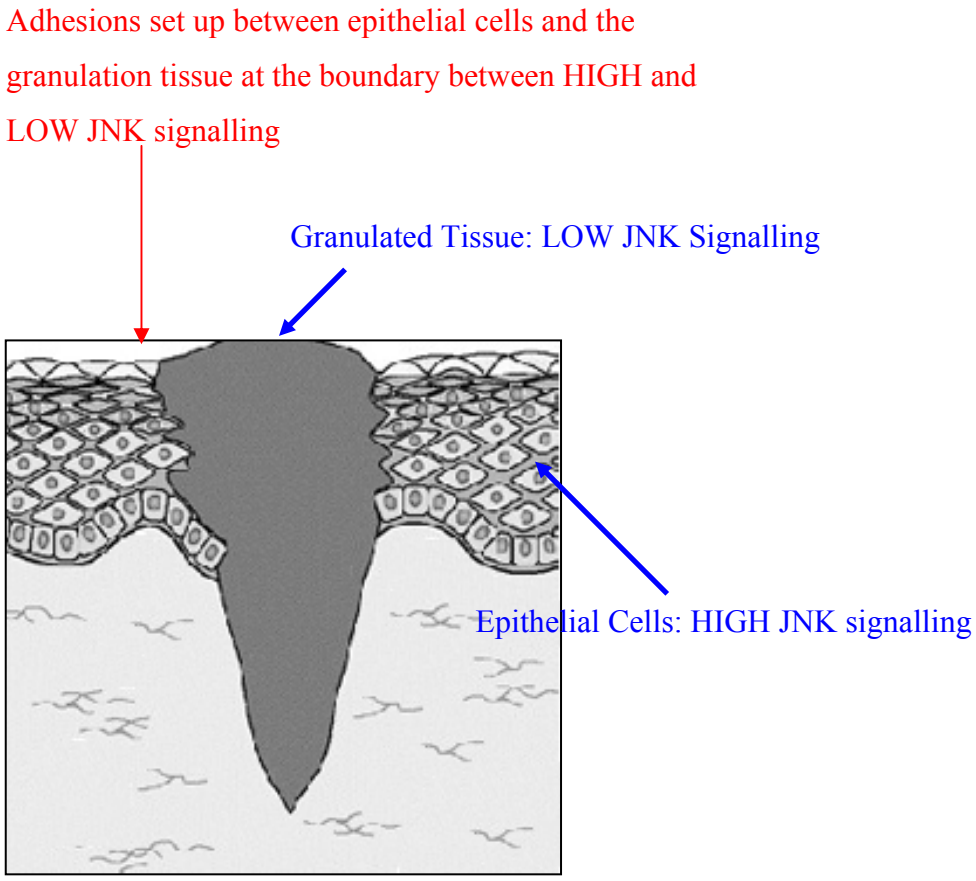

Figure 6.4: Hypothesis outlining a possible role for *pacman* during wound healing by regulation of the JNK signalling pathway. Pacman suppresses JNK signalling pathway in the granulated tissue of the wound clot producing a LOW to HIGH JNK boundary between the granulation tissue and the leading edge epithelial cells. This gradient of JNK signalling promotes cell sheeting sealing to begin.

6.3 Future Research

Further experiments that would help to characterize Pacman's role in wound healing of *Drosophila melanogaster* include:

1. Immunohistochemistry using Pacman antibody at wound sites:
In order to further test the hypothesis that Pacman inhibits the JNK signalling pathway in the exposed connective tissue (granulation tissue) during wound healing to create a JNK signalling gradient. This work would be best in embryos as Immunohistochemistry experiments have already been performed using them for dorsal closure. Embryo wounding would require a laser to produce small and consistent wounds across many samples (Wood et al. 2002). Antibodies for JNK signalling pathway members could also be used. A *puckered* antibody would be very useful to have for staining experiments and Western Blotting experiments.

2. Quantitative PCR:
To further quantify the changes in expression levels of the JNK signalling pathway in *pacman* mutants the quantitative PCR experiments should be continued firstly with new *puckered* and *rp49* primer sets. This could be followed by other JNK signalling pathway members and up stream activators such as *tak1* which was shown to increase in *pacman* mutant testes by microarray experiments. Other tissue types could be used for RNA extraction such as wounded tissue or wing imaginal discs which may have a higher level of JNK signalling expression due to the process of thorax closure taking place during larval development. These experiments are currently being carried out by a second year PhD student in the Newbury lab, Chris Jones, using Taqman quantitative RT-PCR.

3. Western Blotting experiments:
To further characterize the interaction between *pacman* and the JNK signalling pathway. Western Blotting experiments using the phospho *basket* antibody could be repeated using wing imaginal discs for tissue extracts. This may lead to a stronger change in JNK signalling expression in *pacman* mutants. Other

antibodies may be tested, Puckered being a prime example if an antibody is available. A suitable control for the Basket antibody would also to advisable. The *flw* strain mention in Section 5.1.6 may be a consideration. Western Blotting experiments using anti Basket antibodies pJNK (G7) from Santa Cruz Biotechnology and antiACTIVE JNK from Promega showed only the monophosphorylated form of *basket* band for genotype *flw1*/Y ;; puc^{A251}/+. The antibody used in this thesis only binds to the diphosphorylated form. Therefore Western Blotting experiments with *pacman* mutants using phospho *basket* (Sigma) would result in no band at the expected size of the *basket* protein.

4. New control fly strain:

Chris Jones of the Newbury lab has recently produced a new fly strain which will act as a control for the *pacman* mutants. This fly strain has the P-element, which was used to produce the *pacman* mutants, cleanly removed. Therefore the only difference between these new flies and each *pacman* mutant is the deleted region of the *pacman* gene i.e. the genetic background is identical. This new control could be used for further infection experiments and ageing experiments as more data is required for both to determine if the effects seen are significant.

5. Microarray experiments of wounded mutant tissue:

A plan was designed for a microarray experiment to investigate changes in expression of specific genes during wound healing in the pcm^5 mutant compared to the wild type control flies. Genes of interest would include the JNK signalling pathway members, upstream activators of this pathway (e.g. *tak1*) and innate immunity regulators (e.g. *relish*, *toll*). Unfortunately there was no time to perform this microarray experiment in the time scale of this thesis. Here is a brief explanation of the microarray plan (Appendix 6): wild type and pcm^5 flies are wounded on the abdomen with a small scalpel (Method 2.6) then allowed to heal for 4 hours. Any changes in expression may be small and localised to the abdomen therefore the flies are dissected to leave only the empty abdomen. These tissue samples along with unwounded controls for both strains would then be sent for microarray analysis at the Affymetrix array facility, Glasgow. This microarray data would provide valuable information about both the genes that are activated/inhibited in wild type flies after wounding and also the gene expression

that is affected by a *pacman* mutation. The genes whose expression is seen to change in the *pacman* mutants would be good targets for further analysis. (Boutros et al. 2002; Etter et al. 2002; Drnevich et al. 2004)

The results outlined in this thesis have detailed a link between *pacman* and the JNK signalling pathway during wound healing of *Drosophila melanogaster* and probably other epithelial cell sheeting movements. This highlights a novel specific and targeted regulation of a signalling pathway through degradation by the exoribonuclease *pacman* during the biological process of wound healing. Thus the work in this thesis has laid the foundations for further work on specific regulation of signalling pathways via degradation by *pacman* during morphogenetic processes.

a Appendices:

Appendix 1:

Primer sequences for Jes1 and Big1 which span the *pacman* gene were used to identify the different *pacman* mutations

Jes1 (Forward): 5' TCC CGA TCA CGA TGA AGA CC 3'
Big1 (Reverse): 5' ACT GCC GCC TCA GAT CTG 3'

Appendix 2:

Primer sequences for pcm5F and pcm5R which were used to identify the pcm^5 mutation in the *pacman puckered* double mutants.

pcm5F (Forward): 5' ACG CGT CAG TAC GCC AAC AA 3'
pcm5R (Reverse): 5' TCT TGG GAC GGT ACG CCT GT 3'

Appendix 3:

Primer sequences for melLacZF and melLacZR which were used to identify the presence of the *pucLacZ* reporter gene in the *pacman puckered* double mutants.

melLacZF (Forward): 5' CTG GCG TAA TAG CGA AGA GG 3'
melLacZR (Reverse): 5' CAG CAG CAG ACC ATT TTC AA 3'

Appendix 4:

Primer sequences for pucF/R and rp49F/R which were used for Semi Quantitative PCR experiments to measure the levels of *puckered* mRNA of *pacman* mutants.

pucF (Forward): 5' ACA CTA CAA CGG CAA CGT CA 3'
pucR (Reverse): 5' TCG TCA CAT GCC AGA TTC TC 3'
Amplicon Size: 421bp

rp49F (Forward): 5' CCA GTC GGA TCG ATA TGC TAA 3'
rp49R (Reverse): 5' GTT CGA TCC GTA ACC GAT GT 3'
Amplicon Size: 121bp

Appendix 5:

Primer sequences for Dpuc3F/R, Dpuc4F/R, Drp491F/R and Drp492F/R which were designed for Real-Time Quantitative PCR experiments to measure the levels of *puckered* mRNA of *pacman* mutants.

Dpuc3F (Forward): 5' TGT GAA TCG AGA AAC GCA 3'
Dpuc3R (Reverse): 5' CTT TGT ATA TGA CTC ACG CT 3'
Amplicon Size: 141bp

Dpuc4F (Forward): 5' CAC CTG AAT AGT CCT AGC AA 3'
Dpuc4R (Reverse): 5' CCT CGC TAT CCG ACT T 3'
Amplicon Size: 136bp

Drp491F (Forward): 5' CAA GGG ACA GTA TCT GAT G 3'
Drp491R (Reverse): 5' CAG TAA ACG CGG TTC T 3'
Amplicon Size: 141bp

Drp492F (Forward): 5' TCG GTT ACG GAT CGA ACA 3'
Drp492R (Reverse): 5' GTA AAC GCG GTT CTG C 3'
Amplicon Size: 113bp

Appendix 6:

Microarray Plan: *Drosophila* whole transcriptome long-oligonucleotide array

To analysis the changes in gene expression between wild type (OregonR) and mutant (*pacman*^{5}) flies after wounding using microarrays. Looking particularly at the genes of the JNK signalling pathway and those involved in cell shape changes.

Experimental Design:

Samples:		
OregonR	unwounded	
	wounded	4 hrs healing
pacman^{5}	unwounded	
	wounded	4 hrs healing

Need ~ 50 abdomen carcasses to give ~ 50µg of total RNA per hybridization reaction
Each sample type/condition has four hybridization reactions
Therefore need ~ 200 abdomen carcasses per sample type/condition

Appendices:

1. Collect 3-5 day old flies raised at 19˚C and wound on abdomen.
2. Allow flies to heal for 4 hours.
3. Put flies on ice. Cut off head and thorax and pull out ovaries.
4. Place abdomen carcasses in 1.5ml micro centrifuge tubes and put in liquid nitrogen.
5. Store at -70˚C
6. Homogenise samples in 300µl of TRIzol for 30-60 secs on ice.
7. Store at -70˚C till ready to send to flychip.

Analysis:

To analysis the results we would like to compare gene expression in

1. Unwounded wild type flies to unwounded mutant flies.
2. Wounded wild type flies to wounded mutant flies.
3. Unwounded wild type flies to wounded wild type flies.
4. Unwounded mutant flies to wounded mutant flies.

b References:

Agnes, F., M. Suzanne and S. Noselli (1999). "The Drosophila JNK pathway controls the morphogenesis of imaginal discs during metamorphosis." Development **126**(23): 5453-62.

Alberts, B., D. Bray, J. Lewis, R. Martin, K. Roberts and J. D. Watson (1994). Molecular Biology of The Cell, Garland Publishing.

Altan, Z. M. and G. Fenteany (2004). "c-Jun N-terminal kinase regulates lamellipodial protrusion and cell sheet migration during epithelial wound closure by a gene expression-independent mechanism." Biochem Biophys Res Commun **322**(1): 56-67.

Ashburner, M. (1989). Drosophila: A laboratory handbook, Cold Spring Harbour Laboratory Press.

Azouz, A., M. S. Razzaque, M. El-Hallak and T. Taguchi (2004). "Immunoinflammatory responses and fibrogenesis." Med Electron Microsc **37**(3): 141-8.

Babcock, D. T., A. R. Brock, G. S. Fish, Y. Wang, L. Perrin, M. A. Krasnow and M. J. Galko (2008). "Circulating blood cells function as a surveillance system for damaged tissue in Drosophila larvae." Proc Natl Acad Sci U S A **105**(29): 10017-22.

Barr, R. K. and M. A. Bogoyevitch (2001). "The c-Jun N-terminal protein kinase family of mitogen-activated protein kinases (JNK MAPKs)." Int J Biochem Cell Biol **33**(11): 1047-63.

Barreau, C., L. Paillard and H. B. Osborne (2005). "AU-rich elements and associated factors: are there unifying principles?" Nucleic Acids Res **33**(22): 7138-50.

Bashirullah, A., R. L. Cooperstock and H. D. Lipshitz (2001). "Spatial and temporal control of RNA stability." Proc Natl Acad Sci U S A **98**(13): 7025-8.

Bashirullah, A., S. R. Halsell, R. L. Cooperstock, M. Kloc, A. Karaiskakis, W. W. Fisher, W. Fu, J. K. Hamilton, L. D. Etkin and H. D. Lipshitz (1999). "Joint action of two RNA degradation pathways controls the timing of maternal transcript elimination at the midblastula transition in Drosophila melanogaster." Embo J **18**(9): 2610-20.

Bashkirov, V. I., H. Scherthan, J. A. Solinger, J. M. Buerstedde and W. D. Heyer (1997). "A mouse cytoplasmic exoribonuclease (mXRN1p) with preference for G4 tetraplex substrates." J Cell Biol **136**(4): 761-73.

References:

Bement, W. M., C. A. Mandato and M. N. Kirsch (1999). "Wound-induced assembly and closure of an actomyosin purse string in Xenopus oocytes." Curr Biol **9**(11): 579-87.

Bidla, G., M. Lindgren, U. Theopold and M. S. Dushay (2005). "Hemolymph coagulation and phenoloxidase in Drosophila larvae." Dev Comp Immunol **29**(8): 669-79.

Bosch, M., F. Serras, E. Martin-Blanco and J. Baguna (2005). "JNK signaling pathway required for wound healing in regenerating Drosophila wing imaginal discs." Dev Biol **280**(1): 73-86.

Botella, J. A., I. A. Baines, D. D. Williams, D. C. Goberdhan, C. G. Proud and C. Wilson (2001). "The Drosophila cell shape regulator c-Jun N-terminal kinase also functions as a stress-activated protein kinase." Insect Biochem Mol Biol **31**(9): 839-47.

Boutros, M., H. Agaisse and N. Perrimon (2002). "Sequential activation of signaling pathways during innate immune responses in Drosophila." Dev Cell **3**(5): 711-22.

Boutros, M., N. Paricio, D. I. Strutt and M. Mlodzik (1998). "Dishevelled activates JNK and discriminates between JNK pathways in planar polarity and wingless signaling." Cell **94**(1): 109-18.

Bownes, M. (1975). "A photographic study of development in the living embryo of Drosophila melanogaster." J Embryol Exp Morphol **33**(3): 789-801.

Brand, A. H. and N. Perrimon (1993). "Targeted gene expression as a means of altering cell fates and generating dominant phenotypes." Development **118**(2): 401-15.

Brazma, A., P. Hingamp, J. Quackenbush, G. Sherlock, P. Spellman, C. Stoeckert, J. Aach, W. Ansorge, C. A. Ball, H. C. Causton, T. Gaasterland, P. Glenisson, F. C. Holstege, I. F. Kim, V. Markowitz, J. C. Matese, H. Parkinson, A. Robinson, U. Sarkans, S. Schulze-Kremer, J. Stewart, R. Taylor, J. Vilo and M. Vingron (2001). "Minimum information about a microarray experiment (MIAME)-toward standards for microarray data." Nat Genet **29**(4): 365-71.

Bustin, S. A. (2000). "Absolute quantification of mRNA using real-time reverse transcription polymerase chain reaction assays." J Mol Endocrinol **25**(2): 169-93.

Bustin, S. A. (2002). "Quantification of mRNA using real-time reverse transcription PCR (RT-PCR): trends and problems." J Mol Endocrinol **29**(1): 23-39.

Campos-Ortega, J. A. a. H., V. (1985). The embryonic development of drosophila melanogaster, Springer-Verlag.

References:

Caponigro, G. and R. Parker (1996). "Mechanisms and control of mRNA turnover in Saccharomyces cerevisiae." Microbiol Rev **60**(1): 233-49.

Chanda, S. K., S. White, A. P. Orth, R. Reisdorph, L. Miraglia, R. S. Thomas, P. DeJesus, D. E. Mason, Q. Huang, R. Vega, D. H. Yu, C. G. Nelson, B. M. Smith, R. Terry, A. S. Linford, Y. Yu, G. W. Chirn, C. Song, M. A. Labow, D. Cohen, F. J. King, E. C. Peters, P. G. Schultz, P. K. Vogt, J. B. Hogenesch and J. S. Caldwell (2003). "Genome-scale functional profiling of the mammalian AP-1 signaling pathway." Proc Natl Acad Sci U S A **100**(21): 12153-8.

Chang, L. and M. Karin (2001). "Mammalian MAP kinase signalling cascades." Nature **410**(6824): 37-40.

Chen, H. W., M. J. Marinissen, S. W. Oh, X. Chen, M. Melnick, N. Perrimon, J. S. Gutkind and S. X. Hou (2002). "CKA, a novel multidomain protein, regulates the JUN N-terminal kinase signal transduction pathway in Drosophila." Mol Cell Biol **22**(6): 1792-803.

Chernukhin, I. V., J. E. Seago and S. F. Newbury (2001). "Drosophila 5'-->3'-exoribonuclease Pacman." Methods Enzymol **342**: 293-302.

Chin-Sang, I. D. and A. D. Chisholm (2000). "Form of the worm: genetics of epidermal morphogenesis in C. elegans." Trends Genet **16**(12): 544-51.

Ciapponi, L. and D. Bohmann (2002). "An essential function of AP-1 heterodimers in Drosophila development." Mech Dev **115**(1-2): 35-40.

Coller, J. and R. Parker (2005). "General translational repression by activators of mRNA decapping." Cell **122**(6): 875-86.

Cooper, L., C. Johnson, F. Burslem and P. Martin (2005). "Wound healing and inflammation genes revealed by array analysis of 'macrophageless' PU.1 null mice." Genome Biol **6**(1): R5.

Cooperstock, R. L. and H. D. Lipshitz (1997). "Control of mRNA stability and translation during Drosophila development." Semin Cell Dev Biol **8**(6): 541-9.

de Ruiter, N. D., R. M. Wolthuis, H. van Dam, B. M. Burgering and J. L. Bos (2000). "Ras-dependent regulation of c-Jun phosphorylation is mediated by the Ral guanine nucleotide exchange factor-Ral pathway." Mol Cell Biol **20**(22): 8480-8.

DeVeale, B., T. Brummel and L. Seroude (2004). "Immunity and aging: the enemy within?" Aging Cell **3**(4): 195-208.

Dobens, L. L., E. Martin-Blanco, A. Martinez-Arias, F. C. Kafatos and L. A. Raftery (2001). "Drosophila puckered regulates Fos/Jun levels during follicle cell morphogenesis." Development **128**(10): 1845-56.

References:

Drnevich, J. M., M. M. Reedy, E. A. Ruedi, S. Rodriguez-Zas and K. A. Hughes (2004). "Quantitative evolutionary genomics: differential gene expression and male reproductive success in Drosophila melanogaster." Proc Biol Sci **271**(1554): 2267-73.

Etter, P. D. and M. Ramaswami (2002). "The ups and downs of daily life: profiling circadian gene expression in Drosophila." Bioessays **24**(6): 494-8.

Fenteany, G., P. A. Janmey and T. P. Stossel (2000). "Signaling pathways and cell mechanics involved in wound closure by epithelial cell sheets." Curr Biol **10**(14): 831-8.

Fernandez, B. G., A. M. Arias and A. Jacinto (2007). "Dpp signalling orchestrates dorsal closure by regulating cell shape changes both in the amnioserosa and in the epidermis." Mech Dev **124**(11-12): 884-97.

Fischer, N. and K. Weis (2002). "The DEAD box protein Dhh1 stimulates the decapping enzyme Dcp1." Embo J **21**(11): 2788-97.

Galko, M. J. and M. A. Krasnow (2004). "Cellular and genetic analysis of wound healing in Drosophila larvae." PLoS Biol **2**(8): E239.

Glise, B., H. Bourbon and S. Noselli (1995). "hemipterous encodes a novel Drosophila MAP kinase kinase, required for epithelial cell sheet movement." Cell **83**(3): 451-61.

Glise, B. and S. Noselli (1997). "Coupling of Jun amino-terminal kinase and Decapentaplegic signaling pathways in Drosophila morphogenesis." Genes Dev **11**(13): 1738-47.

Goberdhan, D. C. and C. Wilson (1998). "JNK, cytoskeletal regulator and stress response kinase? A Drosophila perspective." Bioessays **20**(12): 1009-19.

Gosain, A. and L. A. DiPietro (2004). "Aging and wound healing." World J Surg **28**(3): 321-6.

Grima, D. (2002). Analysis of the role of the exoribonuclease *pacman* in *Drosophila* development. Genetics department. Oxford, Oxford University. **Doctor of Philosophy**.

Grima, D. P., M. Sullivan, M. V. Zabolotskaya, C. Browne, J. Seago, K. C. Wan, Y. Okada and S. F. Newbury (2008). "The 5' - 3' exoribonuclease pacman is required for epithelial sheet sealing in Drosophila and genetically interacts with the phosphatase puckered." Biol Cell.

Grinnell, F. (1992). "Wound repair, keratinocyte activation and integrin modulation." J Cell Sci **101 (Pt 1)**: 1-5.

Grose, R. (2003). "Epithelial migration: open your eyes to c-Jun." Curr Biol **13**(17): R678-80.

References:

Grose, R. and P. Martin (1999). "Parallels between wound repair and morphogenesis in the embryo." Semin Cell Dev Biol **10**(4): 395-404.

Hall, A. (1998). "Rho GTPases and the actin cytoskeleton." Science **279**(5350): 509-14.

Harden, N. (2002). "Signaling pathways directing the movement and fusion of epithelial sheets: lessons from dorsal closure in Drosophila." Differentiation **70**(4-5): 181-203.

Harden, N. (2005). "Cell biology. Of grainy heads and broken skins." Science **308**(5720): 364-5.

Harden, N., J. Lee, H. Y. Loh, Y. M. Ong, I. Tan, T. Leung, E. Manser and L. Lim (1996). "A Drosophila homolog of the Rac- and Cdc42-activated serine/threonine kinase PAK is a potential focal adhesion and focal complex protein that colocalizes with dynamic actin structures." Mol Cell Biol **16**(5): 1896-908.

Harden, N., M. Ricos, Y. M. Ong, W. Chia and L. Lim (1999). "Participation of small GTPases in dorsal closure of the Drosophila embryo: distinct roles for Rho subfamily proteins in epithelial morphogenesis." J Cell Sci **112 (Pt 3)**: 273-84.

Hoheisel, J. D. (2006). "Microarray technology: beyond transcript profiling and genotype analysis." Nat Rev Genet **7**(3): 200-10.

Homsy, J. G., H. Jasper, X. G. Peralta, H. Wu, D. P. Kiehart and D. Bohmann (2006). "JNK signaling coordinates integrin and actin functions during Drosophila embryogenesis." Dev Dyn **235**(2): 427-34.

Hsu, C. L. and A. Stevens (1993). "Yeast cells lacking 5'-->3' exoribonuclease 1 contain mRNA species that are poly(A) deficient and partially lack the 5' cap structure." Mol Cell Biol **13**(8): 4826-35.

Huang, C., Z. Rajfur, C. Borchers, M. D. Schaller and K. Jacobson (2003). "JNK phosphorylates paxillin and regulates cell migration." Nature **424**(6945): 219-23.

Hutson, M. S., Y. Tokutake, M. S. Chang, J. W. Bloor, S. Venakides, D. P. Kiehart and G. S. Edwards (2003). "Forces for morphogenesis investigated with laser microsurgery and quantitative modeling." Science **300**(5616): 145-9.

Ingelfinger, D., D. J. Arndt-Jovin, R. Luhrmann and T. Achsel (2002). "The human LSm1-7 proteins colocalize with the mRNA-degrading enzymes Dcp1/2 and Xrnl in distinct cytoplasmic foci." Rna **8**(12): 1489-501.

Jacinto, A. and P. Martin (2001). "Morphogenesis: unravelling the cell biology of hole closure." Curr Biol **11**(17): R705-7.

References:

Jacinto, A., A. Martinez-Arias and P. Martin (2001). "Mechanisms of epithelial fusion and repair." Nat Cell Biol **3**(5): E117-23.

Jacinto, A., W. Wood, T. Balayo, M. Turmaine, A. Martinez-Arias and P. Martin (2000). "Dynamic actin-based epithelial adhesion and cell matching during Drosophila dorsal closure." Curr Biol **10**(22): 1420-6.

Jacinto, A., S. Woolner and P. Martin (2002). "Dynamic analysis of dorsal closure in Drosophila: from genetics to cell biology." Dev Cell **3**(1): 9-19.

Jasper, H., V. Benes, C. Schwager, S. Sauer, S. Clauder-Munster, W. Ansorge and D. Bohmann (2001). "The genomic response of the Drosophila embryo to JNK signaling." Dev Cell **1**(4): 579-86.

Jasper, H. and D. Bohmann (2002). "Drosophila innate immunity: a genomic view of pathogen defense." Mol Cell **10**(5): 967-9.

Kagawa, S., A. Matsuo, Y. Yagi, K. Ikematsu, R. Tsuda and I. Nakasono (2008). "The time-course analysis of gene expression during wound healing in mouse skin." Leg Med (Tokyo).

Kallio, J., A. Leinonen, J. Ulvila, S. Valanne, R. A. Ezekowitz and M. Ramet (2005). "Functional analysis of immune response genes in Drosophila identifies JNK pathway as a regulator of antimicrobial peptide gene expression in S2 cells." Microbes Infect **7**(5-6): 811-9.

Kaltschmidt, J. A., N. Lawrence, V. Morel, T. Balayo, B. G. Fernandez, A. Pelissier, A. Jacinto and A. Martinez Arias (2002). "Planar polarity and actin dynamics in the epidermis of Drosophila." Nat Cell Biol **4**(12): 937-44.

Karlsson, C., A. M. Korayem, C. Scherfer, O. Loseva, M. S. Dushay and U. Theopold (2004). "Proteomic analysis of the Drosophila larval hemolymph clot." J Biol Chem **279**(50): 52033-41.

Kenna, M., A. Stevens, M. McCammon and M. G. Douglas (1993). "An essential yeast gene with homology to the exonuclease-encoding XRN1/KEM1 gene also encodes a protein with exoribonuclease activity." Mol Cell Biol **13**(1): 341-50.

Kiehart, D. P. (1999). "Wound healing: The power of the purse string." Curr Biol **9**(16): R602-5.

Kiehart, D. P., C. G. Galbraith, K. A. Edwards, W. L. Rickoll and R. A. Montague (2000). "Multiple forces contribute to cell sheet morphogenesis for dorsal closure in Drosophila." J Cell Biol **149**(2): 471-90.

Kim, J., S. Jeon, Y. S. Yang and J. Kim (2004). "Posttranscriptional regulation of the karyogamy gene by Kem1p/Xrn1p exoribonuclease and Rok1p RNA helicase of Saccharomyces cerevisiae." Biochem Biophys Res Commun **321**(4): 1032-9.

References:

Kirchner, J., S. Gross, D. Bennett and L. Alphey (2007). "Essential, overlapping and redundant roles of the Drosophila protein phosphatase 1 alpha and 1 beta genes." Genetics **176**(1): 273-81.

Kirchner, J., S. Gross, D. Bennett and L. Alphey (2007). "The nonmuscle myosin phosphatase PP1beta (flapwing) negatively regulates Jun N-terminal kinase in wing imaginal discs of Drosophila." Genetics **175**(4): 1741-9.

Knox, P., S. Crooks and C. S. Rimmer (1986). "Role of fibronectin in the migration of fibroblasts into plasma clots." J Cell Biol **102**(6): 2318-23.

Knust, E. (1996). "Drosophila morphogenesis: follow-my-leader in epithelia." Curr Biol **6**(4): 379-81.

Knust, E. (1997). "Drosophila morphogenesis: movements behind the edge." Curr Biol **7**(9): R558-61.

Kockel, L., J. G. Homsy and D. Bohmann (2001). "Drosophila AP-1: lessons from an invertebrate." Oncogene **20**(19): 2347-64.

Lamka, M. L. and H. D. Lipshitz (1999). "Role of the amnioserosa in germ band retraction of the Drosophila melanogaster embryo." Dev Biol **214**(1): 102-12.

Lasko, P. (1999). "RNA sorting in Drosophila oocytes and embryos." Faseb J **13**(3): 421-33.

Lehner, B. and C. M. Sanderson (2004). "A protein interaction framework for human mRNA degradation." Genome Res **14**(7): 1315-23.

Letsou, A. and D. Bohmann (2005). "Small flies--big discoveries: nearly a century of Drosophila genetics and development." Dev Dyn **232**(3): 526-8.

Li, G., C. Gustafson-Brown, S. K. Hanks, K. Nason, J. M. Arbeit, K. Pogliano, R. M. Wisdom and R. S. Johnson (2003). "c-Jun is essential for organization of the epidermal leading edge." Dev Cell **4**(6): 865-77.

Liechty, K. W., H. B. Kim, N. S. Adzick and T. M. Crombleholme (2000). "Fetal wound repair results in scar formation in interleukin-10-deficient mice in a syngeneic murine model of scarless fetal wound repair." J Pediatr Surg **35**(6): 866-72; discussion 872-3.

Ligoxygakis, P., S. Roth and J. M. Reichhart (2003). "A serpin regulates dorsal-ventral axis formation in the Drosophila embryo." Curr Biol **13**(23): 2097-102.

Lin, M. D., S. J. Fan, W. S. Hsu and T. B. Chou (2006). "Drosophila decapping protein 1, dDcp1, is a component of the oskar mRNP complex and directs its posterior localization in the oocyte." Dev Cell **10**(5): 601-13.

References:

Lin, M. D., X. Jiao, D. Grima, S. F. Newbury, M. Kiledjian and T. B. Chou (2008). "Drosophila processing bodies in oogenesis." Dev Biol **322**(2): 276-88.

Liu, H., Y. C. Su, E. Becker, J. Treisman and E. Y. Skolnik (1999). "A Drosophila TNF-receptor-associated factor (TRAF) binds the ste20 kinase Misshapen and activates Jun kinase." Curr Biol **9**(2): 101-4.

Lodish, H., A. Berk, P. Matsdaira, C. A. Kaiser, M. Krieger, M. P. Scott, S. L. Zipursky and J. Darnell (2004). Molecular Cell Biology. London, Freeman and Company.

Long, R. M. and M. T. McNally (2003). "mRNA decay: x (XRN1) marks the spot." Mol Cell **11**(5): 1126-8.

Mace, K. A., J. C. Pearson and W. McGinnis (2005). "An epidermal barrier wound repair pathway in Drosophila is mediated by grainy head." Science **308**(5720): 381-5.

Mackay, D. J. and A. Hall (1998). "Rho GTPases." J Biol Chem **273**(33): 20685-8.

Marone, M., S. Mozzetti, D. De Ritis, L. Pierelli and G. Scambia (2001). "Semiquantitative RT-PCR analysis to assess the expression levels of multiple transcripts from the same sample." Biol Proced Online **3**: 19-25.

Martin-Blanco, E. (1997). "Regulation of cell differentiation by the Drosophila Jun kinase cascade." Curr Opin Genet Dev **7**(5): 666-71.

Martin-Blanco, E. (1998). "Regulatory control of signal transduction during morphogenesis in Drosophila." Int J Dev Biol **42**(3): 363-8.

Martin-Blanco, E., A. Gampel, J. Ring, K. Virdee, N. Kirov, A. M. Tolkovsky and A. Martinez-Arias (1998). "puckered encodes a phosphatase that mediates a feedback loop regulating JNK activity during dorsal closure in Drosophila." Genes Dev **12**(4): 557-70.

Martin-Blanco, E. and E. Knust (2001). "Epithelial morphogenesis: filopodia at work." Curr Biol **11**(1): R28-31.

Martin-Blanco, E., J. C. Pastor-Pareja and A. Garcia-Bellido (2000). "JNK and decapentaplegic signaling control adhesiveness and cytoskeleton dynamics during thorax closure in Drosophila." Proc Natl Acad Sci U S A **97**(14): 7888-93.

Martin, P. (1997). "Wound healing--aiming for perfect skin regeneration." Science **276**(5309): 75-81.

Martin, P., D. D'Souza, J. Martin, R. Grose, L. Cooper, R. Maki and S. R. McKercher (2003). "Wound healing in the PU.1 null mouse--tissue repair is not dependent on inflammatory cells." Curr Biol **13**(13): 1122-8.

References:

Martin, P. and C. D. Nobes (1992). "An early molecular component of the wound healing response in rat embryos--induction of c-fos protein in cells at the epidermal wound margin." Mech Dev **38**(3): 209-15.

Martin, P. and S. M. Parkhurst (2003). "Development. May the force be with you." Science **300**(5616): 63-5.

Martin, P. and S. M. Parkhurst (2004). "Parallels between tissue repair and embryo morphogenesis." Development **131**(13): 3021-34.

Martin, P. and W. Wood (2002). "Epithelial fusions in the embryo." Curr Opin Cell Biol **14**(5): 569-74.

Mattila, J., L. Omelyanchuk, S. Kyttala, H. Turunen and S. Nokkala (2005). "Role of Jun N-terminal Kinase (JNK) signaling in the wound healing and regeneration of a Drosophila melanogaster wing imaginal disc." Int J Dev Biol **49**(4): 391-9.

McCluskey, J. and P. Martin (1995). "Analysis of the tissue movements of embryonic wound healing--DiI studies in the limb bud stage mouse embryo." Dev Biol **170**(1): 102-14.

McEwen, D. G., R. T. Cox and M. Peifer (2000). "The canonical Wg and JNK signaling cascades collaborate to promote both dorsal closure and ventral patterning." Development **127**(16): 3607-17.

McEwen, D. G. and M. Peifer (2005). "Puckered, a Drosophila MAPK phosphatase, ensures cell viability by antagonizing JNK-induced apoptosis." Development **132**(17): 3935-46.

McLaren, R. S., S. F. Newbury, G. S. Dance, H. C. Causton and C. F. Higgins (1991). "mRNA degradation by processive 3'-5' exoribonucleases in vitro and the implications for prokaryotic mRNA decay in vivo." J Mol Biol **221**(1): 81-95.

Mee, C. J. (2005). "Microarray methods in Drosophila neurobiology." Invert Neurosci **5**(3-4): 189-95.

Mihaly, J., L. Kockel, K. Gaengel, U. Weber, D. Bohmann and M. Mlodzik (2001). "The role of the Drosophila TAK homologue dTAK during development." Mech Dev **102**(1-2): 67-79.

Myers, F. A., H. Francis-Lang and S. F. Newbury (1995). "Degradation of maternal string mRNA is controlled by proteins encoded on maternally contributed transcripts." Mech Dev **51**(2-3): 217-26.

Narasimha, M. and N. H. Brown (2004). "Novel functions for integrins in epithelial morphogenesis." Curr Biol **14**(5): 381-5.

Newbury, S. and A. Woollard (2004). "The 5'-3' exoribonuclease xrn-1 is essential for ventral epithelial enclosure during C. elegans embryogenesis." Rna **10**(1): 59-65.

References:

Newbury, S. F. (2006). "Control of mRNA stability in eukaryotes." Biochem Soc Trans **34**(Pt 1): 30-4.

Newbury, S. F., O. Muhlemann and G. Stoecklin (2006). "Turnover in the Alps: an mRNA perspective. Workshops on mechanisms and regulation of mRNA turnover." EMBO Rep **7**(2): 143-8.

Noselli, S. (1998). "JNK signaling and morphogenesis in Drosophila." Trends Genet **14**(1): 33-8.

Noselli, S. and F. Agnes (1999). "Roles of the JNK signaling pathway in Drosophila morphogenesis." Curr Opin Genet Dev **9**(4): 466-72.

O Morgan, D. (2007). The Cell Cycle: Principles of Control, New Science Press Ltd.

Oehmichen, M. (2004). "Vitality and time course of wounds." Forensic Sci Int **144**(2-3): 221-31.

Page, A. M., K. Davis, C. Molineux, R. D. Kolodner and A. W. Johnson (1998). "Mutational analysis of exoribonuclease I from Saccharomyces cerevisiae." Nucleic Acids Res **26**(16): 3707-16.

Pajulo, O. T., K. J. Pulkki, M. S. Alanen, M. S. Reunanen, K. K. Lertola, A. I. Mattila-Vuori and J. A. Viljanto (2000). "Duration of surgery and patient age affect wound healing in children." Wound Repair Regen **8**(3): 174-8.

Paricio, N., F. Feiguin, M. Boutros, S. Eaton and M. Mlodzik (1999). "The Drosophila STE20-like kinase misshapen is required downstream of the Frizzled receptor in planar polarity signaling." Embo J **18**(17): 4669-78.

Parker, R. and U. Sheth (2007). "P bodies and the control of mRNA translation and degradation." Mol Cell **25**(5): 635-46.

Parker, R. and H. Song (2004). "The enzymes and control of eukaryotic mRNA turnover." Nat Struct Mol Biol **11**(2): 121-7.

Pastor-Pareja, J. C., F. Grawe, E. Martin-Blanco and A. Garcia-Bellido (2004). "Invasive cell behavior during Drosophila imaginal disc eversion is mediated by the JNK signaling cascade." Dev Cell **7**(3): 387-99.

Piekny, A. J. and P. E. Mains (2003). "Squeezing an egg into a worm: C. elegans embryonic morphogenesis." ScientificWorldJournal **3**: 1370-81.

Pinheiro, P., G. Scarlett, A. Rodger, P. M. Rodger, A. Murray, T. Brown, S. F. Newbury and J. A. McClellan (2002). "Structures of CUG repeats in RNA. Potential implications for human genetic diseases." J Biol Chem **277**(38): 35183-90.

Poss, K. D., M. T. Keating and A. Nechiporuk (2003). "Tales of regeneration in zebrafish." Dev Dyn **226**(2): 202-10.

References:

Purves, W. K., G. H. Orians, H. C. Heller and D. Sadava (1998). Life the Science of Biology: The Cell and Heredity, W H Freeman & Co.

Qiu, C., P. Coutinho, S. Frank, S. Franke, L. Y. Law, P. Martin, C. R. Green and D. L. Becker (2003). "Targeting connexin43 expression accelerates the rate of wound repair." Curr Biol **13**(19): 1697-703.

Radonic, A., S. Thulke, I. M. Mackay, O. Landt, W. Siegert and A. Nitsche (2004). "Guideline to reference gene selection for quantitative real-time PCR." Biochem Biophys Res Commun **313**(4): 856-62.

Ramet, M., R. Lanot, D. Zachary and P. Manfruelli (2002). "JNK signaling pathway is required for efficient wound healing in Drosophila." Dev Biol **241**(1): 145-56.

Ransom, R. (1982). A handbook of *Drosophila* development, Elsevier Biomedical.

Raymond, K., E. Bergeret, M. C. Dagher, R. Breton, R. Griffin-Shea and M. O. Fauvarque (2001). "The Rac GTPase-activating protein RotundRacGAP interferes with Drac1 and Dcdc42 signalling in Drosophila melanogaster." J Biol Chem **276**(38): 35909-16.

Redd, M. J., L. Cooper, W. Wood, B. Stramer and P. Martin (2004). "Wound healing and inflammation: embryos reveal the way to perfect repair." Philos Trans R Soc Lond B Biol Sci **359**(1445): 777-84.

Reed, B. H., R. Wilk and H. D. Lipshitz (2001). "Downregulation of Jun kinase signaling in the amnioserosa is essential for dorsal closure of the Drosophila embryo." Curr Biol **11**(14): 1098-108.

Ridley, A. J. (2001). "Rho GTPases and cell migration." J Cell Sci **114**(Pt 15): 2713-22.

Riesgo-Escovar, J. R., M. Jenni, A. Fritz and E. Hafen (1996). "The Drosophila Jun-N-terminal kinase is required for cell morphogenesis but not for DJun-dependent cell fate specification in the eye." Genes Dev **10**(21): 2759-68.

Ring, J. M. and A. Martinez Arias (1993). "puckered, a gene involved in position-specific cell differentiation in the dorsal epidermis of the Drosophila larva." Dev Suppl: 251-9.

Roberts, C. (2002). Investigations into the role of pacman protein during *Drosophila* embryogenesis, and in adult *Drosophila* male fertility., Oxford University.

Sathyanarayana, P., M. K. Barthwal, M. E. Lane, S. F. Acevedo, E. M. Skoulakis, A. Bergmann and A. Rana (2003). "Drosophila mixed lineage kinase/slipper, a missing biochemical link in Drosophila JNK signaling." Biochim Biophys Acta **1640**(1): 77-84.

References:

Scherfer, C., C. Karlsson, O. Loseva, G. Bidla, A. Goto, J. Havemann, M. S. Dushay and U. Theopold (2004). "Isolation and characterization of hemolymph clotting factors in Drosophila melanogaster by a pullout method." Curr Biol **14**(7): 625-9.

Scherfer, C., M. R. Qazi, K. Takahashi, R. Ueda, M. S. Dushay, U. Theopold and B. Lemaitre (2006). "The Toll immune-regulated Drosophila protein Fondue is involved in hemolymph clotting and puparium formation." Dev Biol **295**(1): 156-63.

Scuderi, A. and A. Letsou (2005). "Amnioserosa is required for dorsal closure in Drosophila." Dev Dyn **232**(3): 791-800.

Seago, J. E., I. V. Chernukhin and S. F. Newbury (2001). "The Drosophila gene twister, an orthologue of the yeast helicase SKI2, is differentially expressed during development." Mech Dev **106**(1-2): 137-41.

She, M., C. J. Decker, K. Sundramurthy, Y. Liu, N. Chen, R. Parker and H. Song (2004). "Crystal structure of Dcp1p and its functional implications in mRNA decapping." Nat Struct Mol Biol **11**(3): 249-56.

Shen, J. and C. Dahmann (2005). "Extrusion of cells with inappropriate Dpp signaling from Drosophila wing disc epithelia." Science **307**(5716): 1789-90.

Sheth, U. and R. Parker (2003). "Decapping and decay of messenger RNA occur in cytoplasmic processing bodies." Science **300**(5620): 805-8.

Sheth, U. and R. Parker (2006). "Targeting of aberrant mRNAs to cytoplasmic processing bodies." Cell **125**(6): 1095-109.

Simske, J. S. and J. Hardin (2001). "Getting into shape: epidermal morphogenesis in Caenorhabditis elegans embryos." Bioessays **23**(1): 12-23.

Sluss, H. K., Z. Han, T. Barrett, D. C. Goberdhan, C. Wilson, R. J. Davis and Y. T. Ip (1996). "A JNK signal transduction pathway that mediates morphogenesis and an immune response in Drosophila." Genes Dev **10**(21): 2745-58.

Stevens, A. (1980). "Purification and characterization of a Saccharomyces cerevisiae exoribonuclease which yields 5'-mononucleotides by a 5' leads to 3' mode of hydrolysis." J Biol Chem **255**(7): 3080-5.

Stramer, B. and P. Martin (2005). "Cell biology: master regulators of sealing and healing." Curr Biol **15**(11): R425-7.

Stramer, B., W. Wood, M. J. Galko, M. J. Redd, A. Jacinto, S. M. Parkhurst and P. Martin (2005). "Live imaging of wound inflammation in Drosophila embryos reveals key roles for small GTPases during in vivo cell migration." J Cell Biol **168**(4): 567-73.

Stratagene (2006). "Introduction to Quantitative PCR."

References:

Stronach, B. (2005). "Dissecting JNK signaling, one KKKinase at a time." Dev Dyn **232**(3): 575-84.

Stronach, B. and N. Perrimon (2002). "Activation of the JNK pathway during dorsal closure in Drosophila requires the mixed lineage kinase, slipper." Genes Dev **16**(3): 377-87.

Su, Y. C., C. Maurel-Zaffran, J. E. Treisman and E. Y. Skolnik (2000). "The Ste20 kinase misshapen regulates both photoreceptor axon targeting and dorsal closure, acting downstream of distinct signals." Mol Cell Biol **20**(13): 4736-44.

Su, Y. C., J. E. Treisman and E. Y. Skolnik (1998). "The Drosophila Ste20-related kinase misshapen is required for embryonic dorsal closure and acts through a JNK MAPK module on an evolutionarily conserved signaling pathway." Genes Dev **12**(15): 2371-80.

Sugihara, K., N. Nakatsuji, K. Nakamura, K. Nakao, R. Hashimoto, H. Otani, H. Sakagami, H. Kondo, S. Nozawa, A. Aiba and M. Katsuki (1998). "Rac1 is required for the formation of three germ layers during gastrulation." Oncogene **17**(26): 3427-33.

Sullivan, W., M. Ashburner and R. S. Hawley (2000). *Drosophila* Protocols, Cold Spring Harbour Laboratory Press.

Suzanne, M., N. Perrimon and S. Noselli (2001). "The Drosophila JNK pathway controls the morphogenesis of the egg dorsal appendages and micropyle." Dev Biol **237**(2): 282-94.

Tadros, W., S. A. Houston, A. Bashirullah, R. L. Cooperstock, J. L. Semotok, B. H. Reed and H. D. Lipshitz (2003). "Regulation of maternal transcript destabilization during egg activation in Drosophila." Genetics **164**(3): 989-1001.

Tepass, U. (1999). "Genetic analysis of cadherin function in animal morphogenesis." Curr Opin Cell Biol **11**(5): 540-8.

Tepass, U., D. Godt and R. Winklbauer (2002). "Cell sorting in animal development: signalling and adhesive mechanisms in the formation of tissue boundaries." Curr Opin Genet Dev **12**(5): 572-82.

Theopold, U., D. Li, M. Fabbri, C. Scherfer and O. Schmidt (2002). "The coagulation of insect hemolymph." Cell Mol Life Sci **59**(2): 363-72.

Theopold, U., O. Schmidt, K. Soderhall and M. S. Dushay (2004). "Coagulation in arthropods: defence, wound closure and healing." Trends Immunol **25**(6): 289-94.

Till, D. D., B. Linz, J. E. Seago, S. J. Elgar, P. E. Marujo, M. L. Elias, C. M. Arraiano, J. A. McClellan, J. E. McCarthy and S. F. Newbury (1998). "Identification and developmental expression of a 5'-3' exoribonuclease from Drosophila melanogaster." Mech Dev **79**(1-2): 51-5.

References:

Ting, S. B., J. Caddy, N. Hislop, T. Wilanowski, A. Auden, L. L. Zhao, S. Ellis, P. Kaur, Y. Uchida, W. M. Holleran, P. M. Elias, J. M. Cunningham and S. M. Jane (2005). "A homolog of Drosophila grainy head is essential for epidermal integrity in mice." Science **308**(5720): 411-3.

Usui, K. and P. Simpson (2000). "Cellular basis of the dynamic behavior of the imaginal thoracic discs during Drosophila metamorphosis." Dev Biol **225**(1): 13-25.

Van Aelst, L. and C. D'Souza-Schorey (1997). "Rho GTPases and signaling networks." Genes Dev **11**(18): 2295-322.

Van Aelst, L. and M. Symons (2002). "Role of Rho family GTPases in epithelial morphogenesis." Genes Dev **16**(9): 1032-54.

Wadman, M. (2005). "Scar prevention: the healing touch." Nature **436**(7054): 1079-80.

Walsh, D. (1987). "PCPROBIT: A User-Friendly Probit Analysis Program for Microcomputers." The American Statistician **Vol. 41**(No. 1): pp. 78-78.

Wan, K. C. (2003). genetics department. Oxford, Oxford University. **Doctor of Philosophy**.

Wang, M. C., D. Bohmann and H. Jasper (2003). "JNK signaling confers tolerance to oxidative stress and extends lifespan in Drosophila." Dev Cell **5**(5): 811-6.

Wang, M. C., D. Bohmann and H. Jasper (2005). "JNK extends life span and limits growth by antagonizing cellular and organism-wide responses to insulin signaling." Cell **121**(1): 115-25.

Werner, S. and R. Grose (2003). "Regulation of wound healing by growth factors and cytokines." Physiol Rev **83**(3): 835-70.

Weston, C. R. and R. J. Davis (2002). "The JNK signal transduction pathway." Curr Opin Genet Dev **12**(1): 14-21.

Williams-Masson, E. M., A. N. Malik and J. Hardin (1997). "An actin-mediated two-step mechanism is required for ventral enclosure of the C. elegans hypodermis." Development **124**(15): 2889-901.

Wilusz, C. J., M. Wormington and S. W. Peltz (2001). "The cap-to-tail guide to mRNA turnover." Nat Rev Mol Cell Biol **2**(4): 237-46.

Wolpert, L., Jessell, T., Lawrence, P., Meyerowitz, E., Robertson, E. and Smith, J. (2007). Principles of Development, Oxford university press.

Wood, W., C. Faria and A. Jacinto (2006). "Distinct mechanisms regulate hemocyte chemotaxis during development and wound healing in Drosophila melanogaster." J Cell Biol **173**(3): 405-16.

References:

Wood, W., A. Jacinto, R. Grose, S. Woolner, J. Gale, C. Wilson and P. Martin (2002). "Wound healing recapitulates morphogenesis in Drosophila embryos." Nat Cell Biol **4**(11): 907-12.

Woolner, S., A. Jacinto and P. Martin (2005). "The small GTPase Rac plays multiple roles in epithelial sheet fusion--dynamic studies of Drosophila dorsal closure." Dev Biol **282**(1): 163-73.

Xia, Y. and M. Karin (2004). "The control of cell motility and epithelial morphogenesis by Jun kinases." Trends Cell Biol **14**(2): 94-101.

Zabolotskaya, M. V., D. P. Grima, M. D. Lin, T. B. Chou and S. F. Newbury (2008). "The 5' - 3' exoribonuclease Pacman is required for normal male fertility and is dynamically localised in cytoplasmic particles in Drosophila testis cells." Biochem J.

Zeitlinger, J. and D. Bohmann (1999). "Thorax closure in Drosophila: involvement of Fos and the JNK pathway." Development **126**(17): 3947-56.

Zeitlinger, J., L. Kockel, F. A. Peverali, D. B. Jackson, M. Mlodzik and D. Bohmann (1997). "Defective dorsal closure and loss of epidermal decapentaplegic expression in Drosophila fos mutants." Embo J **16**(24): 7393-401.

Biol. Cell (2008) **100**, 687–701 (Printed in Great Britain) doi:10.1042/BC20080049

Research article

c Publications

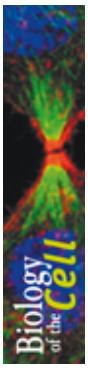

The 5′–3′ exoribonuclease *pacman* is required for epithelial sheet sealing in *Drosophila* and genetically interacts with the phosphatase *puckered*

Dominic P. Grima*, Melanie Sullivan*, Maria V. Zabolotskaya*, Cathy Browne†, Julian Seago‡, Kay Chong Wan†, Yoshio Okada§ and Sarah F. Newbury*[1]

*Brighton and Sussex Medical School, Medical Research Building, University of Sussex, Falmer, Brighton BN1 9PS, U.K., †Department of Biochemistry, University of Oxford, South Parks Road, Oxford OX1 3QU, U.K., ‡Institute for Animal Health, Ash Road, Pirbright, Surrey GU24 0NF, U.K., and §Bio21 corporation, 750 Minami-Uehara, Nakagusuku village, Okinawa, 901-242 Japan

Background information. Ribonucleases have been well studied in yeast and bacteria, but their biological significance to developmental processes in multicellular organisms is not well understood. However, there is increasing evidence that specific timed transcript degradation is critical for regulation of many cellular processes, including translational repression, nonsense-mediated decay and RNA interference. The *Drosophila* gene *pacman* is highly homologous to the major yeast exoribonuclease *XRN1* and is the only known cytoplasmic 5′–3′ exoribonuclease in eukaryotes. To determine the effects of this exoribonuclease in development we have constructed a number of mutations in *pacman* by P-element excision and characterized the resulting phenotypes.

Results. Mutations in *pacman* resulted in flies with a number of specific phenotypes, such as low viability, dull wings, crooked legs, failure of correct dorsal/thorax closure and defects in wound healing. The epithelial sheet movement involved in dorsal/thorax closure is a conserved morphogenetic process which is similar to that of hind-brain closure in vertebrates and wound healing in humans. As the JNK (c-Jun N-terminal kinase) signalling pathway is known to be involved in dorsal/thorax closure and wound healing, we tested whether *pacman* affects JNK signalling. Our experiments demonstrate that *pacman* genetically interacts with *puckered*, a phosphatase that negatively regulates the JNK signalling pathway.

Conclusions. These results reveal that the 5′–3′ exoribonuclease *pacman* is required for a critical aspect of epithelial sheet sealing in *Drosophila*. Since these mutations result in specific phenotypes, our data suggest that the exoribonuclease Pacman targets a specific subset of mRNAs involved in this process. One of these targets could be a member of the JNK signalling pathway, although it is possible that a parallel pathway may instead be affected. The exoribonuclease *pacman* is highly conserved in all eukaryotes, therefore it is likely that it is involved in similar morphological processes, such as wound healing in human cells.

Introduction

The control of mRNA stability is now widely recognized as a key component in the regulation of gene expression. Since the abundance of any given RNA depends upon the rate at which it is transcribed compared with the rate of specific degradation, control of RNA stability is a key factor in the control of gene regulation (Caponigro and Parker, 1996; Cooperstock and Lipshitz, 1997; McCarthy, 1998; Wilusz et al., 2001). In multicellular organisms, it is increasingly evident that differential regulation of mRNA stability is crucial for normal embryonic development. For

[1]To whom correspondence should be addressed (email S.Newbury@bsms.ac.uk).

Key words: *Drosophila*, development, exoribonuclease, RNA degradation, RNA stability.

Abbreviations used: aa, amino acid; HRP, horseradish peroxidase; JNK, c-Jun N-terminal kinase; P-body, processing body; RT-PCR, reverse transcriptase PCR; UTR, untranslated region.

example, in all metazoans studied to date, mRNAs provided maternally that are critical in determining axis formation during early embryogenesis are specifically degraded at a particular point in development (Cooperstock and Lipshitz, 1997; Bashirullah et al., 2001; Tadros et al., 2003). In addition, crucial protein gradients in early *Drosophila* embryos are often dependent on translational suppression of particular target RNAs, such as *nanos* and *hunchback*, followed by their degradation (Macdonald and Smibert, 1996). Therefore transcript degradation during development can be selective and also modulated, suggesting a not-well-studied control of gene expression during development.

In the yeast *Saccharomyces cerevisiae*, the major degradation pathway is in a 5′–3′ direction. The critical exoribonuclease in this pathway is Xrn1p, which degrades mRNAs after they have been decapped (Muhlrad et al., 1994; Johnson, 1997; Meyer et al., 2004; Parker and Song, 2004). Mutations in *XRN1* lead to a number of phenotypes, including larger cell size, increased doubling times, defective sporulation and sensitivity to the microtubule-depolymerizing drug benomyl (Decker and Parker, 1993, 1994; Muhlrad et al., 1994; Johnson, 1997; Sweet et al., 2007). Deletion of *XRN1* in yeast is deleterious, but not lethal, because mRNAs can still be degraded by the 3′–5′ pathway via the exosome (Anderson and Parker, 1998). Xrn1p is not only involved in the normal decay of mRNA, but is required in the major pathway in nonsense-mediated decay (Gatfield et al., 2003), RNA interference (Orban and Izaurralde, 2005) and degradation via microRNAs (Souret et al., 2004; Valencia-Sanchez et al., 2006). Mutations in XRN1 in yeast or silencing of *xrn-1* in *Caenorhabditis elegans* lead to phenotypic defects, suggesting that this enzyme is required for normal cellular processes (Johnson and Gray, 1991; Decker and Parker, 1993, 1994; Muhlrad et al., 1994; Johnson, 1997; Newbury and Woollard, 2004). Previous work has shown that Xrn1p forms a multicomponent complex with the decapping proteins Dcp1p and Dcp2p, the Lsm proteins, the mRNA degradation factor Pat1p and the DEAD-box-containing helicase protein Dhh1p (Tharun and Parker, 1998; Bouveret et al., 2000; Parker and Song, 2004). The majority of these proteins are highly conserved in all eukaryotes studied and are located in cytoplasmic particles that are known as P-bodies (processing bodies) (Sheth and Parker, 2003; Eulalio et al., 2007; Parker and Sheth, 2007). P-bodies have also been observed in human and mouse cells, and these also function as specific sites of mRNA storage as well as decay (Bashkirov et al., 1997; Cougot et al., 2004).

The *Drosophila* gene *pacman* is a functional homologue of *S. cerevisiae* Xrn1p. *Drosophila* Pacman can complement the exonucleolytic activity of yeast Xrn1p and purified Pacman protein can degrade nucleic acids in a 5′–3′ direction (Till et al., 1998; Chernukhin et al., 2001). The *pacman* gene encodes a 184 kDa protein (5.2 kb cDNA) and includes a perfect trinucleotide repeat, $(CAG)_n$, encoding polyglutamine. Expansions of polyglutamine repeats have been implicated in a number of human genetic diseases, including Huntingdon's disease (MacDonald et al., 2003). The *pacman* transcripts are differentially expressed during development, being strongly expressed during oogenesis and during early embryonic development (0–8 h), with particularly abundant expression in the germ band. The *pacman* gene is located on the X chromosome at 18C7 (Flybase., 1996; Till et al., 1998).

In the present study, we have analysed the effect of *pacman* on *Drosophila* development. We constructed a number of mutations in the *pacman* gene and analysed the resulting phenotypes. Remarkably, these mutations resulted in specific defects in dorsal and thorax closure, as well as wing and leg phenotypes. Pacman also affects wound healing, a morphological process that is similar to thorax closure. We also demonstrate that *pacman* interacts genetically with *puckered*, a phosphatase in the JNK (c-Jun N-terminal kinase) pathway which is known to be critical in thorax closure, dorsal closure and wound healing. Our results show that *pacman* has a specific role in developmental processes in *Drosophila* and suggest that it has, directly or indirectly, a regulatory role on the conserved JNK pathway or acts in a parallel pathway.

Results

Construction of *pacman* mutations

In order to understand the role of *pacman* in *Drosophila* development, we used a reverse genetics approach. All available strains carrying a P-element transposon located near *pacman* were first checked by inverse PCR. The nearest P-element *P{EP}EP1526* was located 584 nt downstream of the *pacman* polyadenylation site, between *pacman* and the convergent gene

Figure 1 | Molecular characterization of *pacman*

(**A**) Genomic structure of *pacman.* Exons (■), introns (–), the 'domino' repeat (QQEAQ), the polyglutamine repeat (polyQ) and the polyadenylation (polyA) site are shown. The insertion site of the P-element used to generate deletions in the *pacman* gene is given, as is the downstream gene CG12202 (*Nat1*). The *pacman* alleles described in the present study are given below: gaps represent deletions at the genomic DNA level. Arrows indicate sites of the primers used to characterize these mutants. (**B**) Western blotting of *pacman* homozygous and hemizygous mutant adults showing that the truncated proteins are not detectable (pcm^5) or are poorly expressed (pcm^3 and pcm^6). The molecular masses of these truncated proteins are given in the Materials and methods section. An actin loading control is shown below. (**C**) Agarose gel showing no significant difference in the mRNA levels of the downstream gene *Nat1* between any of the strains tested, as determined by semi-quantitative RT-PCR. The first two strains are controls; (w^{1118}) represents the progenitor stock 11456 carrying the P-element *P{EP}EP1526* inserted between *pcm* and *Nat1*. pcm^5 and pcm^3 are two *pacman* mutants, gDNA represents the genomic DNA control and -ve is the 'no DNA' control. Duplex PCR reactions were carried out using *Nat1* primers and control rp49 primers, and were amplified for 26 cycles.

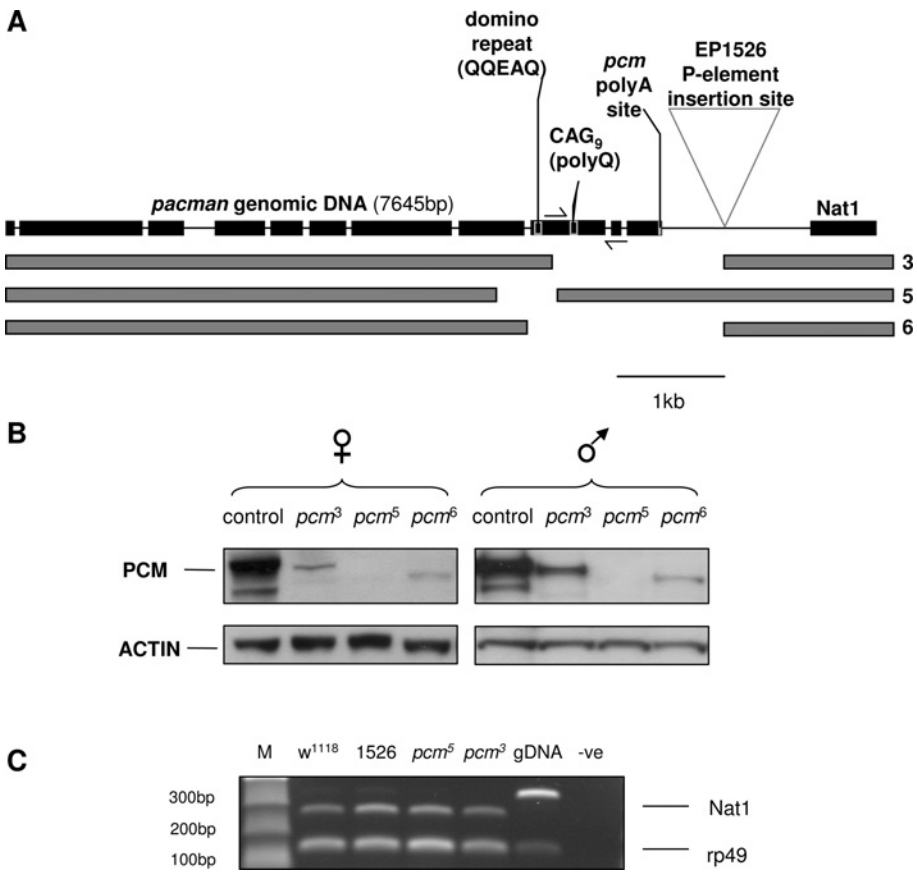

Nat1 (accession number CG12202) (Flybase, 1996). As there were no existing mutations within *pacman* at that time, we used P-element excision of P-element EP1526 in stock 11456 as the starting stock to construct a number of mutant alleles. After mobilization of the P-element, 345 excision lines were checked by PCR for deletion events. A total of seven homozygous viable lines were identified with a deletion in *pacman*. Sequencing of these lines revealed three unique excisions which were predicted to encode truncated *pacman* proteins and where the downstream gene was untouched (Figure 1A). Nine lethal lines proved to include larger deletions, which, by Southern blotting experiments and by further PCR experiments, showed no evidence of lethality due to *pacman*, therefore were not studied further.

In order to analyse the expression of *pacman* in wild-type and mutants, we raised an antibody to Pacman

Figure 2 | Pacman affects zygotic viability

(**A**) Percentages of female offspring of the two different genotypes from the cross *pcm*^{5}/FM7c × *pcm*^{5}/Y at 19°C ($n = 460$) and 25°C ($n = 839$). (**B**) Percentages of female offspring of the two different genotypes from the cross Df(1)JA27/FM7c × *pcm*^{5}/Y showing that, at 19°C, a single copy of the mutant gene significantly reduces viability compared with female siblings [$n = 143$ (19°C) and $n = 254$ (25°C)]. (**C**) Ectopic expression of *pacman* rescues *pacman*-viability phenotypes. At 19°C the viability of female flies carrying the *pacman* transgene [*pcm*^{5}/Df(1)JA27;;hs-*pcm*/+] is completely rescued compared with *pacman* mutant female siblings [*pcm*^{5}/Df(1)JA27;;+/+] (total scored = 458). Percentages relate to percentages of female offspring; 25% of each genotype is expected if there are no effects of *pacman* on viability.

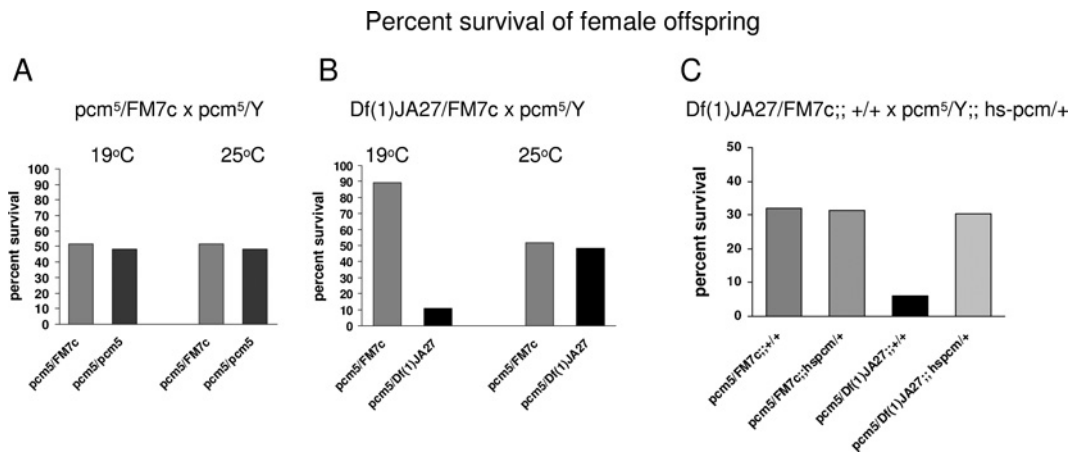

protein. This polyclonal antibody is highly specific to Pacman in that it recognizes a major band of 184 kDa, and is the only band detected which increases in intensity when *pacman* is overexpressed in transgenic flies (data not shown). The minor bands seen in wild-type males and females are most likely due to protein modifications or specific cleavages; we have no evidence for alternative splice forms. The expression of *pacman* in flies carrying mutant alleles was tested by Western blotting using these polyclonal antibodies. Homozygous *pcm*^{3} (where *pcm* is *pacman*) and *pcm*^{6} adults produced truncated protein at levels significantly lower than wild-type, whereas *pcm*^{5} animals expressed undetectable levels of the Pacman protein (Figure 1B). We therefore decided to concentrate on the strongest allele, *pcm*^{5}, for further analysis. In all these mutants, there was no major change in expression of the convergent downstream gene *Nat1*, as detected by semi-quantitative RT-PCR (reverse transcriptase PCR) (Figure 1C).

Exoribonuclease *pacman* affects viability

To determine the zygotic effect of *pacman* on viability we crossed *pcm* heterozygous females (*pcm*^{5}/FM7c) with *pcm*^{5} hemizygous males (*pcm*^{5}/Y) and counted the numbers of the resulting female offspring. If *pacman* has no effect on viability, we would expect equal numbers of homozygous female offspring (*pcm*^{5}/*pcm*^{5}) and heterozygous female offspring (*pcm*^{5}/FM7c). At 19°C and 25°C, this cross resulted in similar numbers of homozygous and heterozygous females (Figure 2A), showing that, at these temperatures, *pacman* mutations have little effect on adult viability, presumably due to residual activity of the truncated Pcm protein. However, reducing the dosage of the *pcm*^{5} mutant allele from two to one in hemizygous females carrying the deficiency Df(1)JA27 results in significantly reduced zygotic viability. The deficiency Df(1)JA27 removes 400 kb of genomic sequence, including the *pacman* gene, as well as 50 neighbouring genes on the X chromosome (Flybase; http://flybase.org). When *pcm*^{5} hemizygous males (*pcm*^{5}/Y) were crossed with heterozygous Df(1)JA27/FM7c females only 10% of the female offspring were of the *pcm*^{5}/Df(1)JA27 genotype compared with 90% *pcm*^{5}/FM7c female siblings at 19°C (50% of each are expected) (Figure 2B). At 25°C, this *pacman* allele has little effect on zygotic viability showing that it, along with our other alleles, *pcm*^{3} and *pcm*^{6}, are cold temperature sensitive (data not shown). This effect is not due to

haplo-insufficiency of the Df(1)JA27 chromosome, as offspring from the cross Df(1)JA27/FM7c × +/+ result in approximately equal numbers of Df(1)JA27/+ and FM7c/+ female offspring (ratio of 1.05:1 observed; 1:1 expected; $n = 117$). These results therefore suggest that the pcm^5 mutation has a deleterious zygotic effect on development at low temperatures. They also show that the pcm^5 allele has some residual activity and is not a null allele.

Expression of *pacman* cDNA rescues the mutant phenotypes

To confirm that the observed effects on viability were due to mutations in the *pacman* gene rather than another mutation on the X chromosome, we generated transgenic flies carrying a full-length cDNA copy of *pacman* in order to rescue the mutation. The 5.2 kb *pacman* open reading frame, plus 5′ and 3′ UTRs (untranslated regions), were cloned into a vector carrying a P-element transposon, and expressed under the control of the heat-shock promoter hsp70Bb pP{CaSpeRhs-*pcm*}. Transgenic flies were then generated using standard techniques. To confirm the expression of the *pacman* cDNA, transgenic flies and embryos carrying this *pacman* construct were subjected to heat-shock (37°C for 30 min, followed by 1 h recovery at 20°C) and the expression analysed by Northern and Western blotting. These experiments confirmed that *pacman* was expressed at high levels at the RNA and protein levels both in adults and embryos following heat shock (data not shown). However, these experiments also showed that expression of this *pacman* transgene was leaky in that it was ubiquitously expressed at low (near wild-type) levels throughout the life-cycle at 19°C. To determine whether these low levels of ectopic expression of *pacman* could rescue its associated mutant defects, the viability of females hemizygous for pcm^5 (pcm^5/Df(1)JA27;;+/+) was compared with these mutants carrying the *pcm* transgene (pcm^5/Df(1)JA27;;hs-*pcm*/+). As shown in Figure 2(C), ectopic expression of *pacman* completely rescued the viability defects associated with the *pacman* mutation at 19°C. These data therefore show that the deleterious effects on development at low temperatures are associated with the pcm^5 allele. These experiments also demonstrate that low levels of ectopic expression of *pacman* do not affect viability in this transgenic [compare pcm^5/FM7c;;+/+ with pcm^5/FM7c;;hs-*pcm*/+, (Figure 2C)].

pacman adults have wing abnormalities and defects in thorax closure

Analysis of pcm^5 mutant adult flies revealed a number of interesting defects. These adults had 'dull' wings, which were often crumpled along the posterior edge with occasional blisters in the posterior half of the wing (Figures 3B and 3E). Figure 3(A) shows a pcm^5 male with dull wings on the right-hand side compared with a male where the *pacman* mutation was rescued by a wild-type copy of *pacman* (pcm^5/Y;;hs-*pcm*/+) on the left. A mutant female pcm^5/Df(1)JA27 with crumpled wings is shown on the right-hand side of Figure 3(B) compared with a heterozygous female (pcm^5/FM7c) on the left-hand side. For pcm^5/pcm^5 females, the penetrance of the dull-wing phenotype was 98% at 19°C ($n = 295$) and 68% at 25°C ($n = 200$), again showing that this *pacman* allele is temperature sensitive. The dull-wing phenotype was fully penetrant at all temperatures in hemizygous females [pcm^5/Df(1)JA27]. Close inspection of the dull wings in these mutants revealed that the surface of the wing was not smooth, but had a regular pattern of raised tissue under each trichome (Figure 3D). This uneven surface would account for the lack of irridescence in the wings of these mutants. This dull-wing phenotype was fully rescued by ectopic expression of the wild-type *pacman* gene (Table 1).

In addition to the above defects, many mutant flies also had 'crooked' legs, where the third pair of legs was bent within the femur (Figure 3G). This defect appeared to reflect a weakness in the legs as these crooked legs were not observed in newly eclosed flies. The penetrance of this phenotype varied with temperature and again was more penetrant at lower temperatures (Table 2). These phenotypes were completely rescued by ectopic expression of *pacman*, as described above. Blistered wings and crooked legs are common phenotypes in flies carrying mutations in genes encoding adhesion proteins or extracellular matrix proteins, such as laminin (Henchcliffe et al., 1993; Brown et al., 2000), or in the focal adhesion protein paxillin (Chen et al., 2005).

The most striking effect of this *pacman* mutation was that of a cleft thorax phenotype (Figures 4B, 4C and 4D compared with wild-type, Figure 4A). At 25°C, females hemizygous for pcm^5 [pcm^5/Df(1)JA27] exhibited a cleft thorax phenotype with a penetrance of 11.6% (Table 2). At lower temperatures, no cleft thorax phenotypes were seen, but dissection of pupal

Figure 3 | Wing and leg phenotypes of *pacman* mutant adults

(**A**) Dull-wing phenotype of *pcm*^{5} male (right-hand side) compared with a mutant male ectopically expressing *pacman* [*pcm*^{5}/Y; pP{CaSpeRhs-*pcm*}/+] (left-hand side). (**B**) Dull and crumpled wing phenotype (arrow) of *pcm*^{5} hemizygous female [*pcm*^{5}/Df(1)JA27] (right-hand side) compared with heterozygous control (*pcm*^{5}/FM7c) (left-hand side). (**C** and **D**) Close-up of the surface of a wild-type (wt) wing (**C**) and a *pcm*^{5} dull wing (**D**) showing a regular pattern of raised tissue, rather than a smooth surface. (**E**) Example of a blistered wing from a *pcm*^{5}/Df(1)JA27 female (arrow). (**F** and **G**) Example of a kinked leg (arrow) from a *pcm*^{5} male where the femur of the third leg is bent (**G**) compared with the wild-type control (**F**).

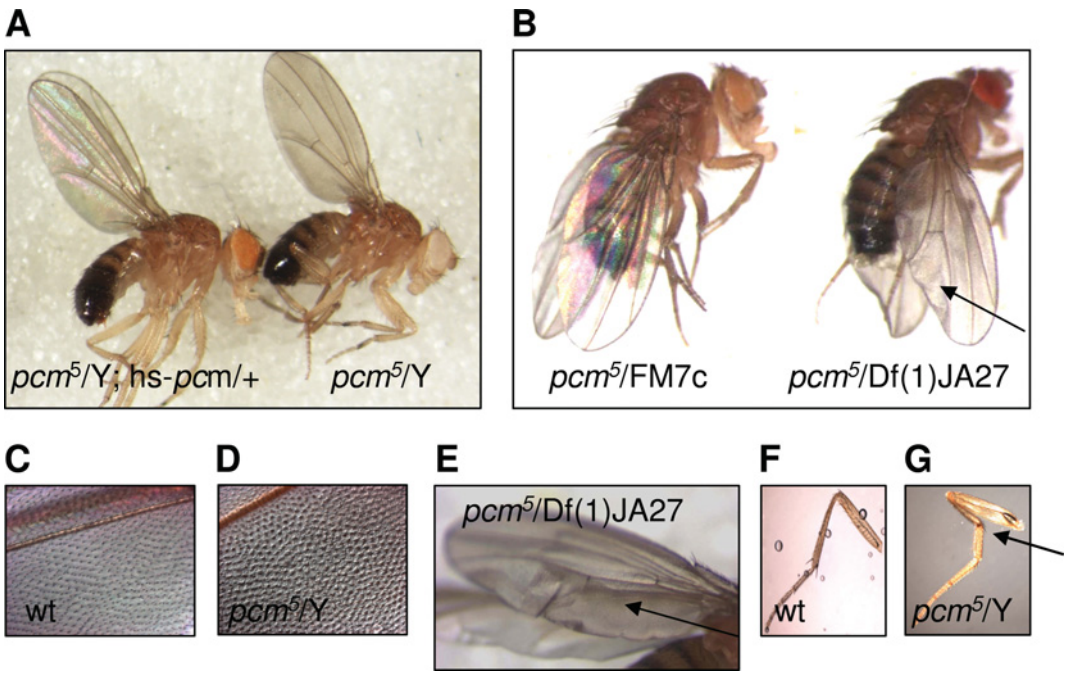

Table 1 | Ectopically expressed Pacman rescues the dull-wing phenotype in both male and female flies at 19°C

The offspring were derived from the cross *w,pcm*^{5}/FM7c;+/+ × *w,pcm*^{5}/Y;pP{CaSpeRhs-*pcm*}/+. If the ectopically expressed *pacman* (hs-*pcm*) did not rescue the dull-wing phenotype we would expect flies carrying the hs-*pcm* construct (*w,pcm*^{5}/Y;hs-*pcm*/+ or *w,pcm*^{5}/FM7c;hs-*pcm*/+) to have orange eyes and dull wings. Note that this pP{CaSpeRhs-*pcm*} construct is leaky and expresses at low levels even when the flies are not subjected to heat-shock.

	Number of phenotype			
	White eye, dull wing	White eye, shiny wing	Orange eye, dull wing	Orange eye, shiny wing
Males				
w,pcm^5/Y;+/+	50	0	–	–
w,pcm^5/Y;*hs-pcm*/+	–	–	0	55
Females				
w,pcm^5/FM7c;+/+	60	0	–	–
w,pcm^5/FM7c;*hs-pcm*/+	–	–	0	65

cases in the large number of dead pupae revealed such severe cleft thorax defects that they had died before emergence. Homozygous or hemizygous mutants (*pcm*^{5}/*pcm*^{5}, *pcm*^{5}/Y) showed a lower frequency of the cleft thorax defect. The severity of this phenotype varied from mild, where there was a bald stripe along the dorsal midline of the thorax, through to medium, where the two halves of the thorax had not conjoined, and then to strong, where the thorax and scutellum were extremely disorganized or one half of the thorax was completely missing (Figure 4D). These phenotypes were completely rescued by the

Table 2 | Percentage of phenotypes of female flies carrying one copy of the mutant *pcm*^{5} allele

These flies resulted from the cross Df(1)JA27/FM7c × *pcm*^{5}/Y. Note that Df(1)JA27/FM7c is not associated with any of these mutant phenotypes.

		Percentage of flies	
Phenotype	Temperature (°C)...	19	25
Crooked legs		53.3	9.4
Blistered wings		13.3	1.0
Cleft thorax		0	11.58
Dull wings		100	100
Number scored		243	295

ectopic expression of *pacman* in the transgenic described above. These cleft thorax phenotypes strongly resemble that of flies carrying mutations in *hemipterous* and *kayak*, which are members of the JNK signalling pathway. Incomplete penetrance and variable expressivity are also observed in *hemipterous* and *kayak* mutants (Zeitlinger et al., 1997; Agnes et al., 1999; Zeitlinger and Bohmann, 1999).

The thorax of *Drosophila* is formed during pupariation when the distal tips of the two imaginal wing discs grow together and fuse along the dorsal midline. The cells at the distal tips of the discs become more elongated as they move together by crawling over the underlying layer of larval cells. The leading cells then seal along the dorsal midline (Zeitlinger and Bohmann, 1999; Martin-Blanco, 2000; Usai and Simpson, 2000). Incorrect fusion leads to the cleft thorax phenotype. If *pacman* is involved in this epithelial spreading we would expect it to be expressed in third instar larvae and early pupae, when this epithelial sheet spreading is taking place. Our Western blotting experiments show that Pacman protein is, indeed, expressed in third instar wandering larvae, and early, mid and late pupae with higher expression of *pacman* at these stages than in second instar larvae and late pupae (Figures 4E and 4F). Therefore the expression of *pacman* is consistent with a role in this process.

If *pacman* is required for thorax closure it would also be expected to be necessary for correct dorsal closure, which is a similar morphological process. Our results show that it is indeed required for this process. Figure 4(G) shows that hemizygous *pcm*^{5} mutant embryos [*pcm*^{5}/Df(1)JA27/FM7c] at 19°C have a severe 'dorsal open' phenotype, which is very similar to that seen in a *kayak*^{1} (DFos) mutant (Zeitlinger et al., 1997) (Figure 4H). This phenotype results from the two epithelial sheets completely failing to join, resulting in the epithelial sheet springing back to give a wrinkled scrap of tissue. The penetrance of this phenotype in *pcm*^{5}/Df(1)JA27/FM7c embryos raised at 19°C is 80%. At 25°C, these embryos show a severe dorsal closure defect, resulting in a large anterior hole (Figure 4J), very similar to that of a *bsk*^{2} (*basket*; JNK) mutant (Figure 4K). The dark-field image of these embryos shows that the denticle belt patterning is not unduly perturbed (Figures 4M and 4N). The cleft thorax, dorsal open and dorsal closure mutant phenotypes provide powerful evidence that *pacman* plays a role in the cell movement, cell adhesion or cell shape change, and show an unexpected link between RNA stability and morphogenesis.

pacman affects wound healing

The epithelial sheet movement involved in thorax closure is a conserved morphogenetic process which is similar to that of dorsal closure in *Drosophila*, hindbrain closure in vertebrates and wound healing in humans (Jacinto et al., 2001). Since *pacman* is highly conserved in eukaryotes, and epithelial sheet sealing is a conserved morphological process, we reasoned that *pacman* might also affect wound healing. To test this, we wounded adult 3–5-day-old females on the underside of the abdomen using a small scalpel, being careful not to damage the underlying tissues. The survival of these flies was then compared with controls. Figure 5 shows that *pcm*^{5} and *pcm*^{3} homozygotes survived much less well than controls. For example, the half-life of *pcm*^{5} homozygotes at 25°C after wounding was 11.2 h compared with 22.4 h in controls (Figure 5B). The survival of unwounded *pcm*^{5} flies was similar to unwounded controls over the time course of the experiment (Figure 5F). The survival rate of the controls may reflect the severity of the wounding procedure or could be as a result of infection (although sterile scalpel blades were used). Statistical analysis of the survival curves confirmed that survival at 48 h and 72 h was significantly different for *pcm*^{3} and *pcm*^{5} homozygotes compared with controls ($P < 0.0001$ for all comparisons).

In order to determine whether this difference in survival of *pacman* mutants after wounding might be particular to the epithelial sheet sealing process,

Figure 4 | Phenotypes of *pacman mutant* flies

(**A**) Dorsal view of a wild-type thorax. (**B**) Mutant homozygous *pcm*^{5} and (**C** and **D**) hemizygous *pcm*^{5} [*pcm*^{5}/Df(1)JA27] females showing the cleft thorax phenotypes. (**E**) Western blot showing expression of *pacman* protein in wild-type larvae, pupae and adults compared with the actin loading control. Pacman is expressed at higher levels in L3, early pupae and mid-pupae during growth and differentiation of the imaginal discs. L1, first instar larvae; L2, second instar larvae; L3, third instar larvae; EP, early pupae; MP, mid-pupae; LP, late pupae; M, adult males; F, adult females. (**F**) Quantification of the Western using the actin loading control. (**G**–**O**) Cuticle preparations of mutant and wild-type embryos. (**G**) Cuticle prep of a *pacman* mutant embryo expressing one copy of the *pcm*^{5} allele [i.e. a hemizygous mutant *pcm*^{5}/*Df(1)JA27* (reared at 19°C)] compared with a *kay*^{1}/*kay*^{1} homozygous mutant (**H**) (Zeitlinger et al., 1997) and wild-type control (**I**). Note that this *pacman* mutant has a dorsal open phenotype resulting from complete failure of dorsal closure and is very similar to that of a homozygous mutant in *kayak* (DFos), encoding a JNK signalling protein. (**J** and **M**) Cuticle prep of a *pacman* mutant embryo expressing one copy of the *pcm*^{5} allele [i.e. a hemizygous mutant *pcm*^{5}/Df(1)JA27 (reared at 25°C)] compared with a *bsk*^{2}/*bsk*^{2} homozygous mutant (**K**) and (**N**). (**J**) and (**K**) show the embryos using bright-field microscopy, which emphasizes the large dorsal holes (arrows). (**M**) and (**N**) show the same embryos using dark-field microscopy, demonstrating that the pattern of denticle belts is not substantially perturbed in these mutants. A wild-type embryo, taken using bright- (**L**) and dark- (**O**) field microscopy is shown for comparison.

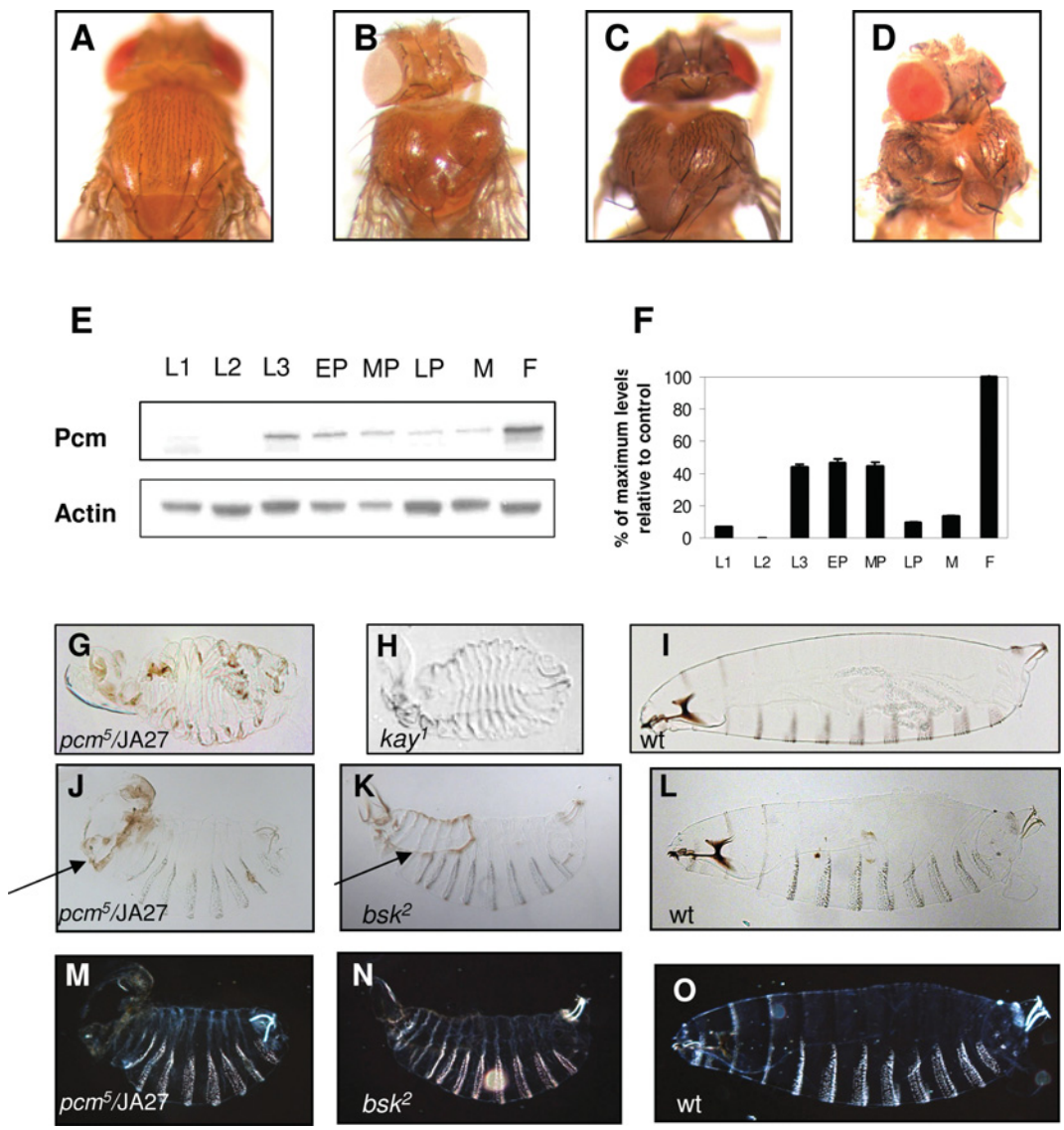

Figure 5 | Survival of *pacman* mutants after wounding

(**A** and **B**) Average half-lives of *pcm*^{3}, and *pcm*^{5} mutants after wounding, together with isogenic controls. Means ± S.E.M. of at least three independent experiments are given. Flies raised at 19°C (**A**) and 25°C (**B**) were used. In all cases, the *pacman* mutants survived significantly less well than controls. (**C** and **D**) Average times of clot formation in *pacman* mutants compared with controls in flies raised at 19°C (**C**) and 25°C (**D**). Means ± S.E.M. of at least three independent experiments are given. (**E** and **F**) Typical survival curves for *pcm*^{5} mutants and controls showing survival of wounded and unwounded flies raised at 19°C (**E**) and 25°C (**F**). The survival of unwounded mutants was not significantly different to that of controls over the time period of the experiment. ●, Control unwounded; ◆, control wounded; ▲, *pcm*^{5} unwounded; ■, *pcm*^{5} wounded.

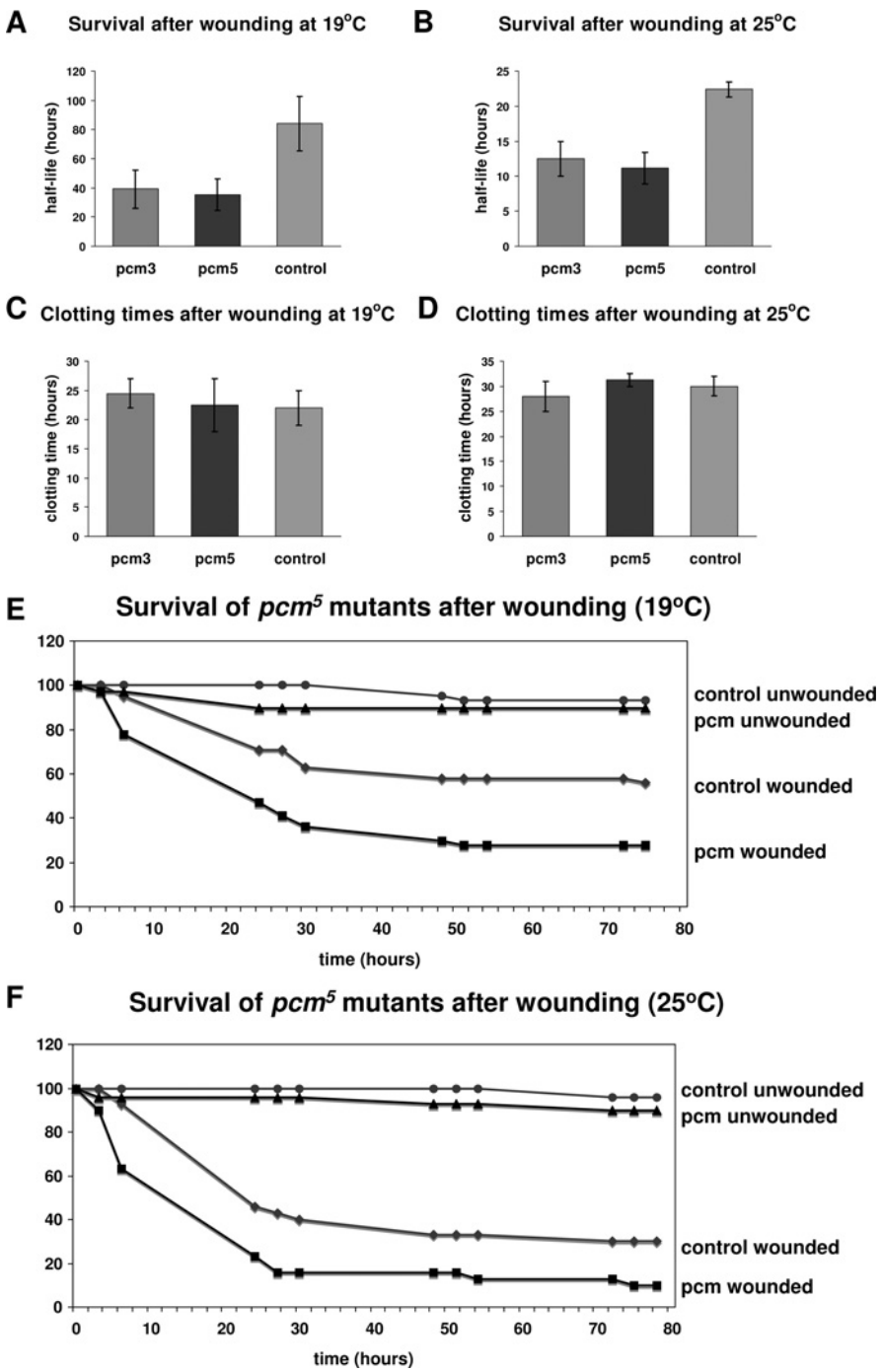

Figure 6 | Phenotypic defects in flies carrying mutations in *pacman* and *puckered*

(**A**) Bristles on the dorsal side of the thorax in a wild-type fly. (**B**) Bald patch at the anterior dorsal midline of a pcm^5/pcm^5;;puc^{A251}/TM6b,Tb,Sb female (arrow).

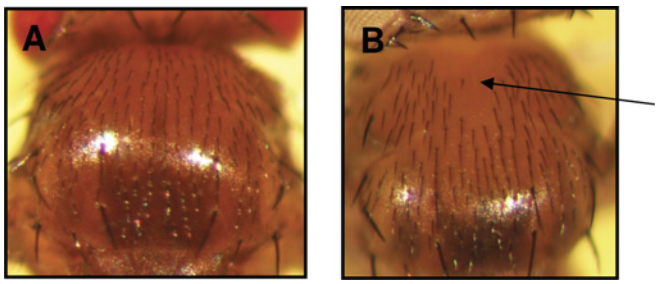

rather than a general metabolic defect, we also followed the formation of the melanin clot over the wound. The clotting process in *pcm* mutants followed a similar time course to that of controls (Figures 5C and 5D). Therefore these results show that *pacman* is required for the normal wound healing process.

pacman interacts with *puckered*, a phosphatase in the JNK signalling pathway

The cleft phenotypes observed closely resemble that observed in flies mutant for genes such as *hemipterous* [JNKK (JNK-activated kinase)], *basket* (JNK) and *kayak* (DFos), which are members of a conserved JNK signalling pathway (Agnes et al., 1999; Zeitlinger and Bohmann, 1999). This JNK signalling pathway has been shown to be crucial in controlling the cellular events that govern epithelial sheet sealing processes, such as thorax closure, dorsal closure and wound healing (Jacinto et al., 2002; Martin and Wood, 2002; Wood et al., 2002; Martin and Parkhurst, 2004). Therefore *pacman* could be involved in the regulation of thorax closure and wound healing by modulating the expression of gene(s) in this pathway. A potential candidate gene is *puckered*, a crucial phosphatase in this pathway, which dephosphorylates the central JNK, *basket*. We reasoned that the phenotypes we observed could be due to mis-regulation of *puckered* expression by *pacman*.

In order to test this hypothesis, we looked for a genetic interaction between *puckered* and *pacman*. The *puckered* allele puc^{A251} is a result of a P-element insertion into the second intron of the *puckered* gene (Martin-Blanco et al., 1998) and are homozygous lethal. The P-element inserted (P{w^+,*lacZ*}A251.1) carries a *lacZ* reporter gene which has been used to monitor the transcriptional activity of the *puckered* promoter (Martin-Blanco et al., 1998). Flies carrying both pcm^5 and puc^{A251} alleles were generated and the phenotypes examined. Male and female flies homozygous (or hemizygous) for *pacman* and heterozygous for puc^{A251} (pcm^5/pcm^5;;puc^{A251}/TM6b,Tb,Sb and pcm^5/Y;;puc^{A251}/TM6b,Tb,Sb) were viable, but showed a number of interesting phenotypic defects. In 58% of males and 70% of females raised at 19°C, there was a 'bald' patch at the anterior end of the dorsal midline, indicating that thorax closure was not quite complete (Figure 6B). When these flies were raised at 25°C, 95% of males and 66% of females had bald patches. All other genotypes had no bald patches (Table 3). Greater than 90% of flies homozygous (or hemizygous) for *pacman* and heterozygous for the *puckered* mutation (pcm^5/pcm^5;;puc^{A251}/TM6b,Tb,Sb and pcm^5/Y;;puc^{A251}/TM6b,Tb,Sb) had dull wings at 19°C and 25°C, indicating that *puckered* did not substantially affect this *pacman* phenotype. This observation therefore suggest that *pacman* affects expression of *puckered*, either by directly regulating the JNK pathway or by regulating a parallel pathway.

Discussion

In the present study we have investigated the effects of a 5′–3′ exoribonuclease *pacman* on *Drosophila* development. This was achieved by constructing mutations in *pacman* and examining the zygotic effect of the resulting phenotypes. Although we did not succeed in generating a null allele, the allelic series we obtained shed light on the function of *pacman* in development. The most striking phenotype observed in *pacman* mutants is a defect in thorax formation such that the two halves of the thorax on the dorsal

Table 3 | Percentage of dorsal bald patches in particular genotypes

Flies of the genotypes in rows 1–4 are relevant offspring from the cross pcm^5/FM7i;;puc^{A251}/TM6b,Tb,Sb × pcm^5/Y;;puc^{A251}/TM6b,Tb,Sb. At least 50 of each genotype were scored.

Row	Genotype Temperature (°C)...	Bald patches (%) 19	25
1	pcm^5/pcm^5;;puc^{A251}/TM6b,Tb,Sb	70	67
2	pcm^5/Y;;puc^{A251}/TM6b,Tb,Sb	58	95
3	pcm^5/FM7i;;puc^{A251}/TM6b,Tb,Sb	0	0
4	FM7i/Y;;puc^{A251}/TM6b,Tb,Sb	0	0
5	pcm^5/Y	0	0
6	FM7i/Y	0	0
7	pcm^5/ pcm^5	0	0
8	pcm^5/FM7i	0	0
9	puc^{A251}/TM6,Tb,Sb	0	0

side do not join together correctly. The dorsal part of the thorax in wild-type *Drosophila* is formed by cells at the tips of the two wing imaginal discs which migrate towards each other over a layer of larval cells and then fuse together along the dorsal midline (Agnes et al., 1999; Martin-Blanco et al., 2000). This epithelial cell movement is very similar to that seen in dorsal closure in *Drosophila*, hindbrain closure in vertebrates, epiboly in *Xenopus* and in wound healing in humans (Jacinto et al., 2002). We also showed that *pacman* affects wound healing in *Drosophila*, which significantly strengthens our hypothesis that *pacman* has a conserved role in epithelial sheet movement. Furthermore, our results in a previous study (Newbury and Woollard, 2004) demonstrate that the *pacman* orthologue *xrn-1* in *C. elegans* is essential for ventral enclosure, which has been shown to be a similar morphological process to dorsal and thorax closure in *Drosophila* (Jacinto et al., 2002; Newbury and Woollard, 2004), although the molecular similarities between the two processes remain controversial. Our results on *pacman* in *Drosophila*, taken together with those on *xrn-1* in *C. elegans*, suggest that the 5′–3′ mRNA degradation pathway is a crucial factor in this morphological process.

Our results presented above, where we have used living organisms, rather than tissue culture cells, suggest that the 5′–3′ mRNA degradation pathway is important for cellular processes. That it is defects in mRNA degradation which lead to the phenotypic defects observed, rather than some other function of Pacman, is suggested by our recent study showing that an exoribonuclease-dead version of Pacman cannot complement the *pacman* mutation (D.P. Grima, S. Hebbes and S.F. Newbury). Our results are in agreement with studies in human tissue culture cells showing that the degradation of unstable RNAs containing AREs (AU-rich elements), such as c-*myc* and c-*fos* is primarily in a 5′–3′ direction (Newbury et al., 2006), emphasizing the importance of this pathway in human cells. Earlier studies, using human tissue culture cell extracts, demonstrating that degradation of short-lived mRNAs such as c-*myc* and c-*fos* are primarily in a 3′–5′ direction via the exosome (Mukherjee et al., 2002; Wang and Kiledjian, 2001) can be explained by the fact that cytoplasmic complexes containing the decapping/5′–3′ degradation enzymes are removed or disrupted during preparation of the extract. Therefore our results support the conclusion that 5′–3′ degradation of mRNAs is important in yeast, *Drosophila* and mammalian cells.

The cleft thorax or dorsal closure phenotypes of *pacman* mutants resemble that of mutations in the JNK signalling pathway. Hypomorphic mutations in *hemipterous*, *basket* and *kayak* or overexpression of the JNK phosphatase *puckered* result in similar cleft thorax defects to those seen in *pacman* mutants. In addition, the JNK pathway, including the phosphatase *puckered*, is known to be involved in the epithelial sheet sealing pathway during wound healing (Ramet et al., 2002). There are a number of ways in which *pacman* might regulate the JNK pathway. Pacman might act directly on *puckered* transcripts, in which case *puckered* transcripts would be expected to be stabilized with a corresponding increase in levels of Puckered protein. This would lead to increased dephosphorylation of its target kinase (the JNK Basket) and down-regulation of the JNK pathway, resulting in defective epithelial sheet sealing. However, this hypothesis seems unlikely as *puckered* mutations would then be expected to suppress (rather than enhance) *pacman* phenotypes, as is seen in hep^1;;puc^{E69} and kay^2/kay^1;;puc^{E69} double mutants (Zeitlinger and Bohmann, 1999). Alternatively, *pacman* may have its primary effects on other transcripts, which in turn affect the expression of *puckered*. It is also possible that *pacman* may act in a pathway that is parallel, rather than linear to, the JNK pathway.

As well as epithelial sheet sealing, the *pacman* phenotypes, such as dull wings and bent legs, would

suggest that *pacman* also affects transcripts in other cellular pathways. A possible target for *pacman* is *paxillin*, a focal adhesion adaptor. Overexpression of Dpax in flies results in bent and/or twisted leg phenotypes and also blistered wings (Chen et al., 2005). Therefore it is possible that the Pacman exoribonuclease directly targets *paxillin* mRNA to ensure that it is expressed at the correct levels in wild-type flies.

Interestingly, we consistently find the phenotypic effects of *pacman* alleles to be more severe in *pacman* mutant females compared with *pacman* mutant males. For example, the enhanced lethality in hemizygous females pcm^5/Df(1)JA27 at 19°C (viability of 2.7% of total offspring) compared with pcm^5/Y at 19°C (viability 13.9% of total offspring) highlights this difference. As yet, we do not understand the differences in phenotypic effects between males and females, but suspect it may be to do with dosage compensation. It is possible that *pacman* mutations may affect the levels of non-coding RNAs that are involved in dosage compensation (Deng and Meller, 2006). If this is the case, then *pacman* mutations may also modulate the levels of expression of genes located on the X-chromosome, resulting in different phenotypic effects in males compared with females.

How could an exoribonuclease, which is relatively non-specific *in vitro* (Chernukhin et al., 2001), selectively affect the expression of particular RNAs, such as those encoding proteins involved in thorax formation? Our work, using *Drosophila* neurons (Barbee et al., 2006), shows that Pacman is localized in cytoplasmic particles, which appear to be analagous to yeast or human P-bodies. In these particles, Pacman is co-localized with other proteins in the 5′–3′ degradation pathway, such as the decapping enzymes dDcp1 and dDcp2, as well as proteins involved in translational repression (Barbee et al., 2006; Lin et al., 2006). In human tissue culture cells, mRNAs appear to be guided to these P-bodies by RNA-binding proteins, such as TTP (tristetraprolin) or by microRNAs (Lai et al., 2003; Kedersha et al., 2005). We speculate that *pacman* target mRNAs are normally transported to P-bodies and then rapidly down-regulated by translational repression and degradation. Reduction in Pacman activity may interfere with the translational repression process, resulting in inappropriate levels of target proteins and down-regulation of the JNK pathway. The finding that *pacman* regulates the JNK pathway is significant in that it will allow us to identify and define targets *in vivo* for this 5′–3′ exoribonuclease. This is a crucial step in understanding the mechanisms whereby ribonucleases can specifically target RNAs and is likely to be relevant to other specific degradation events, such as those that occur during RNA interference.

Materials and methods

Drosophila strains, generation of *pacman* mutants and molecular characterization of mutants

Fly stocks used were obtained from the Bloomington *Drosophila* Stock Center (Indiana University, Bloomington, IN, U.S.A.) unless otherwise indicated. Bloomington stock 11456 carrying the P-element insertion *P{EP}EP1526* was used to create *pcm* mutants by imprecise P-element excision using standard protocols (Greenspan, 2004). Bloomington stock 971 carrying the deficiency Df(1)JA27/FM7c was used to generate hemizygous stocks and to generate balanced stocks of the mutagenized *pcm* lines. Potential mutant lines were screened by duplex PCR using the following primers: jls1, 5′-TCAAAAAGGCAGTGGCATGAG-3′, and jls2, 5′-GTCCGAATCTGATGGGGTCT-3′; and control primers dob1f, 5′-GACATTGTTCAGGGCAAGGCAG-3′ and dob1b, 5′-GGAGCGGTGAGGTCGTTAAATAC-3′. Mutant lines were then checked by Southern blotting for single transposition events. Mutations were characterized at the molecular level by amplification of DNA at either side of the breakpoint using the primers jes1, 5′-TCCCGATCACGATGAAGACC-3′, and big1, 5′-ACTGCCGCCTCAGATCTG-3′, and the DNA was sequenced. To test whether the molecular lesions in the nine lethal lines were due to a deletion in the *pacman* gene, DNA isolated from heterozygotes carrying a viable allele of *pacman* {pcm^2; encoding a slightly truncated *pacman* protein [truncated by 66 aa (amino acids)]}, together with each of the lethal alleles, was subjected to PCR using the primers jls1 and jls2. Since these primers do not result in any product from the pcm^2 chromosome, any PCR product must come from the chromosome carrying the lethal allele. All these lethal alleles resulted in a PCR product of a size comparable with that from a wild-type chromosome. Therefore the lethality of these nine alleles did not result from deletions in the *pacman* gene. The predicted sizes and molecular masses of the three truncated proteins encoded by the alleles pcm^3, pcm^5 and pcm^6 compared with the wild-type protein were as follows: wild-type PCM, 1612 aa, 184.5 kDa; PCM3, 1461 aa, 167.7 kDa; PCM5, 1293 aa, 149.2 kDa; PCM6, 1396 aa, 160.0 kDa. Unfortunately, no null alleles were generated.

To determine whether the deletions within *pacman* affected expression of the downstream gene *Nat1* we used semi-quantitative RT-PCR in duplex reactions with primers for the 'housekeeping' control gene *rp49*, as well as *Nat1* primers. The primers used were: Nat1-34f, 5′-CACTACGACTACATGCGCGATA-3′; Nat1-34r, 5′-GAACTTGGCGCAGATCTCCT-3′; rp49F1, 5′-CAAGGGACAGTATCTGATG-3′; rp49R1 5′-CAGTAAACGCGGTTCT-3′.

Primers were designed to amplify a region of the *Nat1* gene spanning the intron between exons 3 and 4 (Nat1-34f and Nat1-34r) in order to distinguish between genomic DNA

amplicons (324 bp) and cDNA amplicons (244 bp). RNA was extracted from 15 flies from each of the lines tested using the RNeasy extraction kit (Qiagen) and cDNA was prepared using the Superscript III reverse transcriptase kit according to the manufacturer's instructions. All amplicons first appeared faintly at 24 cycles and clearly at 26 cycles. PCR was repeated using the same programme, except that only 26 cycles were used. Positive (gDNA from w^{1118}) and negative (template replaced with water) controls were used to validate the results.

The stock overexpressing *pacman* was generated by cloning a full-length *Drosophila* cDNA, including the 5′ UTR and 3′ UTR, into the P-element transformation vector pP{CaSpeR-hs}, followed by germline transformation of w^{1118} flies using standard methods. Three independently generated lines all gave identical results. All whole fly images were captured using the Nikon DN100 camera attached to a Nikon SMZ800 microscope.

Generation of antibodies, Western blotting and immunostaining

For preparation of an antibody to Pacman, cDNA encoding a 54 kDa C-terminal portion of Pacman was expressed as a histidine-tagged fusion protein in *Escherichia coli* using the expression vector pET28a. The histidine tag was removed by thrombin treatment and the Pacman protein fragment cut from the gel for use in raising antibodies. The rabbit polyclonal antibody was prepared by the company Eurogentec. Although this antibody was made against the C-terminus of the Pacman protein, we know it can detect the truncated Pacman protein encoded by the pcm^5 mutants for two reasons. First, sequencing of the pcm^5 lesion shows that the truncated protein still includes 140 aa of the C-terminal region used to raise the antibody. Secondly, our immunoprecipitation experiments using testes from pcm^5 mutants have shown that this antibody can immunoprecipitate the truncated Pacman protein (Zabolotskaya et al., 2008).

SDS/PAGE and Western blotting was performed essentially as described by Sambrook et al. (1989). Equal numbers of adult flies, raised at 25°C, were used for the samples in each lane. The binding of the polyclonal antibody against Pacman was detected using the ECL® Western blot reagent kit (Amersham). Primary polyclonal anti-Pacman antibody was used at a 1:2000 dilution and the monoclonal anti-actin antibody (Sigma) at 1:10000. The secondary antibodies were monoclonal anti-rabbit HRP (horseradish peroxidase)-conjugated antibody (Sigma) and monoclonal anti-mouse HRP-conjugated antibody (Sigma) both used at a 1:80 000 dilution. Western blotting was quantified using ImageJ software (http://rsbweb.nih.gov/ij/).

Cuticle preps

BL971 females [Df(1)JA27/FM7c] were collected as virgins and allowed to mate with pcm^5 males in a collection cage for 2 days with fresh grape-juice agar and yeast supplied every day. Embryos at the appropriate stage of development were dechorionated in 50% bleach for 3 min before washing twice in distilled water and transferring to a scintillation vial containing 3 ml of 100% methanol and 3 ml of 100% heptane. The vial was shaken vigorously for 1 min to devitellinize the embryos, which then sank to the bottom. The upper layer and interface were siphoned off and the embryos washed twice in methanol. Embryos were then transferred on to a clean microscope slide and the methanol allowed to air dry. Hoyer's medium/lactate (3:1; 50–100 μl) was added and a coverslip placed over the top of the embryos. The slide was then incubated overnight at 65°C to clear and then flattened with a brass weight. Slides were then examined and photographed under dark- or bright-field microscopy on a Axioplan microscope (Zeiss). Similar methods were used for the wild-type and bsk^2 embryos.

Wounding experiments

Female flies were wounded on the ventral side of the abdomen, using a small scalpel, taking care not to damage the underlying tissues, and then placed in food vials. Typically, ten flies for each stock were wounded and compared with ten unwounded controls. The number of flies still alive was recorded every 3 h (during the day) until at least 50% of the mutant flies were dead. These data were then analysed using the statistics computer programme Minitab. The χ^2 test was applied to the data to determine whether there was a significant difference between survival of wounded and unwounded flies after wounding. To determine the time of clot formation, 3–4-day-old flies were wounded as above, and the progression of clot formation recorded at 10, 20, 25, 30, 35, 40, 50 and 60 min.

Acknowledgements

We thank Dr France Docquier for advice on the P-element excision work and Professor Roy Parker for advice and encouragement. We are also grateful to Dawn Field, Helen Glenwright, Alex Blundell and Sarah Allan for technical help. This work was supported by the Leverhulme Trust, the U.K. Biotechnology and Biological Sciences Research Council, the Nuffield Foundation, the Biochemical Society and the Genetics Society.

References

Agnes, F., Suzanne, M. and Noselli, S. (1999) The *Drosophila* JNK pathway controls the morphogenesis of imaginal discs during metamorphosis. Development **126**, 5453–5462

Anderson, J.S. and Parker, R. (1998) The 3′ to 5′ degradation of yeast mRNAs is a general mechanism for mRNA turnover that requires the SKI2 DEVH box protein and 3′ to 5′ exonucleases of the exosome complex. EMBO J. **17**, 1497–1506

Barbee, S.A., Estes, P.S., Cziko, A., Luedeman, R.A., Coller, J.M., Johnson, N., Howlett, I.C., Geng, C., Brand, A., Newbury, S.F., Levine, R.B., Wilhelm, J.E., Nakamura, A., Parker, R. and Ramaswami, M. (2006) FMRP and Staufen containing RNA granules are structurally and functionally related to somatic P-bodies. Neuron **52**, 997–1009

Bashirullah, A., Cooperstock, R.L. and Lipshitz, H.D. (2001) Spatial and temporal control of RNA stability. Proc. Natl. Acad. Sci. U.S.A. **98**, 7025–7028

Bashkirov, V.I., Scherthan, H., Solinger, J.A., Buerstedde, J.-M. and Heyer, W.D. (1997) A mouse cytoplasmic exoribonuclease (mXRN1p) with preference for G4 tetraplex substrates. J. Cell Biol. **136**, 761–773

Bouveret, E., Rigaut, G., Shevchenko, A., Wilm, M. and Seraphin, B. (2000) A Sm-like protein complex that participates in mRNA degradation. EMBO J. **19**, 1661–1671

Brown, N.H., Gregory, S.L. and Martin-Bermudo, M.D. (2000) Integrins a mediators of morphogenesis in *Drosophila*. Dev. Biol. **223**, 1–16

Caponigro, G. and Parker, R. (1996) Mechanisms and control of mRNA turnover in *Saccharomyces cerevisiae*. Microbiol. Rev. **60**, 233–249

Chen, G.C., Turano, B., Ruest, P.J., Hagel, M., Settleman, J. and Thomas, S.M. (2005) Regulation of Rho and Rac signaling to the actin cytoskeleton by paxillin during *Drosophila* development. Mol. Cell. Biol. **25**, 979–987

Chernukhin, I.V., Seago, J.E. and Newbury, S.F. (2001) *Drosophila* 5′ → 3′-exoribonuclease Pacman. Methods Enzymol. **342**, 293–302

Cooperstock, R.L. and Lipshitz, H.D. (1997) Control of mRNA stability and translation during *Drosophila* development. Semin. Cell Dev. Biol. **8**, 541–549

Cougot, N., Babajko, S. and Seraphin, B. (2004) Cytoplasmic foci are sites of mRNA decay in human cells. J. Cell Biol. **165**, 31–40

Decker, C.J. and Parker, R. (1993) A turnover pathway for both stable and unstable mRNAs in yeast: evidence for a requirement for deadenylation. Genes Dev. **7**, 1632–1643

Decker, C.J. and Parker, R. (1994) Mechanisms of mRNA degradation in eukaryotes. Trends Biochem. Sci. **19**, 336–340

Deng, X. and Meller, V.H. (2006) Non-coding RNA in fly dosage compensation. Trends Biochem. Sci. **31**, 526–532

Eulalio, A., Behm-Ansmant, I. and Izaurralde, E. (2007) P bodies: at the crossroads of post-transcriptional pathways. Nat. Rev. Mol. Cell Biol. **8**, 9–22

Flybase (1996) The *Drosophila* genetic database. Nucleic Acids Res. **24**, 53–56

Gatfield, D., Unterholzner, L., Ciccarelli, F.D., Bork, P. and Izaurralde, E. (2003) Nonsense-mediated mRNA decay in *Drosophila*: at the intersection of the yeast and mammalian pathways. EMBO J. **22**, 3960–3970

Greenspan, R.J. (2004) Fly Pushing: The Theory and Practice of *Drosophila* Genetics. Cold Spring Harbor Laboratory Press, Cold Spring Harbor, NY

Henchcliffe, C., Garcia-Alonso, L., Tang, J. and Goodman, C.S. (1993) Genetic analysis of laminin A reveals diverse functions during morphogenesis in *Drosophila*. Development **118**, 325–337

Jacinto, A., Martinez-Arias, A. and Martin, P. (2001) Mechanisms of epithelial fusion and repair. Nat. Cell Biol. **3**, E117–E123

Jacinto, A., Woolner, S. and Martin, P. (2002) Dynamic analysis of dorsal closure in *Drosophila*: from genetics to cell biology. Dev. Cell **3**, 9–19

Johnson, A.W. (1997) Rat1 and Xrn1p are functionally interchangeable exoribonucleases that are restricted to and required in the nucleus and cytoplasm respectively. Mol. Cell Biol. **17**, 6122–6130

Johnson, K.H. and Gray, D.M. (1991) An estimate of the nearest neighbour base-pair content of 5S RNA using CD and absorption spectroscopy. Biopolymers **31**, 385–395

Kedersha, N., Stoecklin, G., Ayodele, M., Yacono, P., Lykke-Andersen, J., Fitzler, M.J., Scheuner, D., Kaufman, R.J., Golan, D.E. and Anderson, P. (2005) Stress granules and processing bodies are dynamically linked sites of mRNP remodeling. J. Cell Biol. **169**, 871–884

Lai, W.S., Kenninton, E.A. and Blackshear, P.J. (2003) Tristetraprolin and its family members can promote the cell-free deadenylation of AU-rich elementc-containing mRNAs by poly(A) ribonuclease. Cell Biol. **23**, 3798–3812

Lin, M.D., Fan, S.J., Hsu, W.S. and Chou, T.B. (2006) *Drosophila* decapping protein 1, dDcp1, is a component of the oskar mRNP complex and directs its posterior localization in the oocyte. Dev. Cell **10**, 601–613

MacDonald, M.E., Gines, S., Gusella, J.F. and Wheeler, V.C. (2003) Huntington's disease. Neuromol. Med. **4**, 7–20

Macdonald, P.M. and Smibert, C.A. (1996) Translational regulation of maternal mRNAs. Curr. Opin. Genet. Dev. **6**, 403–407

Martin, P. and Parkhurst, S.M. (2004) Parallels between tissue repair and embryo morphogenesis. Development **131**, 3021–3034

Martin, P. and Wood, W. (2002) Epithelial fusions in the embryo. Curr. Opin. Cell Biol. **14**, 569–574

Martin-Blanco, E. (2000) p38 MAPK signalling cascades: ancient roles and new functions. Bioessays **22**, 637–645

Martin-Blanco, E., Gampel, A., Ring, J., Virdee, K., Kirov, N., Tolkovsky, A.M. and Martinez-Arias, A. (1998) Puckered encodes a phosphatase that mediates a feedback loop regulating JNK activity during dorsal closure in *Drosophila*. Genes Dev. **12**, 557–570

Martin-Blanco, E., Pastor-Pareja, J.C. and Garcia-Bellido, A. (2000) JNK and decapentaplegic signaling control adhesiveness and cytoskeleton dynamics during thorax closure in *Drosophila*. Proc. Natl. Acad. Sci. U.S.A. **97**, 7888–7893

McCarthy, J.E.G. (1998) Posttranscriptional control of gene expression in yeast. Microbiol. Mol. Biol. Rev. **62**, 1492–1553

Meyer, S., Temme, C. and Wahle, E. (2004) Messenger RNA turnover in eukaryotes: pathways and enzymes. Crit. Rev. Biochem. Mol. Biol. **39**, 197–216

Muhlrad, D., Decker, C.J. and Parker, R. (1994) Deadenylation of the unstable mRNA encoded by the yeast MFA2 gene leads to decapping followed by 5′–3′ digestion of the transcript. Genes Dev. **8**, 855–866

Mukherjee, D., Gao, M., O'Connor, J.P., Raijmakers, R., Pruijn, G., Lutz, C.S. and Wilusz, J. (2002) The mammalian exosome mediates the efficient degradation of mRNAs that contain AU-rich elements. EMBO J. **21**, 165–174

Newbury, S.F., Muhlemann, O. and Stoecklin, G. (2006) Turnover in the Alps: an mRNA perspective. EMBO Rep. **7**, 143–148

Newbury, S.F. and Woollard, A.C. (2004) The 5′–3′ exoribonuclease xrn-1 is essential for ventral epithelial enclosure during *C. elegans* embryogenesis. RNA **10**, 59–65

Orban, T.I. and Izaurralde, E. (2005) Decay of mRNas targeted by RISC requires XRN1, the Ski complex and the exosome. RNA **11**, 459–469

Parker, R. and Sheth, U. (2007) P-bodies and the control of mRNA degradation and translation. Mol. Cell **25**, 635–646

Parker, R. and Song, H. (2004) The enzymes and control of eukaryotic mRNA turnover. Nat. Struct. Mol. Biol. **11**, 121–127

Ramet, M., Lanot, R., Zachary, D. and Manfruelli, P. (2002) JNK signalling pathway is required for efficient wound healing in *Drosophila*. Dev. Biol. **241**, 145–156

Sambrook, J., Fritsch, E.F. and Maniatis, T. (1989) Molecular Cloning: A Laboratory Manuel (2nd ed.), Cold Spring Harbor Press, Cold Spring Harbor

Sheth, U. and Parker, R. (2003) Decapping and decay of messenger RNA occur in cytoplasmic processing bodies. Science **300**, 805–808

Souret, F.F., Kastenmayer, J.P. and Green, P.J. (2004) AtXRN4 degrades mRNA in Arabidopsis and its substrates include selected miRNA targets. Mol. Cell **15**, 173–183

Sweet, Y.J., Boyer, B., Hu, W., Baker, K.E. and Coller, J. (2007) Microtubule disruption stimulates P-body formation. RNA **13**, 493–502

Tadros, W., Houston, S.A., Bashirullah, A., Cooperstock, R.L., Semotok, J.L. and Lipshitz, H.D. (2003) Regulation of maternal transcript destabilization during egg activation in *Drosophila*. Genetics **164**, 989–1001

Tharun, S. and Parker, R. (1998) Analysis of mutations in the yeast mRNA decapping enzyme. Genetics **151**, 1273–1285

Till, D.D., Linz, B., Seago, J.E., Elgar, S.J., Marujo, P.E., Elias, M., McClellan, J.A., Arraiano, C.M., McCarthy, J.E.G. and Newbury, S.F. (1998) Identification and developmental expression of a 5′–3′ exoribonuclease from *Drosophila melanogaster*. Mech. Dev. **79**, 51–55

Usai, K. and Simpson, P. (2000) Cellular basis of the dynamic behavior of the imaginal thoracic discs during *Drosophila* metamorphosis. Dev. Biol. **225**, 13–25

Valencia-Sanchez, M.A., Liu, J. and Parker, R. (2006) Control of translation and mRNA degradation by miRNAs and siRNAs. Genes Dev. **20**, 515–524

Wang, Z. and Kiledjian, M. (2001) Functional link between the mammalian exosome and mRNA decapping. Cell **107**, 751–762

Wilusz, C., Wormington, M. and Peltz, S. (2001) The cap-to-tail guide to mRNA turnover. Nat. Rev. Mol. Cell Biol. **2**, 237–241

Wood, W., Jacinto, A., Grose, R., Woolner, S., Gale, J., Wilson, C. and Martin, P. (2002) Wound healing recapitulates morphogenesis in *Drosophila* embryos. Nat. Cell Biol. **4**, 907–912

Zabolotskaya, M.V., Grima, D.P., Lin, M.-D., Chou, T.-B. and Newbury, S.F. (2008) The 5′-3′ exoribonuclease Pacman is required for normal male fertility and is dynamically localized in cytoplasmic particles in *Drosophila* testis cells. Biochem. J., doi:10.1042/BJ20071720

Zeitlinger, J. and Bohmann, D. (1999) Thorax closure in *Drosophila*: involvement of Fos and the JNK pathway. Development **126**, 3947–3956

Zeitlinger, J., Kockel, L., Peverale, F.A., Jackson, D.B., Mlodzik, M. and Bohmann, D. (1997) Defective dorsal closure and loss of epidermal decapentaplegic expression in *Drosophila* fos mutants. EMBO J. **16**, 7393–7401

Received 31 March 2008/3 June 2008; accepted 11 June 2008

Published as Immediate Publication 11 June 2008, doi:10.1042/BC20080049